"THE INFLUENCE OF RIBOSOMAL PROTEINS ON THE ACTION OF RIBOSOME-INACTIVATING PROTEINS"

Hilda Romero-Zepeda, BA, MSc., U.A.Q., MEX.

A thesis submitted for the degree of

Doctor of Philosophy

at the University of Warwick

Plant Biochemistry/Molecular Cell Biology

Department of Biological Sciences

University of Warwick

Coventry, West Midlands, CV4 7AL

United Kingdom

1999

PAGE
NUMBERS
CUT OFF
IN THE
ORIGINAL

CONTENTS

ii. List of Tables

iii. List of Appendices

iv. List of Figures

v. Acknowledgements

vi. Declaration

All the results presented in this thesis were obtained by the author. Where appropriate, the sources of information and materials have been specifically acknowledged in the text. Some of the results presented in chapter 4 have been presented in SAPS Congress at Sweden, 17-20 September 1997. None of the work contained in this thesis has been used for a previous application for a degree.

Hilda Romero-Zepeda

vii. Abbreviations and units

Å	angstrom unit = 10^{-10}m (0.1nm)
A-site	aminoacyl-tRNA site on ribosome
A_{260}	absorbance at 260 nm
ADP	adenosine diphosphate
AMV	avian myeloblastosis virus
Arg	arginine
Asn	asparagine
ATP	adenosine triphosphate
dATP	deoxyadenosine triphosphate
b, bp	base, base pair
BSA	bovine serum albumin
Ci	Curie
Ca^{2+}	calcium, divalent cation
cpm	counts per minute
CTP	cytidine triphosphate
dCTP	deoxycytidine triphosphate
Da	dalton
DEP	diethylpyrocarbonate
DNase	deoxyribonuclease
DNA	deoxyribonucleic acid
cDNA	complementary deoxyribonucleic acid
dsDNA	double stranded deoxyribonucleic acid
dNTP	deoxynucleoside triphosphate
ddNTP	dideoxynucleoside triphosphate
dpm	disintegrations per minute
DTT	dithiothreitol
E-site	binding site on ribosome for outgoing tRNA
E. coli	*Escherichia coli*
EDTA	ethylenediamine-tetraacetic acid
EF1	elongation factor 1
EF 2	elongation factor 2

17

EGTA	ethyleneglycol-bis(2-aminoethylether)N,N,N′,N′-tetraacetic acid
FF	fast flow
g	acceleration due to gravity
Glu	glutamic acid
Gln	glutamine
GTP	guanosine triphosphate
dGTP	deoxyguanosine triphosphate
HEPES	N-2-hydroxyethylpiperazine-N'-2-ethane sulphonic acid
HPLC	high performance liquid chromatography
IPTG	isopropyl-β-D-thiogalactoside
K_M	Michaelis constant= substrate concentration at which the rate of an enzyme-catalysed reaction is half the maximum
kb	kilobase
kDa	kilodalton
K_{cat}	catalytic constant (also called turnover number)= maximum or limiting reaction rate of an enzyme divided by the enzyme conc.
l	litre
M	molarity
Mr	molecular mass relative to 1/12 of the atomic mass ^{12}C
Mg^{2+}	magnesium, divalent cation
met	methionine
ml	millilitre
mol	mole
mol. wt.	molecular weight
mM	millimolar
mRNA	messenger ribonucleic acid
ng	nanogram
P-site	peptidyl site on ribosome
PAGE	polyacrylamide gel electrophoresis
PAP	pokeweed antiviral protein
PBS	phosphate buffered saline
PEG	polyethyleneglycol

pH	$-\log_{10} [H^+]$
pI	isoelectric point
pRDVI	pGEM-based plasmid containing 23S rRNA domain VI
p.s.i.	pounds per square inch (lb/in^2)
RIPs	ribosome inactivating proteins
RNA	ribonucleic acid
RNA_T	domain VI - RNA transcript
rRNA	ribosomal ribonucleic acid
RTA	ricin toxic A-chain
rRTA	recombinant ricin toxic A-chain
RNase	ribonuclease
rpm	revolutions per minute
r-proteins	ribosomal proteins
ssRNA	single stranded RNA
SDW	sterile distilled water
SDS	sodium dodecyl sulphate
TCA	trichloroacetic acid
TEMED	N,N,N',N'-tetramethyl-ethylenediamine
TP50	large subunit proteins or 50S subunit total proteins
Tris	tris-(hydroxymethyl)-aminomethane
tRNA	transfer ribonucleic acid
Trp	tryptophan
Tyr	tyrosine
dTTP	deoxythymidine triphosphate
u	units
UV	ultraviolet
μg	microgram
μl	microlitre
v/v	volume per volume
w/v	weight per volume
w/w	weight per weight
X-gal	5-bromo-4-chloro-3-indolyl-β-D-galactopyranoside

viii. Abstract

Ribosome-inactivating proteins (RIPs) are produced by many plants and inhibit ribosome function through an N-glycosidase activity that removes a single adenine residue from a universally-conserved stem-loop structure close to the 3' end of the large subunit rRNA. This site specific action is also retained on 'naked' rRNA, but usually with a much lower catalytic efficiency. Although all known RIPs are active on mammalian ribosomes, their activity on ribosomes from other sources varies considerably. In the work reported, the action of two RIPs with different substrate specificities has been studied on ribosomes and sub-ribosomal derivatives from *Escherichia coli*. The RIPs are pokeweed antiviral protein (PAP), a single chain RIP from the leaves of *Phytolacca americana* and the catalytically active A-chain (RTA) from the heterodimeric toxic lectin ricin from the endosperm of the castor oil bean. The former RIP is active on native *E. coli* ribosomes, whereas the latter is inactive but both are active on naked rRNA. Hence, it is postulated that the ribosomal proteins in the native ribosome either allow, in the case of PAP, or prevent, in the case of RTA, action on the target site in the rRNA. The aim of the work is to use ribosome dissociation and reconstitution techniques to study the relationship between ribosomal proteins and the activity of PAP and RTA.

The initial part of the work concerned establishing conditions under which both PAP and RTA show high levels of discrimination in activity between native ribosomes and naked rRNA substrates. A buffer that contained Ca^{2+} in place of the more usual Mg^{2+} was shown to produce such discrimination. However, in the case of RTA action, the relatively mild treatments resulting in ribosome dissociation were sufficient to allow action. Various subparticles were prepared from purified 50S subunits through the successive removal of ribosomal proteins by increasing ionic strength. As more proteins were split off, the activity of PAP decreased, whereas the activity of RTA remained nearly constant. This is consistent with the hypothesis that ribosomal proteins modulate the activity of the two RIPs differently.

In an attempt to use a small, defined RNA substrate with which to study the influence of ribosomal proteins on RIPs' activity, the region encoding domain VI of 23S rRNA (containing the RIP target site) was sub-cloned from a cloned *rrn*B operon using PCR and used as a template for the synthesis of transcripts *in vitro*. These transcripts were susceptible to depurination by PAP, but for unknown reasons were refractory to RTA. Using gel retardation analysis, it was shown that total 50S ribosomal proteins (TP50) bound to domain VI transcripts in an RNA sequence specific manner, and that the reconstituted complex was relatively stable. However, the activity of PAP on this reconstituted RNP was equivalent to that on the transcript alone, and RTA was inactive on both. These results are discussed in relation to the influences of Mg^{2+} and Ca^{2+} ions and to the possible role of ribosomal proteins L3 and L6.

1. CHAPTER I:

Introduction

I. Introduction

N-glycosidase RIPs most commonly exist either as single catalytic chain polypeptides of approximately 30 kDa or they can exist as toxic lectins, in which a catalytic A-chain is joined to a galactose binding β-chain through a disulphide bond. They inhibit the translocation step in protein synthesis through the removal of a single adenine residue from a universally conserved α-sarcin stem-loop in domain VII (domain VI in eubacteria) in the large-subunit rRNA (reviewed in Massiah and Hartley, 1995; and Marchant and Hartley, 1994).

The specificity of RIPs towards their ribosome substrates varies considerably as has been reviewed in Hartley and Lord (1993), but there are few studies about the binding characteristics of the ribosome-inactivating proteins to ribosome components.

In this work, an attempt is made to describe the binding characteristics of three different RIPs: PAP as a single chain (type 1 RIP) found in various tissues of *Phytolacca americana* with a molecular weight of 29 kDa (Ready *et al.*, 1986), which is active on plant, mammalian, yeast and *E. coli* ribosomes; tritin-S (type 1 RIP) found in the endosperm of *Triticum aestivum* which separates into two partially resolved bands of approximately 32.1 and 32.8 kDa with a similar basic charge (Massiah and Hartley, 1995), and which is active on mammalian and yeast ribosomes, but inactive on plant and *E. coli* ribosomes; and finally RTA, the Ricin toxic A-chain well characterised as having low activity on plant ribosomes, but extreme activity on mammalian and yeast ribosomes, and inactive on *E. coli* ribosomes.

The well conserved α-sarcin loop structure of ribosomes and the similarity between RIPs structures (Chaddock *et al.*, 1996) permit the comparison of the recognition of elements for RIPs over 'naked' (deproteinised) rRNA and Ribosomes from several sources. The RIPs' binding phenomenon with and without activity over the ribosomes will be investigated.

Eukaryotic ribosomes and ribosomal proteins are poorly characterised and it is not yet possible to reconstitute activity in eukaryotic ribosomes.

E. coli ribosomes have therefore been used in this work to establish the role of ribosomal proteins and their reaction characteristics, because these ribosomes and ribosomal proteins are well characterised and the role of individual ribosomal proteins in assembly processes is known. Finally, they are substrates for some single chain RIPs and depurination of 23S rRNA which has been reported to occur at an analogous position as in 28S rRNA as it has been reported.

1.2. The Background of the Project

Ribosome inactivating proteins or RIPs are widely distributed in Angiosperms. They occur in different plant organs (seeds, leaves, roots and tubers) in concentrations ranging from a few µg to several hundred mg per 100g of tissue. They catalytically and irreversibly inactivate the 60S subunit of eukaryotic ribosomes rendering it incapable of binding elongation factor 2 (Stirpe and Barbieri, 1986). Now it is known that RIPs are also active on prokaryotic ribosomes (Marchant and Hartley, 1994). In plants, it is known that in most cases, the ribosomes are sensitive to their endogenous RIPs. Toxicity is avoided by targeting the RIP to the extracellular matrix or the vacuole (reviewed by Hartley *et al.*, 1996).

A major application of RIPs (particularly ricin) is in the construction of immunotoxins in which specific monoclonal antibodies are conjugated with potent toxins in order to target the toxin to specific cells *in vivo* and destroy them. These targets include neoplastic cells, lymphocytes involved in autoimmune reactions and virally infected cells (Dosio *et al.*, 1993; Wachinger *et al.*, 1993; Lee-Huang *et al.*, 1994; Girbes *et al.*, 1996; and for reviews: Barbieri *et al.*, 1993; Hartley and Lord, 1993).

RIPs are also being used increasingly to probe ribosome structure and function, particularly the role of ribosomal RNA (rRNA) in protein synthesis.

1.2.1. Protein Biosynthesis

Protein biosynthesis is of central importance for all living systems, the assembly of polypeptide chains from amino acids and their subsequent modifications leading to the final three dimensional protein structure are exceptionally complex processes. The role

of the ribosome in cells is to synthesise the polypeptide chain specified by the mRNA; hence it has both a decoding and a catalytic function (Arnstein and Cox, 1992). The rRNA structure in the vicinity of the RIP target site, has been shown to be important in binding the elongation factors (Moazed *et al.*, 1988). The depurination or endonucleolytic cleavage of this rRNA structure results in the loss of ribosome function, and thus the enzymes responsible are known as ribosome-inactivating proteins (RIPs).

1.2.2. Ribosomes

Ribosomes are the essential organelles for the synthesis of proteins in all living cells. The ribosomes are ancient and complex. They are large ribonucleoprotein particles that are responsible for the translation of the genetic information encoded in the messenger RNA in proteins. Five different classes of ribosomes can be distinguished: the 70S ribosome of eubacteria, the 80S ribosome of eukaryotic cytoplasmic, the archaebacterial ribosome, chloroplast and mitochondrial ribosomes, all with a general common anatomy but varying in both number and size. Their architecture and their assembly are also complex (Noller and Nomura, 1987). It is well known that proteins are synthesised by ribosomes and that these large polymerases catalyse the construction of polypeptides by linking amino acids in the specific sequence directed by their mRNA templates (Moore, 1997ab).

Prokaryotic ribosomes have molecular weights around 2.5×10^3 kDa; and eukaryotic ribosomes are almost twice as big, and each ribosome synthesises only one polypeptide at a time, regardless of origin (reviewed by Matheson *et al.* 1995).

1.2.2.1. Morphology and composition of the ribosome

The ribosome is composed of two subunits, one being approximately twice as large as the other with 34 protein molecules in the 50S subunit of the *E. coli* ribosome and about 50 in the 60S subunit from eukaryotic cytoplasmic ribosomes (Noller *et al.*, 1995; Wool *et al.*, 1995; Moore, 1997b).

Electron microscopy, x-ray and neutron scattering has been used to obtain the perception of the shape of ribosomes (Prince *et al.*, 1983). In a general way, the 50S

subunit has a spherical or globular shape, which contains the L7/L12 stalk on one side. the central protuberance in the middle and the L1 ridge on the other side. The largest dimension of the 50S subunit is about 24-25nm (Noller and Nomura, 1987).

The 30S subunit is divided into a body and a head. The body contains two-thirds of the mass of the particle, and one-third belongs to the head. Near the body/head junction some kind of platform extends to a cleft. The largest dimension of the particle is about 24-25nm (reviewed by Noller and Nomura, 1987).

The consensus about the relative orientation of the 30S and 50S subunits in the 70S particle suggest that the platform side of the 30S subunit faces the concave side of the 50S subunit, with the head of the 30S particle positioned between the L1 ridge and the central protuberance. The internal architecture has been suggested as a channel-like feature that may correspond to positively stained segments of the ribosome (Kolb *et al.*, 1997). This concept is based mainly on the fact that a c-terminal sequence of about 30 to 40 amino acid residues long of the nascent, growing polypeptide chain is protected against proteinases in crude ribosome preparation. Although there is a controversy about the existence and/or the length of the suggested intraribosomal tunnel, Kolb *et al.* (1997) reported a 50 to 100Å tunnel length.

Stark *et al.* (1997) have determined the three-dimensional structure of the 70S *E. coli* ribosome in various phases of the elongation cycle, through an electron cryo-microscopy and angular reconstitution to a level of 18-23Å. Their results show that the positions of the tRNAs bound to the A- and P-, and to the P- and E-sites in the pre- and post-translocation states are that:

> a) the P-site tRNA is positioned directly above the bridge connecting the small and the large ribosomal subunit,
> b) in the pretranslocational state, the A-site tRNA is fitted snugly against the
> > P-site tRNA under an angle of approx. 50°, towards the L7/L12
> side of the ribosome,

c) the E-site tRNA lies between the side lobe of the 30S subunit and the L1 protuberance,

d) in the structure of ribosome binding the 'ternary complex' of EF-Tu and the aminoacyl-tRNA and GTP, the 3D reconstruction shows the ternary complex spanning the inter-subunit space with the acceptor domain on the tRNA reaching into the decoding centre,

e) the domain 1 of the EF-Tu is bound to the L7/L12 stalk and the 50S body underneath the stalk,

f) finally, domain 2 of the EF-Tu is oriented towards the S12 region of the 30S subunit.

The **Table 1** shows the consensus morphology and composition of the ribosomes.

Finally, data obtained from immunoelectron microscopy (IEM) and neutron diffraction studies, have shown the spatial arrangement of r-proteins in the ribosomes **(Table 2)**.

It is noteworthy that there is a protein-protein interaction made during ribosome assembly. Noller and Nomura (1987) suggested that such interactions are likely to occur during the assembly of the subunits, and at least some of the assembly map dependencies reflect this **(Table 2)**.

1.2.2.2. The function of the ribosome

The function of the ribosome is to catalyse the synthesis of proteins as directed by the messenger RNAs. It is able to translate the information encoded by the messenger RNAs into the correct sequence of amino acids in the polypeptide chain and although the fundamental reaction of the protein synthesis is the peptidyl transfer, it is still not fully understood either from the mechanistic point of view, or from the point of view of the functions of the components involved (Franceschi et *al.*, 1997).

Table 1. Consensus morphology and composition of the ribosomes from

   Escherichia coli
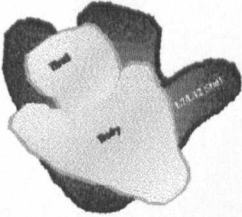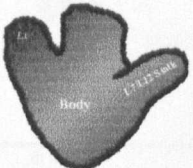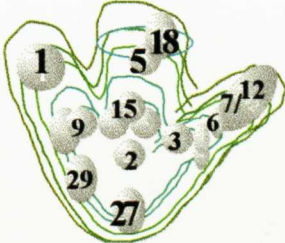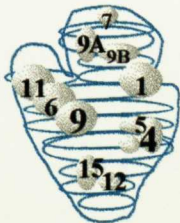
Structure	Composition	Morphology	Reference
70S ribosomes	23S rRNA 16S rRNA 5S rRNA 52 r-proteins		Prince *et al.*, 1983, Oakes *et al.*, 1990, Verschoor *et al*, 1996; Kolb *et al.*, 1997; Stark *et al.* 1997.
50S subunit	23S rRNA 5S rRNA 31 r-proteins		Prince *et al.*, 1983; Oakes *et al.*, 1990.
30S subunit	16S rRNA 21 r-proteins		Prince *et al.*, 1983; Oakes *et al.*, 1990.

Table 2. *E. coli* subunits' r-proteins composition, characteristics, assembly map and suggested spatial arrangement

E. coli

Ribosome Subunit	r-Proteins	Residues	Mol. Wt.	Assembly maps	Spatial arrangments
50S	L1	233	24,559		
	L2	269	29,416		
	L3	209	22,258	For	
	L4	201	22,087	50S subunit´	
	L5	178	20,171	assembly map	
	L6	176	18,832	see:	
	L7	120	12,220	Nierhaus, 1989	
	L9	147	15,431		
	L10	165	17,737		
	L11	141	14,874		
	L12	120	12,178		
	L13	142	16,019		
	L14	123	13,541		
	L15	144	14,981		
	L16	136	15,296		
	L17	127	14,364		
	L18	117	12,770		
	L19	114	13,002		
	L20	117	13,366		
	L21	103	11,565		
	L22	110	12,227		
	L23	99	11,013		
	L24	103	11,185		
	L25	94	10,694		
	L26=S20	86	9,553		
	L27	84	8,993		
	L28	77	8,875		
	L29	63	7,274		
	L31	62	6,971		
	L32	56	6,315		
	L33	54	6,255		
	L34	46	5,381		
	S1	557	61,159		
	S2	240	26,613		
	S3	232	25,852		
	S4	203	23,137	For	
	S5	166	17,151	30S subunit´	
	S6	135	15,704	assembly map	
	S7	177	19,732	see:	
	S8	129	13,996	Nierhaus, 1989	
	S9	128	14,569		
	S10	103	11,736		
	S11	128	13,728		
	S12	123	13,606		
	S13	117	12,968		
	S14	97	11,063		
	S15	87	10,001		
	S16	78	9,191		
	S17	83	9,573		
	S18	74	8,896		
	S19	91	10,299		
	S20	86	9,553		
	S21	70	8,369		

50S: Rohl and Nierhaus, 1982; Wittmann, 1982; Hackl and Stoffler-Miolicke, 1988; Nierhaus, 1989; Egebjerg *et al.*, 1990; Arnstein and Cox, 1992.

30S: Wittmann, 1982; Ramakrishnan *et al.*, 1984; Noller and Nomura, 1987; Moore, 1988; Van Heel, 1997.

The general process of protein synthesis is composed of three main stages: initiation, elongation and termination. A brief description of the mechanism of protein synthesis in *E. coli* follows. In initiation, the 30S subunit binds to mRNA in the vicinity of the initiation codon(s) in the mRNA (AUG or GUG) by a way of a region of base sequence complementarity consisting of 4-7 base pairs between the 3' end of 16S rRNA and the mRNA. Formyl methionyl tRNA binds to the initiation codon positioned in the partial P site in the 30S subunit, followed by the attachment of the 50S subunit, the hydrolysis of GTP and the release of initiation factors bound to the 30S subunit. During elongation, there is a codon-directed binding of an aminoacyl tRNA to the empty ribosome A site, followed by peptide bond formation between the amino group of this aminoacyl residue and the carboxyl group of the aminoacyl residue attached to the tRNA in the P site. This is catalysed by peptidyl transferase, an integral activity of the 50S subunit. Following peptide bond formation, the peptidyl tRNA in the A site is physically shifted to the P site by the translocation of the ribosome along the mRNA in a 5' – 3' direction by the length of one codon in a GTP hydrolysing reaction. The elongation cycle continues until a stop codon is encountered in the A site. This causes the peptidyl transferase to transfer its peptidyl moiety to water, causing the termination and release of the nascent polypeptide chain. The ribosome then dissociates into its subunits. Subunits once more are available for binding to initiation sites on free mRNA or to mRNA to which ribosomes are already attached (Arnstein and Cox, 1992).

1.2.2.3. The *E. coli* ribosome

E. coli is the reference organism for ribosome research, although it does not mean that it is representative of the state of ribosome research in general. About 80% of the RNA in a bacterial cell is found in ribosomes (Moore, 1997). The *E. coli* ribosome consists of 38% protein and 62% rRNA (Noller and Nomura, 1987), with a molecular weight of 2.25×10^3 kDa (Dahlberg and Zimmermann, 1992) and consists of two particles, namely the 50S and 30S subunits. All the *E. coli* r-proteins have been sequenced either by protein sequencing, by DNA sequencing of their genes, or by both. All these have been well characterised and similar enterprises are under way for archaebacterial thermophile (Draper, 1994) and rat ribosomes now completed in terms

of primary structures (Wool et al., 1995). The small subunit of the E. coli ribosome consists of 21 proteins and a single rRNA molecule, and the large subunit consists of 34 different proteins and two rRNA molecules. E. coli ribosome subunits can be totally disrupted and reconstituted with relative ease. It might mean that both the prescription for this complicated assembly process and the information necessary to form the quaternary structure of the ribosome resides completely in the primary sequences of the proteins and rRNAs taking part (Nierhaus, 1994).

1.2.3. The 30S and 50S Subunits

There are two large ribosomal subunits containing their respective ribosomal RNA. The small subunit contains a single species, usually in the range of 1500-1800 nucleotides (nt) and is referred to as small subunit rRNA or 16S-like rRNA (Draper, 1994). The large subunit contains one large rRNA (23S in prokaryotes, 25S / 28S in eukaryotes) and one (prokaryotes) or two (eukaryotes) small rRNAs. The small rRNAs are 5S found in all ribosomes except mitochondrial ribosomes and 5.8S found in eukaryotic ribosomes. The latter RNA is homologous to the 3' end of eubacterial 23S rRNA (reviewed by Arnstein and Cox, 1992). Both subunits plays an important role in protein biosynthesis, they have interactions within the two ends of tRNA. Noller et al. (1995) considered these two subunits with their rRNAs as relics of molecular evolution, which may have pre-existed as small and functionally independent RNA structures.

Noller et al. (1995), have suggested that in the 30S subunit, about 75% of the 16S rRNA is considered to be sufficiently constrained to allow unambiguous placement of the various structural elements providing extensive information about the location and nature of protein- rRNA interactions. Most of its 21 distinct proteins are globular and contain an average of 28% α-helix and 20% β-structure (Arnstein and Cox, 1992). Most of the 30S subunit's r-proteins are basic, and only S1, S2 and S6 are acidic. Hence, the interaction between the negatively charged rRNA and the basic proteins contribute to the stability of the ribosome. The 30S subunit's 16S rRNA plays an active role in the initiation, elongation, and termination steps of protein synthesis (Dahlberg, 1989).

The model of the 30S subunit structure, has been approached by using four different techniques:

a) molecular modelling based on the phylogenetically determined secondary structure (Noller, 1984),

b) the spatial arrangement of r-proteins as derived from neutron scattering data (Stern *et al.* 1989),

c) the interaction of proteins with rRNA derived from cross linking experiments (Brimacombe *et al.*, 1990) and

d) Hydroxyl radical probing which is based on the attack of the C1' and C4' by iron-tethered hydroxyl radicals, making a chain scission, which was identified by primer extension (Noller *et al.* 1995).

The functional regions of 16S rRNA are probably located on the surface of the ribosome. The phylogenetic studies have shown those 16S rRNA sequences of both bacteria and eukaryotes, including chloroplasts and mitochondria, follow a common pattern of secondary structure. Is noteworthy that the small ribosomal subunit is capable of self-assembly *in vitro* from the 16S rRNA and ribosomal proteins. The *in vitro* self-assembly has been used to suggest the spatial arrangement of the proteins within the small subunit (Moore, 1988).

The 50S subunit or large subunit structure is less well characterised that the small one, because of its greater complexity. Most of its 31 different proteins are also basic with only L7 and L12 as acidic proteins. The 50S subunit's 23S rRNA is around 2900 nucleotides, folded into a bihelical-like secondary structure, and this subunit shows a peptidyl transferase and a translocase activity on the ribosome (Arnstein and Cox, 1992). Moazed and Noller (1989) have reported that the elongation factor EF-Tu and EF-G compete for the binding site on the ribosome. EF-G and EF-Tu have been reported to interact with the highly conserved α-sarcin/ricin loop nucleotide

sequence around position A_{2660} which is the site of the action of the cytotoxins α-sarcin and ricin (Zimmerman *et al.*, 1990; Nierhaus *et al.*, 1993).

The 50S subunit is also capable of self-assembly in vitro from the 23S rRNA, 5S rRNA and the large subunit proteins (TP50). (Nierhaus, 1990). In each subunit, approximately one third of the ribosomal proteins bind independently to the rRNA and are referred to as primary-binding proteins. They may organise the rRNA structure in a way that facilitates the interaction of the remaining proteins and rRNA conformational changes have been strongly implicated to important aspect of assembly (Powers *et al.*, 1993).

1.2.4. Ribosomal RNA Operons

It has been reported that eubacteria possess between 1 and 10 RNA operons per genome (Hui and Dennis, 1985) whereas eukaryotes have many hundreds of transcription units per genome. *E. coli* contains seven independent RNA transcriptional units with almost identical sequences per chromosome (*rrn*A, *rrn*B, ...*rrn*H) in the region of the mature rRNA (Kiss *et al.*, 1977; Noller and Nomura, 1987). Brosius *et al.* (1981) determined the complete DNA sequence for the *rrn*B transcriptional unit, which is the model for the gene organisation and primary structure for the rRNA form of *E. coli*.

1.2.5. Ribosomal RNA

The role of RNA, which can serve as genetic material, has an enzymatic function in ribozymes and also an adapter role in protein synthesis, which have been analysed extensively (Cech, 1987). RNA has a very similar, covalent structure to DNA, showing the difference between having a ribose sugar instead of a 2'-deoxyribose, and having a uracil instead of a thymine (these have a similar structure but where a thymine has a methyl group, a uracil has a hydrogen atom). The RNA structure contains a Watson-Crick base pairing which provides a simple structure code for secondary structures and helical pairing. However, structural determination from crystallography and NMR spectroscopy show that non-Watson-Crick base pairs and sequence-specific contacts between the bases and the sugar-phosphate backbone are very common in non-perfectly paired regions of

33

RNA where the RNA has non-helical regions (Varani and Pardi, 1994). The catalytic activity of ribozymes is mediated by the crucial tertiary contacts that allow RNA to assume its active 3D shape (or to act as a protein-binding site).

Besides the well-known roles of RNA as a mediator of genetic information from DNA to protein (mRNA), as an adapter molecule (tRNA) and as an integral component of the ribosome (rRNA) it has become clear that RNA is involved in a great diversity of other functions in the cell. RNA is the only macromolecule that has the flexibility to fulfil the requirements of a carrier of genetic information and of a catalyst.

The functional role of ribosomal RNA with its highly conserved structures, has been identified for containing: the decoding site, the peptidyl transferase active centre, the binding sites for the elongation factors, and other functional centres of the ribosome required for protein synthesis (Noller, 1991).

1.2.5.1. Structure of rRNA

Most of the secondary structure of ribosomal RNA is conserved among different species, from prokaryotes to eukaryotes, where the exceptions are the expansion sequences of eukaryote rRNA. The different expansion sequences are located in the same regions in many higher eukaryote rRNA, but differ widely in sequence and length (Lundquist and Nygard, 1997).

The rRNA is able to fold into several structural motifs such as bulge loops, interior loops, multibranched loops and stem loops, either singly or together because of its single stranded nature and its ability to form non-Watson-Crick base pairings. They give to the rRNA a higher degree of structural freedom than dsDNA (Pleij, 1990).

The secondary structure of rRNA is dominated by A-form helix stem regions throughout the molecule and separated by single stranded regions appearing as loops. The base pairing between the single-stranded regions in the secondary structure can make tertiary interactions within the ribosome. One of the possibilities of forming these tertiary interactions is given by the interactions between a loop region, and

single-stranded regions outside the loop, described as pseudoknot formation, through a Watson-Crick pairing (Pleij, 1990).

1.2.5.2. The 23S rRNA

The important role that 23S rRNA plays in protein biosynthesis, specifically at a step in peptide bond formation has been reviewed (Noller *et al.*, 1992; Draper, 1994). The greater complexity of 23S-like rRNA relative to 16S-like rRNA, makes it difficult to study its structure and functions in the ribosome, especially considering that the folding and numerous ribosomal proteins can influence performance of rRNA. Also, it is well known that within this rRNA, some fragments show properties of the whole ribosome, such as the ability to interact with antibiotics (Purohit and Stern, 1994; Fourmy *et al.*, 1996), and with mRNA and tRNA (Purohit and Stern, 1994).

The prediction of the 23S rRNA secondary structure was done mainly through the prediction of classical base pairing (Watson-Crick pairs). This is done by comparative sequence analysis where, given an alignment of two or more sequences, sites were sought where similar structure can be maintained by classical base pairing, despite nucleotide replacements (Westhof and Michel, 1994). The 23S-like ribosomal rRNA consists of six major structural domains that are brought together by long-range base pairing interactions that probably form structure and assemble proteins independently during rRNA transcription **(Table 3)**. **Table 3** shows the regions involved in long range interactions. The domains also contain specialised functional sites (Noller, 1984).

Brosius *et al.* (1981ab) obtained the complete nucleotide sequence of the 23S ribosomal RNA gene from *E. coli*. They reported the 2,904 nucleotide sequence and also confirmed numerous post-trascriptionally modified nucleotides (reviewed by Noller and Nomura, 1987). Although there is a consensus about secondary structure models for *E. coli* 23S rRNA, there is not yet a consensus in terms of the structure of the loops, since it is not possible to predict non Watson-Crick base pairing interactions. The existence of each helix obtained mainly by comparative sequence analysis has undergone revision in recent years. So far, 23S rRNA has been recognised as having 5'- and 3'- end sequences as base pairs and so further long-range base - paired

Table 3. Major Domains of 23S rRNA from *Escherichia coli* ribosomes and their long range interactions

Domain	Base Ranges	Long-range Interactions	
Domain I	16 - 524	16-25	/ 515 - 524
Domain II	579 - 1261	579 - 585	/ 1255 - 1261
Domain III	1295 - 1645	1295 - 1298	/ 1642 - 1645
Domain IV	1648 - 2009	1656 - 1664	/ 1997 - 2004
Domain V	2043 - 2625	2043 - 2054	/ 2615 - 2625
Domain VI	2630 - 2882	2630 - 2637	/ 2781 - 2788

Domains project from a central loop created by pairing of the 5' and 3' ends of the *E. coli* 23S rRNA molecule. Domains are brought together by long-range base pairing (from Noller, 1984, and Noller and Nomura, 1987).

36

interactions partition the chain into identifiable structural domains (Noller and Nomura, 1987). *In vitro* reconstitution experiments from purified molecular components have demonstrated that all of the information needed for correct assembly of the subunit is contained in the structure of the ribosome molecular components. In the 50S subunit, the *in vitro* assembly reaction takes place with the 23S rRNA, 5S rRNA and the r-proteins, involving two steps with different reaction conditions because of the complexity of this larger subunit. The assembly reaction also shows the cooperative binding pathway of proteins to rRNA, presenting two main and independent nucleation sites. The above situation is similar to that presented by the assembly in vivo, but it does not establish the dependence or independence of nucleation sites for the subunit. (Dijk and Littlechild, 1979; Röhl and Nierhaus, 1982; Datta *et al.*, 1986; Franceschi and Nierhaus, 1990; Romero *et al.*, 1990; Ostergaard *et al.*, 1998).

Nitta *et al.* (1998$_{ab}$) showed experimental results suggesting that 23S rRNA is directly involved in the peptide bond formation. They showed that although several reports have indicated that the eubacterial peptidyltransferase reaction does not require all the r-proteins, this reaction of the naked 23S rRNA by itself suggested that 23S rRNA seems to be the peptidyltransferase itself.

1.2.5.3. Domain VI of *E. coli* 23S rRNA

Domain VI is one of the six *E. coli* 23S rRNA domains (corresponding to domain VII of eukaryotic large subunit rRNA) designated I to VI by Raué *et al.* (1988). Domain VI lies at the 3' end of *E. coli* 23S rRNA, and it is a component of the site of the elongation factor binding to the ribosome and also the site of action of ribotoxins. According to Leffers *et al.* (1988), within domain VI of 23S rRNA from *E. coli*, double helices are numbered 1 to 9, where helix 2 contains (helix 90 in Raué's, *E. coli* 23S rRNA numbering) a universally, conserved region of 14 nucleotides, which is the site of action of RIPs. Furthermore, domain VI can be divided into a highly conserved subdomain VIA and a less conserved VIB (Leffers *et al.*, 1988). The site of the action of RIPs is found within the subdomain VIA. T7 transcripts of domain VI have been made and the structure determined (Leffers *et al.*, 1988; Uchiumi *et al.*, 1997). This domain has been found to bind ribosomal proteins L3 and L6. L3 has been found to bind directly to the rRNA, the binding localised to domain VIA and most protection

effects due to L3 have been found in the vicinity of α-sarcin loop (Leffers *et al.* 1988; Uchiumi *et al.*, 1999).

1.2.5.4. The α-sarcin loop

The α-sarcin loop or helix 90 (Raué's *E. coli* numbering) is the sole universally conserved region (Raué *et al.*, 1988), located in domain VI of *E. coli* 23S rRNA **(Figure 1(a))**. This loop in *E. coli* 23S rRNA (nucleotides 2646-2674) is despicted in the secondary structure as a stem-loop or as a continuous helix, distorted by a bulged G_{2655} and with a G_{2659}AGA tetraloop **(Figure 1)**.

Orita *et al.* (1993) investigated the α-sarcin loop structure using a dodecaribo-nucleotide that mimics the α-sarcin loop in 28S ribosomal RNA, which forms an RNA hairpin structure with a GAGA loop and a stem of four base pairs. They found that the tetraloop is formed of an unusual G: A base pair formed by the first G and the last A of the GAGA tetraloop. The phosphodiester backbone between the first G and the A in the second position of the same tetraloop extends, changing the shape of the tetraloop, which seems to help the ribotoxin to access the universally conserved region. Furthermore, the crystal structure of a 29-nt RNA (E73) containing the 28S rRNA α-sarcin loop sequence, determined by NMR (Szewczak *et al.*, 1993; Szewczak and Moore, 1995; Seggerson and Moore, 1998), showed a bulged nucleotide G10 (G_{2655} in *E. coli* 23S rRNA, G_{4319} in rat 28S rRNA) that reaches across the major groove and interacts with the phosphate backbone of the opposite strand. Adjacent to G10 is a reversed Hoogsteen U-A base pair, U11-A20, followed by a side by side A6 base pair, which together generate a cross strand adenine stack. A GNRA tetraloop closed by C-G base pair (C13-G18) caps the loop (Seggerson and Moore, 1998).

Seggerson and Moore (1998) showed results of NMR studies of two variants of E73: G10A and Pro-SRL. G10A is identical to that of E73 except that an adenine replaces G10. PRO-SRL (27-nt RNA) contains the prokaryotic α-sarcin loop sequence but it lacks the C8 and A21 and so it differs from the eukaryotic α-sarcin loop. **Figure 1(b)** shows the PRO-SRL sequence reported by Seggerson and Moore (1998).

Figure 1. The α-sarcin domain of 23S rRNA.

(a) A portion of *E. coli* 23S rRNA with α-sarcin domain. (From Leffers *et al.*, 1988)
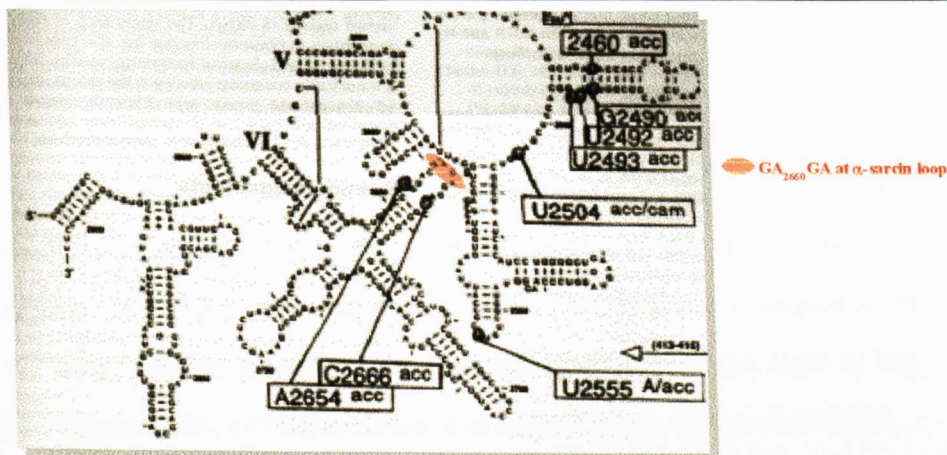
(b) PRO-SRL (*E. coli* 23S rRNA α-sarcin loop). (From Seggerson and Moore, 1998)
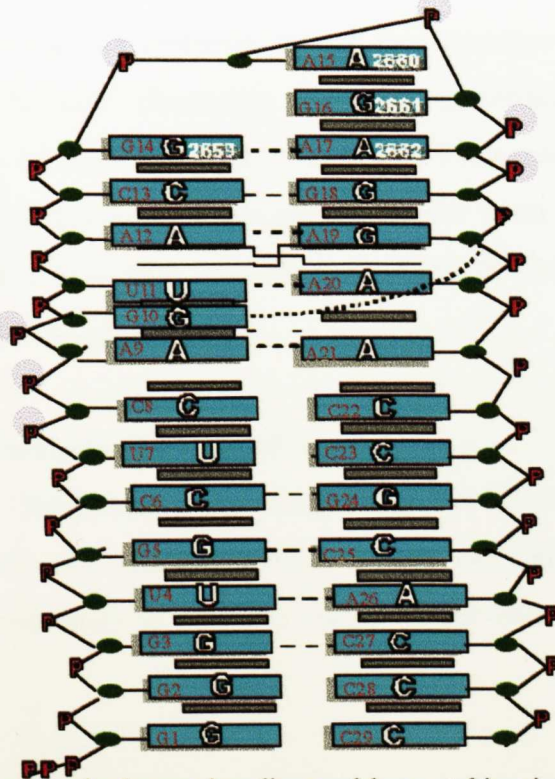
Schematic diagram of the hydrogen bonding and base staking interactions in part of the oligoribonucleotide that mimics the sarcin/ricin loop in 23S rRNA (Seggerson and Moore, 1998). Sugars are represented by filled circles and phosphate groups are represented by P, which are within a circle when the phosphate has a nonhelical chemical shift. Base stacking interactions are shown by filled rectangles. Watson-Crick base pairing is denoted by dashes, and non-Watson-Crick pairing by dots. The crossed shaded bars at G19-A20 show stacking of a base on the 3'end of the loop with a residue on the 5' side and viceversa (from Szewczak *et al*, 1993). PRO-SRL refers to Prokaryotic sarcin/ricin loop, a 29 base oligonucleotide mimicking *E. coli* 23S rRNA α-sarcin loop.

Results have shown that the α-sarcin stem-loop structure might be the first essential contact site for both elongation factors (Moazed *et al.*, 1988; Douthwaite *et al.*, 1995; Munishkin and Wool, 1997; Wilson and Noller, 1998). This has been deduced mainly from the observation that the single cleavage after G_{2661}, exclusively impaired the binding of each of the elongation factors. The intrinsic ribosomal functions, such as the formation of 70S ribosomes from subunits, tRNA binding to A-, P-, and E- sites, peptidyltransfer and EF-G independent (spontaneous) translocation, were not affected at all. Hence the α-sarcin loop structure is characterised by two universally conserved features. (Zimmerman *et al.*, 1990; Nierhaus *et al.* 1992). The first is the sequence of the dodecamer in the loop, and the second is the structural weakness of the stem as has been suggested by Nierhaus *et al.*, (1992) because it is the substrate of the ribotoxins.

α-Sarcin is a ribonuclease (produced by the mold *Aspergillus giganteus*, Endo *et al.* (1990)) that inhibits protein biosynthesis in cell-free systems from a variety of prokaryotes such as *E. coli* ribosomes and the archebacterium *Sulpholobus solfataricus* (reviewed by Jiménez and Vásquez, 1985) and eukaryotes. This ribonuclease specifically hydrolyses a single phosphodiester bond linking to the 3' side of G_{4325} in 28S rRNA or to G_{2661} in *E. coli* ribosomes (23S rRNA). Both are present in the 'universal' sequence $GA_{2660}GA$.

1.2.6. Ribosome inactivating proteins (RIPs)

N-glycosidase active, Ribosome Inactivating Proteins (RIPs) are a group of structurally and functionally related proteins which can attack and irreversibly inactivate eukaryotic ribosomes so that they are no longer able to function in protein synthesis.

1.2.6.1. Nomenclature and classification of RIPs

The classification was proposed by Stirpe and Barbieri (1986) who designate those RIPs existing in nature as single chain proteins or glycoproteins as type 1 and those consisting of an A- (catalytically active chain) covalently linked to a B- (cell binding chain) with lectin properties as type 2. Type 1 RIPs and the toxic A-chain, both

exhibit sequence homologies in their enzymatic chains and possess rRNA N-glycosidase activity, inhibiting protein biosynthesis.

Classically, RIPs have been categorised, based on their structural characteristics:

The **type 1** RIPs: Some of these are N-glycosylated. They occur as monomeric proteins or single chain proteins, N-glycosidases. They have a molecular mass around 30 kDa. Although type 1 RIPs show the inhibition of protein synthesis in cell-free systems, they are considerably less toxic to eukaryotic cells (by a factor of 10^2-10^4) than the type 2 RIPs, since the former lack the means of initially binding to the surface of cells (Olsnes and Pihl, 1982). Nevertheless, some of them have shown activity not only with eukaryotic ribosomes but also with prokaryotic ribosomes in cell free systems. (Hartley *et al.*, 1991; Chaddock *et al.* 1996).

The **type 2** RIPs: These are heterodimeric proteins with an A-chain that appears to be structurally and functionally related to the RIPs type 1, is disulphide linked to a galactose-binding B-chain of around 30 kDa. These type 2 RIPs are less common than their type 1 counterparts, and they are potent cytotoxins owing to the cell binding ability of the B-chain which promotes the obligatory first step in toxin uptake. Only two type 2 RIPs have been shown to exhibit extremely low cytotoxicity, but *in vitro* protein synthesis inhibition, they are equivalent to the other type 2 RIPs (reviewed by Chaddock *et al.* 1996). In type 2 RIPs, binding results because the B-chain recognises galactose-containing receptors on sensitive cells in the internalisation of RIPs and transports them (reviewed by Gluck *et al.* 1992) to the ER complex. In this, it is assumed that the disulphide bond is reduced, thus separating the two chains and allowing translocation of the A-chain to the cytosol.

The **Table 4** summarises some of the type 1 and type 2 RIPs' characteristics.

Table 4. Characteristics of some type 1 and type 2 RIPs.

RIP name	type	M. wt. (kDa)	N-Glycosylated	Inhibition of cell-free protein synthesis IC_{50} (nM)	Tissue	Species	References
Barley seed RIP	1	29.9		2.13	seed	*Hordeum vulgare*	Asano *et al.*, 1984; Coleman & Roberts; 1981
Dianthin 30	1	29.5	Yes	0.3	leaves	*Dianthus caryophyllus*	Stirpe *et al.*, 1981
Dianthin 32	1	31.7		0.12	leaves	*Dianthus caryophyllus*	Stirpe *et al.*, 1981
Gelonin	1	30.0	Yes	0.06	seeds	*Gelonium multiflorum*	Stirpe *et al.*,1980
Gypsophilin	1	28.0	No		leaves	*Gypsophila elegans*	Yoshinari *et al.* 1997
Momordin	1	29.0	Yes	0.06	seeds	*Momordica charantia*	Stirpe *et al.*, 1981
Mor-I	1	27.9		0.063	seeds	*Marah oreganus*	Shih *et al.* 1998
Mor-II	1	27.6		0.071	seeds	*Marah oreganus*	Shih *et al.* 1998
Pepocin	1	26.0	No		sarcocarp	*Cucurbita pepo*	Yoshinari *et al.* 1996
PAP	1	29.0		0.24	leaves	*Phytolacca americana*	Irvin *et al.* 1980; Barbieri
PAP II	1	30.0		0.25	leaves	*Phytolacca americana*	*et al.* 1982; Bolognesi
PAP-S	1	29.2		0.04	seeds	*Phytolacca americana*	*et al.*1990.
Saporin	1	29.5	No		s & l	*Saponaria officinalis*	Olsnes & Pihl, 1973
Leaf tritin	1	37.2			leaves	*Triticum aestivum*	Stirpe *et al.* 1983; Ferreras *et al.*, 1993.
Seed tritin	1	32.0	No	2.0	seeds	*Triticum aestivum*	Roberts and Stewart, 1979; Massiah & Hartley, 1995.
Volvarin	1	29.0	.	0.5	fruiting bodies	*Volvariella volvacea*	Qi-Zhi *et al.*, 1998
Abrin	2	63.8	Yes	88.0	seeds	*Abrus precatorius*	Olness & Pihl, 1973a
Abrin A-chain		30.0	No	0.5		*Abrus precatorius*	Olness & Pihl, 1973b
Modecin2		63.0	Yes		roots	*Adenia digitata*	Gasperi-Campani *et al.*
Modecin A-chain		28.0				*Adenia digitata*	1978.
Ricin	2	65.0	Yes	84.0	seeds	*Ricinus communis*	Olness & Pihl, 1973
Ricin A-chain		30.0	Yes	0.1		*Ricinus communis*	Olness & Pihl, 1973
Volkesin	2	62.0	Yes	43.3	leaves	*Sambucus ebulus*	Barbieri *et al.* 1984
Volkesin A-chain		29.0		0.37		*Sambucus ebulus*	Barbieri *et al.* 1984
Viscum	2	60.0	Yes	84.0	leaves	*Viscum album*	Olness *et al.* 1982
Viscum A-chain		29.0		3.5		*Viscum album*	Olness *et al.* 1982

1.2.6.2. Mode of action of RIPs

RIPs are site specific rRNA N-glycosidases that catalyse the removal of a single adenine base from the conserved loop of the 28S rRNA of eukaryotic ribosomes, or the 23S rRNA of prokaryotes (Hartley *et al.*, 1991). The removal is done by hydrolysing the N-glycosidic bond between the base and the ribose of the adenine at the position A_{4324} in rat 28S rRNA, at position A_{2660} in prokaryotic 23S rRNA. This RNA modification interferes with the elongation factor binding and disrupts protein synthesis (Wool et *al.*, 1990).

Depurination of *E. coli* 23S rRNA occurs at A_{2660}, in a functionally equivalent position to the target adenine of eukaryotic 26/28S rRNA (A_{4324} in rat liver) (Hartley *et al.*, 1991; Chaddock *et al.*, 1996). RIPs act enzymatically, and approximately 10 molecules of PAP will kill an animal cell, moreover, a single molecule of the Ricin A chain is sufficient to kill a cell and a single molecule will inactivate approximately 1500 ribosomes min^{-1} (Gluck *et al.*, 1992). All RIPs inactivate mammalian ribosomes, although only some RIPs are capable of attacking ribosomes from plants, fungi, protists, and bacteria. But the extreme cytotoxicity of the heterodimeric RIPs, such as ricin, together with highly efficient RIPs activities of the single chain RIPs, have prompted the widely held view that RIPs play a defensive role in plants, protecting them against predators and pathogens. Single chain RIPs including PAP are potent inhibitors of plant viruses, at concentrations as low as 25ng/ml (Irvin, 1975, Kubo *et al.* 1990). It has also been reported that PAP inhibited plant viruses from seven groups (five RNA virus group and two DNA virus groups) when assayed on the leaves of appropriate indicator plants (Chen *et al.* 1991). In that context, Kumon *et al.* (1990) showed that physical association between the virus and the RIP was not required for antiviral activity. In these cases, the pathway proposed for PAP is that when a virus infects a cell, PAP apparently also gains entrance and disrupts cellular protein synthesis, thus killing virus-infected cells and thereby preventing viral replication. (Bonness *et al.*, 1994).

Nevertheless, the mechanism of antiviral action of RIPs described above cannot account for the described inhibitory effects of RIPs on the Human Immuni-deficiency Virus (HIV) gene expression in acutely and chronically infected macrophages and T-

cells. It was shown that the type 1 RIP trichosanthin selectively inhibited both HIV RNA and protein accumulation without affecting the host cell gene expression (McGrath *et al.* 1989).

1.2.6.3. Structure and function of RIPs

It has been suggested that the heterodimeric structure of type 2 RIPs is the result of a fusion between a gene encoding a single-chain RIP (analogous to a type 1 RIPs) and a lectin gene. It is possible that such an event has occurred more than once since the several species in which type 2 RIPs are found are not closely related taxonomically.

Katzin *et al.* (1991) have proposed a putative model for the active site of the ricin A-chain. It contains the residues Tyr80, Tyr123, Glu177, Arg180 and Trp211, which are invariant in all of the N-glycosidase RIPs sequenced to date. In addition to these invariant residues, Asn78, Arg134, Gln173, Glu208 and Asn209 are highly conserved active site residues. Site-directed mutagenesis studies from several laboratories have shown that the substitution of Arg180 and Glu177 for one of several other residues, reduces the ribosome-inactivating capacity of the mutant polypeptides by a factor of $\geq$ 100 (Schlossman *et al.*, 1989; Frankel *et al.*, 1990; Ready *et al.*, 1991). Monzingo *et al.* (1993) have shown that the three dimensional structural alignments of some type 1 and type 2 RIPs are very similar and the organisation of the putative active-site is highly conserved. Their common enzymatic activity suggest basic similarities in the tertiary and the quaternary structure for this class of proteins. Detailed X-ray crystallographic structures for gelonin, mirabilis antiviral protein, ricin and PAP are known. (Montfort *et al.*, 1987; Katzin *et al.*, 1991; Rutember and Robertus, 1991; Miyano *et al.*, 1992; Monzingo *et al.*, 1993; Hosur *et al.*, 1995).

Modelling studies on the X-ray analysis of substrate analogues in the ricin A-chain active site, proposed by Monzingo and Robertus (1992), have suggested that the Tyr80 side chain rotates to a standard orientation on substrate binding. The major differences in protein folding tend to concentrate in the C-terminal region and surface loop structures. The active site shows a highly conserved structure, with the only major difference being in the orientation of the conserved Tyr80. The model shows that the target adenine is presented to the catalytic centre in a 'sandwich' between two

conserved tyrosines. Two mechanisms of acid-catalysed depurination have been proposed. Both suggest nucleophilic attack by a water molecule of an oxycarbonium ion intermediate, with the conserved residues Arg180 and Glu177 being directly involved. A mechanism for catalysis by RIPs, proposed by Ready *et al.* (1991), asserts that Glu177 stabilises an oxycarbonium ion on the ribose attached to the target adenine in the rRNA substrate, and Arg180 is involved in binding to the sugar-phosphate backbone through electrostatic interaction. Hydrolysis of the N-glycosidic bond is envisaged as being facilitated by the partial protonation of the target adenosine (which is in between of two tyrosine residues) through its hydrogen bonding and the positive charge developed on the ribose. **(Figure 2)**

The entry of cytotoxic lectins into cells is based on the fact that cytotoxic lectins bind opportunistically to the surface of target cells by reversible interaction between the B-chain and carbohydrate moieties containing terminal galactose residues occurring on both glycoproteins and glycolipids. Mammalian cells contain an abundance of such binding sites, ensuring a high concentration of bound toxin. A proportion of the surface-bound toxin is internalised by the target cell. It has been shown that ricin enters cells by endocytosis, primarily (Moya *et al.*, 1985) but not exclusively, via clathrin coated pits and vesicles (van Deurs *et al.* 1985). A large proportion of the ricin taken into cells is either recycled back to the cell surface or is delivered into lysosomes where it is presumably degraded. A small proportion of ricin avoids recycling or degradation and it is from this pool that the ricin A-chain crosses an intracellular membrane to reach its ribosomal substrates in the cytosol.

1.2.6.4. Effects of RIPs action on the function of the ribosomes

It is now and generally recognised that rRNA is responsible for the basic biochemistry of protein synthesis, including peptide bond formation, translocation and binding of aminoacyl-tRNA and supernatant factors (Wool *et al.*, 1990). Noller (1991) even suggested that rRNA plays a direct catalytic role, the ribosomal proteins merely facilitating the optimal structure of the rRNA. Moazed *et al.* (1988) provided direct evidence for the involvement of the α-sarcin/ricin loop in protein synthesis, concluding

Figure 2. A schematic illustration of the proposed mechanism
of RTA action (from Mozingo and Robertus, 1992)
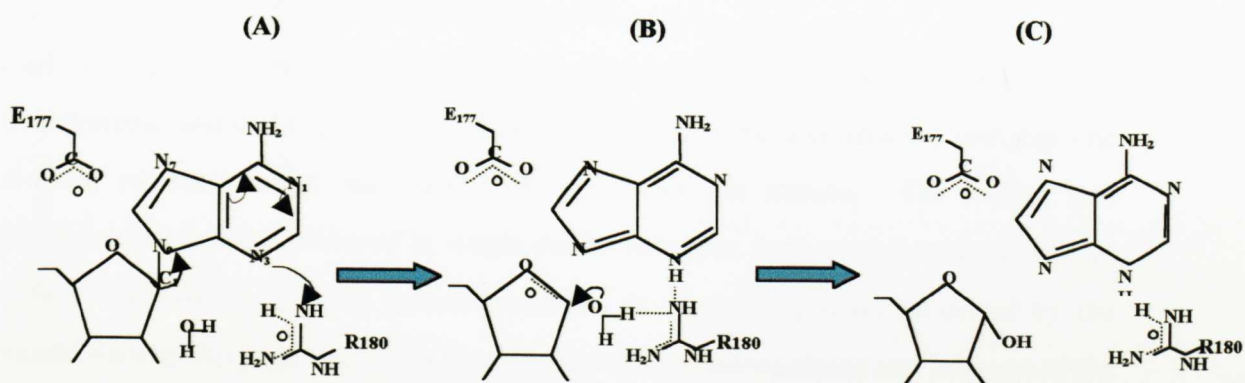
A) Bond breaking between ribose and adenine. Arg180 stabilises the
anion character of the adenine through protonation at N3 (A). Glu177
stabilises the cation character of the ribose (B).

B) Arg180 activates water for its attack on ribose to yield (C) products.

that it was part of the binding site for the elongation factors EF-Tu and EF-G (translocase).

Osborn and Hartley (1990) showed in the reticulocyte lysate cell free system that the N-terminal dipeptide of rabbit β-globin -methionine: valine- was formed on ricin-modified ribosomes and that the subsequent translocation of this dipeptide was blocked, showing that translocation was the step that received most inhibition.

1.2.7. The Action and Specificity of RIPs on Ribosomes

Early studies on the effects of type 2 RIPs on the inhibition of protein synthesis in cell-free systems, showed that the 60S ribosomal subunit alone was affected and that one A-chain molecule could inactivate 1500 ribosomes per minute. The finding that ribosome inactivation occurred in simple buffer solutions suggested that there was no cofactor requirement. Also, because α-sarcin (a cytotoxic protein produced by the mould *Aspergillus giganteus*) acts as a specific rRNA endonuclease and because of the similarities between the partial reactions of protein synthesis inhibited by α-sarcin and ricin as well as related RIPs, Endo *et al.* (1987) investigated the possibility that ricin may also act on rRNA.

It is interesting to mention that one of the methods reported for the assay of the N-glycosidase activities of RIPs on their ribosome substrates, makes use of the fact that the phosphodiester bounds on either side of the depurinated ribose are sensitive to amine-catalysed hydrolysis at acidic pH by a β-elimination reaction (Peattie, 1979). The resulting fragments are then separated on a polyacrylamide or agarose gel. The extent of depurination can then be calculated following densitometric scanning of the ethidium bromide stained gel using 5.8S rRNA as an internal standard (Osborn, 1990).

Furthermore Endo *et al.* (1987) and Endo and Tsuguri (1987) revealed the precise nature of the ricin-catalysed modification in 28S rRNA, where Adenine, at position 4324 (numbered from 5' end of 28S rRNA) had been removed, leaving the sugar-phosphate backbone intact. Thus ricin acts as a highly specific hydrolase, cleaving a single N-glycosidic bond among c.7000 nucleotide residues in rRNA. Endo and co-

47

workers subsequently went on to show that several RIPs act on rat liver ribosomes in an analogous manner to RTA. Stirpe *et al.* (1988) showed that the 28S rRNA of rabbit reticulocyte ribosomes and the 26S rRNA of yeast ribosomes also produced a diagnostic aniline-labile site with RTA and a variety of type 1 RIPs.

It is highly significant that Adenine A_{4324} lies near the centre of a 14 nucleotide sequence that is the most strongly conserved structural feature of the large rRNA from the large ribosomal subunit and which has remained largely unchanged throughout evolution (Raué *et al.*, 1988). **(Figure 3)**

Recently, work from Stirpe's laboratory (Barbieri *et al.*, 1997) has shown that under certain conditions, many RIPs possess a non-specific N-glycosidase activity which hydrolytically removes adenines from a wide variety of substrates in a sequence-independent manner. The authors have termed this the polynucleotide: adenosine glycosidase activity and its substrates include DNA, viral RNA and synthetic poly (A) in addition to rRNA. Although the authors claim that this activity may play a role in both the cytotoxic and antiviral activities of RIPs, they fail to reconcile their findings with the more widely accepted sequence specific action first described by Endo and Tsurugi (1987).

Some RIPs require a cofactor in order to exert their depurination activity. Coleman and Roberts (1981) found that the inhibition of protein synthesis in cell-free systems by tritin (a type 1 RIP) had a marked requirement for ATP. In addition Massiah and Hartley (1995) confirmed this requirement, showing the RNA-glycosidase activity of tritin-S on reticulocyte and yeast ribosomes, was greatly stimulated by ATP.

1.2.7.1. Tritin-S - a type 1 RIP-

Tritin-S, a type 1 RIP is purified from wheat seeds (Massiah and Hartley, 1995). Tritin-S was identified as a basic protein with a Mr of 32kDa. Tritin-S is inactive on ribosomes from wheat germ, wheat seed endosperm and *E. coli*, but active on yeast and rabbit reticulocyte ribosomes. Tritin-S shows a marked requirement for ATP in its action. Its activity has been reported (Massiah and Hartley, 1995) to be stimulated of

Figure 3. α-sarcin/ricin stem-loop. The universally conserved region of his domain.
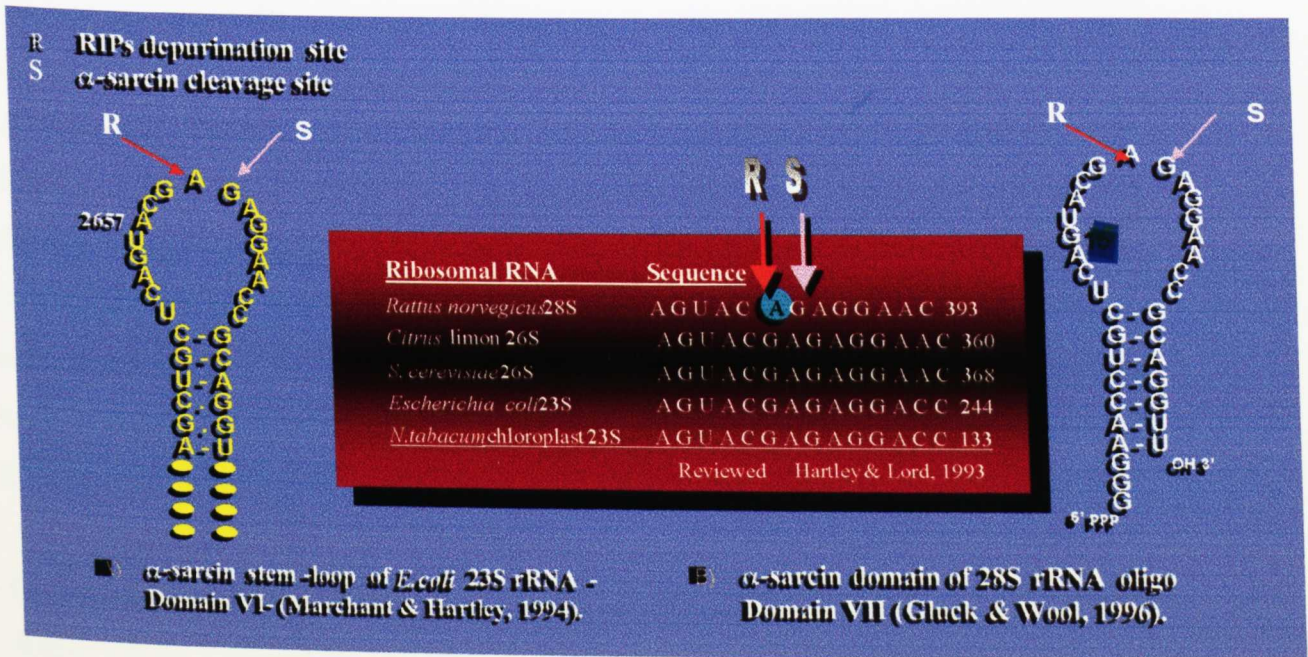
R) RIPs depurination site.

S) α-Sarcin cleavage site.

A) α-Sarcin/ricin stem-loop of *E. coli* 23S rRNA domain VI (Marchant and Hartley, 1994).

B) Oligo mimicking the α-sarcin domain of rat 28S rRNA (Gluck and Wool, 1996).

The numbers at the right of the sequences refer to the distance in nucleotides from the depurination site to the 3'end of the rRNA.

the order of 4-fold on yeast ribosomes and 220-fold on reticulocyte ribosomes when assayed in the presence of ATP.

1.2.7.2. Pokeweed Antiviral Protein (PAP) -a type 1 RIP-

Pokeweed antiviral protein (PAP) is a type 1 ribosome inactivating protein (RIP) from the plant *Phytolacca americana* (pokeweed), that is believed to play a role in the plant's defence as an antiviral agent. It is located in the cell wall and it protects the plant from viral attack by entering the cytoplasm when the plasma membrane is breached by viral infection since inhibition of its own ribosomes would block viral replication (Ready *et al.* 1986). PAP has the additional ability to inactivate prokaryotic ribosomes. It cleaves the bond between A_{2660} and the ribose of the prokaryotic 23S rRNA (Hartley *et al.*, 1991), which is structurally and functionally equivalent to the cleavage position (A_{4324}) of eukaryotic 28S rRNA. Marchant and Hartley (1995) showed that PAP - catalysed depurination is not dependent on the α-sarcin tetraloop structure (section 1.2.5.4.). After working with six mutations within the α-sarcin/ricin loop, it was also found that the base G_{2661} does not appear to be critical for activity, as it is for RTA catalysed depurination.

1.2.7.3. Ricin and ricin toxic A-chain (RTA) -a type 2 RIP-

Ricin: a type 2 Ribosome Inactivating Protein. Ricin from *Ricinus communis* (castor oil bean) is the best-studied example of type 2 RIPs. It is composed of a 32 kDa A-chain linked by a single disulphide bond to a 34 kDa B-chain (Lord *et al.*, 1994). Ricin is synthesised as a precursor form termed preproricin which consists of the A- and B-chains linked by an interchain linker peptide together with an N-terminal signal sequence (Richardson *et al.*, 1989).

Ricin is highly active on mammalian ribosomes and will also depurinate plant ribosomes, including those derived from *Ricinus communis*, though the activity on the latter is approximately 2×10^4-fold lower (Harley and Beevers, 1982). RTA has attracted increasing interest in recent years because of its potential applications in chemotherapy (Thrush *et al.*, 1996).

Ricin A-chain (RTA) was found to bind only to the 60S subunit of rat liver ribosomes, but it has been shown too, that RTA is not able to bind to *E. coli* ribosomes (Hedblom *et al.*, 1976). It was confirmed by Marchant and Hartley (1995) that RTA is not active on *E. coli* ribosomes under near physiological reaction conditions, and so activity can only be determined on 'naked' rRNA. It was found also that RTA catalysed depurination is dependent on the tetraloop structure. After work with six mutations within the α-sarcin/ricin loop, it was also found that the identity of the base G_{2661} is critical for RTA activity.

1.2.8. The Susceptibility of Plant and *E. coli* ribosomes to RIPs

Under the appropriate conditions a given RIP does not present the same N-glycosidase activity on ribosomes from different sources, despite the fact that they show the same conserved RIP target site in their large subunit. Cawley *et al.* (1977) found that wheat germ ribosomes required a 5000-fold higher concentration of ricin A-chain to inhibit their activity than it required for a comparable inhibition of rat liver ribosomes. *E. coli* ribosomes were completely resistant to the toxin. Earlier studies showed that plant cytoplasmic ribosomes are much less sensitive to RIPs in general than are mammalian ribosomes, and that *E. coli* ribosomes, were completely resistant to RIPs in general (Batielli *et al.*, 1984). It was widely accepted view that prokaryotic ribosomes are insensitive to RIPs and for that reason, *E. coli* has been used successfully as a host for the production of the biologically active recombinant ricin A-chain (rRTA) (O'Hare *et al.*, 1987, Piatak *et al.*, 1988). However, attempts to express some RIPs like with MAP (Mirabilis Antiviral Protein) or PAP (Pokeweed Antiviral Protein), both type 1 RIPs were unsuccessful. Their expression resulted in a severe inhibition of growth of *E. coli*, when an attempt to obtain the recombinant protein was made (Habuka *et al.*, 1989). The reason for their inhibition became apparent when it was discovered that *E. coli* ribosomes were sensitive to several type 1 RIPs (Hartley *et al.*, 1991).

In summary, ribosomes from mammals and *Saccharomyces cerevisiae* are highly sensitive to most RIPs. Higher plant ribosomes are moderately resistant to the A-chains of the toxic lectins, for example ricin and abrin A-chains, and cereal seed ribosomes are resistant to their homologous RIPs. Finally *E. coli* ribosomes, so far,

present complete resistance to the A-chains of ricin and abrin, but are moderately sensitive to several type 1 RIPs.

1.2.8.1. Comparison between PAP and RTA

PAP and Ricin are two members of a family of RIPs that are characterised by their ability to catalytically depurinate eukaryotic ribosomes. In contrast to RTA (the Ricin toxic A-chain), PAP inactivates prokaryotic ribosomes. PAP and RTA have different RNA recognition elements as has been shown by Marchant and Hartley (1995) (tetraloop structure is required for the action of RTA, but not of PAP, and unlike RTA, PAP does not require G at position 2661), and this may account, at least in part, for the fact that PAP but not RTA catalyses the depurination of *E. coli* ribosomes.

Despite the fact that the primary structure conservation among the RIPs is highly variable (17-80%), their tertiary structures are well conserved. Their 3D structure is extremely similar as reported by Monzingo and Robertus (1992) and Monzingo *et al.* (1993) showed that the α-carbon traces for tertiary structures of RTA and PAP are virtually superimposable. Chaddock *et al.* (1996) used the information from the X-ray structures of RTA and PAP in order to design gross polypeptide switches and specific peptide insertions. Their work suggested that the carboxy-terminus of the RIPs (PAP 219-262) did not contribute to ribosome recognition. Polypeptide swaps in the amino-terminal half of the proteins affected ribosome inactivation.

Chaddock *et al.* (1996) also showed that directed substitution of RTA sequences into PAP, at those three loop regions that were different in both structure and composition, had little effect on the ribosome inactivation characteristics of the mutant PAP, suggesting that the loops were not crucial for prokaryotic ribosome recognition. Since the prokaryotic rRNA can serve as a substrate for RTA-dependent N-glycosidase activity when stripped of ribosomal proteins, and the rRNA target sequence is conserved, the molecular basis of this difference in RIPs specificity was considered as a complex phenomenon. Monzingo *et al.* (1993) suggested that a small number of polypeptide regions, which were identified as having sufficiently different tertiary structures, warranted research as possible ribosome-specificity determinants. It might mean that regions of RIPs protein structure, possibly quite distinct from the active site

determine ribosome specificity. Nevertheless, Chaddock *et al.* (1996) created RTA/PAP hybrid proteins in order to examine their ability to inactivate ribosomes, through specific peptide swaps and gross polypeptide swaps. These experiments were validated, once x-ray structure analysis of PAP and RTA showed the highly conserved tertiary structure. So far, no conclusion has been reached and experiments are continuing.

1.2.9. RNA Identity Elements required for recognition and catalysis by RIPs

Endo *et al.* (1987) and Endo and Tsurugi (1988) found that the RTA could depurinate deproteinised 28S rRNA with an identical specificity to that of 28S rRNA in native ribosomes. This demonstrated that ribosomal proteins are not required for the sequence specificity of the modification site. They show that intact 28S rRNA is not required for activity, an evidence by finding that the 553-nucleotide fragment generated from the 3' end on 28S rRNA by endogenous RNase could serve as a substrate following its deproteinisation.

It was suggested that RTA has a similar affinity for both ribosomes and rRNA, and that the native conformation of rRNA in the ribosomes, which is probably dependent on ribosomal proteins, is required for efficient catalysis. The only additional requirement for these substrates is that they retain their secondary structure. Endo and Tsurugi (1987) also showed that deproteinised *E. coli* rRNA served as a substrate for RTA modification, but it was demonstrated that the depurination occurred at two sites, A_{2660} in 23S rRNA (corresponding to A_{4324} in rat 28S rRNA) and A_{1014} in 16S rRNA. Analysing the structures around these depurination sites, it was revealed that they all contain the sequence 'GAGA', which could in theory exist in a tetraloop.

However the same structural motif occurs at a further four sites in both *E. coli* ribosomes and rat rRNAs which are not modified by RTA in either ribosomes or deproteinised rRNA as reported by Endo and Tsurugi (1988). After further work, Endo *et al.* (1991) showed the requirements for recognition and catalysis by using a synthetic oligoribonucleotide of 35 nucleotides (35-mers) that mimics the primary and secondary structure of the rat 28S rRNA target site. It was found that there was an absolute requirement for an adenine (A*) in the sequence GA*GA, and that the helical

stem is present. Although the length of the stem could be reduced from seven to a minimum of three base pairs there is an important role to the existence of a stem to tether the tetraloop structure.

The activity of RTA was eliminated by altering the nucleotides in the 'universal' sequence surrounding the adenine, and by changing the position in the loop of GAGA, where the minimum substrate is GAGA tetraloop shut off by Watson-Crick base pairs **(Figure 4)**. It is important to underline that only those ribosomes engaged in protein biosynthesis can serve as substrates for α-sarcin cleavage. Wool *et al.* (1990) used antibiotic inhibitors of protein biosynthesis in order to show that reticulocyte ribosomes were sensitive to α-sarcin only when peptidyl tRNA is in the ribosomal A site prior to translocation, suggesting that the α-sarcin site alternate between open and closed states during translation.

1.2.9.1. Structural and sequence requirements of the α-sarcin/ricin loop for RIPs
        action

RIPs have also been reported to be active on DNA, but there is a discrepancy between the results presented. In an early report, Endo *et al.* (1991) showed that a stem loop DNA 32-mer which contained the α-sarcin/ricin loop was not a substrate for RTA, but Chen *et al.* (1998) showed that a stem loop DNA 10-mer was a substrate for RTA catalysed hydrolysis, with a K_m (which is related to the affinity of the enzyme for its substrate) of 2.6 μM (similar to the K_m shown by RTA on the 10 base synthetic oligoribonucleotide) and a K_{cat} (which is related to the breakdown for the enzyme: substrate complex to product) of 0.38 min^{-1}. The above results suggested that the active site of RTA might accommodate structural differences between RNA and DNA, by reorganising the nucleotide loop conformation that is required for catalysis. On the other hand, the equivalent K_m values for the action of RTA on the stem loop RNA A-10 and DNA *A-10 indicates the negligible influence on substrate binding of the 2' hydroxyl groups (Chen *et al.*, 1998). Orita *et al.* (1996) showed that the oligonucleotide with stem-GAGA-stem, and stem-G*AGA-stem, (* refers to deoxynucleotide) both showed similar sensitivity to depurination by RTA.

Figure 4. RNA identity elements required for recognition and catalysis by ricin
A-chain

(A)
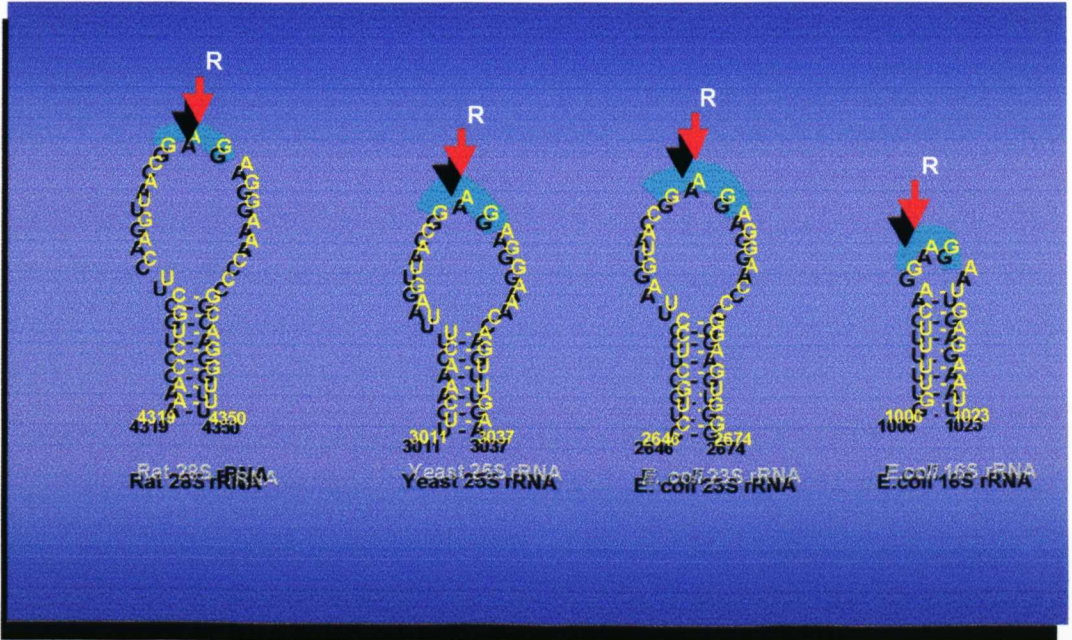
(B)
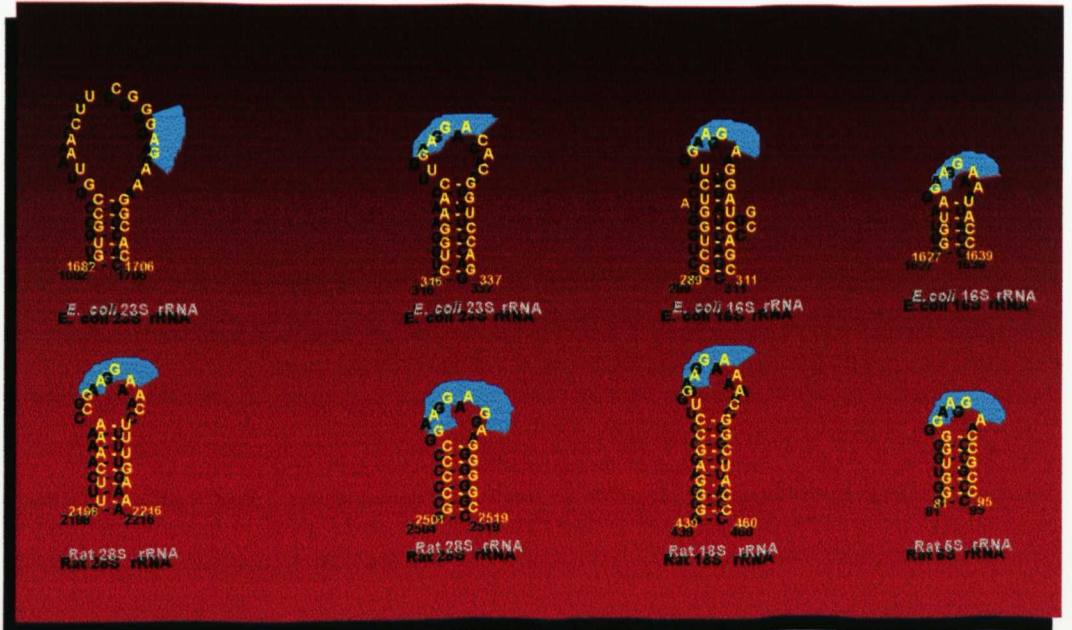
(A) Represents the ricin A-chain sensitive structures in rat, yeast and *E. coli* rRNAs

(B) Ricin A-chain insensitive structures in *E. coli* and rat rRNAs.

(R) RIPs depuration site

Chen *et al.* (1998) showed the substrate specificity by performing mutations on the structural components. They found that adenosine, AMP, dinucleotide AG, and tetranucleotide GAGA were not hydrolysed by RTA even in the presence of a stoichiometric excess of RTA, relative to the substrates

So far, RTA is catalytically active only on RNA structures with the stem loop structural motif, and assays suggest that the energy of activation for depurination by RTA is therefore obtained from the combined interactions between the enzyme and the substrate adenine as well as the adjacent GAGA tetraloop stem structure. (Chen *et al.*, 1998)

1.2.10. RNA Native Structure and rRNA Protein Interactions in Ribosomes

Chaddock *et al.* (1996), have identified regions of the RIP primary sequence that may be important in ribosome recognition and Munishkin and Wool (1995) have identified a ribo-nucleo-protein-like (RNP-like) (a highly conserved sequence protein) structural motif in the ricin A-chain that may mediate binding to ribosomal RNA.

Chen *et al.* (1998) worked on the mechanism and specificity for RTA, using the RNA stem loop structures of 10-18 nucleotides which contained a GAGA tetraloop, the required substrate motif. They found that the kinetic parameters K_m, K_{cat} and K_{cat}/K_m were found to be pH-dependent, and that the optimal pH is near 4.0. It was suggested that these results could be an effect of the protonation of ionizable groups in the RTA or in the rRNA substrate with pKa values near 4.5. The protonation of two adenines in the stem-loop structure could assist binding to RTA because the N1 of adenine has a pKa near 4 (Legault and Pardi, 1997). Also, it was found that the preferred substrate was a 14-base stem loop RNA, showing that smaller or larger oligoribonucleotides have lower K_{cat}, but all have the same K_m values of approx. 5µM (Chen *et al.*, 1998).

The influence of pH was apparently found to place the stem loop RNA or RTA in a conformation that enhances catalysis. The catalytic competence of the RTA-ribosome complex at neutral pH suggested that the structural components of the intact ribosomes are necessary for efficient catalysis at the physiological pH. It also

suggested the possibility that the interaction within the GAGA-containing tetraloop recognised by RIPs, adopts an alternative conformation as a function of pH (Chen *et al.*, 1998).

1.2.10.1. The effect of the action of divalent cations on rRNA structure and RIP activity

Divalent metal ions can interact electrostatically with the sugar phosphate backbone of rRNA. The binding of divalent metal ions (or divalent cations in this case) to single-stranded RNA homopolymers reaches saturation close to one metal ion per two phosphate ions, and in the absence of other cations their dissociation constants are in the neighbourhood of 0.1 to 10mM. Divalent metal ions might bridge the two phosphates, requiring a constrained phosphodiester backbone with an accompanying reduction in entropy and cost in energy. Thus, divalent cations bind more tightly to homopolymer helices where the phosphates are structurally constrained and two phosphates on opposite strands are sufficiently close in the rRNA to bind single metal ions (reviewed by Pan *et al.*, 1993).

In the review made by Pan *et al.* (1993), the cations were considered as basic elements for reducing the electrostatic repulsion between the negatively charged phosphates of rRNA backbone (which means that divalent cations are extremely effective in stabilising the rRNA double helix). Mg^{2+}, Ca^{2+} and Mn^{2+}, through electrostatic interactions, apply within the context of binding with those phosphates of the rRNA backbone. In this way, the positive charge on the divalent metal ion can stabilise the transition state by binding to negatively charged nonbridging oxygens.

In the majority of the studies of RIP action on ribosomes *in vitro* the reactions were performed in a simple Tris/Mg^{2+}/ KCl buffer (a near physiological buffer), or in buffers containing little free Mg^{2+}. Moreover, the activity of RTA with oligoribonucleotides has routinely been assessed in a buffer containing 3 mM $MgCl_2$ and 2.5 mM EDTA

(Endo *et al.*, 1991; Gluck *et al.*, 1992). EDTA is added to reduce the concentration of magnesium to 0.5mM that was thought to be optimal for RTA activity (Endo, unpublished data).

It has been found that high concentrations of Mg^{2+} can partially overcome the inhibition of protein synthesis in both α-sarcin and ricin-modified ribosomes (Cawley *et al.*, 1979; Terao *et al.*, 1988). This could mean that the alterations in conformation could be partially reversed by this ion, presumably through the formation of salt bridges between neighbouring phosphate groups in the rRNA backbone. Other research work has suggested that the α-sarcin/ricin stem loop may adopt different conformations in the presence and absence of Mg^{2+}, an effect that has important implications for the changing activity of RIPs on their substrates. Further work done on the activity of RTA and α-sarcin on synthetic oligoribonucleotides mimicking the α-sarcin/ricin stem loop has confirmed this (Leffers *et al.*, 1988; Endo *et al.*, 1991; Gluck *et al.*, 1992; Gluck *et al.*, 1994).

Gluck and Wool (1996) reported that RTA had no enzymatic activity unless a divalent cation and a chelating agent capable of forming a complex with the cation were present in the reaction mixture. They experimented on a series of solutions of $MgCl_2$/EDTA of different concentrations, as well as with $CaCl_2$/EDTA, $MgCl_2$/EGTA and $CaCl_2$/EGTA. The results showed that although a Mg^{2+} concentration of 0.5 mM was thought to be optimal for RTA activity, the enzymatic activity was not observed in Mg^{2+} containing solutions in the absence of EDTA, on the 35mer oligonucleotide prepared to mimic the structure at the site of action in 28S rRNA. Catalysis by RTA in the presence of EDTA was observed to be significantly more efficient with calcium than with magnesium.

The buffer conditions could be thought to affect either the structure of the rRNA substrate, or the structure of RTA, or to remove or inactivate an inhibitory contaminant in the toxin preparation, or all of these (Gluck and Wool, 1996). However, no requirement has been reported for cofactors for RTA activity (Massiah and Hartley, 1995) when native eukaryotic ribosomes are the substrate rather than

synthetic oligoribonucleotides. This suggests also that the complex with divalent cations and chelating agents affects the structure of the synthetic oligoribonucleotide used in the *in vitro* assay (Gluck and Wool, 1996).

1.2.10.2. Ribosomal proteins influence on RIPs activity

More than a dozen ribosomal proteins bind directly and independently to rRNA in *E. coli* ribosomes and homologues of most of these are found in archaebacteria and eukaryotes as well. They vary greatly in the size and in the complexity of the rRNA-binding site that is recognised. Ribosomal proteins are an important part of the ribosome structure, and they participate in the self assembly processes of ribosomal subunits, helping to obtain the final conformation as it has been reviewed through the present work. (Leffers *et al.*, 1988; Draper, 1994).

While the preferred substrate for RTA is 26/28S rRNA in a native 60S ribosomal subunit, 'naked' 26/28S rRNA can also act as a substrate but the K_{cat} for the latter reaction is approximately 10^5-fold lower than the former (Endo *et al.*, 1990). This suggests that the native secondary structure of ribosome associated 26/28S rRNA is important for the action of RIPs and that ribosomal proteins may play an important role in maintaining this rRNA conformation, and/or in providing a high affinity binding site for the toxin (Gluck and Wool, 1996; Vater *et al.*, 1995).

Since prokaryotic rRNA can serve as a substrate for RTA activity when stripped of ribosomal proteins, the well conserved α-sarcin loop structure of the rRNA and the similarity between the RIPs' structures (Chaddock *et al.*, 1995), suggest that the presence of ribosomal proteins either allow (in the case of PAP) or prevent (in the case of RTA) depurination activity.

Hedblom *et al.* (1976) described studies on the binding characteristics of ricin and its subunits to eukaryotic ribosome components. They obtained a value of 0.87 for the number of ricin molecules bound per ribosome, indicating that there was only one ricin binding site per ribosome and suggesting an enzyme-substrate-like complex between them, with a stable interaction between rat liver ribosomes and RTA. However, this

report is at variace with the kinetic parameters for the action of RTA on ribosomes, and other methods, for example gel retardation, have failed to detect a stable association (I. Wool, personal communication).

Ippoliti *et al.* (1992), have identified a covalent complex between saporin (the RIP extracted from *Saponaria officinalis*) and ribosomal proteins from yeast (*Saccharomyces cereviseae*), by means of chemical crosslinking and immunological or avidin-biotin detection. They found a main complex (mol. wt. approx. 60 kDa) formed only with a protein from a 60S subunit of yeast ribosomes, and not detected with ribosomes from *E. coli*, a resistant species. This observation supports the hypothesis of a molecular recognition mechanism involving one or more ribosomal proteins, which could provide a 'receptor' site for the toxin and favour optimal binding of the target adenine A_{4324} to the active site or the RIP. In this study Ippoliti *et al.* (1992) suggested that the molecular mechanism by which the toxin recognises its target is mediated by protein-protein as well as protein-RNA interactions. The enzyme: substrate-like complex is probably stabilised by molecular contacts over and above the binding of rRNA/A_{4324} to the active site of the RIP, and they showed that at least one ribosomal protein (mol. wt. 30 kDa) from the 60S subunit comes into contact with saporin and is crosslinked. This was fully consistent with the observation that RIPs are more active on the whole ribosome than on isolated rRNA.

Many workers have described the specificity of RIPs in relation to their ability to inactivate self and non-self ribosomes, and have attempted to explain why RIPs have evolved specificity for ribosomes. However, little work has been described where the features necessary for ribosome recognition and interaction have been investigated. Rather, most mutagenesis experiments have concentrated on the determination of the catalytic mechanism. It was recently suggested that the electrostatic potential of the residues surrounding the active site was important in determining ribosome specificity (Chaddock *et al.*, 1996).

1.3. Aims of the Project

1.3.1. General:

To study the influence of ribosomal proteins on the action of Ribosome-Inactivating Proteins

1.3.2. Particular aims:

- To study the binding characteristics of RIPs with different ribosomes and 'naked' (deproteinised) ribosomal RNA.
- To evaluate the role of ribosomal proteins in sensitising the *E. coli* ribosomes to RIPs' action.
- To differentiate between the binding phenomenon and the RIPs' activity with ribosomes.

2. CHAPTER II:

MATERIALS AND METHODS

Materials:

PAP (Pokeweed antiviral protein from the leaves of *Phytolacca americana* a kind gift from Dr. Marchant), tritin-S (RIPs from *Triticum aestivum* seeds), and RTA (recombinant Ricin A chain **rRTA**, RIPs from *Ricinus communis*, a kind gift from Dr. Chaddock). Note recombinant Ricin A chain **rRTA** would be named as RTA.

Suppliers of Reagents and Chemicals: All reagents used were of analytical grade if available and were obtained from the following sources, unless indicated otherwise in the text:

⇒ **Aldrich Chemical Co. Ltd**., Poole, Dorset: ammonium persulphate, Tween-20.

⇒ **Amersham International Plc**., Aylesbury, Buckinghamshire: Hybond-C nitrocellulose membrane, Hybond-N nylon membrane, [^{35}S]-dATP (>1000Ci/mmol), γ–^{32}P-ATP (7000Ci/ mmol), ([^{14}C]- formaldehyde, 30-50 mCi/ mmol).

⇒ **BDH (Merck Ltd)**, Poole, Dorset: Acetic acid, acrylamide, ammonium sulphate, aniline, boric acid, bromophenol blue, calcium chloride, citric acid, di-sodium hydrogen orthophosphate, Duolite MB6113 mixed resin, ethanol, ethylenediamine-tetraacetic acid (EDTA), ethylenedioxydiethylenedinitriolotetra-acetic acid (EGTA), formamide, glycerol, N-2 hydroxyethylpiperazine-N-2 ethane sulphonic acid (HEPES), isopropanol, liquid paraffin colourless, lithium chloride, magnesium chloride, magnesium sulphate, 2-mercaptoehtanol, 2[N-morpholino] ethanosulfonic acid (MES), methanol, Nonided P40, orthoboric acid, potassium acetate, potassium hydroxide, 'Repelcote^{TM}', sodium acetate, sucrose, trichloroacetic acid (TCA), Triton X-100, Tris-(hydroxymethyl)-aminomethane (Tris), urea, zinc chloride.

⇒ **Becton Dickinson and Co.**, Oxnard, California, USA: Falcon Microtest III 96-well microtitre plates, 50ml conical Falcon tubes.

⇒ **Boehringer Mannheim UK Ltd.**, Lewes, East Sussex: ATP, calf liver tRNA, DNase I, RNase-free, DTT, 2[N-morpholino] ethanosulfonic acid (MES).

⇒ **Bio-Rad Laboratories Ltd.,** Hemes Hempstead, Hertfordshire: Biogel P6, pre-stained molecular mass markers.

⇒ **Difco Laboratories Ltd.,** Detroit, Michigan, USA: Bacto-tryptone, Bacto-agar.

⇒ **Eastman Kodak Co.,** Rochester, New York, USA: LX-24 developer, FX-40 fixer, Unifix.

⇒ **Fisons Ltd.,** Loughborough, Leicestershire: Ammonia solution, ammonium chloride, ammonium sulphate, formaldehyde, N, N'-methylene bisacrylamide, caesium chloride, calcium chloride, magnesium chloride, β-mercaptoethanol, polyethylene glycol PEG-6000, phenol, potassium dihydrogen orthophosphate, potassium chloride, sodium acetate, sodium chloride, sodium dodecylsulphate (SDS), trichloroacetic acid (TCA), Tris- (hydroxymethyl)-aminoethane (Tris).

⇒ **Fuji Photo Film (UK) Ltd.,** London: x-ray Films (RX).

⇒ **Gibco-BRL, Life technologies Plc.,** Uxbridge, Middlesex: Agarose, various modification and restriction enzymes: *Eco*RI, *Bam*HI, 10mM NTP Mix (ATP, CTP, GTP, UTP) SuperScript™ II RNase H⁻ reverse transcriptase, T4 DNA ligase, T4 DNA polymerase, T4 polynucleotide kinase, SP6 RNA Polymerase, Taq DNA Polymerase; sucrose (Ultrapure grade), 1Kb DNA ladder.

⇒ **Johnson Matthey Plc.,** Royston, Hertfordshire: silver nitrate.

⇒ **Melford Laboratories Ltd.,** Biochemical & Chemical Manufacturing., Ipswich, Suffolk: 5-Bromo-4-chloro-3-indolyl, β-D-galactoside (X-GAL)

⇒ **Oxoid (Unipath Ltd.),** Bsingstoke, Hampshire: yeast extract.

⇒ **Pierce Europe BV,** Holland: Disposable polystyrene columns (2ml), Pd-10 (Sephadex G25) columns, Slide-A-lyzer 10,000 MW Cassette.

⇒ **Pharmacia LKB Biotechnology AB,** Uppsala, Sweden: CM-Sepharose Fast Flow, Sephadex G-25.

⇒ **Polaroid Corporation,** Cambridge, UK: 665 / 667 photographic Film.

⇒ **Premier Brands UK Ltd.,** Stafford: dried skimmed mild ('Marvel').

⇒ **Promega Ltd.,** Madison, Wisconsin, USA: Untreated rabbit reticulocyte lysate, nitroblue tetrazolium (NBT), 5-bromo-4-chloro-3-indolyl phosphate (BCIP), RNasin[R] Ribonuclease Inhibitor.

⇒ **QIAGEN Ltd.,** Crawley, West Sussex, UK: QIAprep spin plasmid kit, QIAGEN mini-, midi-, and maxi- preps.

⇒ **Rhone-Poulenc Ltd.,** Manchester: polyethylene glycol 6000.

⇒ **Sigma Chemical Co. Ltd.,** Poole, Dorset: Adenine, agarose RNase-free, ampicillin, 8-anilino-1-naphthalene sulphonic acid (ANS), chloramphenicol, donkey anti-sheep IgG alkaline phosphatase conjugate, bovine serum albumin (BSA), diethylpyrocarbonate (DEPC), dithiothreitol, ethidium bromide, Ficoll type 400, guanidine hydrochloride, imidazole, inorganic pyrophosphatase, isopropyl β-D-thiogalactopyranoside (IPTG), lysozyme, magnesium chloride, molecular mass markers, 2[N-morpholino] ethane sulphonic acid (MOPS), propanol, spermidine, spermine, sodium borate, ribonuclease A, rubidium chloride, Sephadex G-50-40, trichloroacetic acid (TCA), N,N,N',N' tetramethyl-ethylenediamine (TEMED), thiamine, Triton X-100, trypsin, uracil, xylene cyanol FF.

⇒ **Ultra Violet Products (UVP) Inc.,** Upland, CA, USA: Grab-IT Image, Annotating Grabber 2.04.5, Synoptics Ltd.

⇒ **United States Biochemical (USB) Corporation,** Cleveland, Ohio, USA: Sequenase Version 2.0, DNA Sequencing Kit (containing Labelling nucleotide mix, Termination mixes, and Sequenase)

⇒ **Whatman LabSales Ltd.,** Maidstone, Kent: filter papers.

⇒ **Purified recombinant ricin A-chain** was a gift from Zeneca Pharmaceuticals, Alderley Park, Cheshire. (RTA).

$\Rightarrow$ All other chemicals were obtained from **BDH, Fisons, Rhone-Poulenc, Fluka Chemicals, Gillingham, Dorset,** and **May and Baker Ltd.,** Dagenham, Essex, and were of analytical grade.

Methods:

2.1. Purification of Tritin-S from Wheat Seeds

All procedures were carried out at 4°C unless otherwise specified. Tritin-S-containing fractions were detected by assaying each fraction for immunoblotting, SDS-PAGE Coomassie® Blue and Silver staining, and for N-glycosidase activity on rabbit reticulocyte ribosomes. 200 g of Wheat seeds (*Triticum aestivum* L., var. Hunter) were ground in a coffee grinder and were homogenised in 600 ml of 100mM Tris/Cl pH 8.5, 100 mM KCl, 4mM $MgCl_2$, and 5 mM DTT, by ten 20 secs. bursts at full power using a polytron homogeniser (Kinematica, Lucerne, Switzerland). The homogenate was filtered through Miracloth (Calbiochem, La Joya, CA, USA) and the filtrate centrifuged at 10,000 rpm, 4°C for 20min in a GSA rotor (Sorvall, Stevenage, Herts, UK). The resulting supernatant liquid was centrifuged at 50,000 rpm and 4°C for 3 h in a 60 Ti rotor (Beckman, High combe, Bucks, UK) (Massiah and Hartley, 1995). Supernatant proteins were precipitated by the addition of ammonium sulphate to 55% saturation and the precipitate, which had formed, was removed by centrifugation and additional solid $(NH_4)_2SO_4$ was added until 85% saturation was achieved.

The precipitate that formed contained the inhibitor, and it was dissolved in the smallest possible volume (20 ml) of 5mM sodium phosphate buffer, pH 7.0 (Roberts and Stewart, 1979; Barbieri *et al.* 1987).

2.1.1. Sephadex G 50-40 Chromatography

A crude protein extract was prepared from 200g wheat seeds and a 55-85% (w/v) ammonium sulphate cut made in accordance with Massiah and Hartley (1995) procedure. Aliquots were taken from both the crude extract and from ammonium sulphate cut and analysed by PAGE (section 2.2.). The Sephadex G 50-40 column was used to further purify tritin-S (MW 32 kDa, reported by Roberts and Steward (1979),

Hartley and Lord (1993) and Massiah and Hartley (1995)). The protein solution was applied to a Sephadex G 50-40 coarse column (2.6 x 35-cm) previously equilibrated with 5mM sodium phosphate buffer, pH 7.0 at 4°C. The column was eluted with the same buffer at a rate of 2 litres/hour. The solution of eluted proteins obtained from Sephadex G 50-40 was loaded onto a CM-Sepharose FF column (section 2.1.2.).

2.1.2. CM-Sepharose Fast Flow Chromatography

The protein-containing front peak from Sephadex G 50-40 (Sigma, Chem. Co., St Lois MO. USA) was collected and then applied to a CM-Sepharose Fast Flow column (30cm x 5 cm) equilibrated 5mM sodium phosphate buffer, pH 7.0 (Massiah and Hartley, 1995). In order to remove the unbound proteins, the column was extensively washed with the same buffer solution until the A_{280} value of the eluted pregradient fraction, had been reduced to approximately 0.01. The elution of the bound proteins was carried out by the application of 1 litre of a linear gradient from 0 to 500 mM NaCl in the same buffer at a flow rate of 120 ml/h (Barbieri *et al.* 1987). The proteins in each fraction were monitored by the measurement of the Absorbance at 280nm, which was plotted against each fraction to obtain a protein elution profile. As it has been reported (Massiah and Hartley, 1995), tritin-S was eluted at NaCl concentration of 100-200mM. Aliquots were taken from the fractions and were analysed by SDS-PAGE (section 2.2.).

2.1.3. SP-Sepharose Fast Flow Chromatography

A second step in cation exchange was necessary in an attempt to further purify tritin-S, therefore SP FF was chosen. The protein fractions containing tritin-S from CM-Sepharose FF (section 2.1.2.) were pooled and applied to a SP-Sepharose column. Like the CM-Sepharose Fast Flow column, the SP-Sepharose column was equilibrated with 5mM Na phosphate, pH 7.0. The unbound proteins were removed by washing the column with column buffer and the elution of the bound proteins was carried out by the application of 1 litre of linear gradient of 0-0.5M NaCl in the same buffer, at 4°C, overnight at a flow rate of 60ml/h.

The protein fractions containing tritin-S were collected, stored at -20°C and concentrated by ultrafiltration using a centricon concentrator.

2.2. SDS-Polyacrylamide Gel Electrophoresis (SDS-PAGE)

Protein separation was carried out using 15% - mini acrylamide gels, as described in standard published protocols (Laemmli, 1970). Protein samples were dissolved in an equal volume of 1x concentration of the sample buffer (1.25 ml 0.5M Tris/Cl pH 6.8, 0.2g SDS, 2 ml glycerol, 0.5 ml β-mercaptoethanol, 10 mg bromophenol blue, 6.25 ml water). Prior to loading, each sample was boiled for 5 minutes to ensure denaturation. Once the protein samples were loaded, the proteins were electrophoresed at 25-30 mA towards the positive electrode for 3-3.5 h. The tank buffer consists of 25mM Tris base, 250mM glycine pH 8.6, and 0.1% (w/v) SDS.

2.2.1. Silver Staining of SDS-Polyacrylamide Gels

Following electrophoresis, the gels were soaked in 50% (v/v) methanol to remove glycine. The methanol solution was changed three times, after 4 hours, after 8 hours and after 12 hours. The methanol was poured off and the gel washed briefly in deionised water. The staining solution used was 0.8g silver nitrate plus 4 ml distilled water, added drop wise with stirring to 21 ml 0.36% (w/v) fresh NaOH plus 1.4 ml ammonia solution and finally 75 ml distilled water was added and mixed. This was prepared immediately prior to use, poured onto the gel, and shaken on a rotary shaker for 20 minutes to ensure that all the gel was exposed to the stain. The gel was then washed four times with deionised water (SDW) for periods of 5 minutes each, on a rotary shaker. The water was replaced with developing solution (500 ml distilled water plus 2.5% (w/v) citric acid and 0.3 ml formaldehyde solution -to 38%-) and shaken continuously until silver stain bands appeared. The gel was subsequently washed in deionised water and colour development stopped by the addition of 45% methanol/10% acetic acid. The gel was left in the stop solution for 15 minutes prior to drying in an Easy Breeze gel dryer or Bio-Rad gel dryer.

2.2.2. Non-denaturing Polyacrylamide Gel Electrophoresis

The separation of RNP complexes was carried out using 12%, 29:1 acrylamide/bisacrylamide - non-denaturing acrylamide gels as described in standard published protocols (Sambrook *et al.*, 1991; Batey and Williamson, 1996; Serganov *et al.*, 1996). After titration, dissociation, and competition experiments (sections 2.17, 2.18. and 2.19.), 2µl of type III loading buffer (30% glycerol, 0.25% bromophenol blue, 0.25% xylene cyanol), were added to the samples. The RNA-protein complex samples were immediately loaded onto the non-denaturing gel in 0.5x TBE buffer. Gels (15.5 cm wide, 12cm long, and 0.05 cm thick) were pre-run for one hour at 20mA at 4°C. Samples volumes of 10µl were loaded onto the gel and electrophoresed for 1.45-4 hours depending on the RNA sample. The gel was dried on a Bio-Rad gel dryer, placed into a Harmer cassette, and put down to X-ray film.

2.2.3. 2D-Polyacrylamide Gel Electrophoresis

Ribosomal proteins were separated by two-dimensional polyacrylamide gel electrophoresis in a system in which the first dimension was an acrylamide gel containing urea, whereas the second dimension contained urea but no SDS (Geyl *et al.*, 1981). Geyl *et al.*, (1981) protocol consists in a 1st dimension rod gel, containing 6M urea, 4% acrylamide, pH 5.0, and the 2nd dimension slab gel consisting of 6.2M urea, 18.6% acrylamide, pH 4.6.

2.2.3.1. First dimension gel

4% (w/v) acrylamide-6M urea first dimension gels were cast in gel tubes (150 x 3mm-inside diameter) to a height of 100mm allowing 1 hour for polymerisation. Gels were set up in a tank containing a cathode solution (10x consists of 1.8M potassium acetate and 4.9% (v/v) acetic acid glacial, pH 5.0) in the lower reservoir and an anode solution (10x consists of 200mM Tris, 4.5% (v/v) acetic acid glacial, pH 4.0) in the upper reservoir. The ribosomal proteins samples (1-2mg/ml) are dissolved in sample loading buffer (consisting of 6M urea, 0.1M DTT, 10% (v/v) upper electrode buffer: (v/v), and basic fuchsin (0.5mg/ml) (mixture of several dyes containing rosaniline as the main component)). The gels were placed in the electrophoresis chamber, filled up both buffer reservoirs with electrode buffer. The bubbles were eliminated and the samples

were applied at the top of gels. The gels were electrophoresed at 4°C, first 30min at 1 mA per gel and then increasing the current to 4 mA per gel during 7 hours or until the tracking dye reached the bottom).

2.2.3.2. Electrophoresis in the second dimension

The 2nd dimension slab gel consisted of 6.2M urea, 18.6% acrylamide, final pH 4.6, 0.5M KOH and 5.4% (v/v) acetic acid. Immediately the first dimension gel was placed on the top of each groove. A small spatula was inserted into the groove and run it along underneath the first dimension gel back and forth to eliminate air bubbles and to minimise any local heterogeneity of gel concentration which may have been introduced with the first dimension gel. The gels were placed into the electrophoresis tank containing the buffer reservoir (10x consists of 1.8M glycine, 1.5% (v/v) acetic acid (glacial)). Gels were electrophoresed at 70V, during 18 hours at 4°C. Gels were immersed in stain solution (45% (v/v) methanol, 10% (v/v) glacial acetic acid, 0.25% (w/v) Coomassie Brilliant blue R250) for 1 hour and then destained in 40% (v/v) ethanol, 10% (v/v) acetic acid, with three changes, until the background was acceptable.

2.3. Western Blotting of SDS-Polyacrylamide Gels

Western blotting was carried out essentially by the method of Sambrook *et al.* (1991). TBS based buffers and block solutions required for the blot were prepared as follows: 1 litre of TBS (10 mM Tris/Cl pH 8.0, 150 mM NaCl) was prepared and 200 ml aliquoted to a separate bottle. To the remaining 800 ml TBS, 1.2 ml Tween was added, stirred and aliquots of 1 x 200 ml and 1 x 400 ml of the TBS-T (10mM Tris/Cl pH 8.0, 150mM NaCl, 1% (v/v) Tween 20) were transferred to separate bottles. To the remaining 200 ml TBS-T, dried milk (Marvel) was added (5%). Then 2 x 20ml aliquots of TBS-T-Marvel were removed to separate universal flasks and stored at 4°C.

After SDS-PAGE, the gel was removed and assembled in the blotting apparatus ensuring that the nitro-cellulose (Hybond-C) was on the positive side of the polyacrylamide gel. The protein transfer was carried out in the transfer buffer (1.44% (w/v) glycine; 0.3 (w/v) Tris, 20% (v/v) methanol) at 100 mA for 1.5 hours. At the end of the transfer, the gel was removed to 50% (v/v) methanol for silver staining, and the

nitro-cellulose placed in 100 ml of block solution (TBS-T-Marvel: 10mM Tris pH 8.0, 150mM NaCl, 0.1% v/v Tween 20 and 5% w/v powder milk) and shaken on a rotary shaker for 45 minutes. To develop the blot, the blocking solution was poured off the blot and primary antibody solution or pre-immune serum (10ml TBS-T-Marvel plus 40 µl anti-tritin-S antibodies), was added and shaken vigorously on a rotary shaker for three hours. The primary antibody was poured off and the nitro-cellulose filter washed in 100 ml TBS-T four times for 5 minutes each in a shaker. Secondary antibody solution (20ml TBS-T-Marvel plus 3 µl anti-rabbit alkaline phosphatase conjugate making a 1/7500 dilution) was poured over the nitro-cellulose filter, shaken and placed on a rotary shaker for one hour. The filter was then washed twice in 100 ml TBS-T for 5 minutes each time, followed by 2 washes in 100 ml TBS also for 5 minutes each time. The blot was removed and the surface liquid removed by gently placing it between filter paper. 10ml developing solution (100 mM Tris/Cl pH 9.5, 100 mM NaCl, 5mM MgCl$_2$) plus 66 µl of NBT solution (50mg/ml) plus 33 µl of BCIP solution (500mg/ml) (prepared just prior to use), were added to the dry filter in a clean dry box, ensuring complete contact between the developer and the nitro-cellulose filter. Colour development was stopped by replacing the developing solution with 200ml-stop solution (20 mM Tris/Cl pH 8.0, 5 mM EDTA).

2.4. Concentration of Protein Samples

2.4.1. Ammonium sulphate precipitation

The method used here, of precipitation by increasing ionic strength, exploits the hydrophobic nature of protein surfaces in solution. Solid ammonium sulphate was added slowly to the protein solution at 4°C with gentle stirring until the desired final saturation was reached (Harris, 1989). Precipitated proteins were pelleted by centrifugation at 7500 rpm and 4°C for 10 min in a Sorvall GSA rotor and resuspended in the minimum volume of the appropriate buffer.

2.4.2. Ultrafiltration using Centricon Concentrator

The Centricon - 10 unit, with a semi-permeable membrane of molecular weight cut off 10 kDa, was used according to the manufacturer's instructions for the small-scale concentration of protein samples.

2.4.3. Estimation of Protein Concentration

The Coomassie® Plus Protein Assay Reagent (PIERCE) was based on the absorbance shift from 465 nm to 595 nm that occurs when Coomassie®Blue G-250 binds to a protein in an acidic solution. It was used to quantify the protein content of the protein sample. Known concentrations of Bovine Serum Albumin (PIERCE) were used to construct a standard curve. This kit was used according to the manufacturer's instructions for the small-scale concentration of protein samples, until the desired concentration was achieved (based on Harris (1989) work).

In addition, SDS-PAGE silver staining was used to quantify the protein contents. In this case known concentrations of RTA (ricin A-chain) were used to construct a standard curve rather than bovine serum albumin, and these two were compared against the purified tritin-S protein samples.

2.5. Ribosome Extraction

2.5.1. Rabbit reticulocyte ribosomes

Non-nuclease treated rabbit reticulocyte lysate was layered over a 1-ml cushion of 1.0M sucrose in Endo (TKMg) buffer, contained in a 3ml-ultracentrifuge tube, and the ribosomes were pelleted at 100,000 rpm and 4°C for 40 minutes in a TL-100.3 rotor. After sequential aspiration of the supernatant and sucrose layers, the ribosome pellet was rinsed with TKMg buffer and then resuspended in 2 ml of the same buffer using an acid washed glass rod. The ribosomes were pelleted as before, rinsed once with TKMg buffer and resuspended in the same buffer. Typically 1 ml of lysate yielded 1-2 mg of ribosome.

2.5.2. Wheat germ ribosomes

Wheat germ lysates were prepared by the method of Jackson and Larkins (1976). Lysate (1ml) was layered over a 1 ml cushion of 1.0 M sucrose in TKMg buffer, in a 3ml ultracentrifuge tube, and centrifuged at 100,000 rpm and 4°C for 1 h in a Beckman TL-100.3 rotor. The supernatant liquid was aspirated off and the ribosome pellet was rinsed once with TKMg buffer and then resuspended in the same buffer. Typically, 1 ml of lysate yielded 5 mg of wheat germ ribosome.

2.5.3. *E. coli* ribosomes

An overnight culture of *E. coli* DH1 (10ml) grown at 30°C in LB media was used to inoculate 500 ml of LB media (1% inoculum). The culture was grown at 37°C to an apparent 0.35-0.4 of A_{600}. Cells were rapidly cooled in a dry-ice/ ethanol bath and then harvested by centrifugation at 4000 rpm in a Beckman JA-10 rotor at 4°C for 10 minutes. The supernatant liquid was decanted and the pelleted cells resuspended in 5 ml of ice cold resuspension buffer (50 mM Tris/Cl pH 7.8, 14mM magnesium acetate, 60mM KCl and 6 mM β-mercaptoethanol). The cells were mechanically broken in a French press pressure cell at 10,000 lb/in². The lysate was centrifuged at 15,000 rpm in a Beckman JA-20 rotor at 4°C for 20 minutes. The supernatant liquid was taken and the ribosomes pelleted by performing a 100,000-rpm centrifugation at 4°C for 60 minutes. The supernatant liquid was then discarded and the pelleted ribosomes resuspended in 1 ml of 1x TKMg buffer (25 mM Tris/Cl pH 7.6, 25 mM KCl and 5mM $MgCl_2$). The concentration of ribosomes was calculated from A_{260}.

2.5.4. Storage of ribosomes

Assuming that a 1mg/ml solution of rRNA had an A_{260} nm of 25 (Sambrook *et al.* 1991), the ribosome concentration could be estimated as approximately twice that of the rRNA concentration as there would be roughly equal weight contributions of rRNA and the protein in the ribosome (Wool, 1979). Isolated ribosomes were stored in TKMg buffer, at a final concentration of 10-40 mg/ml, at -70°C.

2.5.5. Preparation of *E. coli* ribosomal subunits
2.5.5.1. Nierhaus's (1990) protocol for ribosome dissociation

The protocol was based on Nierhaus's (1990) methodology. The pellet of *E. coli* ribosomes (section 2.5.3.) was resuspended in a 100 μl dissociation buffer 2 (named subunit dissociation condition, consisting of 20mM Hepes-KOH pH7.6, 1mM $MgCl_2$, 300mM NH_4Cl, 2mM spermidine, 0.2mM spermine, 5mM 2-mercaptoethanol) to a final concentration of 40μg/μl. The ribosome solution was layered onto a 30ml sucrose gradient (0-40% w/w, made up with the same buffer 2) and centrifuged for 11h at 21000rpm (100,000 x g) in a SW28 rotor, at 4°C. An ISCO system (ISCO Inc, USA) was used to fractionate the sucrose gradient and to measure the absorbance at 254 nm.

Fractions containing 30S and 50S ribosomal subunits were pelleted respectively, by 1h centrifugation at 100,000 rpm in a 100.3TL rotor. Finally, the pellets were resuspended in buffer 3 (20mM Hepes-KOH pH 7.6, 4mM MgCl$_2$, 30mM NH$_4$Cl, 2mM spermidine, 0.2mM spermine, 5mM 2-mercaptoethanol). A$_{260}$ readings were measured and the concentrations of subunits were calculated (section 2.5.4.).

2.5.5.2. Preparation of *E. coli* ribosomal subunits (30S and 50S)

A dissociation buffer (20mM Tris/Cl, pH 7.6, 4mM MgCl$_2$, 100mM NH$_4$Cl) and a standard buffer (20mM Tris/Cl pH 7.6, 10mM MgCl$_2$, 100mM NH$_4$Cl), were used instead of buffers 2 and 3 from Nierhaus's (1990) general methodology (section 2.5.5.1.). The materials and solutions were treated with 0.1% DEP and ultrafiltration (boiling DEP solutions to destroy DEP). During this procedure, the NH$_4$Cl, concentration was kept constant and low because it has been reported that, not only are translation factors removed, but also high concentrations can removed some ribosomal proteins (Bochkariov, 1996; personal communication). The following procedure was employed after the standardisation.

◊ The pellet of *E. coli* ribosomes (section 2.5.3.) was resuspended in a 100 µl dissociation buffer to a final concentration of 40µg/µl as a maximum critical concentration for dissociation. A 5-25% (w/w) sucrose gradient was made up instead of 0-40% (w/w), with the dissociation buffer. The ribosome solution was layered onto a 30ml sucrose gradient (5-25% w/w) and centrifuged for 11h at 21000rpm (100,000 x g) in a SW28 rotor, at 4°C. An ISCO system was used to fractionate the sucrose gradient and to measure the absorbance at 254 nm. The fractions were collected and precipitated using PEG-6000 to a final concentration of 10% and the magnesium concentration was increased to 10mM by adding MgCl$_2$. The mixtures were stirred at 4°C for 12h. Ribosomal subunits were pelleted by 1h centrifugation at 100,000 rpm in a 100.3TL rotor. The pellet was resuspended in the TKMg buffer so that sample could be analysed.

2.5.5.3. Preparative 'zonal' ultracentrifugation

Preparative 'zonal' ultracentrifugation was prepared at the Max Planck Institut fuer Molekulare Genetik: AG Ribosomen, Berlin, at Dr. Francois Franceschi's group. The protocol was based on Nierhaus's (1990) methodology. The pellet of *E. coli* ribosomes (section 2.5.3.), was resuspended, but a dissociation buffer (20mM Tris/Cl, pH 7.6, 4mM $MgCl_2$, 100mM NH_4Cl) (section 2.5.5.2) was used instead of buffer 2 (spermidine and spermine containing buffer) (Nierhaus, 1990). Two runs of 7,500A_{260} units were ultracentrifuged in a preparative 'zonal' rotor, in 0-40% (w/v) sucrose (Ultrapure grade, RNase free, Gibco) in dissociation buffer (20mM Tris/Cl pH 8.0, 1mM $MgCl_2$, 200mM NH_4Cl and 4mM 2-mercaptoethanol) at 21,000 rpm for 18h in a Beckman T5 rotor. A 50% (w/v) sucrose solution (Aldi stores) was used to push the sucrose gradient out from the 'zonal' rotor to be fractionated. Fractions containing 30S and 50S ribosomal subunits were collected respectively, and pelleted at 100,000 g for 24 h in a 45 Ti rotor. Finally, the pellets were resuspended in TKMg buffer (25mM Tris/HCl pH 7.6, 25mM KCl and 5mM $MgCl_2$ instead of buffer 3 (20mM Hepes-KOH pH 7.6, 4mM $MgCl_2$, 30mM NH_4Cl, 2mM spermidine, 0.2mM spermine, 5mM 2-mercaptoethanol) (Nierhaus, 1990). A_{260} readings were measured and the concentration of subunits was calculated (section 2.5.4.).

2.6. 'naked' rRNA

2.6.1. SDS / phenol / chloroform method

Approximately 9,000 µg of *E. coli* ribosome were diluted to 400 µl in SDW with a final SDS concentration of 0.5%. 200 µl of phenol was added and vortexed briefly. 200 µl of chloroform was then added, mixed and the aqueous phase was removed to a fresh tube and the phenol/chloroform extraction procedure repeated twice more at room temperature. A final chloroform extraction was performed before precipitating the rRNA from the aqueous phase by adding to it 1/10th of its volume of 2M sodium acetate pH 6.0 and twice its volume of ethanol and storage at -20°C for at least 30 minutes. The rRNA was pelleted in a microfuge for 15 minutes at room temperature, the aqueous phase removed and the rRNA pellet washed in 70% ethanol. The pellet was dried and resuspended in SDW.

2.6.2. Extraction for use in RIP assays

The 'naked' rRNA used in assays with RIPs was isolated from ribosome preparations by the method of Noller (1980). The whole extraction procedure was carried out at 4°C in the buffer conditions to be used in the RIP depurination assay in order to maintain the secondary structure as far as possible. rRNA was extracted by 3 phenol/chloroform extractions in the presence of 0.5% SDS followed by 2 chloroform extractions. The rRNA was precipitated from the aqueous phase by the addition of 1/10th of its volume of 7M NH_4 acetate and 2.5 times its volume of absolute ethanol (stored at -20°C for at least 30 minutes), and then washed in 70% ethanol twice. The pellet was dried and resuspended in a suitable volume of the appropriate buffer.

2.7. Aniline Cleavage of Depurinated rRNA in assays for RIP Activity

Varying concentrations (10ng/µl to 100 ng/µl) of PAP, tritin-S and RTA were incubated with 30-40 µg of ribosomes (*E. coli*, wheat germ, yeast and rabbit reticulocyte ribosomes) or 15 µg naked rRNA in 1x TKMg buffer (25mM Tris/HCl pH 7.6, 25mM KCl and 5mM $MgCl_2$). The total volume was made up to 20 µl with 2x TKMg buffer and sterile distilled water (SDW), such that the buffer was at a final concentration equal to the original concentration. The incubations were performed at 30°C for 30 minutes on a dry heating block. The reactions were terminated by the addition of SDW and SDS to a final concentration of 1% in a 200 µl volume, and the mixture was vortexed vigorously. The rRNA was extracted using the phenol/chloroform method: 100 µl of phenol was added to the reaction, and the mixture vortexed. This was followed by the addition of 100 µl chloroform and further vortexing. This mixture was centrifuged at 13,000-rpm/ room temperature for 5 minutes. The upper aqueous phase was removed to a fresh Eppendorf tube, and the extraction repeated twice. The rRNA was precipitated by the addition of 0.1 volume of 7 M ammonium acetate and 2.5 volumes of absolute ethanol at -20°C or in dry ice for at least 30 minutes. The mixtures were then centrifuged in a microfuge at 4°C/13,000 rpm/15 minutes. The supernatant liquids were discarded and the pellets washed twice in 70% ethanol at -20°C and spun at 13,000 rpm for 5 minutes. The supernatants were removed and the pellets dried in a vacuum dessicator for 15 minutes. The rRNA pellets were resuspended in 10 µl SDW, and 1 µl used in a 1:400 dilution for

76

spectrophotometer estimation of rRNA content at 260 nm. Following rRNA quantification, 4 μg rRNA were treated with 20 μl 1M aniline/acetic acid pH 4.5 (D'Alessio, 1982), and the reactions incubated at 50°C for 2 minutes. The rRNA was again precipitated using ammonium acetate and ethanol as described above. The pellets were dried in a vacuum for 15 minutes. The dry pellets were resuspended in a solution of 60% deionised formamide in 0.1x TPE (1x TPE: 36mM Tris/Cl pH 8.0, 30mM NaH_2PO_4, 1mM EDTA-Na_2). For the controls, 4 μg of non aniline treated rRNA were each added to the same quantity of additional Eppendorf tubes containing 20 μl 60% deionised formamide in 0.1xTPE. The rRNA extracts were then heat denatured at 65°C for 5 minutes, put on ice, and 3 μl rRNA sample buffer added (50% glycerol, 0.1% bromophenol blue).

2.7.1. Electrophoresis and Visualisation of RNA

The rRNA samples were electrophoresed in 1.2% (w/v) agarose (RNase free) in 0.1x TPE, 50% (v/v) deionised formamide. The agarose was dissolved in distilled water plus 0.1xTPE and 50 ml of deionised formamide. The agarose was then poured onto gel trays previously soaked for 2 hours in 0.1M sodium hydroxide and then rinsed with deionised water. Wells were individually flooded with 60%-deionised formamide in 0.1xTPE, and samples of 25 μl loaded into the wells. 1 litre of 0.1xTPE running buffer was poured into each of the two reservoirs of the gel tank and the gel was electrophoresed at 25mA towards the positive electrode until the dye front had travelled half the length of the gel. Gels were stained for 30 minutes in 500 ml of water containing ethidium bromide (2μg/ml). The gels were subsequently destained in 500 ml of distilled water for 30 minutes then photographed under UV light with Polaroid 667 and 665 film. Agarose gel exposure times were held constant for all gels. Quantification of aniline fragments was achieved by densitometer quantification and using 5S rRNA as an internal control.

2.8. Assay for Binding of Labelled RIPs to Ribosomes

2.8.1. Sucrose gradients

5 - 25 % linear sucrose gradients were prepared and rabbit reticulocyte, wheat germ and *E. coli* ribosomes that had been incubated with RIPs were each layered over the 5 ml sucrose gradient, and centrifuged at 40,000-60,000 rpm and 4°C for 2-3h (several assays) in a Beckman 60.1 Ti rotor. After sequential aspiration of the sucrose layers

and their fractionation into 0.5 ml Eppendorf tubes, the fractions were detected by Absorbance at 260nm, to obtain the sedimentation profile. The presence of the RIP in the fractions was determined by the methods described below.

2.8.2. Semi-quantitative method

The fractions were analysed by western dot blotting using an appropriate anti-RIP antiserum.

2.8.3. Dot blotting

A piece of Hybond-N nylon membrane was soaked in 1x TKMg buffer (25mM Tris/HCl pH 7.6, 25mM KCl and 5mM $MgCl_2$) for 15 minutes and then placed in the dot blot manifold on top of 2 pieces of 3MM paper soaked in 1x TKMg buffer. The wells were filled with 1x TKMg buffer and a vacuum applied until all the fluid had passed through the membrane. The wells were then refilled with PBS buffer. PAP, tritin-S, RTA RIPs and *E. coli*, yeast, wheat germ, rabbit reticulocyte ribosomes in 1x TKMg buffer were added to the wells. The vacuum was again applied and the wells were washed twice with 1 ml of 1x TKMg buffer. The filter was immunoblotting using the develop methodology from western blot.

2.8.4. Radioactive labelling of RIPs (quantitative)

RTA was reductively alkylated according to Rice and Means (1971). 0.1 mg of the protein to be labelled was adjusted to pH 9.0 with 0.1M NaOH. Water was added to a volume of 0.1 ml. To the solution cooled in ice, 10 μl of 0.04 M ^{14}C-formaldehyde (30-50 mCi/mmol) were added to give a 4- or 5- fold excess over the amino groups in the protein. This was followed after 30 secs. by four 2μl sequential additions of sodium borohydride, (5 mg per ml, sufficient to reduce all of the formaldehyde), at 30 secs. intervals. To ensure complete reduction of the formaldehyde, an additional 10 μl of sodium borohydride solution were added after 1-min. It was possible to increase the extent of labelling by repeating the process.

2.8.5. Assay for the binding of Labelled RIPs to Ribosomes: A quantitative method

In a typical experiment 40-50 pmol of washed ribosomes or ribosomal subunits were reacted with 10-1500 pmol of labelled RIPs in a final volume of 0.2-0.3 ml of TKMg buffer for 30 min at 37°C. Centrifugation of this small volume in a Beckman type 40 rotor at 39,000rpm for 10 min was carried out to pellet all the ribosomes and ribosomal subunits. The supernatant liquid was carefully removed and a 100μl aliquot was counted in 3.5 ml of Brays solution. The pellet was resuspended in 50μl of buffer, then transferred to a scintillation vial. The centrifuge tube was rinsed with an additional 50μl of buffer and the combined 50μl aliquots were counted in 3.5 ml of Brays solution. Background values were subtracted from the radioactivity recovered in the pellets of the corresponding experimental tubes (Endo and Tsurugi, 1988).

2.8.6. An Alternative Assay for Binding RIPs to Ribosomes: A qualitative method

40-50 pmol of washed ribosomes or ribosomal subunits were reacted with 10-1500 pmol of labelled RIPs in a final volume of 0.2-0.3 ml of solution of 25 mM triethanolamine-HCl (pH 8.0), 50 mM NH_4Cl, 2.5 mM magnesium acetate, and 0.5 mM dithiothreitol. After incubating at 37°C as above, a small volume of dimethylsuberimidate was added to a final concentration of 2mg/ml and the tubes were incubated at 0°C for 12-15 h. The dimethylsuberimidate was added for the purpose of covalently crosslinking any resulting ricin-ribosome complexes. The contents of the tubes were layered over 1ml pads of 0.2 M sucrose in buffer A in polycarbonate tubes and centrifuged for 30 min at 39,000 rpm in a Beckman type 40 rotor. Samples were treated as above.

2.9. The Action of RIPs on 'naked' rRNA and *E. coli* Ribosomes

Varying concentrations of RIPs (PAP/RTA) (340ng/ml to 0.34 ng/ml) were incubated either with 30 μg of 'naked' rRNA or with 30 μg of *E. coli* ribosomes in order to achieve a 1:1 to 1:0.001 molar ratio of substrate to RIP in each of the log dilutions. 1x TKMg buffer was used as reaction buffer. RNA extracted from the mixtures was subjected to the aniline cleavage of depurinated rRNA for RIP activity methodology as above.

2.10. Maintenance of bacterial stocks and transformation with plasmids

2.10.1. Growth and Storage of Bacterial Cultures

E. coli strains DH1 and DH5 were maintained on Luria-Bertani (LB) plates by streaking and subsequent incubation at 37°C overnight. Each plate consists of 10g/l Bacto-tryptone, 5g/l yeast extract, 10g/l sodium chloride, containing 2% (w/v) Bacto-agar.

2.10.2. Preparation of Competent Cells for Plasmid transformation

E. coli strain DH5 was made competent essentially by the method of Hanahan (1983; 1985), as follows: a 5ml culture of *E. coli* strain DH5 was grown in LB medium at 37°C and shaken at 250rpm overnight. To the 50ml pre-warmed LB medium was added 0.5ml overnight culture. This was then grown at 37°C and shaken at 250rpm until it had reached OD_{600} of approx. 0.5. The culture was cooled on ice for 10-15min, before the cells were harvested at 2000xg (GH3.7 rotor, Beckman GPR bench centrifuge) for 5 min at 4°C. The cell pellet was resuspended in 17ml RF1 (consisting of 100mM rubidium chloride, 50mM manganese chloride tetrahydrate, 30mM potassium acetate, 10mM calcium chloride, 15% (v/v) glycerol, with the pH adjusted to 5.8 with glacial acetic acid) then held on ice for 15 min. The cells were harvested as before, resuspended in 4ml RF2 (consisting of 10mM MOPS. 10mM rubidium chloride, 75mM calcium chloride, 15% (v/v) glycerol, with the pH adjusted to 6.8 with sodium hydroxide), then held on ice for at least 15min, before transformation.

2.10.3. Transformation of Competent Bacterial Cells with Plasmids

E. coli strain DH5 was transformed as follows: to 100μl competent cells was added 1μl DNA before incubating on ice for 40min. The cells were heat-shocked at 42°C for 90 secs, then plated onto LB-agar plates containing 50μg/ml ampicillin. The plates were incubated at 37°C overnight.

2.11. DNA manipulations

2.11.1. Plasmid Preparation

Large-scale alkaline lysis preparations of plasmid DNA ('maxipreps') were carried out as a modification of the method of Sambrook *et al.* (1991). Single colonies of

transformed *E. coli* were grown in 25ml LB medium (or LB medium supplemented with 50μg/ml ampicillin) at 37°C in an orbital shaker and shaken at 200rpm for 5 h. A 34mg/ml chloramphenicol solution was added and shaked for further 3 hours. After that, the cultures were added to 500ml LB medium and incubated overnight. A small volume (200μl) of each culture was saved and stored at -70°C. The rest of the cultures were harvested at 27,000xg (SS-34 rotor, Sorvall RC-5B centrifuge) for 30min at 4°C, the supernatant liquids were discarded, and each pellet resuspended in 100ml SET (consisting of 25mM Tris-HCl pH 8.0, 10mM EDTA, 438mM sucrose). 7.2ml of a solution of 4mg/ml chicken egg white lysozyme in SET were added to each pellet solution and then held on ice for 10min. To each preparation was added 100ml lysis solution (200mM sodium hydroxide, 1% (w/v) SDS), the samples gently mixed, then incubated on ice for 10min, before 150μl 3M sodium acetate pH 4.7, was added and the samples incubated on ice for a further 10min. The precipitate was centrifuged at 27,000xg (SS-34 rotor, Sorvall RC-5B centrifuge) for 20min at 4°C, the supernatant liquid transferred to a fresh Oakridge tube and treated with 5μl 10mg/ml RNase A at 37°C for 15min. The preparation was phenol/chloroform extracted twice, precipitated with 0.6 of its volume of propan-2-ol for at least 10min, centrifuged for 10min as before, and the DNA pellet resuspended in 1.6ml sterile distilled water, 0.4ml 4M sodium chloride, and 2ml 13% (w/v) PEG6000, and precipitated on ice for 1h. The DNA was pelleted in a microcentrifuge at 11,600xg for 15min at 4°C, washed with 100μl 70% (v/v) ethanol, dried in a vacuum desiccator, and resuspended in 100μl TE. The DNA was stored at -20°C.

2.11.2. Large scale plasmid purification by caesium chloride density centrifugation

Overnight cultures of *E. coli* DH1 cells in 10ml LB medium Amp[50] (50μg/ml ampicillin) were grown at 37°C in an orbital shaker (200rpm). 10ml of the overnight culture was used to inoculate 500ml of LB media Amp[50] in a 2L flask. The cells were allowed to grow at 37°C shaken at 200rpm, until the apparent A_{600} was between 0.35 and 0.4. A 34mg/ml chloramphenicol solution was added to achieve a complete inhibition of protein synthesis (170μg/ml chloramphenicol final concentration, Sambrook *et al.*, 1991) and shaked for further 3 hours. The cells were cooled on ice for 10min before being pelleted by centrifugation at 5000rpm for 10min at 4°C

(Beckman JA-10 rotor). The supernatant liquid was removed and the cells resuspended in 7.2ml SET (25mM Tris/Cl pH 8.0, 10mM EDTA, 15% sucrose) prior to adding 7.2ml of lysozyme (4mg/ml) made up in SDW. The mixture was transferred to an 1 litre flask and left at room temperature for 5 minutes. 12ml of 10% Triton X-100 was added and the mixture boiled briefly over a Bunsen flame with constant swirling to prevent burning. The flask was then placed in a boiling water bath for 1 minute before being immersed in a water/ice bath for 5 minutes. The lysis mixture was transferred to Oakridge tube and cell debris pelleted by centrifugation at 20,000rpm for 45 minutes at 4°C (Beckman JA-20 rotor). The supernatant liquid was removed, placed in a fresh Oakridge tube and 0.5 of its volume of 7.5M ammonium acetate added. This mixture was left on ice for 20 minutes before being centrifuged at 15,000rpm for 10 minutes at 4°C (Beckman JA-20 rotor). The supernatant liquid was again transferred to a fresh Oakridge tube and 0.7 of its volume of isopropanol added. This was held at -20°C for 20 minutes. Nucleic acid was pelleted by centrifugation at 15,000rpm for 10 minutes at 4°C (Beckman JA-20 rotor). The supernatant liquid was removed and the pellet dried under vacuum. The pellet was resuspended in 4ml of low TE (10mM Tris/Cl pH 8.0, 0.1mM EDTA). The TE / nucleic acid solution was placed in a small beaker and 4.3g of caesium chloride, 0.25ml of ethidium bromide (10mg/ml) and 0.25ml SDW added. The mixture was gently stirred until all the caesium chloride had dissolved. The solution was filtered through glass wool into a heat sealable tube (5ml). The tubes were balanced to within 0.01g and heat-sealed. The gradients were centrifuged at 52,000rpm for 16 hours at 20°C in a Beckman ultracentrifuge.

The lower plasmid DNA band was removed by first piercing the top of the tube with a needle and then withdrawing the plasmid DNA using a needle and syringe inserted just below the plasmid DNA band. The ethidium bromide was extracted with isopropanol equilibrated with TE and saturated with caesium chloride until a solution completely free of ethidium bromide was obtained. The DNA solution was diluted with 4 volumes of low TE and 1/10th of the volume of the original volume of solution (prior to dilution with 4 volumes of low TE) of 3M sodium acetate pH 6.0 was added. Twice the new volume of ethanol was added and the solution placed on dry ice for 30 minutes. Plasmid DNA was pelleted by centrifugation at top speed in a microfuge for

10 minutes at 4°C. The pelleted DNA was washed twice in 70% ethanol, dried under vacuum and resuspended in 400μl of TE.

2.11.3. Minipreparation of plasmid DNA

Small-scale alkaline lysis preparations of plasmid DNA ('minipreps') were carried out as a modification of the method of Sambrook *et al.* (1991). Single colonies of transformed *E. coli* were grown in 5ml LB medium (or LB medium supplemented with 50μg/ml ampicillin) at 37°C and shaken at 200rpm overnight. A small volume (200μl) of each culture was saved and stored at -70°C. The rest of the cultures were harvested at 2000xg (GH3.7 rotor, Beckman GPR bench centrifuge) for 10min at 4°C, the supernatant liquids were discarded, and each pellet resuspended in 85μl SET (25mM Tris-HCl pH 8.0, 10mM EDTA, 438mM sucrose). 5μl of a solution of 40mg/ml chicken egg white lysozyme in SET were added to each pellet solution and then held on ice for 10min. To each preparation was added 200μl lysis solution (200mM sodium hydroxide, 1% (w/v) SDS), the samples gently mixed, then incubated on ice for 10min, before 150μl 3M sodium acetate pH 4.7, was added and the samples incubated on ice for a further 10min. The minipreps were microcentrifuged at 11,600xg for 10min at 4°C, the supernatant liquids transferred to fresh Eppendorf tubes, 1.5μl 10mg/ml RNase A was added and the tubes incubated at 37°C for 60min. The minipreps were phenol/chloroform extracted twice, and the DNA precipitated with 1/10th of its volume of 3M-sodium acetate pH 6 and twice its volume of absolute ethanol on dry-ice for 15min, before micro-centrifugation at 11,600xg for 15 min at 4°C. The supernatant liquids were discarded, and each DNA pellet washed with 100μl 70% (v/v) ethanol before drying in a vacuum-desiccator. The DNA pellets were resuspended in 11μl TE (10mM Tris-Cl pH 7.5, 1mM EDTA) and stored at -20°C.

2.11.4. Plasmid purification using Magic Minipreps (QIAGEN)

Alternatively, Plasmid purification using Magic Minipreps (QIAGEN) was carried out according to the manufacturer's instructions.

2.11.5. Precipitation of DNA from Aqueous Solutions

DNA was precipitated from aqueous solutions by the addition of 0.1 of its volume of 7M NH_4 acetate and 2.5 times its volume of absolute ethanol. This solution was mixed and placed on dry ice for at least 30 minutes. Precipitated DNA was pelleted by centrifugation in a microfuge for 30 minutes at $4^{\circ}C$. The supernatant liquid was decanted and the pellet washed twice with 70% (v/v) ethanol. The DNA pellet was dried in a vacuum desiccator and then resuspended in a suitable volume of SDW or TE.

2.11.6. Quantification of DNA Concentration

DNA concentrations were calculated from the A_{260} value obtained using a Shimadzu UV-160A spectrophotometer where $1A_{260}/ml$ is equivalent to a DNA concentration of $50\mu g/ml$.

2.11.7. Restriction Digestion of DNA

DNA was digested using BRL restriction enzymes. Digests were performed according to the manufacturer instructions for each enzyme using the supplied digestion buffer. Up to $1\mu g$ of DNA was digested in a standard reaction in a final volume of $20\mu l$.

2.11.8. Separation of DNA Fragments by Agarose Gel Electrophoresis

DNA was electrophoretically separated on a gel consisting of 0.8% agarose in 0.5x TBE (45mM Tris borate, 1mM EDTA) using 0.5x TBE as running buffer. One fifth of the volume of the loading buffer (15% Ficoll, 0.25% bromophenol blue) was added to the DNA samples prior to loading onto the gel. The samples were electrophoresed at 70V until sufficiently resolved. The gels were soaked in SDW containing $2\mu g/ml$ ethidium bromide for 20 minutes and then in SDW for 10 minutes prior to visualising the DNA using an UV transilluminator. The gels were photographed using Polaroid 665 or 667 film and alternatively using Grab-IT system.

2.11.9. Recovery of DNA Fragments from agarose gels

The Geneclean (Bio101) technique was used to recover the DNA fragments from the agarose gels for subsequent ligation. The portion of the gel containing the DNA

fragment to be isolated was excised from the gel using a clean scalpel blade and the gel slice weighed. TBE modifier (0.5ml/g) and sodium iodide solution (4.5ml/g) were added to the gel slice and the mixture heated to 60°C for 5 minutes until the gel slice had completely dissolved. Glass milk solution (5μl) that had been thoroughly resuspended beforehand was added to the DNA solution and mixed. The glass milk was allowed to bind to the DNA at room temperature for 5-10 minutes. The glass milk was then pelleted by centrifugation in a microfuge for 10secs, the supernatant liquid removed and the pellet resuspended in 0.4ml of the wash solution. The glass milk was repelleted as previously, the supernatant liquid removed and the pellet again resuspended in 0.4ml of the wash solution. This washing procedure was repeated 3 times. The final pellet was resuspended in 10μl of SDW and held at 60°C for 10 minutes. The glass milk was pelleted and the supernatant liquid, containing the DNA was removed to a fresh Eppendorf tube. Electrophoresing an aliquot of the sample on an agarose gel (section 2.11.8) checked the recovery.

2.11.10. Dephosphorylation of linearized DNA

DNA that had been digested with a restriction enzyme was phenol/chloroform extracted and precipitated (sections 2.6.1. and 2.11.5.). The pelleted DNA was resuspended in 44μl of SDW and 5μl of 10x buffer added (1mM $ZnCl_2$, 1mM $MgCl_2$, 10mM Tris/Cl pH 8.3). 1 unit of calf intestinal phosphatase (CIP) was added to 100 pmoles of 5' termini to obtain protruding 5' termini. The mixture was incubated for 30 minutes at 37°C. The CIP was inactivated by heating at 75°C for 10 minutes in the presence of 5mM EDTA pH 8.0. The reaction mixture was then phenol/chloroform extracted. The dephosphorylated DNA was precipitated (section 2.11.5.) and resuspended in SDW.

2.11.11. Ligation of DNA

DNA molecules to be ligated were combined and the volume made up to 7μl with SDW. The insert DNA was added in a 5-fold molar excess over the vector DNA. The solution was heated to 45°C for 5 minutes so that all DNA ends were available for ligation. T4 DNA ligase (1μl of 1 unit/μl), 1μl of 5mM ATP and 1μl of 10x T4 DNA ligase buffer were added and the reaction incubated at 16°C overnight. The 10x T4

DNA ligase buffer was 200mM Tris/Cl pH 7.6, 50mM MgCl$_2$, 50mM DTT and 50µg/ml BSA. Half of the ligation reaction was then transferred into a suitable bacterial host made competent for transformation (sections 2.10.2. and 2.10.3.).

2.11.12. Annealing of two complementary oligonucleotides

500pmoles of each of the 2 oligonucleotides to be annealed were combined in an Eppendorf and 3µl of 10x the annealing buffer added (100mM Tris/Cl pH 7.6, 50mM MgCl$_2$). The volume was made up to 30µl with SDW. The annealing mixture was heated to 65°C for 2 minutes and then held at 55°C for 30 minutes before being allowed to cool slowly to 30°C.

2.11.13. PCR amplification

The PCR amplification is a methodology for the *in vitro* amplification of Domain VI from pKK3535 template DNA sequences (Brosius *et al.*, 1981) by the simultaneous forward and reverse primer extension of complementary strands of DNA. PCR was carried out, as described in standard published protocols (Taylor, 1991; Sambrook *et al.*, 1991). The following PCR reaction mixture was prepared: 4µl 10x PCR buffer (200mM Tris/Cl pH 8.4, 500mM KCl), 1µl 150mM MgCl$_2$, 1.6µl 2.5mM stock dNTP pH 7.0, 2.5µl Forward Primer (10pmol/µl) and 2.5µl Reverse Primer (10pmol/µl), 5-10ng template DNA, 0.5µl Taq DNA Polymerase (5U/µl), SDW to a total volume of 20µl reaction mixture. The contents were mixed and 15µl of liquid paraffin was overlaid. The mixture was centrifuged briefly to collect the contents to the bottom, and the Eppendorf tubes were incubated in an automatic thermocycler, at 94°C for 3min to completely denature the template. 35 cycles of PCR amplification were perform as follows: a) denaturing: 94°C for 30secs, b) annealing: 55°C for 30 secs, and c) extending: 72°C 1 min. Further incubation was done for additional 10 min at 72°C followed by maintaining the reaction at 4°C. The amplification products were analysed by agarose gel electrophoresis (section 2.13.1.) and stored at -20°C.

2.12. *In vitro* transcription

In vitro transcription followed the methodology described at sections 2.14.3. and 2.14.4. for synthesis of rRNA domain VI.

86

2.13. Electrophoresis and visualisation of DNA

2.13.1. 0.8% (w/v) Agarose Slab Gels

For the analysis of plasmid DNA and the restriction of endonuclease digest fragments, DNA was electrophoresed as described previously (section 2.11.8.).

2.13.2. Polyacrylamide sequencing gels

For the sequencing of plasmid DNA, the two strands of the double-stranded plasmid DNA were denatured with 5M sodium hydroxide (1μl per 20μl DNA) for 5minutes at room temperature. Meanwhile a Biogel P6 column was set up as follows: A few small chromic acid washed glass beads were placed in the bottom of a 0.5ml Eppendorf tube (with a small hole punched through the bottom). The wet Biogel P6 was placed on this to gel the tube and this was then placed in a 1.5ml Eppendorf tube. The column was microcentrifuged at 8000xg for 30secs, twice, transferred to another 1.5ml Eppendorf tube and centrifuged again until it was dry. The column was placed in a third tube, the denatured DNA solution was added and microcentrifuged at 8000xg for 45secs, twice. The denatured DNA was used immediately for sequencing.

DNA sequencing was carried out using the USB Sequenase (Version 2.0) DNA Sequenase Kit following the manufacturer's protocol. The sequencing primers were annealed to the denatured plasmid DNA as follows: 1.5μl (0.8 pmol) sequencing primer and 8μl denatured DNA was added to 1μl TM buffer (100mM Tris/Cl pH 7.5, 100mM magnesium chloride). The primer was then annealed to the template at 37 °C for 20–45 minutes.

Meanwhile, a labelling reaction mixture was made as follows: 1μl 0.1M DTT, 2μl Labelling nucleotide mix (1.5μM dGTP, 1.5μM dCTP, 1.5μM dTTP; diluted 1:5 with SDW), 0.5μl (5μCi) [^{35}S]-dATP, and 2μl Sequenase enzyme (diluted 1:8 with TE) per $n + 1$ reactions. A microtitre plate was labelled 'G, A, T, C' along four separate rows, and numbered from 1-n along the columns for the reactions. Into the bottom of each well was placed 2.5μl of the relevant Termination mix (each termination mix contains 80μM dGTP, 80μM dATP, 80μM dTTP, 80μM dCTP, 50mM sodium chloride, and 8μM of the relevant dideoxynucleotide). Once the annealing reaction was complete,

5.5µl of the labelling mixture was placed onto the side of each tube. The tubes were then microcentrifuged briefly and a timer was started (counting down from 5 min). From the first tube, 3.5µl were placed onto the side of the wells of each 'G, A, T, C' termination mix for the reaction. This step was repeated for each of the *n* reactions and should be completed within 5min. After which time the microtitre plate was centrifuged briefly in an IEC Centra-4X centrifuge. The plate was incubated at 37 °C for 5min, the 4µl stop mix (consisting of 95% (v/v) deionised formamide, 20mM EDTA, 0.05% (w/v) bromophenol blue, 0.05% (w/v) xylene cyanol FF) was placed onto the side of each well before centrifugation as above. The samples were then heated to 75-85 °C for 2min, before loading onto a 15% polyacrylamide sequencing gel.

The polyacrylamide gel was made as follows: 25.6g urea was placed in a 200ml beaker, 25ml SDW, 9ml 40% acrylamide solution (38% (w/v) acrylamide, 2% (w/v) N, N'-methylene bis-acrylamide) and 6ml 10x TBE (890mM Tris/borate, 25mM EDTA) were added, and the mixture stirred until the urea had dissolved. When the gel was ready to pour, 320µl 10% (w/v) ammonium persulphate and 70µl TEMED were added, the solution mixed and poured into a gel mould, ensuring there were no trapped air bubbles. A well former was inserted and the gel left to polymerise. The gel was initially pre-warmed for 15min at 40°C, and the urea flushed out of the wells prior to use. The samples (2.4 - 4 µl) were electrophoresed at 40W in 1x TBE (89mM Tris/borate, 2.5mM EDTA). After electrophoresis, the gel adhered to one of the plates, as the other plate was coated with Repelcote™ was fixed in 10% (v/v) methanol/10% (v/v) glacial acetic acid for 30 min before it was dried, placed into a Harmer cassette, and put down to X-ray film.

2.14. RNA manipulation

2.14.1. Sequencing of RNA

Sequencing of rRNA and primer extension was carried out largely according to the Moazed *et al.* (1986). rRNA samples were prepared from ribosomes using the SDS / phenol / chloroform method. The oligonucleotide to be used for sequencing was ^{32}P-end labelled (section 2.14.5.2).

2.14.1.1. Hybridisation

The hybridisation mixture was composed of 5pmoles of ^{32}P-end labelled oligo-nucleotide, 4 µg RNA, 2µl 5x hybridisation buffer (250mM Hepes / KOH pH 7.0, 25mM sodium borate, 500mM KCl) and SDW to 10µl. The hybridisation mixture was placed in a heating block at 90 °C for 1 min. The mixture was then allowed to cool slowly to approx. 45 °C.

2.14.1.2. Primer Extension

The extension mixture contains 2µl 2.5x extension mix (125mM Tris/Cl pH 8.5, 125mM KCl, 25mM DTT, 25mM MgCl$_2$ and 250µM of each dNTP), 1.0µl SDW, 1.0µl hybridisation mix, and 1.0µl of a 1:10 dilution of AMV reverse transcriptase (1.7 units/µl). Dideoxy sequencing reactions (Sanger *et al.*, 1977) contain 1.0µl of dideoxy nucleotide stock (T, C, G, or A: 25µM stock) instead of 1.0µl SDW. The extension reaction was allowed to proceed at 42 °C for 30minutes. One µl of chase mix (1mM each dNTP and 1.7 units/µl AMV reverse transcriptase) was then added. The reaction was allowed to proceed for a further 15 minutes at 42 °C. The products of the extension reaction were precipitated by adding 1µl of glycogen (10µg), 1/10th of its volume of 3M sodium acetate pH 6.0 and 2.5 times its volume of ethanol and placing it on dry-ice for 30 minutes. The precipitated nucleic acids were pelleted in a microfuge for 15 minutes, the supernatant liquid was removed and the pellet washed with 70% ethanol. The pellet was dried and resuspended in the loading buffer.

The products of the reaction were separated on a 7M urea, 6% acrylamide, 1x TBE sequencing gel (section 2.13.2.). The products were visualised by autoradiography.

2.14.2. Synthesis of RNA *In vitro*

The construction of a vector for the *in vitro* transcription of RNA domains was similar to that described for domain VI (Leffers *et al.*, 1988), where appropriate PCR fragment from the *rrn*B operon of *E. coli* was prepared from the plasmid pKK3535 (Brosius *et al.*, 1981) and cloned into a pGEM-4Z. The *Bam*HI digestion strategy was employed to generate the 3'end of domain VI (section 2.11.7.).

The domain was synthesised from the recombinant plasmid termed pRDVI linearized with BamHI. Completed linearization was checked by agarose gel electrophoresis (section 2.13.1.). The digestion mixture was extracted twice with one volume of phenol and once with one volume of chloroform, and the DNA was precipitated with three volumes of ethanol, washed with 70% (v/v) ethanol, dried and dissolved in the transcription buffer. Transcription was carried out as follows:

2.14.3. Synthesis of domain VI RNA (unlabelled transcript)

2pmoles of template DNA were prepared by digestion with BamHI restriction enzyme (section 2.14.2.). In a microfuge tube, the following components were mixed in the order given, at room temperature: RNase-free SDW, 10µg linearized plasmid, 10µl 0.1M DTT, 10µl of NTP stock (5mM each NTP), 20µl 5x transcription buffer (200mM Tris/Cl, 30mM $MgCl_2$, 10mM spermidine/Cl), 10µl (10units/µl) RNasin[R] 6µl (7-12 units) SP6 RNA polymerase. The reagents were mixed by gently tapping the outside of the tube. The reaction was incubated for 1.5-2 hours at 37 °C. After incubation, 10µl RNase-free pancreatic DNase I (10 units/µl) were added and then incubated for a further 15 minutes at 37 °C. The transcript was recovered by conventional phenol: chloroform rRNA extraction (Section 2.6.1.) and ethanol precipitation. The RNA transcript was resuspended in 50µl TKCa buffer and analysed using a 2% agarose: formamide RNA analytical gel.

Alternatively, in order to attempt to obtain a higher yield of domain VI - RNA transcript, the Weitzmann et al. (1990) and Nitta et al. (1998) methodologies were used, where the transcription reaction was carried out as above but 5 units of yeast inorganic pyrophosphatase were added to the transcription reaction. The reaction was incubated for 5h at 37°C. The methodology reported by Weitzmann et al. (1990), showed that the transcription was stopped after DNase (100u) was added and the incubation was continued for a further 15min at 37 °C. The transcript was extracted once more using the phenol: chloroform rRNA extraction (section 2.6.1.). The aqueous phase was passed through S300 in HEN buffer (50mM Hepes pH 7.3, 100mM NaCl, 5mM EDTA). The transcripts were precipitated with ethanol and the pellet was resuspended in 800µl rRNA buffer (5mM K acetate pH 5.0, 1mM Mg

acetate). This mixture was dialysed against 200ml rRNA buffer, using a Slide-A-lyzer 10,000 NW (Pierce) cassette, overnight at 4°C and again for 4 hours after change of buffer. Ethanol precipitation was carried out. The RNA transcript was resuspended in 50μl TKCa buffer and analysed using 2% agarose: formamide RNA analytical gel.

The methodology reported by Nitta *et al.* (1998), showed that the transcription was stopped by 10μl of 500mM EDTA pH 8.0. The white precipitated Mg^{2+} pyrophosphate was dissolved before carrying out the transcription extraction using phenol: chloroform and ethanol precipitation (section 2.6.1.). The transcript was dissolved in 200μl QA buffer (50mM MOPS-KOH, pH 7.0, 400mM NaCl and 15% ethanol). The sample was applied to a QIAGEN spin column (minipreps) previously equilibrated by QAT buffer (QA buffer + Triton X-100 1%). The spin column was washed with 1ml QA buffer and the transcripts were eluted from the column with 400μl QRU buffer (50mM MOPS-KOH pH 7.0, 1M NaCl, 1% Ethanol and 6M Urea). The recovered transcript was dialysed (using a Slide-A-lyzer 10,000 MW (Pierce) cassette) against self-folding buffer (50mM Hepes-KOH pH 7.5, 20mM Mg acetate , 400mM NH₄Cl) overnight at 4°C, the buffer was changed and the transcript was dialysed for a further 4 hours. Ethanol precipitation was carried out. The RNA transcript was resuspended in 50μl TKCa buffer and analysed using 2% agarose: formamide RNA analytical gel.

2.14.4. Synthesis of Radiolabelled RNA domain VI Probes (^{32}P-CTP labelled transcripts).
The reaction for synthesis of RNA domain VI radiolabelled probes was carried out according to section 2.14.3. but with one difference: 2μl fresh [^{32}P]-CTP (sp. act. 3000 Ci/mmol; 10μCi/μl) was used instead of 2μl of water. Radiolabelled transcript was resuspended in 50μl TKCa buffer and analysed throughout 2% agarose: formamide RNA analytical gel.

2.14.5. End-labelling of RNA transcripts
For labelling RNA transcripts as well as the reactions described at section 2.14.3. the transcript was treated as follows:

a) Dephosphorylation of RNA transcripts were carried out as described at section 2.11.10.

b) T4 polynucleotide kinase for end labelling of RNA transcripts:

The end-labelling of synthetic oligonucleotides and RNA transcripts by phosphorylation with bacteriophage T4 polynucleotide kinase was carried out according to Sambrook *et al.* (1991). The polynucleotide kinase reaction was carried out as follows: 67.5pmol RNA transcript or oligonucleotide were mixed with 3μl 10x bacteriophage T4 polynucleotide kinase buffer (included in the T4 kinase kit, Promega), 1μl of [γ-^{32}P] ATP (sp. act. 5000 Ci/mmol; 20μCi/μl in aqueous solution) and made up to a total volume of 20μl. 0.5μl (10 units/μl) bacteriophage T4 polynucleotide kinase was added to the reaction mixture. The mixture was incubated for 45 minutes at 37 °C. Following incubation, the mixture was incubated for 10min at 68°C to inactivate the bacteriophage T4 polynucleotide kinase. A second reaction was carried out adding 5-8 additional units of enzyme and incubation was continued for a further 30 minutes at 37°C. The mixture was heated to 68 °C for 10min to inactivate the enzyme.

Meanwhile a Biogel P6 column was set up as follows: A few small chromic acid washed glass beads were placed in the bottom of a 0.5ml Eppendorf tube (with a small hole punched through the bottom). The wet Biogel P6 was placed over this and this was then placed in a 1.5ml Eppendorf tube. The column was microcentrifuged at 8000xg for 30sec twice, transferred to another 1.5ml Eppendorf tube and centrifuged again until it was dry. The column was placed in a third tube, the labelled material solution was added and microcentrifuged at 8000xg for 45secs twice in order to separate it from the unlabelled and from the free [γ-^{32}P] ATP.

2.15. Partial and Total Deproteinisation of 50S subunits
The following procedures were carried out according to Nierhaus (1990).

2.15.1. The NH$_4$Cl/Ethanol Split Procedure

This methodology was used to split off the proteins L1, L5, L6, L7/L12, L10, L11, L16, L25, L31 and L33, resulting in the core subparticle P37 (1.5). 3500A$_{260}$ units of 50S subunits were diluted in 100ml buffer containing 10mM imidazole/Cl pH 7.4, 1.5M NH$_4$Cl, 20mM MgCl$_2$, and 1mM 2-mercaptoethanol, to a final concentration of 35A$_{260}$ units/ml. The mixture was heated to 37°C. Two lots of 50ml of pre-warmed ethanol were added to the mixture consecutively and shaken gently in between for 10min at 37°C. The mixture was centrifuged at 16,000xg for 30min. The pellet was resuspended in 7ml buffer 4 (20mM Tris/Cl pH7.4, 4mM Mg acetate, 400mM NH$_4$Cl, 0.2mM EDTA, 5mM 2-mercaptoethanol) and dialysed overnight against 10 volumes of the same buffer. The mixture was then clarified by a low-speed centrifugation and the supernatant liquid contained the P37 (1.5) subparticle. This subparticle was stored at − 70°C, after measuring the concentration in A$_{260}$ units/ml.

2.15.2. The LiCl-Split Procedure

This methodology was used to split off the proteins L1, L5, L6, L9, L7/L12, L10, L11, L14, L15, L16, L18, L19, L24, L25, L27, L28, L30, L31, L32 and L33, resulting in the production of the 3.5 core subparticle. 50S subunits were diluted in buffer 10 (10mM Tris/Cl pH7.6, 10mM Mg acetate) containing 3.5M LiCl to a final concentration of 20A$_{260}$ units/ml. The mixture was incubated for 5 hours at 0 °C and shaken gently, once every hour. After the incubation, the mixture was centrifuged at 40,000 rpm for 5 hours. The pellet obtained was the 3.5 core subparticle. This was resuspended in 2ml of buffer 6 (20mM Tris/Cl pH7.4, 20mM Mg acetate, 400mM NH$_4$Cl, 1mM EDTA, 5mM 2-mercaptoethanol). This subparticle was stored at −70°C, after measuring the concentration in A$_{260}$ units/ml.

2.15.3. The 66% Acetic Acid Procedure

The method of preparation the RNA using 66% acetic acid, was carried out according to the Nierhaus's (1990) protocol for isolation of total proteins from 50S subunits (TP50), described in the following section 2.16.1., but after the first centrifugation at 10,000g for 30min, the RNA pellet was resuspended in SDW. Further purification was carried out by phenol/chloroform extraction (section 2.6.) and ethanol precipitation.

RNA was visualised (section 2.7.1.) by RNA agarose / formamide analytical gel electrophoresis.

2.16. Preparation of total 50S subunit proteins (TP50)

2.16.1. Isolation of the total proteins from 50S subunits

Total 50S subunit proteins were a kind gift from Dr. Francois Franceschi at the Max Planck Institut fuer Molekulare Genetik: AG Ribosomen, Berlin. They were prepared according to Nierhaus's (1990) published protocol. $350A_{260}$ units of 50S subunits were diluted in 1ml buffer 3 (20mM Hepes-KOH pH 7.6, 4mM $MgCl_2$, 30mM NH_4Cl, 2mM spermidine, 0.2mM spermine, 5mM 2-mercaptoethanol). 0.1x its volume 1M Mg acetate and twice its volume of acetic acid were added to the mixture. The mixture was stirred for 45 min at 0 °C and then it was centrifuged at 10,000xg for 30 min. 5 volumes of acetone were added to the supernatant liquid and it was kept at -20°C for 3 hours. The mixture was centrifuged at 10,000xg for 30 min and the supernatant liquid was discarded. The residual acetone was removed from the pellet, by placing it in a desiccator for 30 minutes.

The pellet was resuspended in 1ml buffer 5 (20mM Tris/Cl pH 7.4, 4mM Mg acetate, 400mM NH_4Cl, 0.2mM EDTA, 5mM 2-mercaptoethanol, 6M Urea), yielding about 300 e.u/ml (section 2.16.2.) and dialysed overnight against the same buffer. The dialysis buffer was changed three times at 45min intervals using buffer 4 (20mM Tris/Cl pH 7.4, 4mM Mg acetate, 400mM NH_4Cl, 0.2mM EDTA, 5mM 2-mercaptoethanol) to ensure that no buffer 5 remained in the suspension. This was then centrifuged at 5,000xg for 5 min.

2.16.2. Quantification of TP50 in solution

Dialysed resuspended pellet of proteins (section 2.16.1.) were centrifuged briefly and Absorption at 230nm was measured in order to quantify the e.u./ml (according to the Nierhaus's (1990) published protocol). It was important to consider the following approximations for the quantification:

a) for TP50: 1 A_{230} unit = 220µg = 10 e.u.

b) for TP30: 1 A_{230} unit = 220µg = 8 e.u.

c) for TP70: 1 A_{230} unit = 220μg = 10 e.u.

d) 1 A_{260} unit of 50S = 36 pmol = 1 e.u. TP50

e) 1 A_{260} unit of 30S = 72 pmol = 1 e.u. TP30

f) 1 A_{260} unit of 70S = 24 pmol = 1 e.u. TP70

e.u. refers to equivalent units

2.16.3. Storage of TP50

The solution was quantified, analysed and finally stored in small aliquots at -70 °C.

2.17. Reconstitution of ^{32}P-RNA Transcript from Domain VI with TP50

Considering the data shown in Section 2.16.2., the ratio for the reconstitution of the domain VI - RNA transcript with TP50 was calculated in order to add the r-proteins in near stoichiometric amounts with respect to the rRNA (Nierhaus, 1990). Considering 1mol of 23S rRNA is approx. 1.05 x 10^6 g, 1 mol of Domain VI - RNA transcript (MW calculated from sequence) is approx. 98706g and that 36pmol 50S requires 1e.u. TP50 (section 2.16.2.), the quantity of TP50 to be added to each probe was calculated.

2.18. Gel retardation experiments for the reconstituted ^{32}P-RNA Transcript

2.18.1. Non-Denaturing Gel Electrophoresis

Non-denaturing gel electrophoresis for gel retardation experiments were carried out as described at section 2.2.2. Aliquots containing equivalent cpm between samples to be compared, or aliquots containing a constant amount of reconstituted Domain VI - RNA transcript (as indicated in the experiment) were fractionated by electrophoresis. Gels were pre-run for 30min at 20mA, and 4°C.

2.18.2. ^{32}P-RNA:TP50 Association Experiments

The complex between Domain VI - RNA transcript and TP50 was observed as a mobility shift (Batey and Williamson, 1996) in a non-denaturing polyacrylamide gel (section 2.18.1). A constant amount of labelled probe RNA transcript (0.0184 to 0.184pmol) was incubated with various concentrations of TP50 (ratios based on section 2.16.2.) in Mobility Shift buffer (MSB). MSB consists of: 10mM Hepes/KOH pH 7.5, 50mM potassium acetate, 0.1mM EDTA, 0.1mg/ml tRNA, 5μg/ml heparin,

and 0.01% Nonidet P40 (Batey and Williamson, 1996). Reaction volumes of 20µl were incubated for one hour at 25°C and one hour at 4°C before adding 2µl of type III loading buffer (30% glycerol, 0.25% bromophenol blue, 0.25% xylene cyanol). The RNA-protein complex samples were immediately loaded onto the non-denaturing gel (section 2.2.2.). The gel was dried on a Bio-Rad gel dryer, placed into a Harmer cassette, and put down to X-ray film.

Alternatively, in order to minimise the influence of time between reaction and loading periods, the experiment was carried out as above described but seven reactions were performed at: 120, 60, 30, 20, 10, 5 and 0 min of incubation period in MSB at 25°C just prior adding 2µl type III loading buffer. The samples were loaded immediately on to the 12% acrylamide non-denaturing gel. The samples were electrophoresed for 4 hours at 20mA, 4°C and under non-denaturing conditions (0.5x TBE tank buffer) (section 2.2.2.). The gel was dried on a Bio-Rad gel dryer, placed into a Harmer cassette, and put down to X-ray film.

2.18.3. ^{32}P-RNA:TP50 Complex Stability

The complex between Domain VI - RNA transcript and TP50 were observed as a mobility shift using the method of Batey and Williamson, (1996) and analysed in a non-denaturing polyacrylamide gel (section 2.18.1). A constant amount of labelled transcript (0.0184-0184pmol as indicated) was incubated in a 1:10 ratio transcript: TP50 (ratios based on section 2.16.2.) in Mobility Shift buffer (MSB). Dissociation experiments were conducted by incubating the complex for two hours at 25°C in the conditions described on section 2.18.2. prior to adding unlabelled RNA transcript (1:15:10 ^{32}P-RNA$_T$:TP50:RNA$_T$ ratio). Aliquots were taken at various time points and 1µl of load buffer type III was added and immediately loaded onto a non-denaturing polyacrylamide gel (section 2.2.2.). The gel was dried at Bio-Rad gel dryer, placed into a Harmer cassette, and put down to X-ray film

Alternatively, in order to minimise the influence of time between reaction and loading periods, the experiment was carried out as described above but eight reactions were performed at: 60, 50, 40, 30, 20, 10, 5 and 0 min of incubation after the unlabelled

RNA transcript competitor was added to the mixture. The incubation was carried our under the above conditions (2h at 25°C), prior adding 2µl type III loading buffer. The samples were loaded immediately on to the 12% acrylamide non-denaturing gel and electrophoresed for 3 hours at 20mA at (section 2.2.2.). The gel was dried on a Bio-Rad gel dryer, placed into a Harmer cassette, and put down to X-ray film.

2.18.4. Effect of temperature on RNA transcript before complex stability assay

Denaturing / renaturing experiments were carried out on the RNA transcripts before the gel retardation experiments, either:

a) heating to 90°C for one minute and cooling it in ice for two min,

b) heating to 90°C for one minute and cooling it down slowly until 40°C,

c) without heating the sample,

TP50 was then added to perform the stability assay as described at section 2.18.2.

2.18.5. The Alternative RNA Transcript Reconstitution Experiment: Change of MSB for TKCa Buffer

The alternative RNA transcript reconstitution experiment was carried out according to Nierhaus (1990) with the modifications described, in order to assay the influence of the reaction buffer for RIP sensitivity (section 2.7.) on the reconstituted Domain VI - RNA transcript/TP50 complex. 0.2pmol of ^{32}P-RNA and 0.087 e.u. TP50 (1:15 RNA: TP50) were dissolved in 20µl reaction buffer: either TKCa or MSB. [TKCa buffer consists of: 25mM Tris/HCl pH 7.6, 25mM KCl and 5mM CaCl$_2$ (Endo *et al.*, 1991) and Mobility Shift buffer (MSB) consists of: 10mM K-Hepes pH 7.5, 50mM potassium acetate, 0.1mM EDTA, 0.1mg/ml tRNA, 5µg/ml heparin, and 0.01% Nonidet P40 (Batey and Williamson, 1996)]. The reconstitution experiment was carried out as described at section 2.18.2. Samples were layered on a Biogel P6 chromatographic column. The Biogel P6 chromatographic column was set up as follows: A few small glass beads were washed in chromic acid and placed in the bottom of a disposable mini column (5cm height x 0.5cm inner radio). The wet Biogel P6 was placed in this and the column was equilibrated with buffer under test. Domain VI: TP50 complex solution was applied to the column, and eluted with the buffer under test. A further quantity of buffer was added to the column, and 0.2ml of eluted

fractions were collected and the cpm was measured in a scintillation counter. cpm/µl was plotted against each fraction to obtain an RNA elution profile.

2.18.6. Detection of complex formation by sucrose gradient centrifugation: based on Nierhaus's (1990) protocol

0.2pmol of ^{32}P-RNA transcript were mixed with 0.087e.u. TP50 to give a 1:15 ratio, for assembly in 200µl of buffer to be tested. The mixture was incubated for 20min at 44°C and then the sample was layered on to a sucrose gradient 10-30% (w/v) made up in either TKCa buffer or buffer 6. TKCa consists of: 25mM Tris/HCl pH 7.6, 25mM KCl and 5mM CaCl$_2$. Buffer 6 consists of: 20mM Tris/Cl pH7.4; 20mM Mg acetate, 400mM NH$_4$Cl, 1mM EDTA, 5mM 2-mercaptoethanol. The gradients were centrifuged at 250,000xg for 2 h 45 min (Beckman SW60 rotor). The gradient was fractionated and the cpm was measured. The cpm/µl were plotted against the fraction number.

3. CHAPTER III:

ISOLATION, PURIFICATION AND STANDARDISATION OF RIPs AND RIBOSOMES

3.1. Introduction

It has been reported that RIPs inhibit protein synthesis in a number of eukaryotic and prokaryotic cell-free translation systems. In order to study the interaction of ribosome-inactivating proteins and the ribosomes, an evaluation will be made of the binding characteristics of RIPs (PAP, tritin-S, and RTA) with *E. coli* ribosomes and the role of ribosomal proteins in sensitising the *E. coli* ribosomes to react with RIPs *in vitro*.

It is known that considerable variation exist in the activities of RIPs on the ribosomes of different kinds of organisms. The general characteristics of RIPs PAP, tritin-S and RTA are summarised in **Table 5**. **Table 5** shows that PAP is highly active on plant, mammalian, yeast and *E. coli* ribosomes (Ready *et al.*, 1986; Hartley *et al.*, 1991; Marchant and Hartley, 1995). Tritin-S is active on mammalian and yeast ribosomes, but does not show activity on plant and *E. coli* ribosomes (Hartley and Lord, 1993; Massiah and Hartley, 1995). RTA is highly active on mammalian and yeast ribosomes but only slightly active on plant ribosomes, and inactive with *E. coli* ribosomes (Hedblom *et al.*, 1976; Harley and Beevers, 1982; Endo and Tsurugi, 1987; Endo *et al.* 1987; Richardson *et al.*, 1989).

Currently, two different procedures are followed to purify type 1 and type 2 RIPs. Type 1 RIPs are purified, essentially, by cation exchange chromatography on carboxymethyl or sulfopropyl derivatized matrices (Roberts and Stewart, 1979; Stirpe *et al.*, 1983; Barbieri *et al.*, 1987; Massiah and Hartley, 1995; Yoshinari *et al.*, 1996). This take advantage of the basicity of most of single chain RIPs (Barbieri *et al.*, 1987; Hartley and Lord, 1993) which have a pIs > 9.5 which corresponds to extreme alkalinity (Roberts and Stewart, 1979; Habuka *et al.*, 1993; Massiah and Hartley, 1995; Yoshinari *et al.*, 1996).

Table 5. Activity Characteristics of tritin-S, PAP and RTA on different ribosomes.

Ribosome Inactivating Proteins	Ribosomes from			
	Plant	Mammalian	Yeast	E. coli
PAP	XXX	XXX	XXX	XX
tritin-S	no	XXX	XXX	no
RTA	X	XXX	XXX	no

- PAP: Highly active on plant, mammalian, yeast and *E. coli* ribosomes
- tritin-S: Inactive on plant and *E. coli* ribosomes and active on mammalian and yeast.
- RTA: Low activity on plant ribosomes, active on mammalian and yeast ribosomes and inactive on *E. coli* ribosomes.

XXX = Highly active
XX   = Moderately active
X   = Weakly active
no   = No activity

Barbieri *et al.* (1987), have even scaled up the above general cation exchange chromatographic procedure, for a pilot scale preparation, with minor adaptation for each RIP. The rationale of these procedures is based on the basic nature of RIPs at a basic pH, which allows it to bind to the column, and the incorporation of a salt gradient which increases the ionic strength of the column buffer, thereby increasing the competition between buffer ions and proteins for the charged groups of the ion exchanger. This reduces the interaction between the ion exchanger and the proteins until the proteins are eluted. Type 2 RIPs are purified, essentially, by affinity chromatography on acid-treated Sepharose, or other galactose-containing stationary phases followed by elution with galactose or lactose (Olsnes and Pihl, 1982). This is possible because of the lectin properties of their B-chains (Barbieri *et al.*, 1993).

For purposes of comparison, the substrates for N-glycosidase activity by RIPs were also isolated, purified and standardised. Ribosome fractions prepared from rabbit reticulocyte, wheat germ or *E. coli* were purified by ultra-centrifugation (as described in sections 2.5.1., 2.5.2. and 2.5.3. respectively) with a constant amount of 10mM $MgCl_2$, in order to avoid subunit dissociation (Gesteland, 1966; Kurland, 1971; Unlenbeck, 1995). For ribosomal RNA purification, a combination of phenol, SDS and stabilising buffers were used in order to remove virtually all the ribosomal proteins and to maintain the secondary structure of the rRNA (Noller *et al.*, 1995).

All the initial assays were performed in $Tris/KCl/MgCl_2$ buffer as described by Endo and Tsurugi, (1987). 1mM ATP was added for tritin-S N-glycosidase activity, in order to satisfy the requirement for tritin-S activity as is well documented (Roberts and Stewart, 1979; Carnicelli *et al.*, 1992; Taylor *et al.*, 1994; Massiah and Hartley, 1995).

3.2. The Chromatographic Two Steps Procedure for tritin-S Purification
The tritin-S isolation (section 2.1.) and purification (sections 2.1.1., 2.1.2. and 2.1.3.) procedure were monitored by SDS-PAGE (section 2.2.) and by N-glycosidase activity (section 2.7.) on rabbit reticulocyte ribosomes (extracted according to 2.5.1.).

A crude extract was prepared from wheat seeds and a 55-85% (w/v) ammonium sulphate cut was made in accordance with Massiah and Hartley(1995) procedure. The

Sephadex G50-40 column was used to further purify tritin-S. Based on the basicity (Barbieri *et al.*, 1987) of tritin-S (pI approx. of 10.13, Habuka *et al.*, 1993), as shown by Massiah and Hartley (1995), further purification was carried out by CM-Sepharose FF chromatographic column. Bound proteins were eluted with a linear gradient from 0-500mM NaCl as described in section 2.1.2. The proteins in each fraction were monitored by the measurement of the absorbance at 280nm which was plotted against each fraction to obtain a protein elution profile, where the salt gradient was established across the chromatographic run recorded. Tritin-S was eluted from the column at a concentration of NaCl of approx. 100-200mM as reported by Massiah and Hartley (1995).

However, a second step in cation exchange was necessary in an attempt to further purify tritin-S, therefore SP Sepharose FF was chosen (section 2.1.3.). The chromatographic procedure was carried out taking the same considerations than were used for the CM-Sepharose FF, and using a 0-500mM NaCl to elute the tritin-S at a concentration of NaCl approx. 100-200mM. Once more, proteins in each fraction were monitored by the measurement of the absorbance at 280nm, which was plotted against each fraction.

Figure 5(I) shows the main protein bands of approximately 30 kDa, which eluted from SP Sepharose at 100-200mM NaCl and run as a close doublet as is shown in tracks 1 to 4. A western blot was performed using rabbit polyclonal antibodies prepared by A.Massiah (Massiah and Hartley, 1995).

Figure 5(II) shows the Western analysis of the positive reaction between the rabbit polyclonal tritin-S antibodies and tritin-S.

Since the measurement of the absorbance at 280nm plotted against each fraction showed a peak (data not showed) and since the peak was analysed by SDS-PAGE and Western analysis and the peak fraction correlates with a 30-kDa major protein band on the electrophoretic pattern, it is assumed that the major protein band corresponds to tritin-S. All tritin-containing fractions were collected and dialysed for 36h against water at 4°C with

103

Figure 5. SDS-PAGE of fractions from SP-Sepharose Fast Flow used in the final purification of Tritin-S.
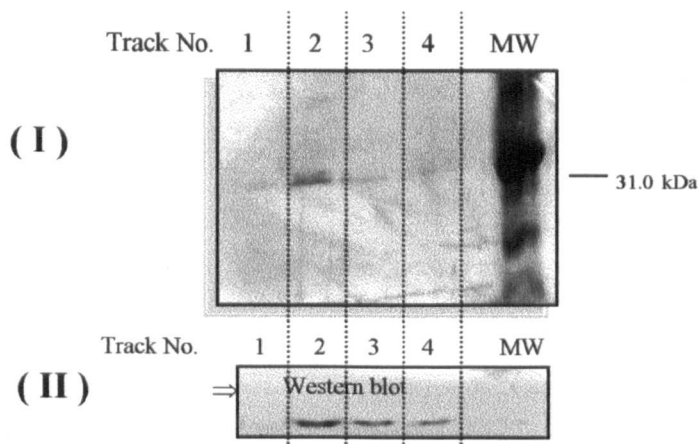
(I) Aliquots of 20µl from SP-Sepharose FF fractions were analysed in a 12% SDS-Polyacrylamide gel electrophoresis, and made visualised by silver staining (section 2.2.1.). Tracks 1-4 (**a** and **b**) correspond to the peak shown by the profile (data not shown) of the measurement of the absorbance at 280nm plotted against each fraction.

(II) Western analysis of positive reaction with the rabbit polyclonal tritin-S antibodies.

Tracks 1-4 (a) analysed by PAGE correspond to tracks 1-4 (b) analysed by Western Blotting.

water changes every twelve hours. The volume was reduced by ultrafiltration through an Amicon Centriprep-10 Concentrator (Amicon, Stone House, Glouc., UK) (section 2.4.2.). The retentate and the eluate from ultrafiltration were analysed by SDS-PAGE (**Figure 6**).

Figure 6 shows the electrophoretic profile from samples after ultrafiltration. The retentate and the eluate samples were analysed at two stages of ultrafiltration (after three and five centriprep concentrator runs):

a) tracks named MW refer to the molecular weight markers (Promega mid-range).

b) tracks 1-2 and 5-6 show the electrophoretic pattern of samples obtained from the retentate after five and three centriprep concentrator runs respectively, and

c) tracks 3-4 and 7-8 show the electrophoretic pattern of samples obtained from the eluate after five and three centriprep concentrator runs respectively.

Figure 6 shows that the second stage retentate samples (after five centriprep concentrator runs, tracks 1 and 2), show a prominent protein which appears as a doublet of the size expected (32 kDa), characteristic of tritin-S (Massiah and Hartley, 1995). The only additional phenomenon is that the doublet band after the second stage presented four additional minor bands below the major doublet, which seemed to be the product of degradation, and which did not appear on previous electrophoretic profiles (after three centriprep concentrator runs, tracks 4 and 6). The eluate samples (tracks 3-4 and 7-8) showed no protein at either stage.

In order to quantify tritin-S, a standard curve was built using 0, 1, 5, 10, 15, and 25 mg/ml of BSA (bovine serum albumin). The reaction with Coomassie® Blue was carried out using the manufacturer's instructions (Coomassie® Blue Kit solutions) (section 2.4.3.). The absorbance at 595nm was plotted against the BSA concentration, using deionised water as a negative control. Linear regression of the plotted line values was done. The equation $y = mx + b$ was resolved, and the final equation was $y = 0.2137x + 0.05445$, with a correlation factor of $r = 0.9979$. 'x' refers to mg/ml protein., 'y' refers to absorbance at 595nm, 'm' refers to slope of the curve.

Figure 6. SDS-PAGE of Retentate and Eluate from Amicon Centriprep Concentrator for tritin-S.
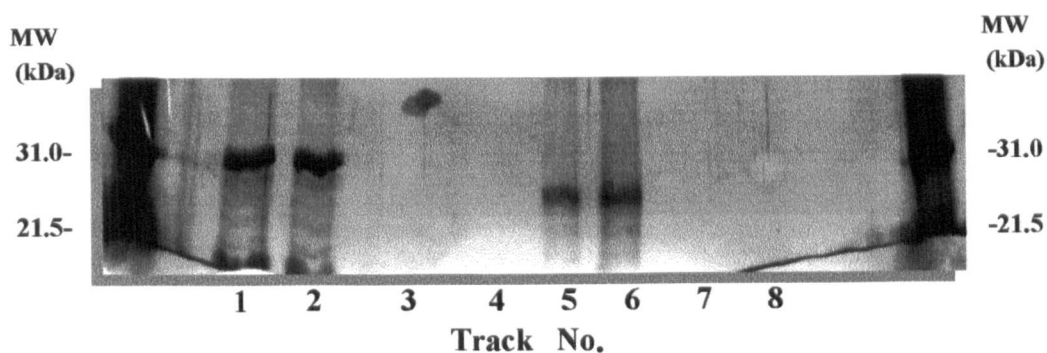
An aliquot of 20μl from the retentate (tracks 1-2 and 5-6) and the eluate (tracks 3-4 and 7-8) from Amicon centriprep concentrator, were analysed in a 12% SDS-Polyacrylamide gel electrophoresis, and made visible by silver staining (section 2.2.1.):

    a)   Tracks MW correspond to the molecular weight markers.

    b) Tracks 1-2 and 5-6 show the electrophoretic pattern of samples obtained from the retentate after five and three centriprep concentrator runs respectively, and

    c) Tracks 3-4 and 7-8 show the electrophoretic pattern of samples obtained from the eluate after five and three centriprep concentrator runs respectively.

A further quantification was carried out where RTA was used as a standard to build a standard curve with known amounts of RTA. **Figure 7** shows the SDS-PAGE silver staining of RTA as control, and tritin-S for protein quantification:

   a) Tracks 1 and 14 contain the molecular weight markers (Mid-range from Promega).

   b) Tracks 2-6 and 8 contain 1.26, 0.5, 0.2, 0.15, 0.10, and 0.05 μg RTA respectively

   c) Tracks 13-9 and 7 contain 1.26, 0.5, 0.2, 0.15, 0.10, and 0.05 μg tritin-S respectively (according to Coomassie® Blue protein quantification Kit, as described previously).

In this gel, the silver staining reaction was carried out longer for quantification purposes; hence the molecular weight markers do not appear as clearly as in **Figure 7**. Nevertheless, the positions of the markers were confirmed by direct observation through the transluminator. Track 7 from tritin-S, even with that overstaining, could not be seen.

It is noteworthy that the basis of the silver staining reaction is not precisely known. However, staining is influenced by the amino acid composition composition where basic and sulphur amino acids give more staining, hence quantification is very problematic (Hames, 1990).

However, the protein quantified by the Coomassie® Blue Kit gave different results from that using the silver stained gel with RTA as standard. The difference between the quantification achieved by the two methodologies appears to be 10 times less for tritin-S using SDS-PAGE than with the Coomassie® Blue Kit. Subsequent amounts of tritin-S were calculated using the Coomassie® Blue Kit.

Figure 7. SDS-PAGE silver stained of RTA as control, and tritin-S for protein quantification

SP-Sepharose FF
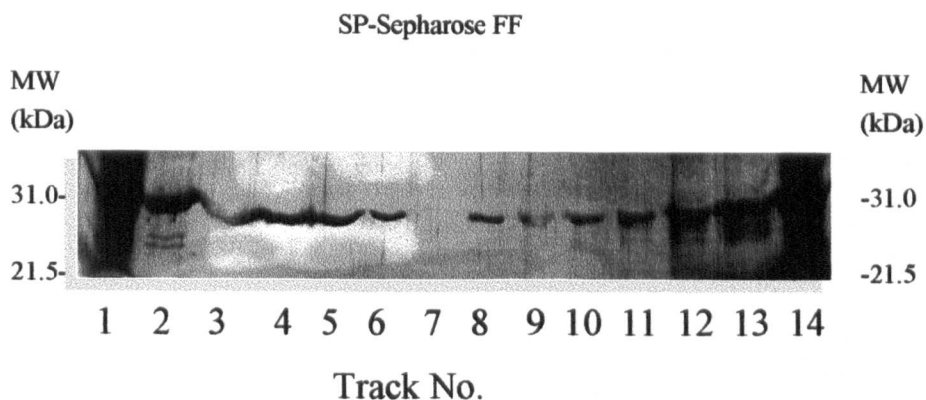
Tracks 1 and 14 contain the molecular weight markers (Mid-range from Promega), tracks 2-13 show the electrophoretic pattern of rRTA as control (tracks 2-6 and 8) and the electrophoretic pattern of tritin-S (tracks 7 and 9-13) as follows:

* 1, 14 = Mid-range molecular weight standard (Promega)
* 2, 13 = 1.26 µg RTA and tritin-S respectively
* 3, 12 = 0.50 µg RTA and tritin-S respectively
* 4, 11 = 0.20 µg RTA and tritin-S respectively
* 5, 10 = 0.15 µg RTA and tritin-S respectively
* 6, 9 = 0.10 µg RTA and tritin-S respectively
* 8, 7 = 0.05 µg RTA and tritin-S respectively

3.3. N-glycosidase Assay for RTA, tritin-S, and PAP

The N-glycosidase activity of RTA, tritin-S and PAP were assay on ribosome extracted from Wheat germ ribosomes (Anderson *et al.*, 1983), non nuclease treated rabbit reticulocyte ribosomes from non-nuclease treated reticulocyte lysate (Promega, Southamton, UK), and from *E. coli* ribosomes (Traub *et al.*, 1971), described in sections 2.5.1., 2.5.2. and 2.5.3. respectively.

In this work as in preliminary work using the RNA N-glycosidase assay, it was confirmed that tritin-S was active on rabbit reticulocyte ribosomes in the presence of 1mM ATP, but inactive on wheat germ and *E. coli* ribosomes, as shown by Massiah, (1994) and Massiah and Hartley, (1995).

Finally, the activity of RTA and PAP on *E. coli* ribosomes, will be review extensively on Chapter IV.

3.4. A Semi-Quantitative Method for RIP-Ribosome Binding

All RIPs inactivate mammalian ribosomes, although, as is well known, only some RIPs are capable of attacking ribosomes from plants, fungi, protists and bacteria (Boness *et al.* 1994). Hedblom *et al.* (1976), Ippoliti *et al.* (1992) and Chaddock *et al.* (1996) all suggested the similar hypothesis that since RTA possesses the correct active site structure to depurinate *E. coli* rRNA, the deciding factor for depurination *in vivo* and *in vitro* would be the presence of ribosomal proteins and their relative ability to interact with RIPs although they approached the problem from different directions. Ippoliti *et al.* (1992) referred to the fact that at least one ribosomal protein was involved in the interaction by the toxin. This was fully consistent with their observation that RIPs were more active on native ribosomes than on isolated rRNA, although is well recognised that a contrary situation occurred with RTA on *E. coli* ribosomes (reviewed extensively on the following Chapter). The analysis by Ippoliti *et al.* (1992), was based on the absence of a covalent complex when *E. coli* ribosomes were challenged with NSBr-modified saporin (which is the saporin reacted with bromoacetic acid N-hydroxysuccinate ester, showing the same inhibitory activity on rabbit reticulocyte lysate as native RTA). It was hypothesised that the resistance of some ribosomes was due to the low stability of the enzyme: substrate complex and / or the

lack of specific protein-protein interaction in the recognition site. Moreover, Hedblom *et al.* (1976) reported that ^{3}H-labelled ricin, bound in a ratio of 1mol/mol of ribosome with a dissociation constant of $3\mu M$ as calculated from a Scatchard plot. The subjects related on the Binding Equation of Scatchart are the molar concentration of the free labelled ricin in the final reaction volume; the number of binding sites per ribosome; the molar concentration of labelled ricin bound and the slope of the plotted line. A value of 0.87 was obtained for the number of ricin molecules bound per ribosome, indicating that there is only one ricin-binding site per ribosome.

It is unclear whether the binding of the RIP to the ribosome is always associated with the subsequent N-glycosidase activity, or whether certain RIPs that are inactive also bind to the ribosomes.

In order to investigate this, the semi-quantitative method as described in section 2.8.2. and based on the work of Ippoliti *et al.* (1992) was carried out. This consists mainly of mixing $1A_{260}$ unit of ribosome with the RIPs to be tested, and fractionating the mixing on 5-25% (w/w) sucrose linear gradient. The gradient was fractionated and the absorbance at 260nm was measured. The fractions are screened through their application to a nitro-cellulose filter held in a dot blot apparatus, and subsequently the filters are reacted with antibodies to identify the RIPs bound to ribosomes. The rRNA from the ribosomes incubated with the RIP was analysed for diagnostic depurination. The procedure allows RIP: ribosome complex formation to be detected, and to determine whether or not depurination of the rRNA occurs.

The RIP binding experiment was carried out in an attempt to detect the binding phenomenon between the three different RIPs, RTA, tritin-S and PAP, and the different ribosomes: rabbit reticulocyte ribosomes (RR ribosomes), wheat germ ribosomes (WG ribosomes) and *E. coli* ribosomes. Prior to obtaining the results from the proposed experiment, RIPs and ribosomes were assayed individually for dot blotting antigenic analysis (**Table 6** and **Table 7**). The antibodies used were anti-RTA, anti-tritin-S, and anti-PAP (a kind gift from M. Bonnes), produced within the Molecular Cell Biology Laboratory at the University of Warwick. **Table 6** shows the

Table 6. Dot blots of RTA, tritin-S and PAP.

RIPs	Primary Antiserum			µg	RIPs					Dot Blotting
		0.001	0.005	0.01	0.02	0.05	0.1	0.15	0.2	
RTA	Anti-RTA	0	0	xx	xx	xx	xx	xx	xx	
tritin-S	Anti-tritin-S	0	0	x	x	x	x	x	xx	
PAP	Anti-PAP	0	0	0	x	x	x	x	xx	
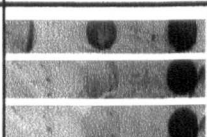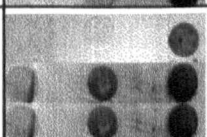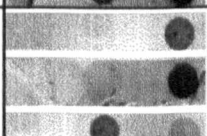
Track No. 1   2   3   4   5   6   7   8   1 2 3 4 5 6 7 8

0 = no reaction   x= reaction

2° antibody: 2.7µl of donkey α-sheep, conjugated to alkaline phosphatase to 20ml TBS-T-Marvel making a 1/7500 dilution.

Table 7. Dot blots of RR, WG and *E. coli* ribosomes showing reaction with RIP antibodies.

RIPs	Primary			μg		ribosomes			
	Antiserum	0	5	10	15	20			
RR	Anti-RTA	0	0	x	x	x			
WG		0	0	0	x	x			
E. coli		0	0	0	x	x			
RR	Anti-tritin-S	0	0	0	0	x			
WG		0	0	x	x	x			
E. coli		0	0	x	x	x			
RR	Anti-PAP	0	0	0	0	x			
WG		0	0	0	x	x			
E. coli		0	0	0	x	x			
Track No.		1	2	3	4	5	3	4	5

0 = no reaction   x= reaction

2° antibody: 2.7μl of donkey α-sheep, conjugated to alkaline phosphatase to 20ml TBS-T-Marvel making a 1/7500 dilution.

dot blots results of RTA, tritin-S and PAP, on a serial dilution of RIPs forming a colorimetric standard reference. **Table 6** shows the expected reaction of RTA, tritin-S and PAP with their respective polyclonal antibodies with a 0.01 μg detection limit in RTA and tritin-S, and 0.02 μg for PAP.

Table 7 shows the Dot blots of RR, WG and *E. coli* ribosomes in serial dilutions assayed for cross reactions with anti-RTA, anti-tritin-S, and anti-PAP antibodies. **Table 7** shows several reactions from different antibodies among the three kind of ribosomes. A possible explanation can be found in the general characteristics of polyclonal antibodies (Harlow and Lane, 1988), that because they are used as whole sera, they will contain the entire repertoire of circulating antibodies found in the immunised animal at the time that the serum was collected. Therefore, it is possible that the serum may contain high titered antibodies that specifically recognise spurious antigens. The serum may contain antibodies against bacteria or fungi that have infected the host animal recently or can cross-react with related antigens, similar to those against which the antiserum has been produced. On the other hand, it is well recognised that this type of possible anti-serum contamination is specific, hence it can not be removed by methods that are designed to lower non-specific backgrounds, for example more extensive blocking of the membrane or vigorous washing. A solution could be blocking the non-specific antibodies by pre-incubating the serum with a preparation that contains ribosomes (Harlow and Lane, 1988). Nevertheless, this experiment was abandoned and different approaches were tried until one was found suitable for subsequent use.

3.5. Radioactive Labelling of RTA as a Model

Based on Hedblom *et al.* (1976), Ippoliti *et al.* (1992) and Rice and Means (1971) experiments and methodologies for the quantitative analysis of the binding phenomenon, a ^{14}C-labelling of RTA as a model was carried out. The procedure described by Rice and Means (1971), has been used for radioactive labelling of proteins *in vitro* in which ^{3}H- or ^{14}C- methyl groups are attached to the protein's

amino group by reductive alkylation. This involves conversion of their amino groups to mono- and dimethylamino groups, where the mild reaction conditions do not alter the physicochemical properties of most proteins.

In order to confirm that the technique of ^{14}C-RTA labelling, through reductive alkylation of RTA by ^{14}C-formaldehyde, would not change the RTA activity towards ribosomes, a reductive alkylation of RTA by non-radioactive formaldehyde was carried out as a control. **Figure 8** compares the results of the activity of RTA and reductively alkylated RTA on RR ribosomes. One method used for confirmation of N-glycosidase activity of RTA on RR ribosomes is the aniline assay. The reaction buffer was that reported by Endo and Tsurugi (1988) (consisting of 25mM Tris/HCl pH 7.6, 25mM KCl and 5mM MgCl$_2$). The rationale for the use of the aniline assay is based on the fact that, once adenine has been removed from the ribosomes and/or 'naked' rRNA, leaving the sugar phosphate back bone intact, these phosphodiester bonds on either side of the depurinated ribose are sensitive to amine-catalysed hydrolysis at acidic pH by a β-elimination reaction (Peattie, 1979). The resulting fragments are then separated on a denaturing polyacrylamide or agarose gel.

Tracks 1-8 show the electrophoretic pattern of rRNA extracted from RR ribosomes after their incubation with:

    a) The reaction buffer alone as a negative control (track 1)

    b) The reaction buffer and aniline treatment as a negative control (track 5)

    c) With RTA and treated RTA in a 1:0.03 and 1:0.06 m.r. (molar ratio) where indicated, as positive control (tracks 2-4)

    d) rRNA from ribosomes treated with native rRNA (tracks 2 and 6) and formaldehyde - treated RTA (tracks 3, 4, 7, 8) subsequently incubated with aniline reagent (tracks tracks 6-8).

Tracks 6-8 show the aniline fragment, produced from rRNA by cleavage following depurination by the RIP. The fragment is equivalent to that reported previously for a depurination at position A$_{4324}$ in the rRNA from rat liver ribosomes (Endo and Tsurugi, 1988; Ippoliti et al., 1992). It can be seen that RR ribosomes have been

Figure 8. Comparative Results of the Activity of RTA on RR ribosomes using RTA with and without a Reductive Alkylation by Formaldehyde.
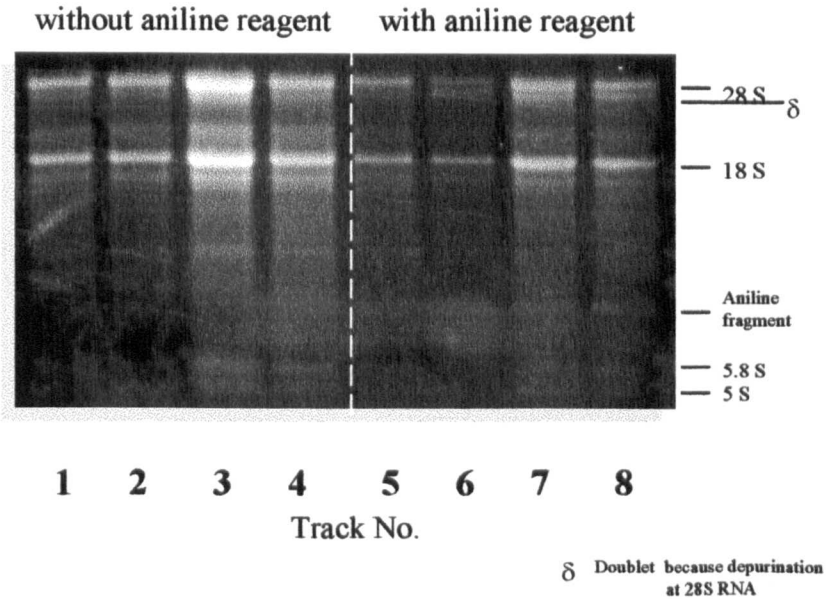
Electrophoretic profile from extracted RNA after incubation of RTA and reductive alkylated RTA with RR ribosomes. 3 μg were loaded onto a 1.2% agarose: formamide gel.

RTA activity on RR ribosomes with and without a reductive alkylation of RTA by Formaldehyde.

1) RR ribosomes
2) RR ribosomes + RTA   (1: 0.06 m.r.)
3) RR ribosomes + treated RTA   (1: 0.03 m.r.)
4) RR ribosomes + treated RTA   (1: 0.06 m.r.)
5) RR ribosomes + Aniline
6) RR ribosomes + RTA + Aniline (1: 0.06 m.r.)
7) RR ribosomes + treated RTA + Aniline (1: 0.03 m.r.)
8) RR ribosomes + treated RTA + Aniline (1: 0.06 m.r.)

115

depurinated by both RTA and treated RTA, even with a minimum concentration of RTA (10ng) (personal communication with Dr. Chaddock, 1996), or with treated RTA (10ng). This demonstrates that the reductive alkylation technique used for RTA ^{14}C labelling does not interfere with the *in vitro* rRNA N-glycosidase activity RTA.

According to previous results two RTA runs were carried out for C-14 labelling according to Rice and Means (1971). Once RTAs (RTA$_1$ and RTA$_2$) were labelled with ^{14}C-Formaldehyde and reduced with sodium borohydride, a dialysis step was carried out to eliminate small subproducts produced by this process. The scintillation counter was used to measure the percentage on ^{14}C- incorporated to RTA. Results obtained showed that this first reaction incorporated 12.8 times less ^{14}C- to that expected specific activity of ^{14}C of 5 x 10^6 cpm/mg protein (Rice and Means, 1971). A further second step labelling was carried out in order to obtain a preparation of specific activity of 5 x 10^6 cpm/mg of ^{14}C-RTA.

Figure 9 shows the SDS-PAGE silver stained electrophoretic pattern of both ^{14}C-RTAs. Tracks 1 and 8 show the mid-range molecular weight markers from Promega. Tracks marked with (-) are separator tracks between those with the ^{14}C-RTA electrophoretic profile. Tracks 2 and 3 show the electrophoretic profile of 16μg of both ^{14}C-RTAs respectively. Tracks 4 and 5 show the electrophoretic profile of 14 and 7 μg of ^{14}C-RTA$_1$ respectively, after a second ^{14}C-labelling process. Finally, tracks 6 and 7 show the electrophoretic profile of 14 and 7 μg of ^{14}C-RTA$_2$ respectively, after a second ^{14}C- labelling process. Generally, ^{14}C-RTA samples show four additional bands of lower molecular weight, products of degradation of the protein which were expected according to Hedblom *et al.*'s (1976) results, and which are not present on those unlabelled samples. The specific activity of the ^{14}C-RTA following two alkylation reactions with ^{14}C-formaldehyde, were approximately 2.07 x 10^{6}cpm/mg. It is noteworthy that labelled RTA obtained was tested for its binding to ribosomes, using sucrose gradient to separate free and bound RIP to ribosome and none was detected. Thus, the use of ^{125}I- instead of ^{14}C- for RTA labelling has been suggested, since the minimum 5 x 10^{6}cpm/mg of ^{14}C-RTA was not achievable a different approach was attempted. This is described in the following Chapters. It was done by analysing the role of r-proteins on RIPs' activity, using as a

Figure 9. SDS–PAGE silver stained electrophoretic pattern of ^{14}C-RTA.
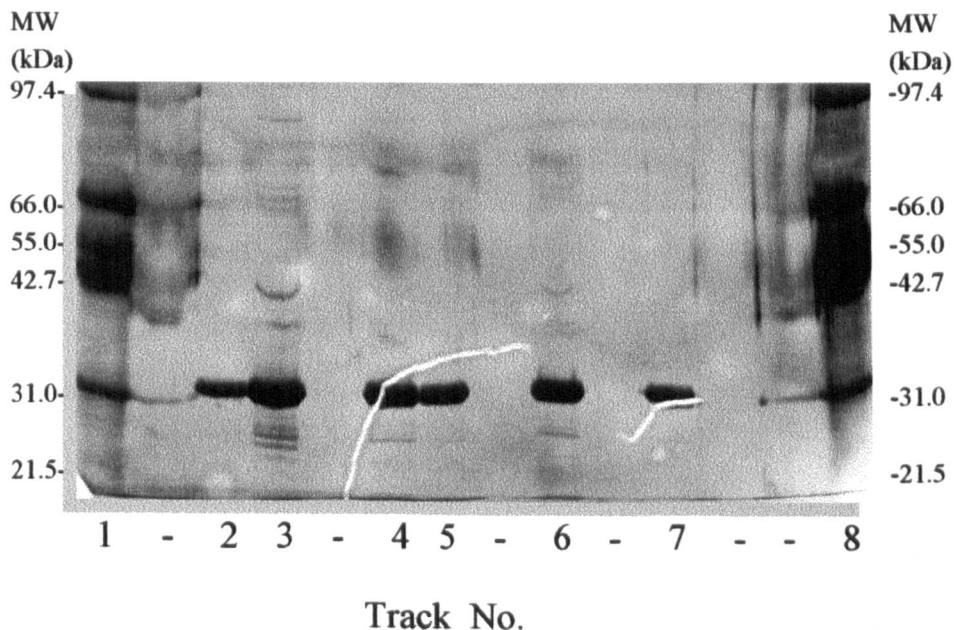
Electrophoretic profile of ^{14}C-RTA and made visible after a silver staining of the SDS-PAGE.

1) Molecular weight markers (Mid-range from Promega)
2) 16 μg ^{14}C-RTA$_1$
3) 16 μg ^{14}C-RTA$_2$
4) 14 μg ^{14}C-RTA$_1$ after a second ^{14}C- labelling proceedure
5) 7 μg ^{14}C-RTA$_1$ after a second ^{14}C- labelling proceedure
6) 14 μg ^{14}C-RTA$_2$ after a second ^{14}C- labelling proceedure
7) 7 μg ^{14}C-RTA$_2$ after a second ^{14}C- labelling proceedure
8) Molecular weight markers (Mid-range from Promega)

model the *E. coli* ribosome, which contains the N-glycosidase activity $GA_{2660}GA$ substrate in its 23S rRNA, but in which the sensitivity to RIPs varies.

3.6. Conclusions

The procedures used for the isolation, purification and quantification of the tritin-S from wheat seeds, were based on published protocols of Roberts and Stewart (1979), Barbieri *et al.*, (1987) and Massiah and Hartley, (1995). A second cation exchange chromatographic step was carried out, and because of the large volumes used in the isolation and purification of tritin-S; ultrafiltration was used for concentration.

The procedures of standardisation included the extraction of ribosomes from three different sources: wheat germ ribosomes, rabbit reticulocyte ribosomes and *E. coli* ribosomes (according to the procedures by Traub *et al.*, 1971; Jackson and Larkins, 1976). Three different RIPs were used, all of them showing a different N-glycosidase activity: PAP (type 1 RIP) which shows activity on plant, mammalian, yeast and *E. coli* ribosomes; tritin-S (type 1 RIP) which shows activity on mammalian and yeast ribosomes, but not on plant and on *E. coli* ribosomes; and RTA (ricin toxic A-chain) (type 2 RIP) which shows activity on plant mammalian and yeast ribosomes but not on *E. coli* ribosomes. Because of the selective activity of RIPs on different substrates is still only partially understood, because it has been reported that RIPs possess the correct active site structure for the depurination of ribosomes, and because is well known that RIPs N-glycosidase activity is carried out in a highly universally conserved rRNA sequence at the 23S-like ribosomal RNA, the intention of the research was to establish the functional activity of the RIPs. It was confirmed that PAP, tritin-S (in presence of 1mM ATP as reported by Massiah and Hartley, 1995) and RTA, all showed activity on rabbit reticulocyte ribosomes. The functional activity of the RIPs also was confirmed in order to establish the 'why and how' of the differences between the RIPs for substrate sensitivity.

With the evolution of knowledge of the RIPs, a series of discrepancies have become apparent. For example the report by Hedblom *et al.* (1970), that a binding ratio for ricin of 1mol/mol of ribosome has a dissociation constant of $3\mu M$ and elsewhere that a

single molecule will inactivate approximately 1500 ribosomes min⁻¹ (Gluck *et al.*, 1992). Or again it, has been suggested that because of the presence or absence of ribosomal proteins and their ability to interact with RIPs, the r-proteins make a difference to substrate sensitivity (Ippoliti *et al*, 1992). On the other hand, in the work on synthetic oligoribonucleotides, where substrates showed sensitivity to RIPs, this was attributed to the identity elements on the tertiary structure of the α-sarcin/ricin loop (Endo *et al.*, 1991).

Two approaches were used in the first part of the research in order to elucidate whether the binding of the RIP to the ribosome is always associated with subsequent N-glycosidase activity, or whether some RIPs can bind to ribosomes without the activity following. The approaches were based on the principle that RIPs bind to ribosomes and if the consequent complexes are subjected to centrifugation, it is possible to differentiate the sedimentation value of the complex of RIP: ribosome and after, its respective activity. The semi-quantitative approach identifies each of the components through sucrose gradient fractions, by specific recognition by RIPs antibodies. The experiments reported show that using the polyclonal antibodies was not discriminatory for ribosomes, thus the approach was inappropriate for the objectives of the research. The second approach, was based on Rice and Means (1971); Hedblom *et al.*, (1976); and Ippoliti *et al.*, (1992), and used the same principle of RIP: ribosome sedimentation profile for its identification after a sucrose gradient fractionation and analysis but using radioactive labelling of RIP instead of its anti-body identification. After the ¹⁴C-radiolabelling of RTA as a model was done, a series of standardisation was carried out also based on the identification of ¹⁴C-RTA as a RIP functionally equivalent to the native RTA. It was demonstrated that both radioactive labelled and native RTA were equivalent, showing that the alkylation process did not disrupt the active site and the subsequent N-glycosidase activity. Nevertheless, labelled RTA obtained and tested for its binding to ribosomes (using sucrose gradient to separate free and bound RIP to ribosome) was not detected. A possible reason for failure of this experiment could be that with the characteristic relatively weak binding of RTA (under the best contidions K_M 5μM), the toxin might be stripped off the ribosome during the sucrose preparation and so, binding was not detectable. In these

terms, an alternative approach based on the differences in sensitivity of the substrates for RIP activity were found. The different substrates consist of: substrate in its native conformation, or after this substrate has been deproteinised, with its subsequent conformational changes and so, difference on substrate sensitivity to RIPs' activity.

The following chapter attempts to give the general characteristics of PAP and RTA activity on both *E. coli* ribosomes and deproteinised ('naked') total rRNA.

4. CHAPTER IV:

GENERAL CHARACTERISTICS OF PAP AND RTA ACTIVITY
ON BOTH *E. COLI* RIBOSOMES AND 'naked' TOTAL rRNA

(as a Model for Research)

4.1. Introduction

The considerable variation that exists in the activities of RIPs on ribosomes from different organisms was reviewed in Chapter III. R-proteins also seem to play a very important role in the efficiency of RIP action. Although it is well known that the activity of RIPs on 'naked' rRNA substrates or synthetic oligonucleotides is present, the K_{cat} is as much as 10^5-fold lower than that with intact ribosomes. (Endo et al., 1987; Endo and Tsurugi, 1988; Hartley et al., 1991; Marchant and Hartley, 1994; Massiah, 1994). Endo et al. (1988), showed that the K_{cat} values for the reaction of the ricin A-chain on rat liver ribosomes and 'naked' rat liver 28S rRNA were 1777 and 0.02 min^{-1} respectively. This showed that the ricin A-chain has a much lower activity on 'naked' rRNA compared with that on 28S rRNA in rat liver ribosomes, and it suggested that, the native conformation of 28S rRNA in ribosomes was required for efficient catalysis. The importance of the secondary structure of the rRNA is emphasised by the fact that denatured 28S rRNA is not depurinated by RTA (Endo et al., 1987). It is possible that the interaction of the rRNA in the vicinity of the α-sarcin/ricin loop with r-proteins, alters the conformation of the rRNA in a way that makes it a more efficient substrate for RIP action. Gross structural changes in rRNA are known to occur on the binding of ribosomal proteins. (Batey and Williamson, 1996).

Massiah (1994) reported that tritin-S did not recognise 'naked' 28S rRNA because it's N-glycosidase activity was not detected at an rRNA: RIP molar ratio of 1:122, which was 18,000 times higher than the minimum m.r. of tritin-S: rRNA (6.8×10^{-3}) required for detectable activity on native ribosomes. N-glycosidase activity on 28S rRNA in reticulocyte ribosomes by tritin-S and RTA was similar. These results could be interpreted to show that tritin-S is more dependent for its action on the native structure of the ribosome than is RTA.

In addition, it has been reported that PAP modifies E. coli 23S rRNA in native E. coli ribosome (Hartley et al., 1991), in contrast to the A-chain of the type 2 RIPs abrin and ricin, which are inactive against bacterial ribosomes. It is recognised that PAP depurinates E. coli ribosomes in the 23S rRNA at position A_{2660} but both PAP and

RTA catalyse depurination of the rRNA in the 'naked' state. RTA has been shown not to bind directly to *E. coli* ribosomes (Hedblom *et al.*, 1976). The kinetic values for the reaction were almost the same for 'naked' 23S rRNA and for 'naked' 28S rRNA, suggesting that RTA is recognising a specific structure in the rRNA. Therefore, it seems that RTA is prevented from binding to *E. coli* ribosomes by interference from ribosomal proteins (Osborne, 1990). In the case of PAP, two mutant recombinant forms have been shown to inhibit eukaryotic protein synthesis *in vitro* but which were not toxic for *E. coli* (Dore *et al.*, 1993). However, Chaddock *et al.* (1996) reported results of the direct analysis of N-glycosidase activity on the same mutants which contradicted Dore *et al.*, (1993). One of the mutants implicates specific amino acids as participants in prokaryotic ribosome recognition while, in the second case, one of the recreated mutants retained its activity towards prokaryotic ribosomes whilst the other was inactive on prokaryotic ribosomes and very poorly active on eukaryotic ribosomes.

It was assumed that from the similarity in the structure of diverse RIPs, and especially the conservation of the active site that they would all recognise the same identity elements in rRNA (Endo *et al.*, 1991). However, work on mutant *E. coli* rRNA showed that PAP has less stringent identity element requirements than RTA (Marchant and Hartley, 1994).

In order to study the role of the r-proteins on the rRNA conformation required for RIP recognition, it is necessary to establish a model of PAP and RTA activity on *E. coli* ribosomes and 'naked' rRNA. In other words, to establish the conditions under which PAP is more active on native *E. coli* ribosomes than in 'naked' rRNA (Chapter V), and to asses the influence of the r-proteins through the successive removal of r-proteins from native subunits and monitoring the reduction in activity of PAP (Chapter VI).

4.2. Activity of PAP on *E. coli* ribosome and 'naked' total rRNA

One method used for confirmation of N-glycosidase activity of PAP on *E. coli* ribosomes and 'naked' rRNA is the aniline assay. Ribosomes and 'naked' rRNA were purified from an *E. coli* DH1 culture as described in sections 2.5.3. and 2.6. A TKMg buffer consisting of 25mM Tris/HCl pH 7.6, 25mM KCl and 5mM $MgCl_2$ (Endo *et al.*, 1991) was used as reaction buffer to assay the RIPs N-glycosidase activity.

Figure 10 shows the results of the N-glycosidase activity of PAP on *E. coli* ribosomes and 'naked' total rRNA. Tracks 1-6 show the electrophoretic pattern of rRNA extracted from *E. coli* ribosomes, and tracks 7-12 show rRNA extracted from 'naked' total rRNA after their respective incubation:

a) with the reaction buffer as negative control (tracks 1 and 7)

b) with PAP in a 1:1 molar ratio (m.r.) as a control without the aniline reagent (tracks 2 and 8)

c) with added aniline reagent for cleaving where depurination has occurred by PAP in serial dilutions of PAP of 1:1, 1:0.1, 1:0.01 and 1:0.001 (where indicated) substrate: PAP m.r. (Tracks 3-6 and 9-12).

Tracks 3, 4 and 9 show the aniline fragment, produced from rRNA cleavage by the activity of the aniline reagent once the PAP's N-glycosidase activity has occurred. The fragment is equivalent to that reported previously for a depurination at position A_{2660} of 23S rRNA (Marchant and Hartley, 1994). N-glycosidase activity of PAP is lower on 'naked' rRNA than on ribosomes by a factor of approx. 10, confirming previous observations (Marchant and Hartley, 1994). Although 23S rRNA contains the sequence $GA_{2660}GA$, the substrate for PAP activity, the results show the influence of r-proteins increases the efficiency of recognition and subsequently N-glycosidase activity. A further two assays were carried out (data not shown) in order to confirm the above results.

Figure 10. N-glycosidase activity of PAP on *E. coli* ribosomes and 'naked' total rRNA.
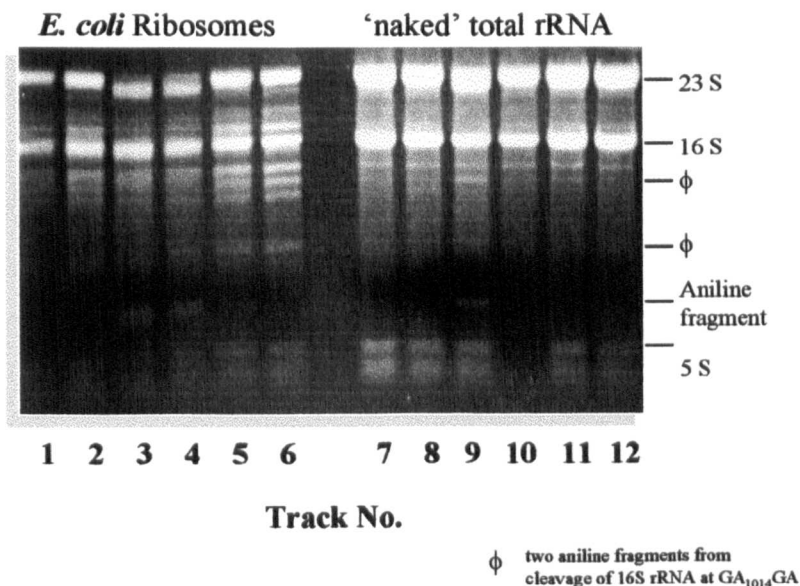
Electrophoretic profile of extracted rRNA after incubation. 3µg were loaded onto a 1.2% agarose: formamide gel. TKMg reaction buffer's final concentration: 25mM Tris/HCl pH 7.6, 25mM KCl, and 5mM $MgCl_2$.

1. *E. coli* ribosomes
2. *E. coli* ribosomes + PAP   (1:1 m.r.)
3. *E. coli* ribosomes + PAP + Aniline   (1:1 m.r.)
4. *E. coli* ribosomes + PAP + Aniline   (1:0.1 m.r.)
5. *E. coli* ribosomes + PAP + Aniline   (1:0.01 m.r.)
6. *E. coli* ribosomes + PAP + Aniline   (1:0.001 m.r.)
7. 'naked' total rRNA
8. 'naked' total RNA + PAP   (1:1 m.r.)
9. 'naked' total RNA + PAP + Aniline   (1:1 m.r.)
10. 'naked' total RNA + PAP + Aniline   (1:0.1 m.r.)
11. 'naked' total RNA + PAP + Aniline   (1:0.01 m.r.)
12. 'naked' total RNA + PAP + Aniline   (1:0.001m.r.)

4.3. Activity of RTA on *E. coli* ribosome and 'naked' total rRNA

Figure 11 shows the results of the N-glycosidase activity of RTA on *E. coli* ribosomes and 'naked' total rRNA in TKMg as the reaction buffer. Tracks 1-4 and 5-8, show the electrophoretic pattern of rRNA extracted from *E. coli* ribosomes and rRNA extracted from 'naked' total rRNA respectively. Tracks 1 and 5 show the substrate electrophoretic pattern as a negative control after it has been incubated with the reaction buffer alone, without either RTA or aniline reagents. Tracks 2 and 6 show the rRNA extracted from the incubation of the substrates with RTA but at a 1:1 substrate: RTA m.r. without cleaving the depurination site. Finally tracks 3 and 4, and 7 and 8, show the rRNA extracted from the incubation of the substrates with RTA and added aniline reagent, at substrate: RTA m.r. of 1:1 and 1:0.1.

None of the tracks showed the aniline fragment produced from the rRNA cleavage by the aniline reagent after RTA, N-glycosidase activity at equivalent amounts to PAP. However PAP showed the diagnostic aniline cleavage fragment (**Figure 10**, section 4.2.). The molar ratio of substrate: RTA was lower than that reported by Marchant and Hartley (1995) who used at least 100 times the amount of RTA for the reaction. RTA N-glycosidase activity assays were carried out twice more in order to confirm the above results (Data not shown). In order to compare PAP and RTA N-glycosidases activities and the influence of r-proteins, the substrate: RIPs molar ratio was maintained for PAP, and increased at least 10 times the amount of RTA for an initial molar ratio of serial dilutions of 1:10 substrate: RIPs.

Marchant and Hartley (1995) reported that the activity of both PAP and RTA was increased at least 10-fold in a reaction buffer containing EDTA compared with the widely used TKMg buffer, when RIP activity was assayed on mutant *E. coli* ribosomes.

Moreover, Gluck and Wool (1996) showed the effect of different complexes of divalent cation: chelating agent on the reaction buffer for RIPs' activity.

Figure 11. N-glycosidase activity of RTA on *E. coli* ribosomes and 'naked' total rRNA.
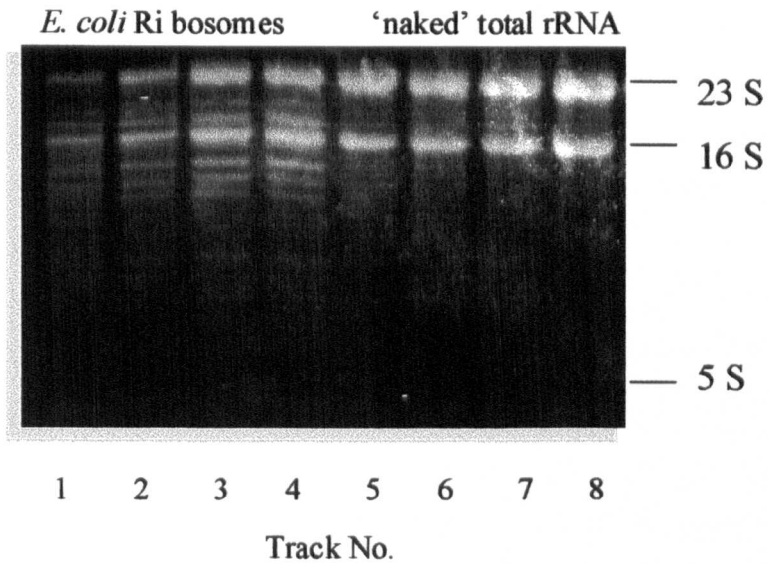
Electrophoretic profile from extracted RNA after incubation. 3μg were loaded onto a 1.2% agarose:formamide gel. TKMg reaction buffer's final concentration: 25mM Tris/HCl pH 7.6, 25mM KCl, and 5mM $MgCl_2$.

1. *E. coli* ribosomes
2. *E. coli* ribosomes + RTA   (1:1 m.r.)
3. *E. coli* ribosomes + RTA + Aniline   (1:1 m.r.)
4. *E. coli* ribosomes + RTA + Aniline   (1:0.1 m.r.)
5. 'naked' total rRNA
6. 'naked' total RNA + RTA   (1:1 m.r.)
7. 'naked' total RNA + RTA + Aniline   (1:1 m.r.)
8. 'naked' total RNA + RTA + Aniline   (1:0.1 m.r.)

4.4. Conclusions

Although it is well known that the majority of RIPs are active on 'naked' substrates or synthetic oligoribonucleotides and that the specificity of depurination at a single site is retained, is well known that the catalytic constant (K_{cat}) is much lower that that with intact ribosomes. (Endo *et al.* 1987; Endo and Tsurugi, 1988; Massiah and Hartley, 1995; Marchant and Hartley, 1995). These results suggest that the r-proteins play a very important role in the activity of RIPs.

The results of the experiments carried out here showed that the N-glycosidase activity of PAP decreased on 'naked' rRNA by a factor of 10x compared to the native substrate, confirming previous observations. Thus the results showed the influence of r-proteins in increasing the efficiency of depurination, possibly because r-proteins support a required rRNA conformation for PAP.

In the case of RTA, it was not possible to establish the differences between the sensitivity of the substrates to RTA at a 1:1 m.r. (substrate: PAP) under TKMg reaction buffer conditions. However, RTA activity has been reported both on a synthetic oligoribonucleotide mimicking the 23S rRNA of *E. coli* ribosomes (Endo et al., 1991) and in mutants of the α-sarcin loop of *Escherichia coli* 23S rRNA (Marchant and Hartley, 1995). Furthermore, the Marchant and Hartley (1995) work showed that the activity of both PAP and RTA was increased at least 10x in a reaction buffer containing EDTA. This observation was consistent with the results presented by Gluck and Wool, (1996) where they analysed the role of divalent cations and chelating agents for RTA activity on a 35mers mimicking the α-sarcin/ricin loop on 26S/28S rRNA.

In order to establish the influence of ribosomal proteins on the efficiency of catalysis by RIPs and in order to search for higher and consistent activity of both RIPs on the substrates, the next step was to seek a reaction medium where those differences between substrate sensitivity to RIPs would become more pronounced and consistent. Chapter V analyses a series of reaction buffers for the RIPs N-glycosidase assay.

5. CHAPTER V:

THE INFLUENCE OF DIFFERENT REACTION BUFFER CONDITIONS ON THE ACTIVITY OF RIPs ON BOTH *E. COLI* RIBOSOMES AND 'naked' TOTAL rRNA

5.1. Introduction

The majority of studies of RIP action on ribosomes *in vitro*, have been done in a buffer (near physiological conditions) of 25mM Tris/HCl pH 7.6, 25mM KCl and 5mM MgCl$_2$ and/ or 3mM Tris, 15mM NaCl, 3mM MgCl$_2$ and 2.5mM EDTA (Endo *et al.*, 1991; Gluck *et al.*, 1992). EDTA is added to reduce the concentration of Mg^{2+} to approx. 0.5mM, thought to be the optimal concentration for RTA activity (Gluck and Wool, 1996).

Gluck and Wool (1996) reinvestigated the dependence of RTA activity on Mg^{2+} and chelating agents. A 35-mer oligoribonucleotide, mimicking the structure at the site of action in ribosomes with 28S-like rRNA, was used for testing RTA activity and the influence of divalent cations-chelating agents. Their results showed an absolute requirement for Mg^{2+}or Ca^{2+} and a significant stimulation of activity in the presence of chelating agents. They showed also that RTA was more active in the presence of Ca^{2+}than Mg^{2+} and in the presence of EDTA than EGTA. According to these results, the divalent cation (Ca^{2+}) and the chelating agent (EGTA) complex had no effect on PAP activity, which is well characterised for having the same mechanism of action as RTA, when the same synthetic 35-mers oligoribonucleotide was used as substrate.

The reduction of α-sarcin activity by 50% on the phosphodiester bond at G$_{4325}$ in 28S rRNA, when the Ca^{2+}- EGTA complex was present, is also reported by Gluck and Wool (1996) which may suggest that the complex affects the RTA as it did to α-sarcin as their results suggested. Nevertheless, pre-treatments on either RTA or of the oligoribonucleotide, or of both, followed by the removal of the cation-chelator complex, did not yield a preparation of either RTA or rRNA that was competent in the N-glycosidase reaction. The addition of the cation-chelator complex to pre-treated RTA and/or on the rRNA as described above, resulted in efficient depurination (Gluck and Wool, 1996). So far, the understanding of the influence of the divalent cation-chelating agent on the N-glycosidase reaction by RIPs has not been reached.

This research project seeks to investigate the influence of ribosomal proteins (r-proteins) on the efficiency of catalysis by RIPs, and to search for higher and consistent activity of both RIPs, PAP and RTA, on *E. coli* ribosomes and their derivatives. The inclusion of EDTA, EGTA, the influence of pH and finally the inclusion of Ca^{2+} instead of Mg^{2+} in the reaction, were tested using the methods of previous researchers (Endo and Tsurugi, 1988; Gluck *et al.*, 1994; Gluck and Wool, 1996). The influence of divalent cation-chelating agent on the activity of PAP and RTA, with the *E. coli* ribosome, and its subparticles was analysed *in vitro*, using the same basis that Gluck and Wool (1996) reported for the 35-mer synthetic oligoribonucleotide mimicking the α-sarcin/ricin loop in 26/28S rRNA.

The *E. coli* ribosome and its derivatives were incubated with serial dilutions of PAP or RTA and different combinations of Mg^{2+}, Ca^{2+}, EDTA and EGTA, were used.

5.2. The Influence of Divalent Cation - EDTA on PAP and RTA activity

Figure 12 compares the results of the activity of PAP on *E. coli* ribosomes and on 'naked' total rRNA in two reaction buffers: TKMg (25mM Tris/HCl pH 7.6, 25mM KCl, 5mM $MgCl_2$) (Endo and Tsurugi, 1987) and TNaMgEDTA (3mM Tris base, 15mM NaCl, 3mM $MgCl_2$, 2.5mM EDTA, pH 5.0) (Gluck and Wool, 1996).

Figure 12 (I), tracks 1-12 show the electrophoretic pattern of rRNA extracted from *E. coli* ribosomes, following incubation with PAP in TKMg buffer (tracks 1-6) or TNaMgEDTA buffer (tracks 7-12). A negative profile is equivalent to the positive profile but it was chosen for presentation so that the results could be seen more clearly. **Figure 12 (II),** tracks 1 -10 show the rRNA extracted from the reaction mixture containing 'naked' total rRNA after their respective incubation with the reaction buffer and PAP in the same order than described for **Figure 12 (I).** In this case the positive profile was sufficiently clear to be used (whereas the negative profile was very light). Tracks 3-4, 9-11 (I), 3 and 8-9 (II) show the aniline fragment, produced from rRNA cleavage by the activity of the aniline reagent after the PAP, N-glycosidase activity has occurred. The fragment is equivalent to that reported previously for a depurination at position A_{2660} of 23S rRNA (Marchant and Hartley, 1994). The activity of PAP towards *E. coli* ribosomes is >10-fold higher in TNaMgEDTA buffer than in TKMg buffer.

131

Figure 12.Comparative Results between the Activity of PAP on *E. coli* ribosomes and 'naked' Total rRNA in both TKMg[(a)] and TNaMgEDTA[(b)] Buffers.
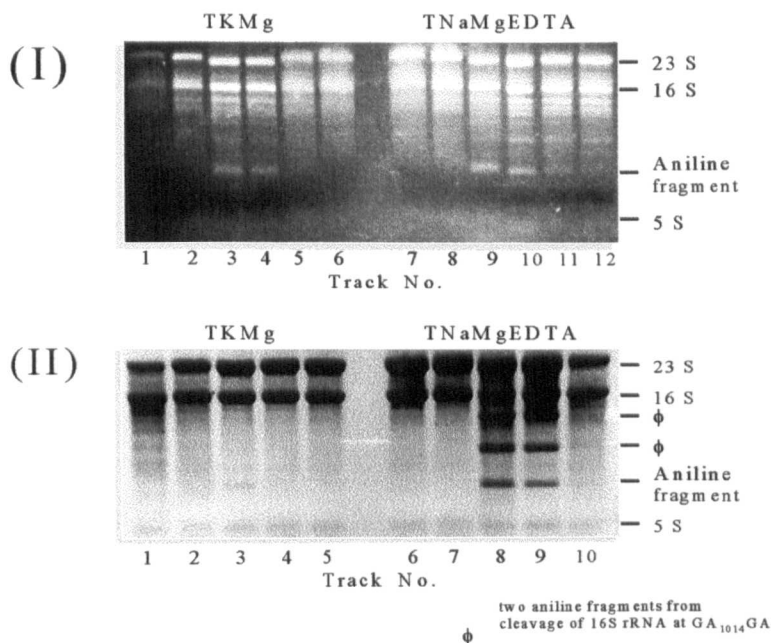
[(a)] TKMg reaction buffer final concentration: 25mM Tris/HCl pH 7.6, 25mM KCl, and 5mM $MgCl_2$.
[(b)] TNaMgEDTA reaction buffer final concentration: 3mM Tris base, 15mM NaCl, 3mM $MgCl_2$, 2.5mM EDTA final pH 5.0. Electrophoretic profile of extracted rRNA after incubation. 3μg were loaded onto a 1.2% agarose: formamide gel.

(I) PAP activity on *E. coli* ribosomes on TKMg (Tracks 1-6) and TNaMgEDTA (Tracks 7-12)

        1. *E. coli* ribosomes
        2. *E. coli* ribosomes + PAP   (1:1 m.r.)
        3. *E. coli* ribosomes + PAP + aniline   (1:1 m.r.)
        4. *E. coli* ribosomes + PAP + aniline   (1:0.1 m.r.)
        5. *E. coli* ribosomes + PAP + aniline   (1:0.01 m.r.)
        6. *E. coli* ribosomes + PAP + aniline   (1:0.001 m.r.)
        7. *E. coli* ribosomes
        8. *E. coli* ribosomes + PAP   (1:1 m.r.)
        9. *E. coli* ribosomes + PAP + aniline   (1:1 m.r.)
        10. *E. coli* ribosomes + PAP + aniline   (1:0.1 m.r.)
        11. *E. coli* ribosomes + PAP + aniline   (1:0.01 m.r.)
        12. *E. coli* ribosomes + PAP + aniline   (1:0.001 m.r.)

(II) PAP activity on 'naked' total rRNA on TKMg (Tracks 1-5) and TNaMgEDTA (Tracks 6-10)

        1. 'naked' total rRNA
        2. 'naked' total rRNA + PAP   (1:1 m.r.)
        3. 'naked' total rRNA + PAP + aniline   (1:1 m.r.)
        4. 'naked' total rRNA + PAP + aniline   (1:0.1 m.r.)
        5. 'naked' total rRNA + PAP + aniline   (1:0.01 m.r.)
        6. 'naked' total rRNA
        7. 'naked' total rRNA + PAP   (1:1 m.r.)
        8. 'naked' total rRNA + PAP + aniline   (1:1 m.r.)
        9. 'naked' total rRNA + PAP + aniline   (1:0.1 m.r.)
        10. 'naked' total rRNA + PAP + aniline   (1:0.01 m.r.)

Figure 12 (II) shows that the activity of PAP on total rRNA was also approx. 10-fold higher the TNaMgEDTA buffer than in the TKMg buffer, since the aniline fragment was present in a 1:1m.r. (substrate:RIPs) in both cases, but only with TNaMgEDTA buffer it was possible to observe activity in a 1:0.1m.r.(substrate:RIPs). Additionally, a second and third extra-bands can be seen, corresponding to the depurination at A_{1014} on 16S rRNA (Tracks 8-9(II)) reported by Marchant and Hartley (1994), which was not shown when TKMg was the reaction buffer.

Figure 12 (I) and **(II)** show results which suggest that, besides the addition of EDTA increasing PAP activity, the combination of this factor with the deproteinisation of the ribosomes, resulted in the activity of PAP on another, well characterised sensitive structure centred on A_{1014} in 16S rRNA. These results differ from those of Gluck and Wool (1996) who found no difference in PAP activity when activity was assumed on the 35-mer oligoribonucleotide (mimicking the α-sarcin/ricin loop in 26/28S rRNA) in the presence of the divalent cation-chelating agent complex.

A possible explanation for the increased sensitivity could be that the depletion of Mg^{2+} by EDTA causes the partial dissociation of the subunits or some other ribosomal structure, which in (I) renders the α-sarcin/ricin loop more accessible to PAP action. In contrast, the RIP-sensitive site in 16S rRNA (A_{1014}) is not made accessible by the treatment.

Figure 13 shows the comparative results between the activity of RTA on *E. coli* ribosomes and on 'naked' total rRNA in both reaction buffers, TKMg and TNaMgEDTA as described for **Figure 12**. Negative and positive profiles are equivalent to their positive and negative profiles respectively on both cases but one or other were chosen for presentation so that the results could be seen more clearly.

Tracks 1-4 and 5-8 show the electrophoretic pattern of rRNA extracted from reaction mixture containing *E. coli* ribosomes and 'naked' total rRNA respectively in TKMg buffer. Tracks 9-12 and 13-16 show rRNA extracted from reaction mixture containing *E. coli* ribosomes and from 'naked' total rRNA respectively in TNaMgEDTA buffer. Tracks 1, 5, 9, and 13 show the control reaction in which either RTA or aniline treatments have been omitted.

Figure 13. Comparative Results between the Activity of RTA on *E. coli* ribosomes and 'naked' Total rRNA in both TKMg[(a)] and TNaMgEDTA[(b)] Buffers.

^(a) TKMg reaction buffer's final concentration: 25mM Tris/HCl pH 7.6, 25mM KCl, and 5mM MgCl$_2$.
^(b) TNaMgEDTA reaction buffer's final concentration: 3mM Tris base, 15mM NaCl, 3mM MgCl$_2$, 2.5mM EDTA final pH 5.0

Electrophoretic profile of extracted rRNA after incubation. 3µg were loaded onto a 1.2% agarose: formamide gel.

(a) RTA activity on *E. coli* ribosomes and 'naked' total rRNA in TKMg buffer.
    1. *E. coli* ribosomes
    2. *E. coli* ribosomes + RTA   (1:10 m.r.)
    3. *E. coli* ribosomes + RTA + aniline   (1:10 m.r.)
    4. *E. coli* ribosomes + RTA + aniline   (1:1 m.r.)
    5. 'naked' total rRNA
    6. 'naked' total rRNA + RTA   (1:10 m.r.)
    7. 'naked' total rRNA + RTA + aniline   (1:10 m.r.)
    8. 'naked' total rRNA + RTA + aniline   (1:1 m.r.)

(b) RTA activity on *E. coli* ribosomes and 'naked' total rRNA in TNaMgEDTA
    9. *E. coli* ribosomes
    10. *E. coli* ribosomes + RTA   (1:10 m.r.)
    11. *E. coli* ribosomes + RTA + aniline   (1:10 m.r.)
    12. *E. coli* ribosomes + RTA + aniline   (1:1 m.r.)
    13. 'naked' total rRNA
    14. 'naked' total rRNA + RTA   (1:10 m.r.)
    15. 'naked' total rRNA + RTA + aniline   (1:10 m.r.)
    16. 'naked' total rRNA + RTA + aniline   (1:1 m.r.)

Tracks 2, 6, 10 and 14 show rRNA extracted from the reaction mixture in their respective reaction buffers with RTA (at a 1:10 substrate: RTA molar ratio) but without aniline treatment. Finally tracks 3-4, 7-8, 11-12, and 15-16, show the rRNA extracted from the reaction mixture in their respective reaction buffers with RTA in a 1:10 and 1:1 (substrate: RTA) molar ratio, followed by aniline treatment.

Tracks 11 and 15 also show the aniline fragment, produced from the rRNA cleavage by the aniline reagent after RTA, N-glycosidase activity. This fragment is equivalent to a depurination at position A_{2660} of 23S rRNA already reported (Hartley *et al.*, 1991; Marchant and Hartley, 1994; Chaddock *et al.* 1996). Track 15 also shows a second and third aniline fragment, which are equivalent to those reported by Marchant and Hartley (1995), and which correspond to the depurination at A_{1014} of 16S rRNA.

The results suggest that the inclusion of EDTA in the reaction buffer increase RTA activity on both *E. coli* ribosomes and 'naked' total rRNA at least 10-fold compared to the TKMg buffer. The results agree partially with those of Gluck and Wool (1996) who showed that RTA had a low, but detectable activity on the 35-mer synthetic oligoribonucleotide in the presence of 5mM EDTA and 5-10mM $MgCl_2$. The detection of RTA activity on *E. coli* ribosomes is a novel finding.

It is noteworthy that the RTA activity on 'naked' total rRNA in a 1:10 m.r. reported by Marchant and Hartley (1995), is also reported by Endo *et al.*, (1991) (reviewed by Hartley and Lord, 1993), where the 23S rRNA was the substrate for RTA activity. The series of experiments was replicated (data not shown) confirming the activity of RTA on both *E. coli* ribosomes and 'naked' total rRNA when EDTA was present.

In order to produce an EDTA buffer with a higher Mg^{2+} concentration, based on the Mg^{2+} concentration of the TKMg buffer, a second set of tests were carried out on a TNaMgEDTA* (3mM Tris base, 15mM NaCl, 5mM $MgCl_2$, 5mM EDTA pH 5.0) reaction buffer (data not shown). The results were similar to those for the original TNaMgEDTA buffer (3mM Tris base, 15mM NaCl, 3mM $MgCl_2$, 2.5mM EDTA pH 5.0 as final concentration).

Mg^{2+} was replaced by Ca^{2+} in the presence of EDTA according to Gluck and Wool (1996) (**Figures 14** and **15**).

Figure 14 shows the comparative results between the activity of PAP on *E. coli* ribosomes and on 'naked' total rRNA, in the reaction buffers, TKMg (25mM Tris/HCl pH 7.6, 25mM KCl, 5mM $MgCl_2$) and TNaCaEDTA (3mM Tris base, 15mM NaCl, 5mM $CaCl_2$, 5mM EDTA, adjusted pH 8.0 with NaOH).

Tracks 1-6(I), 7-12(II) show rRNA extracted from *E. coli* ribosomes, and tracks 13-18(II) show rRNA extracted from 'naked' total rRNA incubated with PAP. Tracks 1(I), 7, 13 (II) are controls and refer to rRNA incubated without PAP. Tracks 9, 14(II) contain the extracted rRNA acting as controls without adding the aniline reagent for cleaving where depurination has occurred using PAP in serial dilutions to give 1:1, 1:0.1, 1:0.01 and 1:0.001 (where indicated) substrate: PAP molar ratios. Tracks 2-5(I) and 8(II) show the aniline fragment from the molar ratios previously reviewed. Track 15 shows a non-specific cleavage-like profile of rRNA by PAP, but where three major bands, one at the reported position for A_{2660} and two at the reported position for A_{1014} depurination, can be seen.

The results shown in **Figure 14** suggest that PAP in combination with Ca^{2+} and EDTA cause non-specific depurination. The generation of the 'smear' of rRNA cannot be due to RNase activity, since its formation is dependent on treatment with aniline.

The N-glycosidase activity of RTA was also analysed in a Ca^{2+}-EDTA buffer. **Figure 15** shows the comparative results of RTA activity in both TKMg and TNaCaEDTA buffers as described for **Figure 14**.

Tracks 1-12 in **Figure 15(I)**, show the electrophoretic pattern of rRNA extracted from *E. coli* ribosomes, and tracks 1-12(II) show rRNA extracted from 'naked' total rRNA, after their respective incubation either with:

a) only the reaction buffer as negative controls (tracks 1 and 7 from (I) and (II) respectively),

Figure 14. Comparative Results between the Activity of PAP on *E. coli* ribosomes and 'naked' Total rRNA in both TKMg[a] and TNaCaEDTA[b] Buffers.
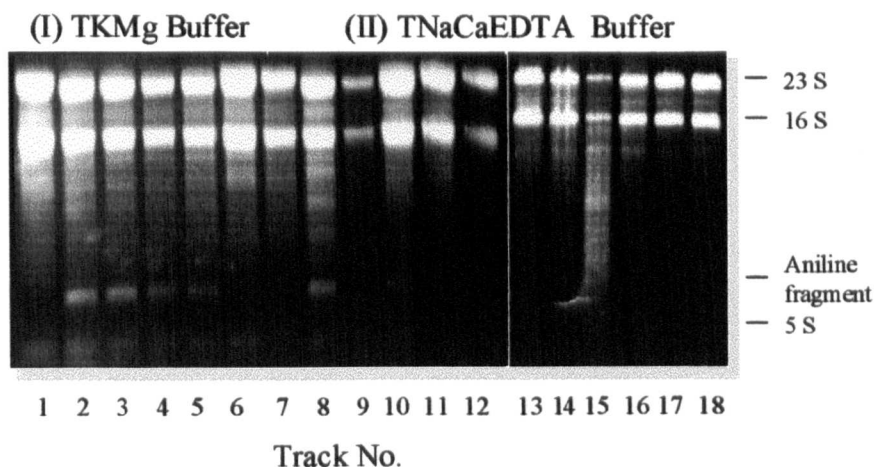
(a) TKMg reaction buffer final concentration: 25mM Tris/HCl pH 7.6, 25mM KCl, and 5mM MgCl$_2$.

(b) TNaCaEDTA reaction buffer final concentration: 3mM Tris base, 15mM NaCl, 5mM MgCl$_2$,   5mM EDTA (adjusted pH 8.0 with NaOH)

Electrophoretic profile of extracted rRNA after incubation. 3μg were loaded onto a 1.2% agarose: formamide gel.

(I) PAP activity on *E. coli* ribosomes on TKMg buffer

    1. *E. coli* ribosomes

    2. *E. coli* ribosomes + PAP + aniline   (1:1 m.r.)

    3. *E. coli* ribosomes + PAP + aniline   (1:1 m.r.)

    4. *E. coli* ribosomes + PAP + aniline   (1:0.1 m.r.)

    5. *E. coli* ribosomes + PAP + aniline   (1:0.01 m.r.)

    6. *E. coli* ribosomes + PAP + aniline   (1:0.001 m.r.)

(II) PAP activity on *E. coli* ribosomes and on 'naked' total rRNA on TNaCaEDTA buffer

    7. *E. coli* ribosomes

    8. *E. coli* ribosomes + PAP + aniline   (1:1 m.r.)

    9. *E. coli* ribosomes + PAP   (1:1 m.r.)

    10. *E. coli* ribosomes + PAP + aniline   (1:0.1 m.r.)

    11. *E. coli* ribosomes + PAP + aniline   (1:0.01 m.r.)

    12. *E. coli* ribosomes + PAP + aniline   (1:0.001 m.r.)

    13. 'naked' total rRNA

    14. 'naked' total rRNA + PAP   (1:1 m.r.)

    15. 'naked' total rRNA + PAP + aniline   (1:1 m.r.)

    16. 'naked' total rRNA + PAP + aniline   (1:0.1 m.r.)

    17. 'naked' total rRNA + PAP + aniline   (1:0.01 m.r.)

    18. 'naked' total rRNA + PAP + aniline   (1:0.001m.r.)

Figure 15. Comparative Results between the Activity of RTA on *E. coli* ribosomes and 'naked' Total rRNA in both TKMg[(a)] and TNaCaEDTA[(b)] Buffers.

Electrophoretic profile of extracted rRNA after incubation. 3μg were loaded onto a 1.2% agarose: formamide gel.

(I) RTA activity on *E. coli* ribosomes in TKMg (tracks 1-6) and in TNaCaEDTA (tracks 7-12)

1. *E. coli* ribosomes
2. *E. coli* ribosomes + RTA   (1:10 m.r.)
3. *E. coli* ribosomes + RTA + aniline   (1:10 m.r.)
4. *E. coli* ribosomes + RTA + aniline   (1:1 m.r.)
5. *E. coli* ribosomes + RTA + aniline   (1:0.1 m.r.)
6. *E. coli* ribosomes + RTA + aniline   (1:0.01 m.r.)
7. *E. coli* ribosomes
8. *E. coli* ribosomes + RTA   (1:10 m.r.)
9. *E. coli* ribosomes + RTA + aniline   (1:10 m.r.)
10. *E. coli* ribosomes + RTA + aniline   (1:1 m.r.)
11. *E. coli* ribosomes + RTA + aniline   (1:0.1 m.r.)
12. *E. coli* ribosomes + RTA + aniline   (1:0.01 m.r.)

(II) RTA activity on 'naked' total rRNA in TKMg (tracks 1-6) and in TNaCaEDTA (tracks 7-12)

1. 'naked' total rRNA
2. 'naked' total rRNA + RTA   (1:10 m.r.)
3. 'naked' total rRNA + RTA + aniline   (1:10 m.r.)
4. 'naked' total rRNA + RTA + aniline   (1:1 m.r.)
5. 'naked' total rRNA + RTA + aniline   (1:0.1 m.r.)
6. 'naked' total rRNA + RTA + aniline   (1:0.01 m.r.)
7. 'naked' total rRNA
8. 'naked' total rRNA + RTA   (1:10 m.r.)
9. 'naked' total rRNA + RTA + aniline   (1:10 m.r.)
10. 'naked' total rRNA + RTA + aniline   (1:1 m.r.)
11. 'naked' total rRNA + RTA + aniline   (1:0.1 m.r.)
12. 'naked' total rRNA + RTA + aniline   (1:0.01m.r.)

138

b) with RTA in a 1:10 m.r. as positive controls (tracks 2 and 8 from (I) and (II) respectively),

c) also shown in the effect of the aniline reagent on rRNA from ribosomes and 'naked' rRNA incubated with RTA in serial dilutions of RTA to give 1:10, 1:1, 1:0.1 and 1:0.01 substrate:RTA molar ratio (tracks 3-6 and 9-12 in (I) and (II) respectively).

None of the tracks 1-12 (I) shows the aniline fragment, although tracks 8 and 9 (II), show a smear-like pattern, similar to the track 15(II) on **Figure 14** where PAP was tested for N-glycosidase activity on 'naked' total rRNA in a TNaCaEDTA buffer.

Figure 15, tracks 9 and 10, show three aniline fragments resulting from the depurination of 23S rRNA at A_{2660} and 16S rRNA at A_{1014}. A similar pattern was seen when RTA was assayed on 'naked' total rRNA **(Figure 13)**. However, the activity in the buffer containing EDTA/Ca^{2+} seems to be similar to the buffer containing Mg^{2+}. The characteristics of tracks 9 and 10, are similar to those shown in **Figure 12** (tracks 8 and 9 for PAP activity of 'naked' total rRNA in a Mg^{2+}-EDTA buffer solution). However, the electrophoretic pattern in tracks 9 and 10 is not as clear and strong as the pattern produced in the assay using PAP.

The activity of both PAP and RTA is approx. 0 to 10-fold higher in the TNaCaEDTA buffer than in the TKMg buffer. There is agreement with Gluck and Wool (1996) in that the EDTA-divalent cation enhances RTA action. However, Gluck and Wool (1996) reported that the EDTA-divalent cation complex, in contrast to the findings presented here, did not enhance the activity of PAP. The experimental systems were not directly comparable, since Gluck and Wool (1996) used the synthetic 35-mer oligoribonucleotide as their substrate.

5.3. The Influence of Ca^{2+}-EGTA on PAP and RTA activity

PAP and RTA activity were tested using the EGTA - divalent cation reaction buffer. **Figure 16** shows the comparative results between the activity of PAP on *E. coli* ribosomes and 'naked' total rRNAs in both TKMg (described previously) and TNaCaEGTA (3mM Tris/HCl pH 7.6, 15mM NaCl, 5mM $CaCl_2$ and 5mM EGTA -adjusted pH 8.0 with NaOH-).

Figure 16. Comparative Results between the Activity of PAP on *E. coli* ribosomes and 'naked' Total rRNA in both TKMg[a] and TNaCaEGTA[b] Buffers.
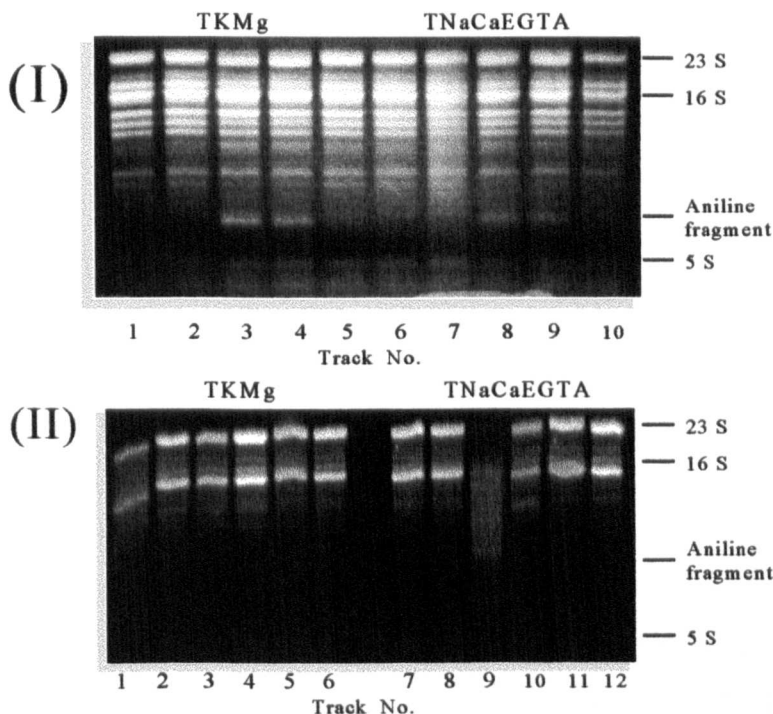
(a) TKMg reaction buffer final concentration: 25mM Tris/HCl pH 7.6, 25mM KCl, and 5mM MgCl$_2$.

(b) TNaCaEGTA reaction buffer final concentration: 3mM Tris base, 15mM NaCl, 5mM MgCl$_2$, 5mM EGTA (adjusted pH 8.0 with NaOH)

Electrophoretic profile of extracted rRNA after incubation. 3μg were loaded onto a 1.2% agarose:formamide gel.

(I) PAP activity on *E. coli* ribosomes in TKMg (tracks 1-5) and TNaCaEGTA (tracks 6-10)

1. *E. coli* ribosomes
2. *E. coli* ribosomes + PAP   (1:1 m.r.)
3. *E. coli* ribosomes + PAP + aniline   (1:1 m.r.)
4. *E. coli* ribosomes + PAP + aniline   (1:0.1 m.r.)
5. *E. coli* ribosomes + PAP + aniline   (1:0.01 m.r.)
6. *E. coli* ribosomes
7. *E. coli* ribosomes + PAP   (1:1 m.r.)
8. *E. coli* ribosomes + PAP + aniline   (1:1 m.r.)
9. *E. coli* ribosomes + PAP + aniline   (1:0.1 m.r.)
10. *E. coli* ribosomes + PAP + aniline   (1:0.01 m.r.)

(II) PAP activity on 'naked' total rRNA in TKMg (tracks 1-6) and TNaCaEGTA (tracks 7-12)

1. 'naked' total rRNA
2. 'naked' total rRNA + PAP   (1:1 m.r.)
3. 'naked' total rRNA + PAP + aniline   (1:1 m.r.)
4. 'naked' total rRNA + PAP + aniline   (1:0.1 m.r.)
5. 'naked' total rRNA + PAP + aniline   (1:0.01 m.r.)
6. 'naked' total rRNA + PAP + aniline   (1:0.001 m.r.)
7. 'naked' total rRNA
8. 'naked' total rRNA + PAP   (1:1 m.r.)
9. 'naked' total rRNA + PAP + aniline   (1:1 m.r.)
10. 'naked' total rRNA + PAP + aniline   (1:0.1 m.r.)
11. 'naked' total rRNA + PAP + aniline   (1:0.01 m.r.)
12. 'naked' total rRNA + PAP + aniline   (1:0.001m.r.)

buffers. Tracks 1-5 (I) and 1-6 (II) show a representative set of the differences of PAP activity on native *E. coli* ribosomes and deproteinised rRNA obtained throughout the whole research project, where deproteinisation results in at least 10-fold less activity of PAP in the TKMg reaction buffer than in the TNaCaEGTA buffer.

There was no difference in PAP activity between the two assays using *E. coli* ribosome as substrate with TKMg and with TNaCaEGTA reaction buffers (Tracks 1-10(I)). This result was different from that obtained in **Figure 14** where the Ca^{2+}-EDTA inclusion was assayed. The Ca^{2+}-EDTA affected the PAP activity on 'naked' rRNA to the extent of having a smeared profile indicative of a non-specific depurination in a 1:1 substrate: PAP m.r. This suggests that Ca^{2+} and EDTA influence PAP activity when the r-proteins are present, but Ca^{2+} and EGTA do not.

Tracks 6-10 (I) and 7-12 (II) show the PAP activity on both substrates (*E. coli* ribosomes and 'naked' total rRNA respectively) but now with the inclusion of Ca^{2+}-EGTA. Tracks 8-9 (I) and 9-10 (II) show the aniline fragment characteristic of the depurination on A_{2660}. Additionally tracks 9 and 10 (II) show the two aniline fragment characteristic of a depurination at position A_{1014}. These aniline fragments appeared with the Ca^{2+}-EDTA inclusion at the same substrate RIP molar ratio, but it was at least 10-fold more sensitive with Ca^{2+}-EGTA, although the aniline fragments' bands were much less strong than when the Mg^{2+}-EDTA reaction buffer was included (**Figure 12**). Moreover, the profile of track 9 (II) **Figure 16** and track 9 (II) **Figure 14** show the non-specific depurination tendency. This suggests that Ca^{2+} in the presence of EDTA or EGTA alters the target site specificity of PAP, so it becomes less stringent.

The N-glycosidase activity of RTA was assayed with Ca^{2+} - EGTA. **Figure 17** shows the comparative results of the activity of RTA on 'naked' total rRNAs in both TKMg (tracks 1-4), and TNaCaEGTA (tracks 5-9). The tracks 7 and 8 show the three aniline fragments, which correspond: one to a depurination at A_{2660} and two to a depurination at A_{1014}. The combination of Ca^{2+}-

141

Figure 17. Comparative Results between the Activity of RTA on 'naked' Total RNA in both TKMg[a] and TNaCaEGTA[b] Buffers.
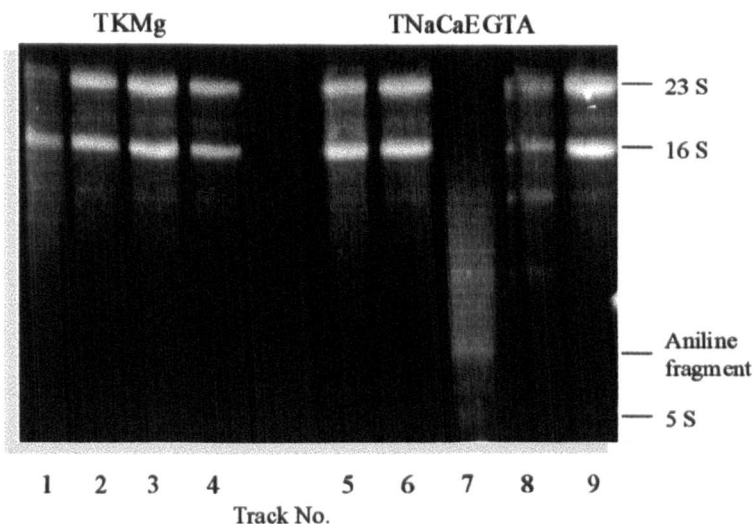
[a] TKMg reaction buffer final concentration: 25mM Tris/HCl pH 7.6, 25mM KCl, and 5mM $MgCl_2$.
[b] TNaCaEGTA reaction buffer final concentration: 3mM Tris base, 15mM NaCl, 5mM $CaCl_2$,   5mM EGTA -adjusted pH 8.0 with Na0H-
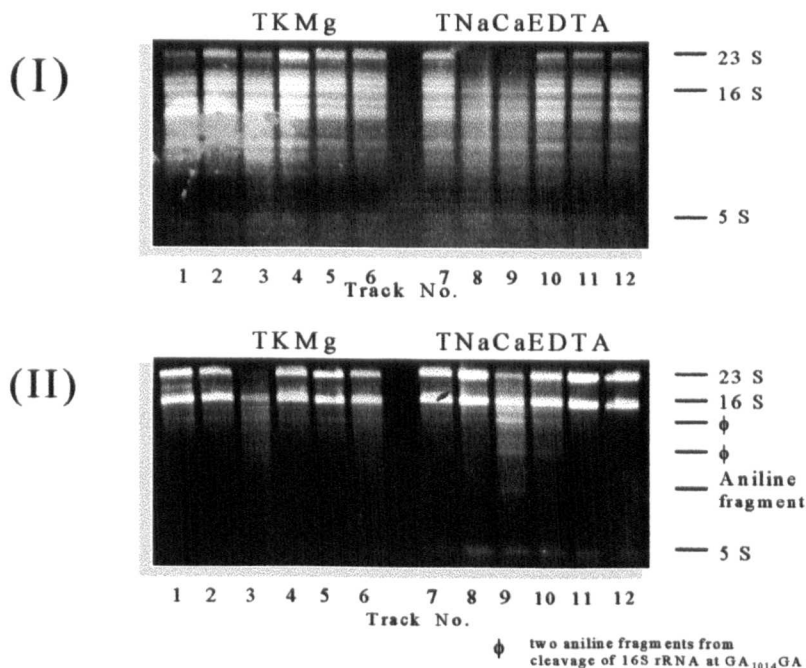Electrophoretic profile of extracted rRNA after incubation. 3μg were loaded onto a 1.2% agarose: formamide gel.

RTA activity on 'naked' rRNA in TKMg (tracks 1-4) and in TNaCaEGTA (tracks 5-9)
    1. 'naked' total rRNA + RTA + aniline   (1:10 m.r.)
    2. 'naked' total rRNA + RTA + aniline   (1:1 m.r.)
    3. 'naked' total rRNA + RTA + aniline   (1:0.1 m.r.)
    4. 'naked' total rRNA + RTA + aniline   (1:0.01 m.r.)
    5. 'naked' total rRNA
    6. 'naked' total rRNA + RTA   (1:10 m.r.)
    7. 'naked' total rRNA + RTA + aniline   (1:10 m.r.)
    8. 'naked' total rRNA + RTA + aniline   (1:1 m.r.)
    9. 'naked' total rRNA + RTA + aniline   (1:0.1 m.r.)

EGTA shows a more degraded rRNA profile, suggesting non-specific depurination. Two additional aniline fragments compared with when Ca^{2+}-EDTA was present are superimposed on this 'smear'. The above result was also similar to that obtain by PAP under the same conditions (**Figure 16**).

Gluck and Wool (1996) showed that RTA was more active on the 35-mer oligoribonucleotide, in Ca^{2+}-EGTA than Ca^{2+}-EDTA, even when the EGTA concentration was higher than that of Ca^{2+}. This did not occur when EDTA was in excess and could explain why in a 5mM Ca^{2+}- 5mM EGTA buffer, the rRNA electrophoretic profile showed a tendency to non-specific depurination. This did not happen for a 5mM Ca^{2+}-5mM EDTA buffer, unless activity on 'naked' total rRNA. A possible explanation might be that the divalent cation-chelating agent complex enhances both RTA and PAP activity. In the absence of r-proteins both complexes (Ca^{2+}/chelating agent) permit non-specific depurination.

5.4. The Influence of Ca^{2+} instead of Mg^{2+} on PAP and RTA activity

Since analysis has established that the activity of PAP and RTA in different Mg^{2+} and Ca^{2+}- chelating agent- containing buffers differed the effects of the replacement of Mg^{2+} with Ca^{2+} was assayed in 'near physiological' buffers lacking chelating agents.

Figure 18 shows the results of the activity of PAP on *E. coli* ribosomes and 'naked' total rRNA in TKCa buffer (25mM Tris/HCl pH 7.6, 25mM KCl and 5mM $CaCl_2$) instead of TKMg buffer described previously.

Figure 18 shows rRNA extracted from reaction mixture containing *E. coli* ribosomes (tracks 1-6) and 'naked' total rRNA respectively (tracks 7-12), following incubation either:

        a) with the reaction buffer alone as negative controls (tracks 1 and 7),

        b) with PAP in a 1:1 m.r. as non-aniline controls (tracks 2 and 8), or

        c) with added aniline reagent for cleaving where depurination has been effected by PAP in serial dilutions of PAP to give 1:1, 1:0.1, 1:0.01, and 1:0.001 (where indicated) substrate: PAP m.r. (tracks 3-6 and 9-12).

Figure 18. Comparative Results between the Activity of PAP on *E. coli* ribosomes and 'naked' Total rRNA in TKCa.

E. coli Ribosomes   'naked' total rRNA

—23 S
—16 S
— φ
— φ
—Aniline fragment
—5 S

1   2   3   4   5   6   7   8   9   10   11   12
Track No.
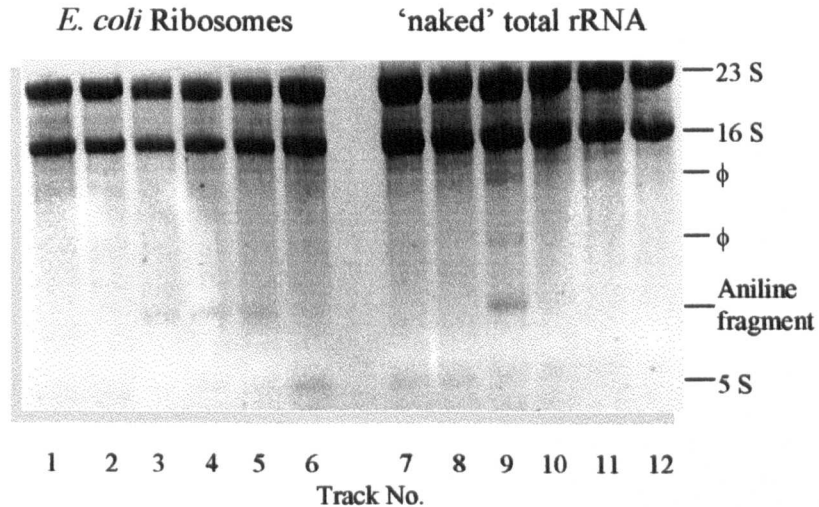
φ   two aniline fragments from
     cleavage of 16S rRNA at $GA_{1014}GA$

TKCa reaction buffer final concentration: 25mM Tris/HCl pH 7.6, 25mM KCl, and 5mM $CaCl_2$.
Electrophoretic profile of extracted rRNA after incubation. 3μg were loaded onto a 1.2% agarose: formamide gel.

PAP activity on *E. coli* ribosomes (tracks 1-6) and on 'naked' total rRNA (tracks 7-12), on a TKCa
        Buffer.
        1. *E. coli* ribosomes
        2. *E. coli* ribosomes + PAP   (1:1 m.r.)
        3. *E. coli* ribosomes + PAP + aniline   (1:1 m.r.)
        4. *E. coli* ribosomes + PAP + aniline   (1:0.1 m.r.)
        5. *E. coli* ribosomes + PAP + aniline   (1:0.01 m.r.)
        6. *E. coli* ribosomes + PAP + aniline   (1:0.001 m.r.)
        7. 'naked' total rRNA
        8. 'naked' total rRNA + PAP   (1:1 m.r.)
        9. 'naked' total rRNA + PAP + aniline   (1:1 m.r.)
        10. 'naked' total rRNA + PAP + aniline   (1:0.1 m.r.)
        11. 'naked' total rRNA + PAP + aniline   (1:0.01 m.r.)
   12. 'naked' total rRNA + PAP + aniline   (1:0.001 m.r.)

Tracks 3-5 and 9 in **Figure 18**, show the aniline fragment, produced from the rRNA cleavage by the aniline reagent, where the PAP's N-glycosidase activity is equivalent to that reported for a depurination at position A_{2660} of 23S rRNA. Track 9 on the other hand, also shows a second and third aniline fragment corresponding to the typical electrophoretic profile of N-glycosidase activity at A_{1014} on 16S rRNA. **Figure 18** shows a marked difference between the activity of PAP on a native *E. coli* ribosomes and on a deproteinised rRNA substrate. The activity of PAP on 'naked' total rRNA is reduced by approximately 100-fold compared to the activity of PAP on *E. coli* ribosomes, since there is only an aniline fragment when 1:1m.r. 'naked' rRNA: PAP (Track 9), and there are aniline fragments at 1:1, 1:0.1 and 1:0.01m.r. *E. coli* ribosomes: PAP (Tracks 3-5).

Finally, it was tested the activity of RTA on E.coli ribosomes and 'naked' total rRNA in TKCa buffer (as reported for **Figure 18**) instead of TKMg buffer described previously (refer forward to data presented in Chapter 6, **Figure 26** -tracks 1-5- and **Figure 27** - tracks 1-5-). It was observed that RTA showed not activity on native *E. coli* ribosomes but activity on 'naked' total rRNA. For the activity on 'naked' total rRNA, it was observed the presence of three aniline fragments, one equivalent to those reported for a depurination at A_{2660} of 23S rRNA and two additional fragments equivalent to those reported for depurination at position A_{1014} of 16S rRNA.

5.5. Summary of the Effect of Divalent Cation-Chelating Agent Complexes and Cation Substitution on N-glycosidase Activity on *E. coli* Ribosomes and on 'naked' total rRNA

Table 8 summarises the data gathered from the analysis and shows the results of the RIPs, PAP and RTA, on *E. coli* ribosomes and 'naked' total rRNA under the several reaction buffer conditions for the N-glycosidase activity during a 30min incubation period at 37°C. The serial dilutions of RIPs concentration is shown, and the code of **x, o, #, -** is also establish at the foot of the table. The colours red and green of the 'X's refer to 23S rRNA (A_{2660}) and to 16S rRNA (A_{1014}) depurination, and/or 23S rRNA depurination respectively where it is indicated. Ca^{2+} / $Mg2^+$ substitution results are also given.

Table 8. Influence of the Reaction Buffer: PAP and RTA activity on *E. coli* ribosomes and 'naked' total rRNA.

REACTION BUFFER INFLUENCE :
PAP and rRTA sensitivity on *E.coli* ribosomes and 'naked' rRNA

Buffer	Composition	E. coli Ribosomes PAP 1:1	1:0.1	1:0.01	1:0.001	rRTA 10:1	1:1	1:0.1	1:0.01	total rRNA PAP 1:1	1:0.1	1:0.01	1:0.001	rRTA 10:1	1:1	1:0.1	1:0.01
TKMg	25mM Tris/Cl pH 7.6, 25mM KCl, 5mM MgCl2	XX	XX	0	0	0	0	0	0	X	0	0	0	0	0	0	0
TKCa	25mM Tris/Cl pH 7.6, 25mM KCl, 5mM CaCl2	XXX	XX	XX	X	0	0	-	-	X	0	-	-	X	X	-	-
TNaMgEDTA	3mM Tris base, 15mM NaCl, 3mM MgCl2, 2.5mM EDTA	XX	XX	X	X	X	0	0	0	uXX	XX	-	-	X	0	0	0
TNaMgEDTA	3mM Tris base, 15mM NaCl, 5mM MgCl2, 5mM EDTA	#	#	-	-	0	0	-	-	XXX	X	-	-	XXX	X	-	-
TNaMgEDTA	3mM Tris/Cl pH 7.6, 15mM NaCl, 5mM MgCl2, 5mM EDTA	XX	X	-	-	0	0	-	-	u	0	0	0	XXX	-	-	-
TNaCaEDTA	3mM Tris/Cl pH 7.6, 15mM NaCl, 5mM CaCl2, 5mM EDTA	#	0	0	0	#	-	-	-	u	0	0	0	uXX	X	0	0
TNaCaEGTA	3mM Tris/Cl pH 7.6, 15mM NaCl, 5mM CaCl2, 5mM EGTA	X	X	0	0	0	0	0	0	u	XX	0	0	u	XX	0	0

X = Slightly active
XX = Active
XXX = Very active
0 = No activity
u = Active, but also giving non-specific depuration products

- = Not determined
# = Non-specific depuration products
X = 23S rRNA depuration
X = 23S and 16S rRNA depuration

146

a) The N-glycosidase activity of PAP is 10-100 fold greater on *E. coli* ribosomes than on 'naked' rRNA.

b) Contrary results were obtained for RTA. This means that ribosomal proteins in native *E. coli* ribosomes, seem to protect the rRNA from the N-glycosidase activity of RTA.

c) The inclusion of a divalent cation - chelating agent complex into the reaction buffer, result in a depurination similar to a non-specific depurination, showing the three additional aniline fragments corresponding one to A_{2660} and two of them to A_{1014} depurination activity, when deproteinised rRNA is the substrate for both PAP and RTA.

d) The non-specific depurination is related to the inclusion of EDTA-Ca^{2+}. However, the visualisation of discrete fragments, resulting from depurination in A2660 in 23S rRNA and A1014 in 16S rRNA show that these sites are still preferential target sites for both PAP and RTA N-glycosidase activity.

The single replacement of Mg^{2+} by Ca^{2+} in a near physiological reaction buffer (25mM Tris/HCl pH 7.6, 25mM KCl and 5mM CaCl$_2$, pH 7.6) was enough to produce a clear profile of the RIPs' activity on both native and deproteinised *E. coli* ribosomes. PAP is more active on *E. coli* ribosomes but less active on 'naked' rRNA, whereas RTA remain inactive on ribosomes, but shows and increased activity on 'naked' rRNA with a TKCa buffer.

The finding that high concentrations of Mg^{2+} can partially overcome the inhibition of protein synthesis in both α-sarcin- and ricin- modified ribosomes (Cawley *et al.*, 1979; Terao *et al.*, 1988) could mean that the alterations in conformation could be partially reversed by this ion. Presumably it could occur through the formation of salt bridges between neighbouring phosphate groups in the rRNA backbone (Cawley *et al.*, 1979; Terao *et al.*, 1988; Pan *et al.*, 1993). The results presente here support this hypothesis for Mg^{2+}, and for Mg^{2+}-EDTA, but not for Ca^{2+} or Ca^{2+}- EDTA or EGTA in the absence of Mg^{2+}.

5.6. Conclusions

The aim of this chapter was to establish the conditions under which RIPs are more active on one substrate than another, in order to study the role of the r-proteins on the activity on ribosomes. Based on the observations of Marchant and Hartley (1995) and Gluck and Wool (1996) about the enhancement of RIPs' activity in the presence of EDTA, the experiments reported here showed results from the utilisation of seven buffers, with a basic pH 7.6-8.0 (near physiological conditions). Each of the buffers was different, both in the nature and concentration of cations and in the presence or absence of a chelating agent. The differences found were attributed to the combination of r-proteins and the nature of the buffers, both of which together exerted an influence. The conditions among the reaction buffers were varied on a controlled basis for this purpose. Acidic pH could enhance the activity of RTA (Marchant and Hartley, 1994) and it could alter the influence of r-protein on changing sensitivity. On the same way, ionic strength as maintained in order to no affect the structure of native ribosome (eg. by unlikely deproteinisation). No main effect was observed.

It was found that the use of divalent cation: chelating agents effectively increased the RIP activity on the substrates and even in some cases, allowed a non-specific depurination. Results showed that under specified conditions, the r-proteins exert an important influence on the sensitivity of the substrates to the RIP's activity. PAP in all cases showed higher activity on the native *E. coli* ribosomes compared to the deproteinised rRNA substrates. Contrary results were found in the case of RTA activity, where, as has been suggested previously, r-proteins seem to play a protective role for RTA action (Endo and Tsurugi, 1987). In all cases, RTA appeared to be more active on the deproteinised rRNA substrate than on native *E. coli* ribosomes. However, it is important to notice that the effect of the depletion of Mg^{2+} both by lowering its concentration by the addition of a chelating agent, and even more by substituting another divalent cation, Ca^{2+}, was to enhance the RIP activity, and to make clearer the effect of the r-proteins on the sensitivity of the substrate to the RIPs. Thus, TKCa buffer was chosen to carry out the following experiments, where, once the ability of the reaction buffer to influence the activity of PAP and RTA consistently was established, it became possible to pursue the main objective of this research, the analysis of the influence of the r-proteins on RIPs' activity. This project is described in the following chapters.

6. CHAPTER VI:

THE INFLUENCE OF RIBOSOMAL PROTEINS ON RIPs-SUBSTRATE SENSITIVITY

6.1. Introduction

The *in vitro* dissociation of rRNA/r-proteins and their re-assembly has been one of the biggest steps in the characterisation of ribosomes and their components. The discovery of the self-assembly phenomenon of the ribosomal subunits is a result of the success in the reconstitution of *E. coli* 30S and 50S subunits (Maruta *et al.*, 1971; Nierhaus and Dohme, 1974; reviewed by Nomura, 1990). Successful reconstitution was achieved using a two step incubation method.

Partial and total deproteinisation procedures have also been established as a means of investigating the interaction of rRNA and r-proteins. Nierhaus (1990) reported the basis and methodology for the deproteinisation procedure. His results are based on the fact that ribosomal proteins can be split off from the ribosome with salt solutions in such a way that the higher the ionic strength, the more proteins are split off. The phenomenon has been called the 'all-or-nothing' phenomenon. For distinct values of the ionic strength, proteins appear together in-groups, in the split fractions with increasing NH_4Cl, LiCl and LiCl/acetic acid concentration. **Figure 19** shows the result of the treatment of 50S subunits by 1.5M NH_4Cl. R-proteins L1, L5, L6, L7, L10, L11, L16, L25, L31 and L33 are removed, leaving the P_{37} subparticle. Increasing the salt concentration (3.5M LiCl) splits off additional r-proteins L9, L14, L15, L16, L19, L24, L27, L28, L30 and L32, leaving the 3.5 core subparticle. Finally L2, L3, L4, L13, L17, L20, L23, L29 and L34 are removed with the addition of 66% HAc, leaving 'naked' rRNA. The sequence in which the ribosomal proteins can be split off roughly reflects the inverse order of the incorporation of proteins during the course of ribosome assembly.

The results shown in previous Chapters suggest that the difference in sensitivity of the *E. coli* ribosomes to PAP and RTA is mostly due to ribosomal proteins, these increase the sensitivity of the α-sarcin/ricin loop to PAP, but inhibit the action of RTA. It is therefore pertinent to ask which groups of r-proteins are responsible for the stimulatory/inhibitory effects on PAP and RTA action. As a first, crude approach to these questions, it was decided to examine the RIP sensitivity of various subparticles of the 50S subunit.

Figure 19. General methodology for partial and total deproteinization of 50S subunits from *E. coli* ribosomes proposed by Nierhaus (1990).
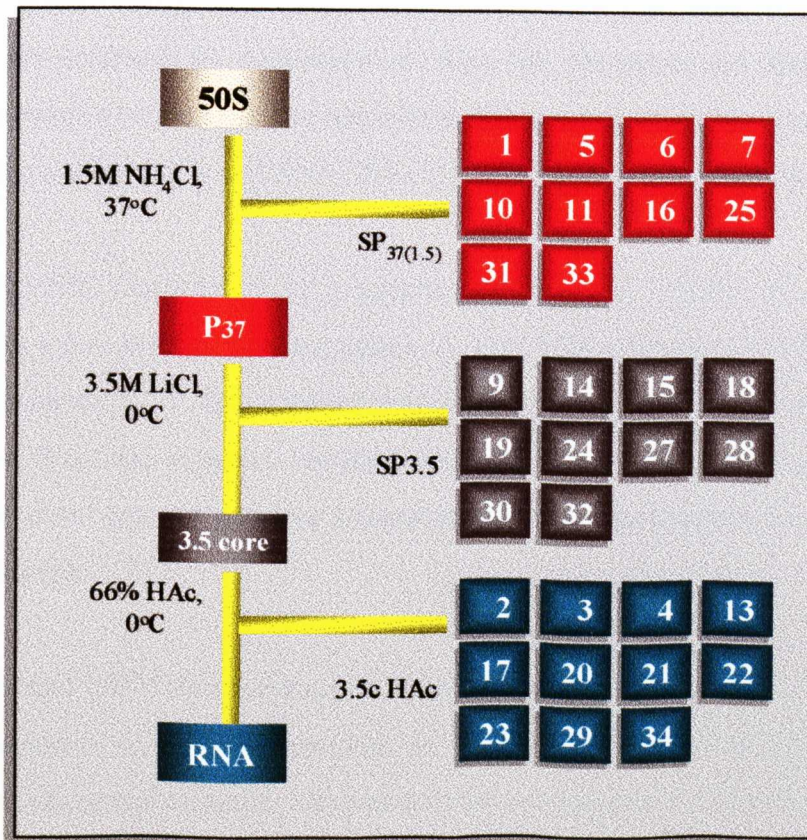
6.2. The *E. coli* Ribosomal Subunits: Their Preparation

Throughout history, the results of studies of the behaviour of ribosomes in the absence of magnesium (removing by dialysis against EDTA) have suggested that the 70S ribosome is dissociated into its 50S and 30S subunits.

Nierhaus, (1990) reported a general protocol for the isolation of 50S subunits with intact 23S rRNA. This general protocol (section 2.5.5.1.) is based on the fact that ribosomes are separated by centrifugation, once the ribosomes are diluted in a low Mg^{2+} concentration buffer, and the subunits equilibrated through the constant amount of spermidine and spermine which are shown to stabilize the dissociated subunits

Nierhaus's (1990) (section 2.5.5.1.) general protocol was applied to *E. coli* DH1 ribosomes in a first attempt at dissociation. *E. coli* DH1 ribosomes were obtained as described in section 2.5.3. Standardisation of centrifugation was carried out in order to separate the ribosomal subunits, varying speed and/or time. Nevertheless, the results showed that there was not a proper separation of the subunits under those conditions (data not shown).

Spirin (1986 and 1990) also summarised the effect of Mg^{2+} removal and ionic strength on the dissociation of *E. coli* ribosomes, i.e. dissociation of the 70S ribosomes into 30S and 50S ribosomal subunits. Magnesium ions are required for particle stability and if their concentration in the medium falls below a critical level, dissociation of the ribosome into two unequal subunits is induced. Moreover, a personal communication with Dr. D.E. Bochkariov (former collaborator of Dr. A. Spirin) confirmed that the depletion of the magnesium concentration was sufficient to obtain the dissociation of *E. coli* ribosomes. Thus, further attempt at the dissociation of ribosomes was carried out according to Bochkariov methodology, described in section 2.5.5.2.

Figure 20 shows the sedimentation profiles of the dissociated subunits of *E. coli* ribosomes applied to sucrose gradients (5-25%) as described in section 2.5.5.2. **Figure 20(a)** shows the sedimentation profile of the dissociated subunits after layering 10.5mg of *E. coli* ribosomes onto the sucrose gradient. Even after increasing the time and

Figure 20. Comparative sedimentation profiles of _E. coli_ ribosomes, dissociated subunits with different quantities of layered ribosomes on sucrose gradient (5-25% w/w).
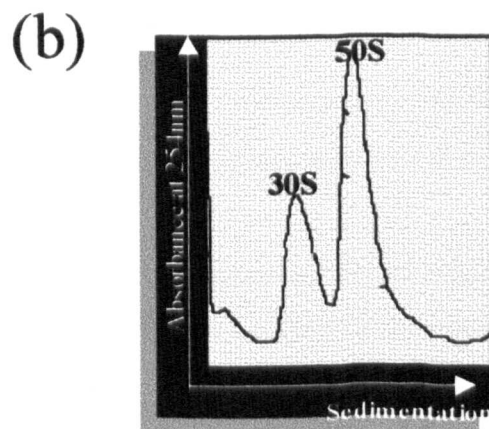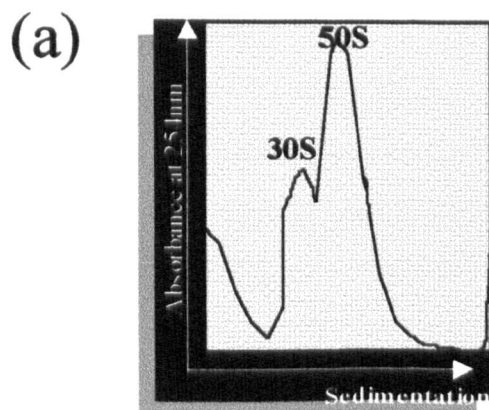
10.5mg _E. coli_ ribosomes, dissociated subunits (a) and 4mg _E. coli_ ribosomes dissociated subunits (b), were fractionated through 5-25% w/w sucrose gradient and the absorbance across the gradients was measured.

speed of centrifugation (data not shown) it was not possible to obtain a sharp sedimentation profile. **Figure 20(b)** shows the sedimentation profile of dissociated subunits after layering 4mg of *E. coli* ribosomes onto the sucrose gradient. Following the conditions for subunit separation stated previously, a sharp profile of the dissociated subunits was obtained.

Having established the final condition for *E. coli* ribosomes dissociation into 50S and 30S subunits, rRNA extraction from the subunits was carried out in order to obtain an electrophoretic profile of 23S and 16S rRNA extracted from 50S and 30S subunits (**Figure 21**) respectively. Tracks 1-6 show rRNA extracted from 50S subunits. Tracks 7-12 show rRNA extracted from 30S subunits. Track B shows rRNA extracted from 70S ribosomes. Tracks 1-6 show the 23S rRNA and the 5S rRNA profile with the additional five bands produced by 23S rRNA degradation. Track 2 shows the lack of 23S and 5S rRNA probably produced due contamination with RNase. None differences between Tracks 1, 3-6 are shown. Tracks 7-12 show the 16S rRNA profile showing only a small amount of degradation (none differences are shown between tracks 7-12).

Because only small quantities of dissociated subunits were obtained, preparative 'zonal' ultracentrifugation was proposed (section 2.5.5.3.).

Figure 22(a) shows the sedimentation profile of dissociated ribosomes separated by 'zonal' centrifugation, carried out at Max-Plank Institut fur Molekulare Genetiks at Berlin. **Figure 22(b)** shows the electrophoretic profile of rRNA extracted from the 50S and the 30S subunits. 1.5µg of each of the extracted RNAs were loaded onto a 1.2% agarose: formamide gel (section 2.7.1.), in order to confirm the dissociation of the ribosomes and assess the purity of the subunits. Tracks 1-3 show the electrophoretic profile of rRNA extracted from 50S subunits (none differences between Tracks 1-3 are shown). Tracks 4-6 show the electrophoretic profile of extracted 16S rRNA from 30S subunits (none differences between Tracks 4-6 are shown). All tracks show more degradation of their respective rRNAs than previous profiles, which may be because the solutions used for the preparation of sucrose gradients were filtered only instead of being filtered and sterilised as previously.

Figure 21. Electrophoretic profile of RNA extracted from *E. coli* ribosomes and subunits.
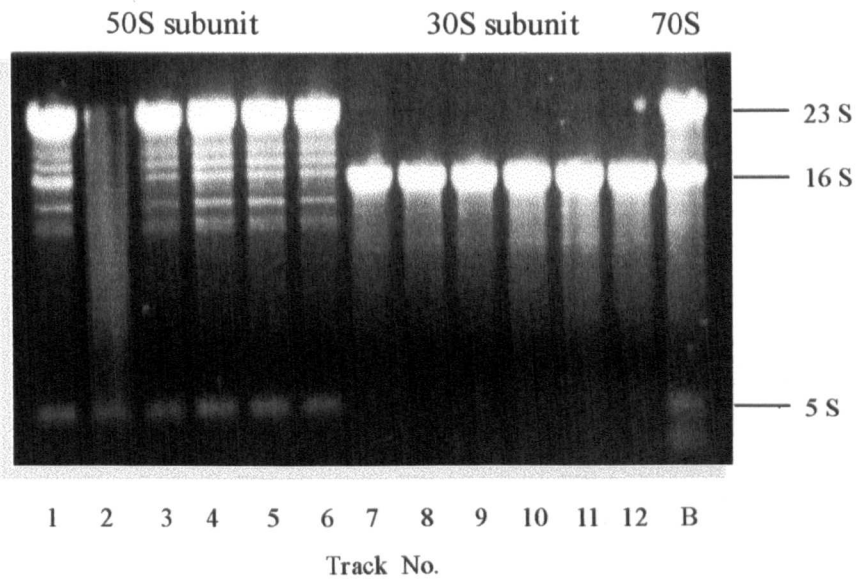
◊ Electrophoretic profile of RNA extracted from sucrose density gradient fractions containing the *E. coli* 50S and 30S subunits. 4-5μg were loaded onto a 1.2% agarose: formamide gel.

◊ RNA extracted from 50S subunit (tracks 1-6), 30S subunit (tracks 7-12) and from total *E. coli* ribosomes as control (track B)

◊ Note: There are not differences between tracks 1-6, but they are numbered and analysed according to the fraction where they were pooled. Same consideration applies to tracks 7-12.

Figure 22. Sedimentation profile[a] and electrophoretic profile[b] of RNA extracted from *E. coli* 50S and 30S subunits fractionated by preparative 'zonal' ultracentrifugation.

(a)

(b)
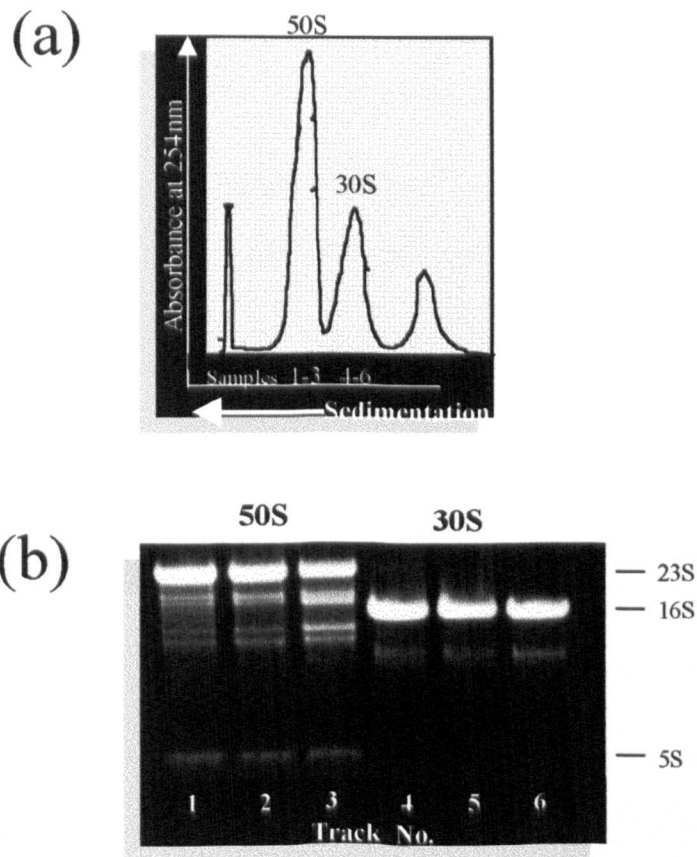
a) 15000A$_{260}$ of *E. coli* ribosomes were dissociated on sucrose gradient by preparative 'zonal' ultracentrifugation.

b) Electrophoretic profile from extracted RNA after *E. coli* ribosomes dissociation into 50S and 30S subunits by 'zonal rotor'. RNA extracted from 50S subunits (tracks 1-3) and from 30S subunits (traks 4-6). 15µg were loaded onto a 1.2% agarose: formamide gel.

◊ Note: There are not differences between tracks 1-3, but they are numbered and analysed according to the fraction where they were pooled. Same consideration applies to tracks 4-6.

As predicted, the preparative 'zonal' ultracentrifugation yielded $12650A_{260}$ 50S subunits and $3200A_{260}$ 30S subunits from $15000A_{260}$ units of *E. coli* ribosomes. The above quantities are equivalent to approximately 500mg of rRNA from the 50S subunit and 150mg of rRNA from 30S subunits obtained in one preparative 'zonal' ultracentrifugation, compared with a hundred-fold lower yield obtained on tube gradients described previously.

In addition, the isolation of the total proteins from 70S *E. coli* ribosomes, 50S and 30S subunits were carried out according to Nierhaus (1990). **Figure 23** shows the 2D electrophoretic profile (section 2.2.3.) of r-proteins from 70S *E. coli* ribosomes, and 50S and the 30S subunits, required to examine the influence of 50S subunit r-proteins (TP50) on RIPs' activity, described in the following Chapter. The 2D-gels show clear profiles of r-proteins from the different samples and the positions of the r-proteins in the 2D electrophoretic pattern, are comparable to those presented by Nierhaus's and Franceschi's group for *E. coli* ribosomes and comparable to those presented by Geyl *et al.* (1981).

6.3. The Influence of Ribosomal Proteins on RIP activity

The replacement of Mg^{2+} by Ca^{2+} in the near physiological TKMg reaction buffer, resulted in higher activity of PAP on native *E. coli* ribosomes and lower on 'naked' rRNA. In the Ca^{2+} buffer, the activity on native 70S ribosomes was approx. 100-fold higher than on 'naked' total rRNA (**Figure 18**). The work detailed in this Chapter follows the influence of r-proteins on the rRNA N-glycosidase activity by the RIPs, PAP and RTA, through partial and total deproteinisation of the subunits. The experiments were carried out using the TKCa reaction buffer in all cases unless otherwise stated.

Figure 24 shows the comparative results of the activity of PAP on *E. coli* 70S ribosomes and 50S and 30S subunits. Tracks 1, 6 and 11 are negative controls and refer to the substrates incubated without PAP. Tracks 2, 7 and 12 contain the extracted rRNA from the different substrates, incubated with PAP at a 1:1 m.r. but without the aniline treatment. Finally, tracks 3-5, 8-10 and 13-15 contain the extracted

Figure 23. 2D electrophoretic profile of TP70[a] , TP50[b] and TP30[c] from *E. coli* 70S ribosomes and 50S and 30S subunits prepared by 'zonal' centrifugation.
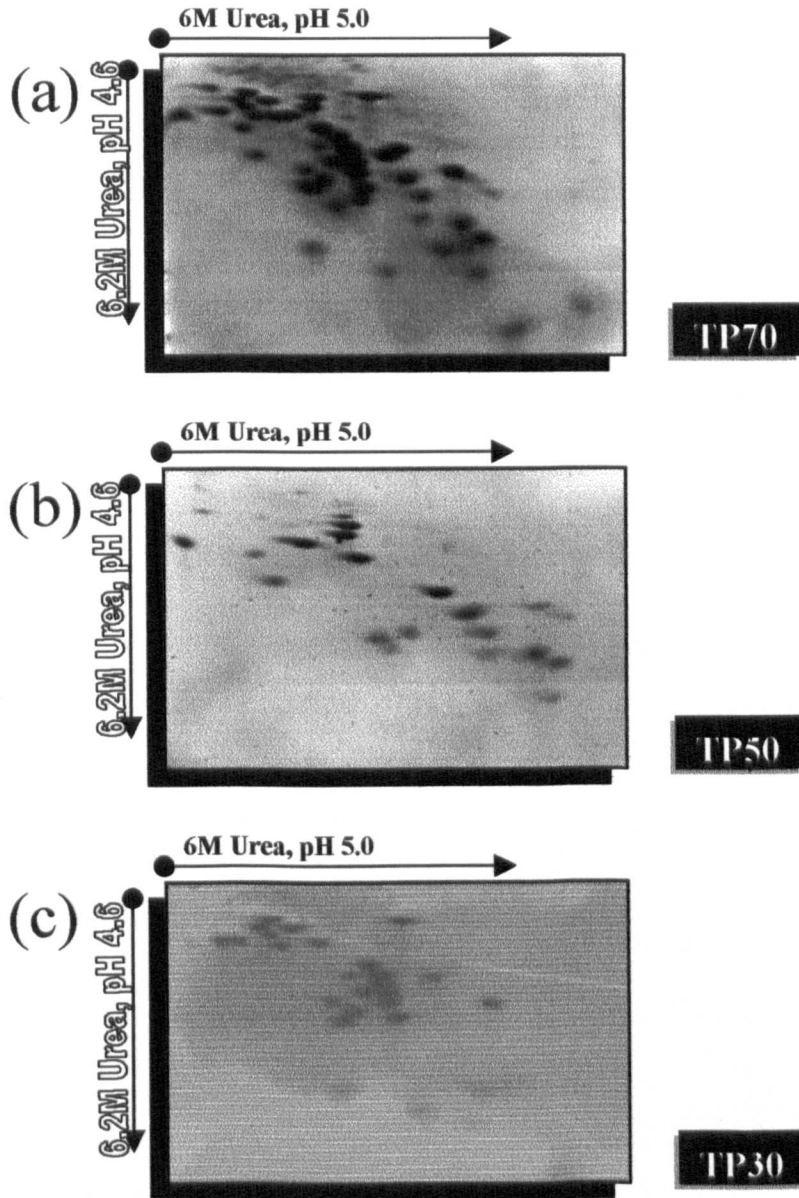
2D electrophoretic profile of TP70[a], TP50[b] and TP30[c] from *E. coli* 70S and 'zonal rotor' dissociated subunits as described by Nierhaus (1990). (sections 2.2.3, 2.2.3.1. and 2.2.3.2.).

Figure 24. PAP activity on *E. coli* ribosomes and their respective 50S and 30S subunits.
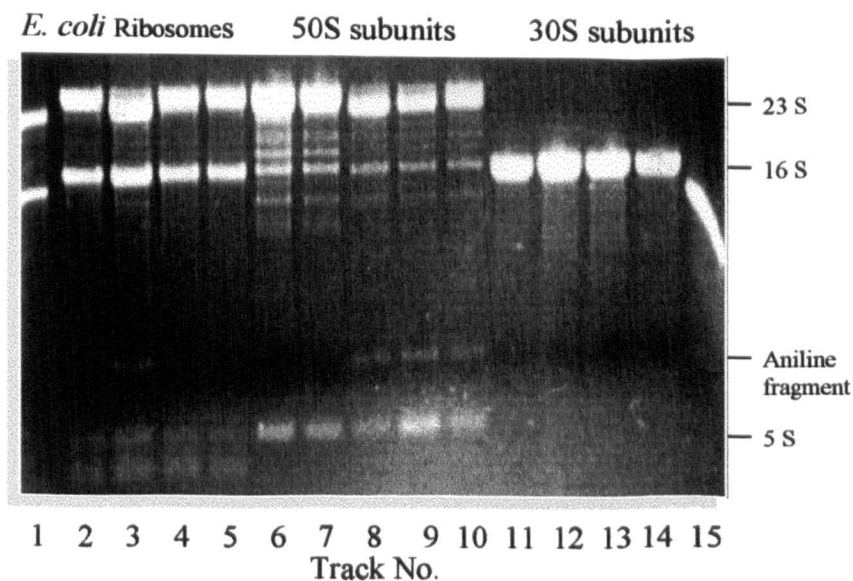
Electrophoretic profile of extracted rRNA after incubation. 3μg were loaded onto a 1.2% agarose: formamide gel. TKCa reaction buffer's final concentration: 25mM Tris/HCl pH 7.6, 25mM KCl, and 5mM CaCl$_2$

PAP activity on *E. coli* ribosomes (tracks 1-5), 50S subunits (tracks 6-10) and 30S subunits (tracks 11-15):

    1. *E. coli* ribosomes
    2. *E. coli* ribosomes + PAP   (1:1 m.r.)
    3. *E. coli* ribosomes + PAP + aniline   (1:1 m.r.)
    4. *E. coli* ribosomes + PAP + aniline   (1:0.1 m.r.)
    5. *E. coli* ribosomes + PAP + aniline   (1:0.01 m.r.)
    6. 50S subunit
    7. 50S + PAP   (1:1 m.r.)
    8. 50S + PAP + aniline   (1:1 m.r.)
    9. 50S + PAP + aniline   (1:0.1 m.r.)
    10. 50S + PAP + aniline   (1:0.01 m.r.)
    11. 30S subunit
    12. 30S + PAP   (1:1 m.r.)
    13. 30S + PAP + aniline   (1:1 m.r.)
    14. 30S + PAP + aniline   (1:0.1 m.r.)
    15. 30S + PAP + aniline   (1:0.01 m.r

rRNA from the different substrates incubated with PAP and with the addition of the aniline reagent for cleaving where depurination has occurred using PAP in serial dilutions of PAP to give 1:1, 1:0.1 and 1:0.01 (where indicated) substrate: PAP molar ratios.

Tracks 3 and 8-10 show the aniline fragment produced from the rRNA cleavage by the aniline reagent, once the PAP's N-glycosidase activity has taken place. The fragment is equivalent to that reported for a depurination at position A_{2660} of 23S rRNA. As expected, none of the rRNA samples extracted from the 30S subunits showed aniline fragments. The activity of PAP on the 50S subunit is between 10 and 100-fold higher than on the 70S ribosome.

Figure 25 shows the comparative results of the activity of PAP on 'naked' rRNAs. Tracks 1-5 show the electrophoretic pattern of rRNA extracted from 'naked' total rRNA after their incubation:

a) with the reaction buffer alone as negative control (track 1)

b) with PAP in 1:1 m.r., but without aniline treatment (track 2)

c) with added aniline reagent for cleaving where depurination has been effected by PAP at substrate: PAP molar ratios of 1:1, 1:0.1 and 1:0.01 (where indicated) (tracks 3-5)

In the same way tracks 6-10 and 11-15 show rRNA extracted from 23S and 16S rRNA respectively after their incubation either (a) with the reaction buffer alone as a negative control (tracks 6 and 11), (b) with PAP in 1:1 m.r. but without aniline treatment (tracks 7 and 12) and (c) with added aniline reagent for cleaving where depurination has occurred using PAP at substrate: PAP molar rations of 1:1, 1:0.1 and 1:0.01 (where indicated) (tracks 8-10 and 13-15).

Tracks 3, 8 and 13 show the fragment produced from the rRNA cleavage by the aniline reagent, after the PAP's N-glycosidase activity (all of them at 1:1 m.r.). The fragments shown in tracks 3 and 8 are equivalent to those reported for a depurination at A_{2660} of 23S rRNA. The two additional fragments in tracks 3 and 13 are equivalent to those

Figure 25. PAP activity on 'naked' RNAs: total RNA, 23S and 16S RNA.
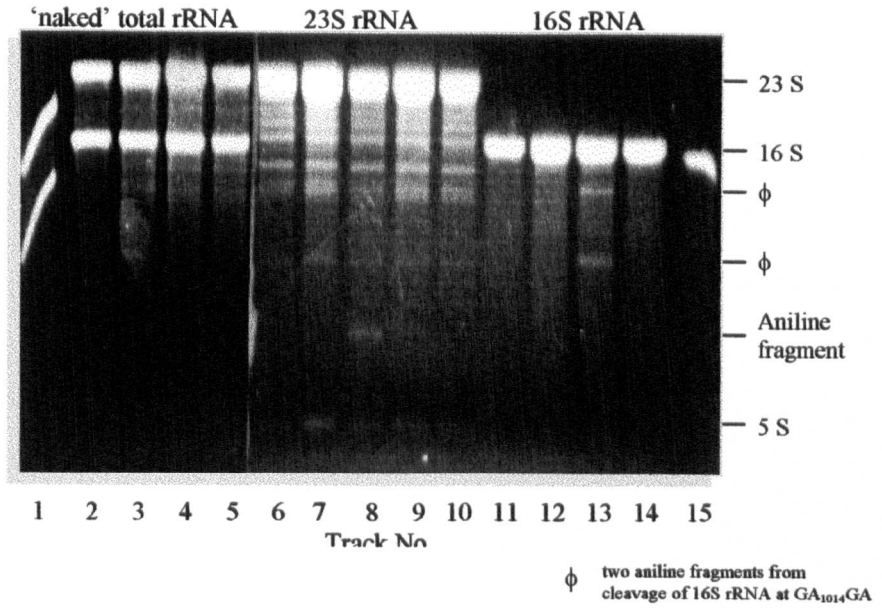
Electrophoretic profile of extracted rRNA after incubation. 3μg were loaded onto a 1.2% agarose: formamide gel. TKCa reaction buffer final concentration: 25mM Tris/HCl pH 7.6, 25mM KCl, and 5mM CaCl$_2$

PAP activity on 'naked' total rRNA (tracks 1-5), 23S rRNA (tracks 6-10) and 16S rRNA (tracks 11-15):
1. 'naked' total rRNA
2. 'naked' rRNA + PAP   (1:1 m.r.)
3. 'naked' rRNA + PAP + aniline   (1:1 m.r.)
4. 'naked' rRNA + PAP + aniline   (1:0.1 m.r.)
5. 'naked' rRNA + PAP + aniline   (1:0.01 m.r.)
6. 23S rRNA
7. 23S + PAP   (1:1 m.r.)
8. 23S + PAP + aniline   (1:1 m.r.)
9. 23S + PAP + aniline   (1:0.1 m.r.)
10. 23S + PAP + aniline   (1:0.01 m.r.)
11. 16S rRNA
12. 16S + PAP   (1:1 m.r.)
13. 16S + PAP + aniline   (1:1 m.r.)
14. 16S + PAP + aniline   (1:0.1 m.r.)
15. 16S + PAP + aniline   (1:0.01 m.r)

reported for a depurination at position A_{1014} of 16S rRNA (Marchant and Hartley, 1995). These latter fragments are not present when native *E. coli* ribosomes are used as substrate. It was confirmed that PAP was approx. 100-fold more active on the native 50S subunit **(Figure 24)** -the starting point for dissociation experiments- than on the 23S rRNA **(Figure 25)**. Conversely the N-glycosidase activity of PAP is undetectable on 30S subunits yet its activity on 'naked' 16S is comparable to that on 'naked' 23S rRNA.

Figure 26 shows the comparative results of the activity of RTA on *E. coli* ribosomes, 50S and 30S subunits. Tracks 1-5 show rRNA extracted from *E. coli* ribosomes. Tracks 6-10 and 11-15 show the electrophoretic pattern of rRNA extracted from 50S and 30S subunits respectively.

a) Tracks 1, 6 and 11 are negative controls and refer to the substrates incubated without RTA.

b) Tracks 2, 7 and 12 contain the extracted rRNA from different substrates, incubated with RTA in 1:10 m.r. but without aniline treatment.

c) Tracks 3-5, 8-10 and 13-15 contain the extracted rRNA from different substrates incubated with RTA and with the addition of the aniline reagent for cleaving where depurination has occurred using RTA in serial dilutions of RTA to give 1:10, 1:1 and 1:0.1 (where indicated) substrate: RTA molar ratio.

The aniline fragment, which has been produced from the depurination at A_{2660} on 23S rRNA from *E. coli* ribosomes by RTA in 1:10 m.r. in TKCa buffer can be seen using high contrast in the image. Tracks 8 and 13 show the fragment produced from the rRNA cleavage by the aniline reagent, after the RTA N-glycosidase activity has taken place. The fragments are equivalent to those reported for a depurination at position A_{2660} of 23S rRNA and at position A_{1014} of 16S rRNA respectively. A comparison of the activity of RTA on 70S ribosomes and 50S and 30S subunits reveals that only the last two are substrates (compare tracks 3, 8 and 13).

Figure 26. RTA activity on *E. coli* ribosomes and their respective 50S and 30S subunits.
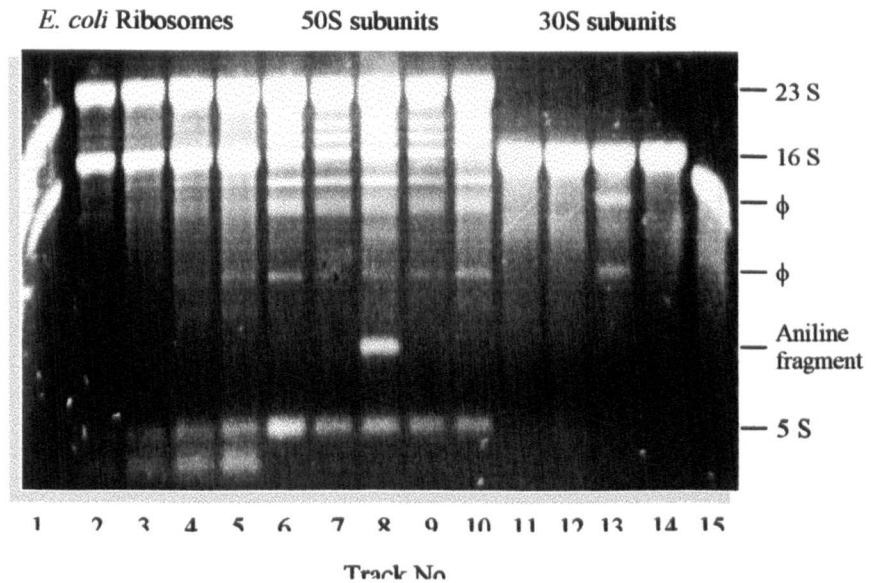
Electrophoretic profile of extracted rRNA after incubation. 3µg were loaded onto a 1.2% agarose: formamide gel. TKCa reaction buffer final concentration: 25mM Tris/HCl pH 7.6, 25mM KCl, and 5mM $CaCl_2$

RTA activity on *E. coli* ribosomes (tracks 1-5), 50S subunits (tracks 6-10) and 30S subunits (tracks 11-15):
1. *E. coli* ribosomes
2. *E. coli* ribosomes + RTA   (1:10 m.r.)
3. *E. coli* ribosomes + RTA + aniline   (1:10 m.r.)
4. *E. coli* ribosomes + RTA + aniline   (1:1 m.r.)
5. *E. coli* ribosomes + RTA + aniline   (1:0.1 m.r.)
6. 50S subunit
7. 50S + RTA   (1:10 m.r.)
8. 50S + RTA + aniline   (1:10 m.r.)
9. 50S + RTA + aniline   (1:1 m.r.)
10. 50S + RTA + aniline   (1:0.1 m.r.)
11. 30S subunit
12. 30S + RTA   (1:10 m.r.)
13. 30S + RTA + aniline   (1:10 m.r.)
14. 30S + RTA + aniline   (1:1 m.r.)
15. 30S + RTA + aniline   (1:0.1 m.r.)

Figure 27 shows the comparative results of the activity of RTA on 'naked' rRNAs. Tracks 1-5 show rRNA extracted from reaction mixtures containing 'naked' total rRNA. Tracks 6-10 and 11-15 show rRNA extracted from 23S and 16S rRNA respectively after their incubation:

a) with the reaction buffer alone as a negative control (tracks 1, 6 and 11)

b) with RTA in 1:10 m.r. but without aniline treatment (tracks 2, 7 and 12)

c) with the added aniline reagent for cleaving where depurination has been effected by RTA in serial dilutions of RTA to give 1:10, 1:1 and 1:0.1 (where indicated) substrate: RTA m.r. (tracks 3-5, 8-10 and 13-15).

Tracks 3, 8 and 13 (**Figure 27**) show the aniline fragment produced from the rRNA cleavage by the aniline reagent, after the RTA N-glycosidase activity (all of them at 1:10 m.r.). The fragments shown on tracks 3 and 8 are equivalent to those reported for a depurination at A_{2660} of 23S rRNA. Tracks 3 and 13 show two additional fragments, which are equivalent to those reported for depurination at position A_{1014} of 16S rRNA. Furthermore, track 13 shows an additional fragment (arrowed) not reported previously, with an approx. 270nt length. Finally, the depurination activity of RTA is similar on dissociated ribosomal subunits and 'naked' rRNAs. However, RTA recognises and catalyses depurination at a second site in 'naked' 16S rRNA (possibly A_{1269}) which is protected in the native 30S subunit.

According to previous results, it is not surprising to find the increased effect of RTA on 'naked' total rRNA, but now also showing activity on 16S rRNA that was not shown on *E. coli* ribosomes. Nevertheless the 'new' additional band produced by RTA N-glycosidase activity on 16S rRNA, with a length similar to the aniline fragment produced from 23S rRNA depurination was unexpected. An explanation could be found after reviewing structures of the rRNA identity elements required for recognition and catalysis by RIPs, where Endo *et al.* (1987; 1991) and Endo and Tsurugi (1988) (further summarised by Hartley and Lord, 1993) showed a potential site for RTA activity $-GA_{1269}GA-$ in 16S rRNA (**Figure 4**). This site was not depurinated in either 30S subunits of 'naked' 16S rRNA under the conditions reported by the authors.

Figure 27. RTA activity on 'naked' RNAs: total RNA, 23S and 16S RNA.
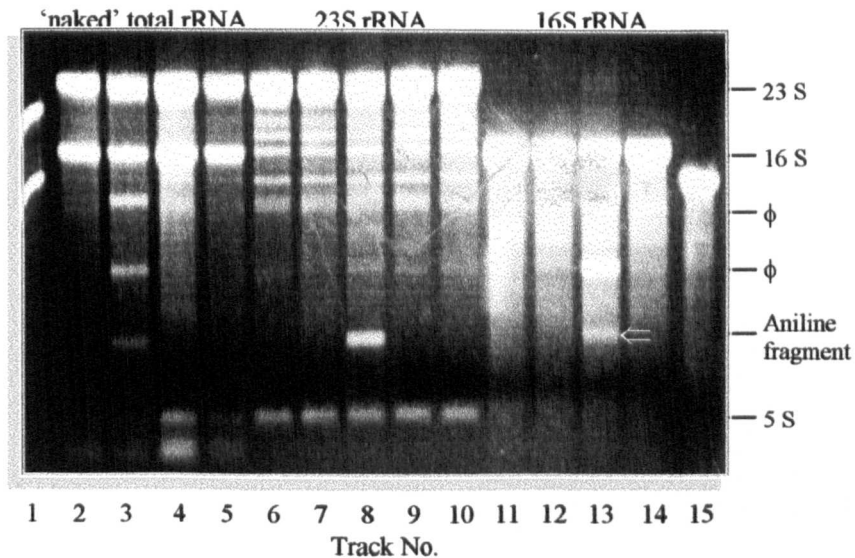
Electrophoretic profile of extracted rRNA after incubation. $3\mu g$ were loaded onto a 1.2% agarose: formamide gel. TKCa reaction buffer final concentration: 25mM Tris/HCl pH 7.6, 25mM KCl, and 5mM $CaCl_2$

RTA activity on 'naked' total rRNA (tracks 1-5), 23S rRNA (tracks 6-10) and 16S rRNA (tracks 11-15):
1. 'naked' total rRNA
2. 'naked' rRNA + RTA   (1:10 m.r.)
3. 'naked' rRNA + RTA + aniline   (1:10 m.r.)
4. 'naked' rRNA + RTA + aniline   (1:1 m.r.)
5. 'naked' rRNA + RTA + aniline   (1:0.1 m.r.)
6. 23S rRNA
7. 23S + RTA   (1:10 m.r.)
8. 23S + RTA + aniline   (1:10 m.r.)
9. 23S + RTA + aniline   (1:1 m.r.)
10. 23S + RTA + aniline   (1:0.1 m.r.)
11. 16S rRNA
12. 16S + RTA   (1:10 m.r.)
13. 16S + RTA + aniline   (1:10 m.r.)
14. 16S + RTA + aniline   (1:1 m.r.)
15. 16S + RTA + aniline   (1:0.1 m.r)

165

Hence, this possible substrate for depurination refers to that present at the 16S rRNA position $GA_{1269}GA$ (which appears as $GA_{1632}GA$ as a mistake made by earlier authors and reviews). After its depurination, the fragments would be expected to have a length of 244 nucleotides (similar to the aniline fragment produced by depurination at A_{2660} on 23S rRNA) and a second larger fragment of approximately 1300 nucleotides, as the results on track 13 from **Figure 27** suggest. Primer extension analysis should be required to confirm this second depurination position at A_{1269}.

The results presented show that in TKCa buffer, PAP is approx. 10-fold more active on 'naked' rRNAs than RTA. Specifically, it is concluded that:

a) PAP >> active on 50S subunit than on 'naked' 23S rRNA

b) RTA has a lower activity than PAP, but does not disciminate between 50S subunits and 'naked' 23S rRNA.

Therefore in future studies, the role of r-proteins in the enhancement of the activity of PAP at $GA_{2660}GA$ will be investigated. Partial deproteinisation of 50S subunits from *E. coli* ribosomes will be carried out and monitored for RIP's activity.

6.3.1. The Influence of r-proteins on the Susceptibility of the 50S Subunit and its
        Subparticles to RIPs

A partial deproteinisation was carried out according to Nierhaus (1990), where firstly the NH_4Cl/Ethanol-split procedure was followed in order to split off L1, L5, L6, L7/12, L10, L11, L16, L25, L31 and L33. The procedure was carried out as described at section 2.15.1. This protocol yields a solution containing mainly P_{37} subparticles, but also some insoluble particles, which can be removed by centrifugation. P_{37} subparticle (the supernatant fraction from the above) and the mixture of particles present before centrifugation, were used as substrates for PAP's activity. They are termed P_{37} subparticles and P_{37} subparticles* respectively.

Figure 28 shows the comparative results of the activity of PAP on the 50S subunit and both: the P_{37} subparticles* and the P_{37} subparticles, all in TKCa reaction buffer.

Figure 28. PAP activity on 50S subunit and subparticles P$_{37}$.
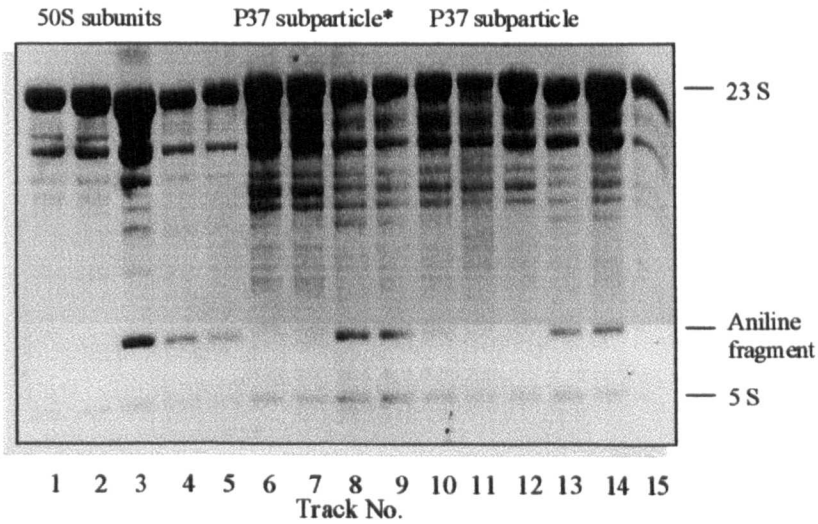
Electrophoretic profile of extracted rRNA after incubation. 3μg were loaded onto a 1.2% agarose: formamide gel. TKCa reaction buffer final concentration: 25mM Tris/HCl pH 7.6, 25mM KCl, and 5mM CaCl$_2$

PAP activity on 50S subunit (tracks 1-5), P$_{37}$ subparticles* (tracks 6-10) (for description of P$_{37}$ subparticles* see text) and P$_{37}$ subparticles (tracks 11-15):

     1. 50S subunit
     2. 50S + PAP   (1:1 m.r.)
     3. 50S + PAP + aniline   (1:1 m.r.)
     4. 50S + PAP + aniline   (1:0.1 m.r.)
   5. 50S + PAP + aniline   (1:0.01 m.r.)
     6. P$_{37}$ subparticles*
     7. P$_{37}$ subparticles* + PAP (1:1 m.r.)
     8. P$_{37}$ subparticles* + PAP + aniline   (1:1 m.r.)
     9. P$_{37}$ subparticles* + PAP + aniline   (1:0.1 m.r.)
     10. P$_{37}$ subparticles* + PAP + aniline   (1:0.01 m.r.)
     11. P$_{37}$ subparticles
     12. P$_{37}$ subparticles + PAP (1:1 m.r.)
     13. P$_{37}$ subparticles + PAP + aniline   (1:1 m.r.)
     14. P$_{37}$ subparticles + PAP + aniline   (1:0.1 m.r.)
     15. P$_{37}$ subparticles + PAP + aniline   (1:0.01 m.r.)

Tracks 1-5 show rRNA extracted from reaction mixture containing 50S subunits of *E. coli* ribosomes. Tracks 6-10 and 11-15 show rRNA extracted from reaction mixtures containing the P_{37} subparticle* and the P_{37} subparticle. The experiment was carried out as follows:

a) with the reaction buffer alone as negative controls (tracks 1, 6 and 11)

b) with PAP in 1:1 m.r. but without aniline treatment (track 2, 7 and 12)

c) with added aniline reagent for cleaving where depurination has been effected by PAP in serial dilutions of PAP to give 1:1, 1:0.1 and 1:0.01 (where indicated) substrate: PAP m.r. (tracks 3-5, 8-10 and 13-15).

Tracks 3-5, 8-9 and 13-14 show the fragment produced from the rRNA cleavage by the aniline reagent, after the PAP's N-glycosidase activity. The fragments shown are equivalent to those reported for a depurination at A_{2660} of 23S rRNA. Tracks 6-10 and 11-15 show similar patterns, hence it is suggested that the presence of resuspended particles in the P_{37} solution, do not influence PAP's N-glycosidase activity. Further experiments including more PAP dilutions to give 1:10, 1:1, 1:0.5, 1:0.1, 1:0.05, 1:0.01, 1:0.001 m.r. (substrate: PAP m.r.), were performed **(Figure 29)**.

Figure 29 shows the comparative percentage depurination profiles for PAP on both the 50S subunit and the P_{37} subparticle substrates. The percentage depurination has been calculated by scanning the ethidium bromide stained gels and measuring the optical density of the aniline fragment. It is expressed as a ratio of the 5S rRNA in order to calculate the percentage depurination. The length of 5S rRNA is 120 nucleotides (Hartley *et al.*, 1991). The percentage depurination values were plotted against the quantity of PAP in ng added in serial dilution of PAP for obtaining 1:1, 1:0.1, 1:0.01 and 1:0.001 m.r. substrate: PAP. Figure 29 shows the quantification of the percentage depurination in relation to the PAP concentration. It was shown that PAP's N-glycosidase activity was approx. 100-fold higher on 50S subunits than on the P_{37} subparticle. The results suggest that the r-proteins removed from the 50S subunit in the preparation of the P_{37} subparticle account for PAP's increased activity on the former substrate. It has being shown (Nierhaus, 1990) that L6 is removed in the

Figure 29. Comparative percentage depurination profile for PAP on both 50S subunit and P$_{37}$ subparticles substrates.
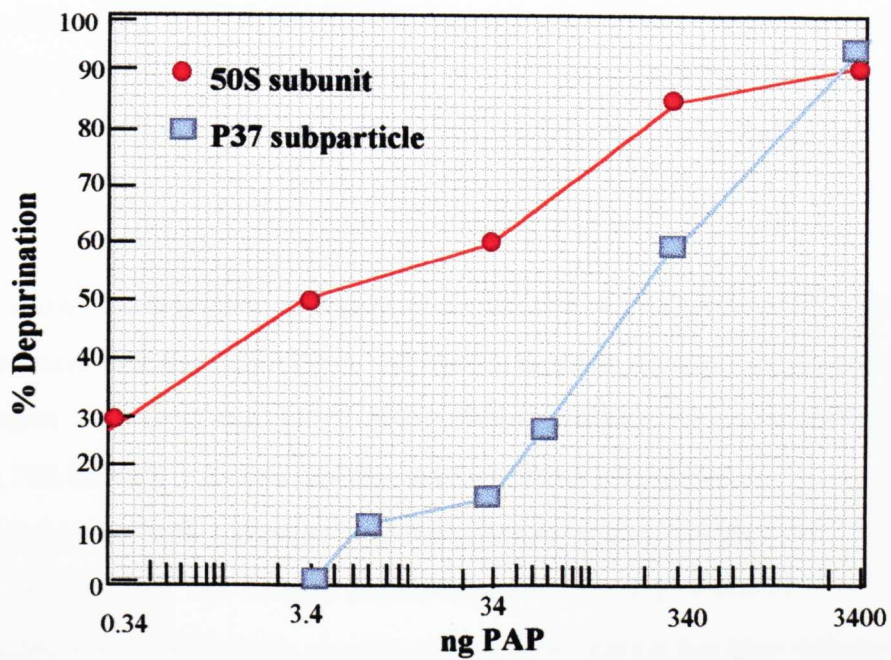
3400ng of PAP corresponds to a
1:10 substrate: PAP molar ratio

preparation of the P_{37} subparticle, and L6 is known to bind to 23S rRNA domain VI and possibly to influence its conformation (Leffers *et al.*, 1988; Uchiumi *et al.*, 1997; Ostergaard *et al.*, 1998; Uchiumi *et al.*, 1999).

Further deproteinisation was carried out according Nierhaus' (1990) LiCl split procedure. Using 3.5M LiCl for the splitting procedure, L1, L5, L6, L7/12, L9, L10, L11, L14, L15, L16, L18, L19, L24, L25, L27, L28, L30, L31, L32 and L33 r-proteins were split off. The procedure was carried out as described at section 2.15.2. where the final solution contained the 3.5 core particle, as it was named by Nierhaus (1990).

Figure 30 shows the comparative results of the activity of PAP on the 50S subunit, the 3.5 core particle and the 23S rRNA, all reactions were carried in a TKCa reaction buffer. Tracks 1-5, 6-10 and 11-15 show rRNA extracted from reaction mixtures containing 50S subunit, 3.5 core particle and 23S rRNA respectively:

a) with the reaction buffer alone as negative controls (tracks 1, 6 and 11)

b) with PAP in 1:1 m.r. but without aniline treatment (track 2, 7 and 12)

c) with added aniline reagent for cleaving where depurination has been effected by PAP in serial dilutions of PAP on 1:1, 1:0.1 and 1:0.01 (where indicated) substrate: PAP m.r. (tracks 3-5, 8-10 and 13-15)

Tracks 3-5, 8 and 13 in **Figure 30**, show the fragment produced from the rRNA cleavaged by the aniline reagent, after the PAP's N-glycosidase activity. The fragments shown are equivalent to that reported for a depurination at A_{2660} of 23S rRNA. **Figure 30** also shows a marked difference between the activity on the native 50S subunit, on a partial deproteinised subparticle (3.5 core subparticle) and on totally deproteinised 23S rRNA. The action of PAP on the latter two substrates is reduced by approx. 100-fold compared with the native 50S subunit. The results confirm the important role of the proteins either in inducing or maintaining or both; the tertiary structure recognised by PAP.

Figure 30. Comparative depurination profile for PAP on 50S subunit, 3.5 core subparticle and 23S RNA.
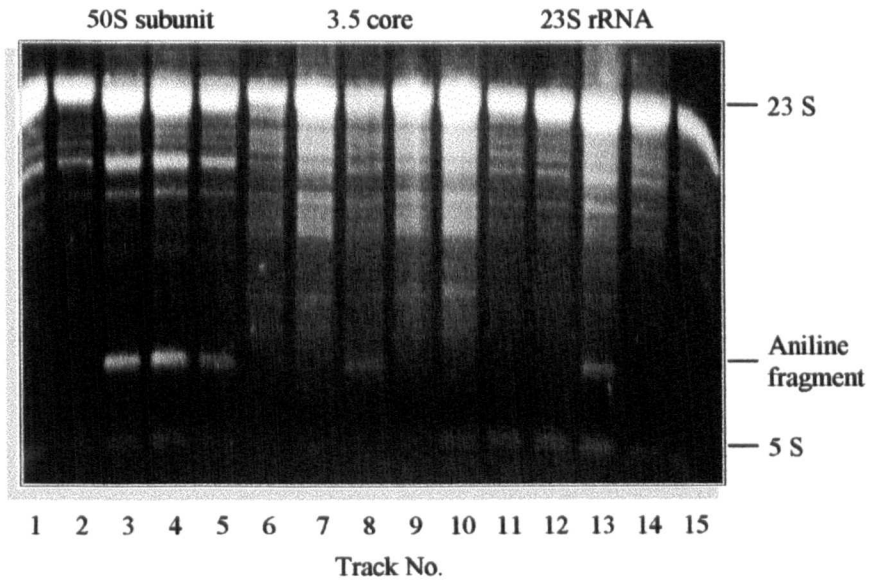
Electrophoretic profile of extracted rRNA after incubation. 3μg were loaded onto a 1.2% agarose: formamide gel. TKCa reaction buffer final concentration: 25mM Tris/HCl pH 7.6, 25mM KCl, and 5mM CaCl$_2$

PAP activity on 50S subunit (tracks 1-5), 3.5 core subparticles (tracks 6-10) and 23S rRNA (tracks 11-15):

    1. 50S subunit
    2. 50S + PAP   (1:1 m.r.)
    3. 50S + PAP + aniline   (1:1 m.r.)
    4. 50S + PAP + aniline   (1:0.1 m.r.)
    5. 50S + PAP + aniline   (1:0.01 m.r.)
    6. 3.5 core subparticle
    7. 3.5 core + PAP   (1:1 m.r.)
    8. 3.5 core + PAP + aniline   (1:1 m.r.)
    9. 3.5 core + PAP + aniline   (1:0.1 m.r.)
    10. 3.5 core + PAP + aniline   (1:0.01 m.r.)
    11. 23S rRNA
    12. 23S + PAP   (1:1 m.r.)
    13. 23S + PAP + aniline   (1:1 m.r.)
    14. 23S + PAP + aniline   (1:0.1 m.r.)
    15. 23S + PAP + aniline   (1:0.01 m.r)

Finally, it has been shown that the activity of RTA was detectable on 50S and on 30S subunits, but undetectable on the native *E. coli* 70S ribosomes. RTA N-glycosidase activity on both subunits, was similar in terms of its activity at a 1:10 m.r. (substrate: RTA). It suggests that it is only in the 70S *E. coli* ribosome substrate that the potential sites for RTA action is inaccessible. Dissociation of 70S tight couples by lowering Mg^{2+} is sufficient to allow access of RTA for its N-glycosidase activity.

Summing up:

- The PAP's N-glycosidase activity on the P_{37} subparticle and 3.5 core subparticle, decreased by a factor of 100-1000, compared to its activity on 50S subunits. The activity of PAP on the 3.5 core subparticle was comparable with that on 'naked' 23S rRNA.

- PAP was not active on A_{1014} on 16S rRNA in native 30S subunits, but it was active on 16S rRNA alone.

- RTA was active on both native 50S and 30S subunits, as well as on 23S and 16S rRNA. The activity on these substrates was similar and the specificity on the 23S rRNA is identical to the 'naked' rRNA. On 16S rRNA, the N-glycosidase activity of RTA produced a 'new' additional aniline fragment suggesting the depurination at a second position $GA_{1269}GA$ of 16S rRNA.

- The successive removal of r-proteins from native 50S subunits caused a reduction in sensitivity of the resulting subparticles to PAP.

6.4. Conclusions

In the present chapter the influence of r-proteins on various substrates' sensitivity to RIPs has been reviewed. The influence of r-proteins was based on the *in vitro* partial and total dissociation of the rRNA/r-proteins (Nierhaus, 1990). r-Proteins were split off from the ribosome with salt solutions in such a way that the higher the ionic strength of the solution, the more the proteins split off.

Previous results have suggested that the r-proteins influence substrate sensitivity to PAP and RTA (Chapters IV and V). Prior to this work, the only substrates tested for PAP's activity were native 70S ribosomes and 'naked' rRNA Thus, the dissociation of *E. coli* ribosomes into 50S and 30S subunits, the partial and total deproteinisation of

50S subunits to obtain the P37 subparticle, the 3.5c subparticle and the 23S rRNA, and finally the search for additional depurination sites in 30S subunits and 16S rRNA, became the aim of this part of the research. The differences between PAP and RTA activity were sought on the partial and total deproteinisation of substrates, in order to assay their sensitivity. In the same way, the point of the differences for RIP activity after the partial deproteinisation was established, based on the knowledge of which proteins were removed by each of the different salt treatments. Substrates, RIP activity, and products of the depurination were monitored by analytical agarose: formamide gel electrophoresis, and the reaction buffer chosen was the TKCa because its use gave a consistent and clear distinction between the different substrates for RIPs N-glycosidase activity (Chapter V).

The length of the main fragment produced by the cleavage of the aniline reagent after the N-glycosidase activity of RIPs was characteristic of the previously reported depurination at $GA_{2660}GA$ in the highly and universally conserved α-sarcin/ricin loop. However, two depurination sites in 16S rRNA at $GA_{1014}GA$ (already established) and putatively the novel site at $GA_{1269}GA$ appeared under some of the different reaction buffer conditions.

RTA was active on native, dissociated 50S and 30S subunits, as well as on 23S and 16S rRNA. The activity on these substrates was of a similar order and the target site in the 50S subunit was identical to that on 'naked' 23S. On 16S rRNA, the N-glycosidase activity of RTA produced a new additional aniline fragment suggesting depurination at a second position $GA_{1269}GA$ on 16S rRNA. This site was previously reported as $GA_{1632}GA$ in error (Endo *et al.*, 1991). However, Endo *et al.*, 1991 found no activity at the correctly identified $GA_{1269}GA$ site under their conditions but changing the conditions to those reported here resulted in depurination at this site.

E. coli ribosomes do not demostrate susceptibility towards RTA at a 1:10 substrate: RIP m.r., but the dissociated subunits are sensitive under these conditions. Of all the different substrates assayed only the native *E. coli* ribosomes were insensitive to RTA action, from which it is inferred that dissociation of the tightly coupled subunits exposed the depurination sites in both subunits.

The experiments reported in the next chapter report the reconstitution of the subribosomal particles consisting of domain VI-RNA transcript from 23S rRNA of *E. coli* ribosomes and TP50 for monitoring PAP activity. Domain VI will be transcribed and an attempt to describe the reconstitution of domain VI transcripts with r-proteins will carried out in order to establish the role of individual proteins in enhancing the activity of PAP.

The confirmation of the depurination sites by primer extension methodology will be reported, and selected approaches will be applied to examining some of the above issues.

7. CHAPTER VII:

CLONING AND *IN VITRO* TRANSCRIPTION OF
DOMAIN VI OF *E. COLI* 23S rRNA AND THE INFLUENCE OF
TP50 PROTEINS

7.1. Introduction

The RIPs' recognition process for activity on different substrates is still only partially understood. rRNA conformation and the role of the r-proteins in obtaining and maintaining an rRNA structure sensitive to RIPs' N-glycosidase activity has been suggested but is still unknown.

23S rRNA comprises six major structural domains (Egebjerg et al., 1989) which fold and assemble proteins during their transcription in vivo (Nowotny and Nierhaus, 1982). Leffers et al. (1988) worked on the structure, assembly and function of domain VI of E. coli 23S rRNA, which contains the highly conserved sequence of the α-sarcin / ricin loop.

In order to gain greater insight into the influence of r-proteins on RIPs' activity, the individual domain VI of 23S rRNA from E. coli ribosomes was transcribed and reconstituted with the total proteins from the 50S subunit (TP50), in which Leffers et al. (1988) have shown that there is an association between domain VI and proteins L3 and L6. Additionally, Uchiumi et al. (1997; 1999) have suggested a possible structural organisation of these proteins within the domain. So, in order to establish the role of the reconstituted-RNP in enhancing PAP activity, transcripts of domain VI were obtained (transcript containing residues 2630-2904, 22 more nucleotides at the 3'end of 23S rRNA than the base ranges 2630-2882 reported by Noller, (1984)) and partial and total reconstitution were attempted using r-proteins that bind to the α-sarcin/ricin loop for testing RIP's activity on these reconstituted substrates.

A possible limitation of using in vitro transcripts of rRNA for reconstitution experiments stems from the finding that transcripts of E. coli full length 23S rRNA are severely compromised in their ability to reconstitute into catalytically active correctly assembled 50S subunits. This is a consequence of the lack of posttrascriptional modifications present in natural 23S rRNA (Green and Noller, 1996). However, these authors have shown by in vitro complementation analysis that nearly all of the functionally important modifications reside in an 80nt sequence extending from positions 2445 to 2524. Significantly for the present study, 50S subunits reconstituted with transcripts from position 2524 to the 3' end of 23S rRNA (including all of domain VI) retained most of their activity. Since the rRNA structure requirements for

functional ribosomes are very stringent, the approach of using transcripts of domian VI for reconstitution and RIP substrate assays is deemed valid.

7.2. Plasmid Construction

Although the use of short oligonucleotides that mimic the α-sarcin/ricin stem loop RNA have provided much information about the identity elements of the RIP target site, and are believed to be similar in structure to the native structure, they have certain limitations. Firstly, the r-protein could affect the structure, as proposed by Meyer *et al.*, (1996) and secondly the transitions in the structure, which have been proposed to occur during protein synthesis (Meyer *et al.*, 1996), require the context of the ribosome. However, Gluck and Wool (1996) have suggested that transcripts and synthetic oligoribonucleotides retain the essential structural features of the native α-sarcin/ricin loop since the specific depurination by RTA and cleavage by α-sarcin on the 26S/28S mimicking oligo, occurs as it occurs in the ribosome (Endo *et al.*, 1988; Nitta *et al.*, 1998).

For cloning and *in vitro* transcription, this work has been based on the following facts (from Sambrook *et al.*, 1991):

1. The development of plasmid vector containing polycloning sites downstream from promoters derived form *Salmonela typhimurium* bacteriophage SP6, allows the synthesis of single-stranded rRNA probes of high specific radio activity. The advantage of the SP6 promoter, is that it is recognised, specifically, by DNA-dependent rRNA polymerases encoded by its respective bacteriophage. Furthermore, the bacteriophage enzyme does not recognize bacterial or plasmid promoters in cloned DNA sequences.

2. *In vitro* transcription of double-stranded DNA templates by bacteriophage DNA dependent RNA polymerases is based on the incubation *in vitro* of a linearized plasmid with the appropriate DNA-dependent rRNA polymerase and the four rNTPs, where the rRNA synthesis is initiated at the bacteriophage promoter site. The rRNA transcript is freed from template DNA by treating the reaction with RNase-free DNase I.

3. There are a large number of plasmid vectors for preparing RNA probes, carrying a cloned copy of the bacteriophage promoter adjacent to a polycloning site. This polycloning site also provides a restriction site downstream from the foreign DNA that can be used to linearize the recombinant plasmid. Furthermore, more complex plasmids are available containing not only the bacteriophage promoters, but also they contain for example, the region of the *E. coli* lacZ gene coding for the α-peptide of β-galactosidase. The insertion of foreign DNA sequences into the polycloning site of these vectors can be scored by the appearance of white colonies on plates containing the chromogenic substrate 5-bromo-4-chloro-3-indolyl-β-D-galactosidase (X-gal).

4. Finally, the bacteriophage promoter fixes the 5' terminus of the transcript, but the downstream site of cleavage determines the 3' terminus by the restriction enzyme. So, the transcription could be directed.

It is well known that transcription *in vitro* by T7 or SP6 RNA polymerases of genes has been used to produce rRNA fragments for the study of both structure and function (Unlenbeck, 1987; Leffers *et al.*, 1988; Weitzman *et al.*, 1990). In *E. coli* there are 7 ribosomal RNA operons per genome (Kiss *et al.*, 1977; Hui and Dennis, 1985) as has been reviewed previously. Each of these operons encodes the 16S, 23S and 5S RNA.

The *rrn*B operon from *E. coli* ribosomes has been cloned and the gene organisation primary sequence determined (Brosius *et al.*, 1981a; Brosius *et al.*, 1981b). It has been cloned in pKK3535 and the entire 11,864-bp sequence is known. Thus, precise rearrangements and site specific alterations of the ribosomal RNA operon are possible.

Figure 31(I) shows a detailed physical map of pKK3535, and **Figure 31(II)** shows domain VI at the 3' end of *E. coli* 23S rRNA sequence. The strategy for the cloning of this fragment is shown in **Appendix 1**, and restriction sites diagram of pKK3535 is shown on **Figure 31.**

Figure 31(I) shows that domain VI lies at the 3' end of *E. coli* 23S rRNA, so domain

Figure 31. Schematic map of hybrid plasmid pkk3535 (I) and domain VI sequence at the 3' end of *E. coli* 23S RNA (II).

(from Brosius *et al.*, 1981a; Brosius *et al.*, 1981b).

(I) Schematic map of the hybrid plasmid pKK3535 (from Brosius *et al.*, 1981). Positions of vector DNA or inserts from other plasmids carrying parts of the *rrn*B operon are indicated on the inner circle. The λ portion of the 7.5-kb fragment is hatched. The genes for the rRNAs and tRNA^Glu are represented by filled bars. Two open reading frames (ORF I and ORF II) flanking the *rrn*B operon are indicated. The tandem rRNA promoters P1 and P2 and their sites of initiation of transcription are indicated by arrows. Putative terminators for the *rrn*B operon are marked as T1 and T2. The ampicillin and tetracycline genes (the latter is interrupted by the 7.5-kb *Bam* H1 insert) of plasmid vector pBR 322 are dotted. The location of restriction enzyme (those with recognize a sequence of six nucleotides) sites are based on the known sequence of pKK 3535 via the primary structures of pBR 322, and location of the rest of the enzymes have been confirmed by digestion of pKK 3535 with various enzymes. Domain IV at the pKK3535 correlates to the black area.

179

VI - DNA fragment (275 bp) was prepared from the *rrn*B RNA operon in plasmid pKK3535 (Brosius *et al.*, 1981b). Forward and Reverse primers were designed including an *EcoRI* and BamH1 restriction site, and used for the PCR DNA-amplification technique based on the work of Saiki *et al.* (1988), which utilises DNA-polymerase (a thermostable enzyme) from *Thermus aquaticus* a thermophilic bacterium (Chien *et al.*, 1976; Kaledin *et al.*, 1980).

Figure 32 (a) and **(b)** shows the physical representation of the *rrn*B gene and primer sequences designed for PCR-DNA amplification, respectively. Figure **32(c)** shows the electrophoretic profile of the PCR products of four identical and separated amplification reactions of domain VI from the pKK3535 plasmid. QIAGEN purification kit was used in order to extract and to purify the PCR products (section 2.11.13.).

PCR product encoding domain VI from 23S rRNA was inserted within the GEM-4Z in order to obtain the required RNA transcript. **Figure 33** shows the pGEM-4Z vector with its polycloning sites downstream from the SP6 promoter. The DNA - domain VI encoding sequence including the added *EcoRI* and *Bam*HI restriction sites also is shown. The arrowed starting point of the SP6 transcription promoter and the circled RIPs depurination site at A_{2660} can be seen.

The insert and vector were ligated and used to transform competent *E. coli* DH5α cells (section 2.10.3). Colonies with recombinant plasmids were selected as white colonies in the presence of x-gal (section 7.2.).

7.3. Characterisation of the Domain VI - containing Plasmid

*Bam*HI and *EcoRI-Bam*HI restriction was carried out on a mini-prep in order to confirm that the transformation was successful. **Figure 34** shows the electrophoretic pattern on a DNA analytical agarose gel (section 2.13.1.) of the plasmid. Track 1 shows the 1kb DNA ladder as length size standard. Tracks 2-4 show the profile of the extracted DNA, DNA *Bam*HI restricted and DNA *Bam*HI-*EcoRI* restricted,

Figure 32. Domain VI from 23S RNA; gene PCR amplification.

(a)

*E. coli rrn*B operon

5' — 16S — 23S — domain VI — 5S — 3'

(b)

Forward Primer:(5'-3'): CGGAATTCCCTCTTGACTCCCCCCGACG
Reverse Primer:(5'-3'): CGGGATCCAAGGTTAAGCCTCACGGTT

(c)

S 1 2 3 4

— 275bp

S) DNA ladder (1Kb)
1-4) 3 μg DNA after PCR
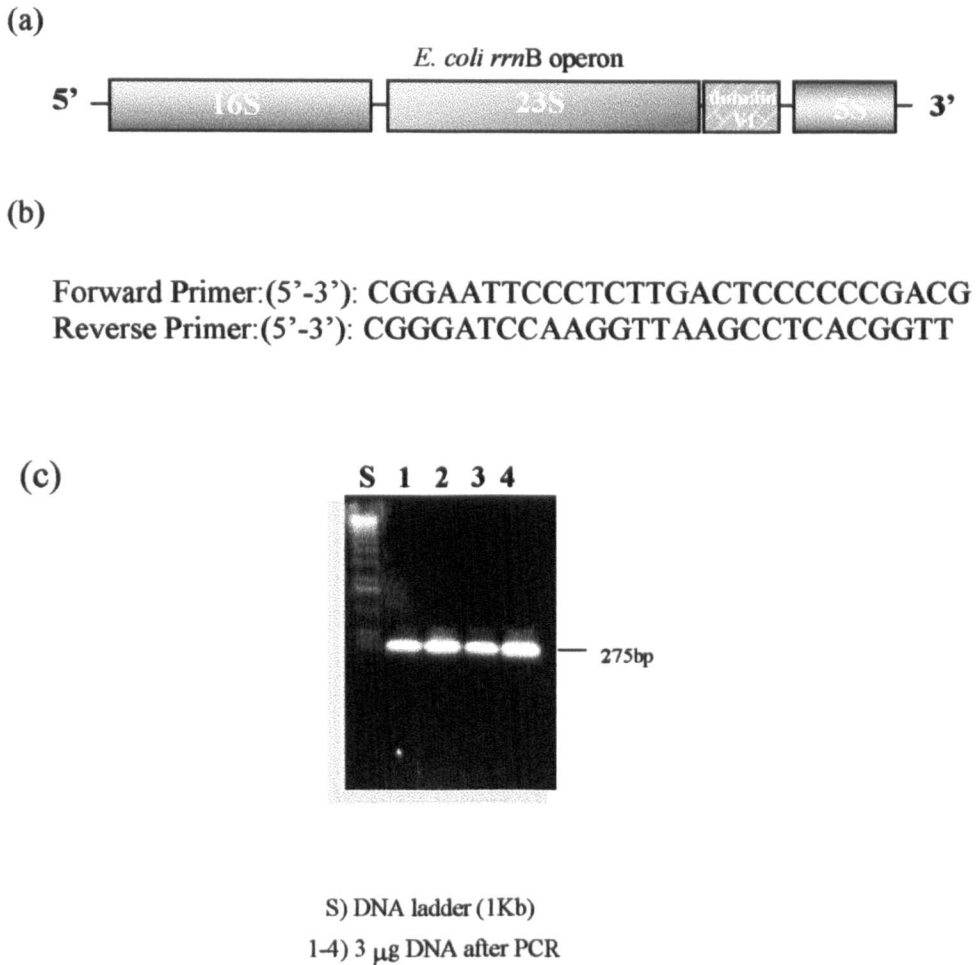
Four identical and separate reactions were carried out in order
to obtain the domain VI PCR products.

(a) Map of *E. coli rrn*B operon showing domain VI.
(b) Primer sequences for PCR, amplification of domain VI DNA.
(c) Agarose gel fractionation of PCR products.

Figure 33. pGEM-4Z Vector and Domain VI-DNA sequence from *E. coli* 23S RNA, *rrn*B operon.

SP6 Transcription start

5'end- GGATT TAGGT GACAC TATAG AATAC

SP6 Promoter

GAATT C GGAGA ACTGA GGGGG GCTGC   TCCTA GTACG

Eco R1

A GAGG ACCGG AGTGG ACGCA TCACT GGTGT TCGGG

TTGTC ATGCC AATGG CACTG CCCGG TAGCT AAATG

CGGAA GAGAT AAGTG CTGAA AGCAT CTAAG CACGA

AACTT GCCCC GAGAT GAGTT CTCCC TGACC CTTTA

AGGGT CCTGA AGGAA CGTTG AAGAC GACGA CGTTG

ATAGG CCGGG TGTGT AAGCG CAGCG ATGCG TTGAG

CTAAC CGGTA CTAAT GAACC GTGAG GCTTA ACCTT

GGAT CCTCT AGAGT CGACC TGCAG GCATG CAAGC

Bam H 1   Xba I   Sal 1/ Acc I/ Hinc II   PstI   Sph 1

TTGTC TCCCT ATAGT GAGTC GTATT   A GAGC 3'end

Hind III   T7 Promoter

pGEM -4Z Vector (2746 bp)

lac Z

SP6
Eco R1
Sac I
Kpn I
Ava I
Sma I
BamH I
Xba I
Sal I
Acc I
Hinc II
Pst I
Sph I
Hind III
T7

SP6 Transcription Start

5'... GGATT TAGGT GACAC TATAG AATAC

SP6 Promoter

GAATT GGAGC TCGGT ACCCG GGGAT CCTCT AGAGT

Eco RI   Sac I   Kpn I   Ava1/Xmal/ Smal   Bam H 1   Xba I

CGACC TGCAG GCATG CAAGC TTGTC TCCCT ATAGT

Sal 1/Acc I/HincII   PstI   Sph 1   Hind III   T7 Promoter

GAGTC GTATT AGAGC ... 3′

The transcript contains the entire domain VI with an additional 12 nucleotides (GAAUACGAAUUC) at the 5' end and an additional six nucleotides (GGAUCC) at the 3' end.

Figure 34. Electrophoretic pattern of plasmid pRDVI, *Bam*HI and BamH1-*EcoRI* restricted.
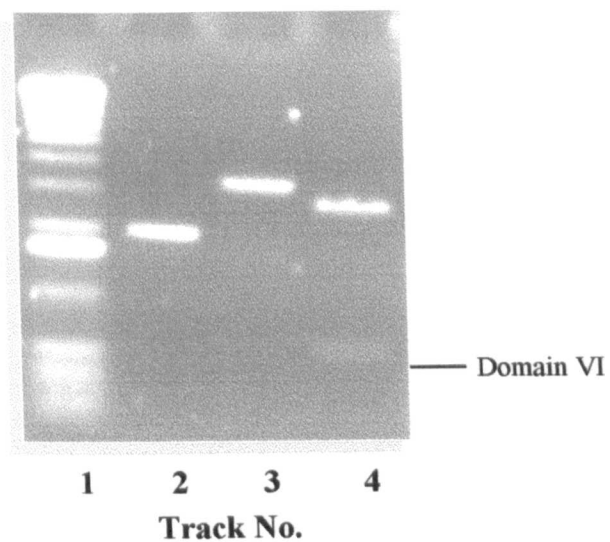
Electrophoretic profile of pRDVI DNA. 1.5μg were loaded onto a 0.8% agarose analytical gel.

1) DNA ladder
2) pRDVI DNA
3) pRDVI DNA *Bam*HI restricted
4) pRDVI DNA *Bam*HI-*EcoRI* restricted

respectively. Track 4 shows a second fragment of approximately 280 nucleotides after *Bam*HI-*EcoRI* restriction that corresponds to the domain VI insert. This recombinant plasmid was termed pRDVI.

Forward and Reverse primers were used for DNA sequencing. **Figure 35** shows the DNA sequencing electrophoresis profile obtained by using the Reverse primer. The domain VI sequence was confirmed and agrees with already published sequence (Brosius *et al.*, 1981a; Leffers *et al.*, 1988).

A large-scale preparation of the sequenced plasmid was made using the caesium chloride method (section 2.11.2.) and/ or the QIAGEN mini and maxi-preps Kits (sections 2.11.1., 2.11.3. and 2.11.4.).

7.4. Transcription of Domain VI from *E. coli rrn*B Operon

Once pRDVI was purified, it was *Bam*HI restricted to linearize DNA as described in section 2.11.7. SP6-RNA polymerase enzyme and rNTPs were used to obtain the RNA transcripts. The DNA template was removed with pancreatic RNase-free DNase and RNA transcripts were obtained through phenol/chloroform extraction (section 2.6.1.).

The RNA transcription and RNA renaturation methodologies of Weitzmann *et al.* (1990) and Nitta *et al.* (1998), were used in an attempt to obtain a higher yield of correctly folded transcripts. Preliminary results showed no difference between them, and the RNasin^R ribonuclease inhibitor methodology was finally used with satisfactory results (sections 2.14.2 and 2.14.3.). **Figure 36** shows the domain VI - RNA transcript electrophoretic profile in a 1.2% agarose: formamide gel compared to the profile of 'naked' total *E. coli* rRNA. Tracks 1 and 2 show 0.5 and 1.0 µg respectively of RNA transcript, using track 3 with 3µg 'naked' rRNA as control.

7.5. Transcript Sensitivity to RIPs

In order to study the role of the r-proteins on the sensitivity of domain VI reconstituted RNP to RIPs, confirmation was required that the domain VI transcript behaved in a similar manner towards RIPs as intact 23S rRNA.

Figure 35. DNA electrophoretic pattern for DNA sequencing, using Reverse primer.

The sequence shown on the right is that surrounding the RIP target site.

Figure 36. Comparative electrophoretic pattern of domain VI - RNA transcripts and 'naked' total RNA as control.
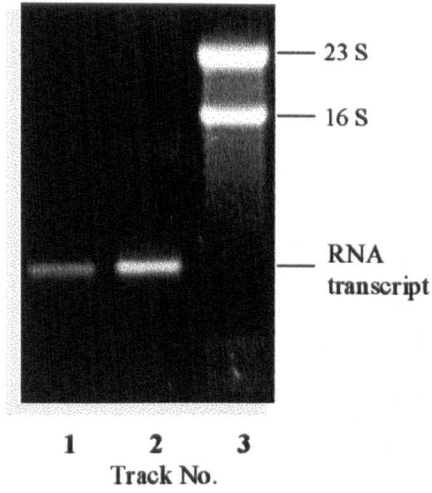
Electrophoretic profile from extracted RNA. 1.2% agarose: formamide gel.

    1) 0.5μg domain VI - RNA transcript
    2) 1.0μg domain VI - RNA transcript
    3) 3.0μg 'naked' total RNA from *E. coli* ribosomes as control

Figure 37 shows the comparative results of the activity of PAP on *E. coli* ribosomes and domain VI - transcript (RNA_T) in a TKCa reaction buffer. Tracks 1-4 show the profile of rRNA from the reaction mixtures of *E. coli* ribosomes, and tracks 5-8 show the profile of rRNA from the reaction mixtures of domain VI - RNA transcript as follows:

a) with the reaction buffer alone as negative control (track 1)

b) with PAP as control in a 1:1 and 1:10 m.r., without aniline treatment (tracks 2 and 5 respectively)

c) with added aniline reagent after PAP activity, in serial dilutions of PAP to give 1:10 (track 6), 1:1 (tracks 3 and 7) and 1:0.1 (tracks 4 and 8) m.r. (Substrate: PAP).

Tracks 3, 4, and 6 show the aniline fragment, produced by the N-glycosidase activity of PAP and after the rRNA cleavage by the aniline reagent where the depurination has occurred. The fragment is equivalent to those reported for a depurination at position A_{2660} of 23S rRNA. These results show a difference between the activity of PAP on native *E. coli* ribosomes, and on RNA_T. The latter is reduced by more than 100 times. tRNA was used as a carrier and it was added after the substrate: RIP reaction in order not to affect the results and in order to enhance the quantity of rRNA recovered from the solution mixtures of above reactions.

The above assay was carried out for PAP and RTA N-glycosidase activity on both 23S rRNA and RNA_T in the TKCa buffer. **Figure 38** shows the comparative results of the activity of PAP and RTA on both substrates. Tracks 1-4 and 11-14 show the pattern of rRNA extracted from the reaction mixtures containing 23S rRNA, and tracks 5-10 show the pattern of the RNA_T reaction mixtures.

Figure 37. Comparative results between the activity of PAP on *E. coli* ribosomes and domain VI - RNA transcript in TKCa buffer.
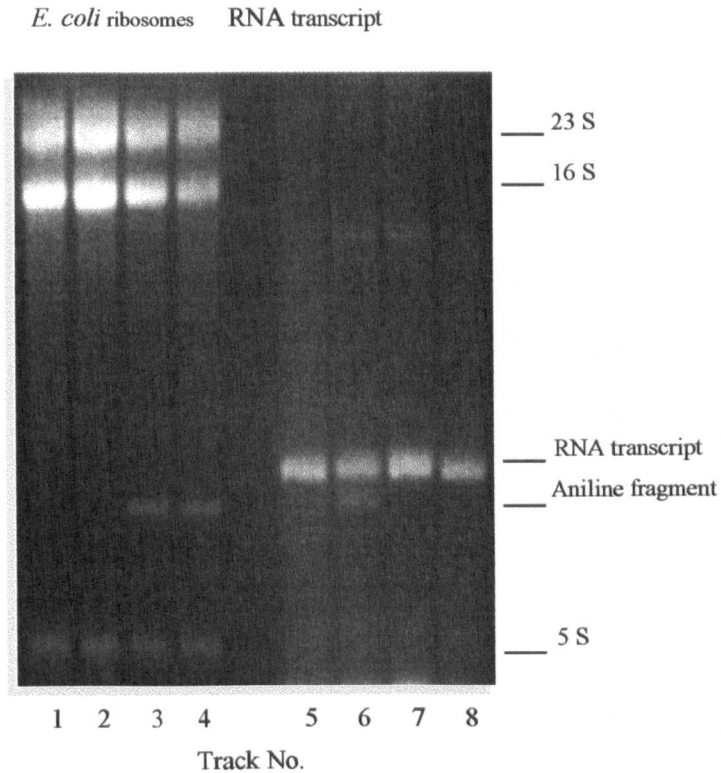
Electrophoretic profile of extracted rRNA after incubation. 3μg were loaded onto a 1.2% agarose: formamide gel. TKCa reaction buffer final concentration: 25mM Tris/HCl pH 7.6, 25mM KCl, and 5mM CaCl₂

PAP activity on *E. coli* ribosomes (tracks 1-4) and on domain VI - RNA transcript (tracks 5-8):

    1) *E. coli* ribosomes
    2) *E. coli* ribosomes + PAP (1:1 m.r.)
    3) *E. coli* ribosomes + PAP + aniline (1:1 m.r.)
    4) *E. coli* ribosomes + PAP + aniline (1:0.1 m.r.)
    5) RNA_T + PAP (1:10 m.r.)
    6) RNA_T + PAP + aniline (1:10 m.r.)
    7) RNA_T + PAP + aniline (1:1 m.r.)
    8) RNA_T + PAP + aniline (1:0.1 m.r.)

Figure 38. Comparative results between the activity of PAP and RTA on 23S RNA and on domain VI - RNA transcript in TKCa reaction buffer.
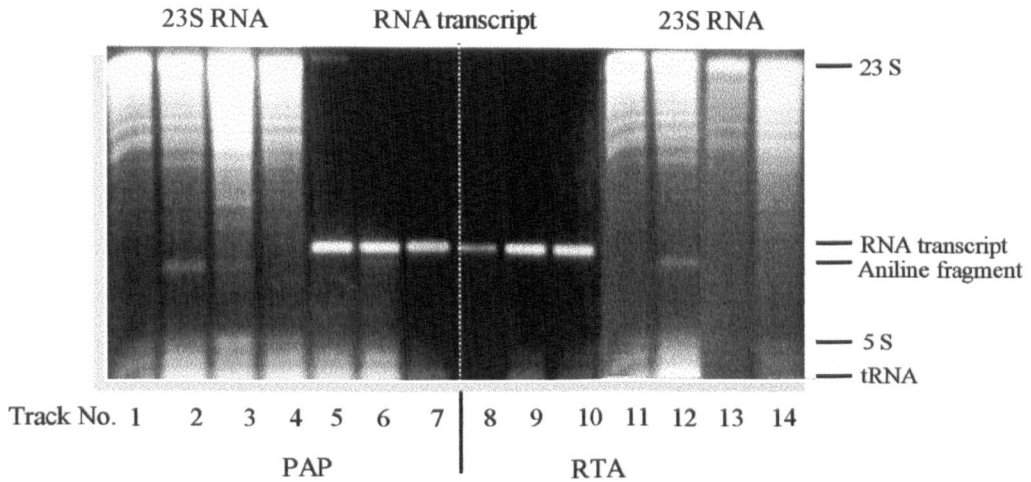
Electrophoretic profile of extracted rRNA after incubation. 3µg were loaded onto a 1.2% agarose: formamide gel. TKCa reaction buffer final concentration: 25mM Tris/HCl pH 7.6, 25mM KCl, and 5mM CaCl$_2$

PAP activity on 23S rRNA (tracks 1-4) and on domain VI - RNA transcript (tracks 5-7), RTA activity on 23S rRNA (tracks 11-14) and on domain VI - RNA transcript (tracks 8-10):

    1) 23S rRNA
    2) 23S rRNA + PAP + aniline (1:10 m.r.)
    3) 23S rRNA + PAP + aniline (1:1 m.r.)
    4) 23S rRNA + PAP + aniline (1:0.1 m.r.)
    5) RNA$_T$
    6) RNA$_T$ + PAP + aniline (1:10 m.r.)
    7) RNA$_T$ + PAP + aniline (1:1 m.r.)
    8) RNA$_T$
    9) RNA$_T$ + RTA + aniline (1:10 m.r.)
    10) RNA$_T$ + RTA + aniline (1:1 m.r.)
    11) 23S rRNA
    12) 23S rRNA + RTA + aniline (1:10 m.r.)
    13) 23S rRNA + RTA + aniline (1:1 m.r.)
    14) 23S rRNA + RTA + aniline (1:0.1 m.r.)

The reactions were carried out as follows:

a) with the reaction buffer alone as negative control (tracks 1,5, 8 and 11)

b) with added aniline reagent and with PAP in serial dilutions of PAP to give 1:10, 1:1 and 1:0.1 (where indicated) substrate:PAP m.r.(tracks 2-4 and 6-7).

c) with added aniline reagent and with RTA in a serial dilutions of RTA to give1:10, 1:1 and 1:0.1 (where indicated) substrate: RTA m.r.(tracks 9-10 and 12-14).

Tracks 2, 3, 6 and 12 show the aniline fragment produced after the RIPs N-glycosidase activity and after the rRNA cleavage by the aniline reagent where depurination has occurred. The aniline fragments shown are equivalent to that reported for depurination at A_{2660} of 23S rRNA. It was confirmed that PAP was at least 10-fold more active on the 23S rRNA than on the RNA_T. No activity on RNA_T was observed even at a RNA_T: RTA m.r. of 1:10.

Finally, **Figure 39** shows the comparative results of the activity of PAP and RTA on RNA_T in TKCa reaction buffer. Samples were analysed in a 2% agarose: formamide RNA analytical gel in order to get a better separation of the fragments. The reactions are as follows:

a) Track 1 shows the RNA_T profile as a negative control.

b) Track 2 shows the RNA_T profile with an added aniline reagent as a control.

c) Tracks 3 and 5 show the profile of the RNA_T with added PAP and RTA respectively to give a 1:10 m.r. substrate: RIP as controls.

d) Tracks 4 and 6 show the profile of the RNA_T with added PAP and RTA respectively to give 1:10 m.r. substrate: RIP, with an added aniline reagent.

Only track 4 shows the aniline fragment produced by PAP's N-glycosidase activity. No activity on RNA_T was observed with RTA. Primer extension was carried out in order to confirm that the depurination has occurred at the adenine equivalent to A_{2660} of 23S rRNA.

Figure 39. Comparative results between the activity of PAP and RTA on domain VI - RNA transcripts in TKCa reaction buffer.
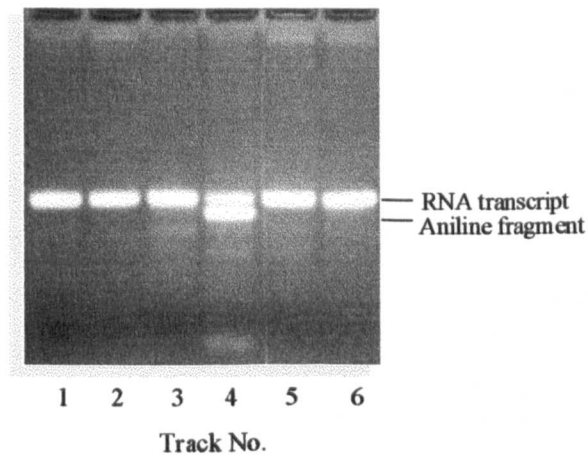
Electrophoretic profile of extracted rRNA after incubation. 3μg were loaded onto a 2.0% agarose: formamide gel. TKCa reaction buffer final concentration: 25mM Tris/HCl pH 7.6, 25mM KCl, and 5mM CaCl$_2$.

PAP activity on domain VI - RNA transcript (tracks 3-4), RTA on RNA$_T$ (tracks 5-6):

1) RNA$_T$
2) RNA$_T$ + aniline
3) RNA$_T$ + PAP (1:10 m.r.)
4) RNA$_T$ + PAP + aniline (1:10 m.r.)
5) RNA$_T$ + RTA (1:10 m.r.)
6) RNA$_T$ + RTA + aniline (1:10 m.r.)

A common method used in the past to determine the site of depurination of large subunit rRNA was the direct sequencing of the fragments released upon aniline treatment after depurination has occurred by RIPs. For example, Endo *et al.* (1988) identified the depurination at A_{4324} in eukaryotic ribosomes by the direct sequencing methodology. Furthermore, Prestle *et al.* (1992) identified the depurination at A_{2660} by the same direct sequencing methodology for 23S rRNA in *E. coli* ribosomes.

Primer extension analysis is based on the fact that reverse transcriptase is unable to read through certain chemically modified or disrupted sequences among the sequencing in the rRNA template (Hagenbuchle *et al.*, 1978; Yovan and Hearst, 1979). Both Primer extension and dideoxynucleotide sequencing methodologies have been well used and recognised as faster, more sensitive and effective methods for identifying where the N-glycosidase activity has occurred on rRNA by RIPs. On primer extension, pauses or stops give rise the premature termination products. The length of the cDNA from the 5' end of the primer to the site of N-glycosidase depurination, where the reverse transcriptase cannot read throughout the site, allows the position of the missing base to be determined, when products of primer extension are electrophoresed alongside dideoxynucleotide sequencing products.

Primer extension analysis was carried out as described in section 2.14.1.2. The 3' end of the primer used 'Prok Prim' anneals 77 bases from the putative depurination site. **Figure 40** shows the primer extension design and the primer sequence, complementary to the bases 2737 to 2753 on the *E. coli* 23S rRNA (Brosius *et al.*, 1981b, numbering) or 6236 to 6252 on the *E. coli rrn*B numbering.

Further aliquots were taken from the RNA extracted from untreated RNA_T and RIPs modified RNA_T with and without aniline treatment **(Figure 39)** for their analysis by primer extension.

Figure 41 shows a sequencing gel of the primer extension on the domain VI – transcript template of 'Prok Prim' and dideoxynucleotide sequencing termination

Figure 40. The sequences and position to which ^{32}P, 5' end-labelled 17 and 19 mers anneal on the RNA for Primer extension analysis of RIPs modified RNA templates.

a) RNA sequencing of α-sarcin/ricin stem loop from 23S rRNA of *E. coli* ribosomes (5'end to 3'end):

α-Sarcin/ricin loop: **CUGCUCCUAGUACG<u>A</u>GAGGACCGGAGUGG** (2646-2674 23S rRNA numbering)

2660   (6145-6173 *rrn*B numbering)

(5'end to 3'end numbering)

b) Oligonucleotides used in Primer extension and rRNA sequencing:

(19mers: 5'end to 3'end) PRT23S: **CCGCATTTAGCTACCGGGC** (2714-2732 23S rRNA numbering)

(6213-6231 *rrn*B numbering)

(5'end to 3'end numbering)

(17mers: 5'end to 3'end) PROK PRIM: **TGCTTTCAGCACTTATC** (2737-2753 23S rRNA numbering)

(6236-6252 *rrn*B numbering)

(5'end to 3'end numbering)

c) Primer extension: representation of Primer annealing for extension experiments.

The numbers below the 5' and 3' ends denote the positions to which the primers anneal. For 23S rRNA numbering, the numbers represent the bases in the 23S rRNA according to the sequence of Leffers *et al.* (1988), and for *rrn*B numbering, the numbers represent the bases in the whole *rrn*B operon according to the sequence from Brosious *et al.* (1988).

Figure 41. Sequencing gel showing the primer extension products of PAP/RTA N-glycosidase activity on domain VI - RNA transcript (RNA$_T$).
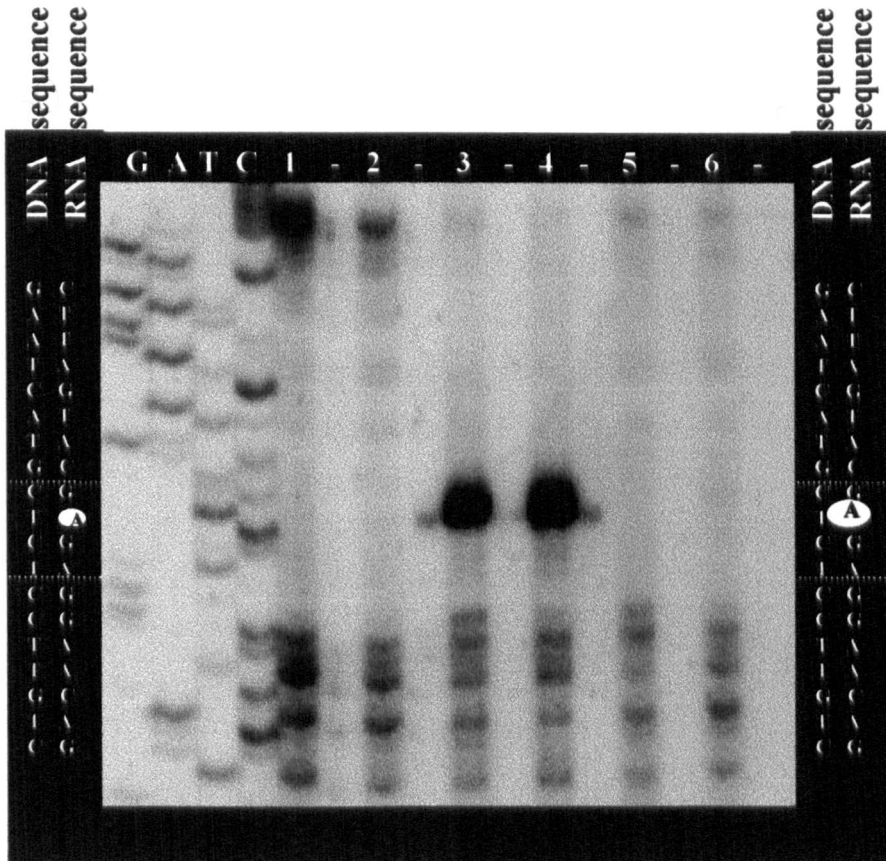
RNA$_T$ was incubated with and without PAP/RTA, with and without aniline reagent (where indicated) and according to the **Figure 39** fully detailed in this Chapter.

Total rRNA was extracted after incubation, and 3μg were used as a template for primer extension as detailed in section 2.14.1.2. The products of primer extension were fractionated on a 6% (w/v) polyacrylamide gel and made visible by autoradiography (section 2.13.2). 'Prok Prim' was used as primer.

1) Domain VI - RNA transcript (RNA$_T$)
2) RNA$_T$+ aniline
3) RNA$_T$ + PAP (1:10 m.r.)
4) RNA$_T$ + PAP + aniline (1:10 m.r.)
5) RNA$_T$ + RTA (1:10 m.r.)
6) RNA$_T$ + RTA + aniline (1:10 m.r.)

GATC represent dideoxynucleotide sequencing reactions from pKK3535 using the same primer as above.

products using pKK3535 as a template using the same primer. Tracks labelled G, A, T and C are the domain VI termination products from *rrn*B in the presence of the corresponding dideoxynucleoside triphosphate reagents. Tracks 1 and 2 with unmodified RNA_T, serve as controls and identify any termination products which result from natural pauses or stops that occur as the reverse transcriptase moves along. Tracks 3 and 4 show the specific termination product (arrowed) induced by PAP treatment but not present in the track 1 used as control.

The products showed identical size and they appear after a C corresponding to the position G_{2661} on *E. coli* rRNA. The stops show that reverse transcriptase could not read through A_{2660} because of its absence in the sequence after the N-glycosidase activity which agrees with other authors (Hartley *et al.*, 1991; Hartley and Lord, 1993; Marchant and Hartley, 1994). The results confirm the RNA electrophoretic profile where it is shown that RNA_T is sensitive to PAP, but not to RTA (**Figure 39**).

7.6. Primer Extension Comparisons with other Substrates

The Primer extensions were done in order to confirm that the putative site of PAP and RTA action were equivalent in all cases, and was carried out on *E. coli* ribosomes and its derivatives tested for substrate sensitivity to PAP and RTA in TKCa reaction buffer. The primers used are described in section 7.5.

Figure 42(a-c) shows a sequencing gel of the products of primer extension reverse transcribed from unmodified substrates (tracks 1, 6, 11, 16, 21 and 24), PAP modified rRNA (tracks 2-3, 7-8, 12-13, 17-18, 22-23 and 25-26) in a 1:1 and 1:10 (substrate: RTA) m.r. as indicated, and RTA modified rRNA (tracks 4-5, 9-10, 14-15 and 19-20) in a 1:10 (substrate: RTA) m.r.

1. **Figure 42(a)** shows the products of primer extension on rRNA extracted from 70S ribosomes (tracks 1-5) and from 'naked' total rRNA (tracks 6-10), after RIPs N-glycosidase activity (tracks 2, 4, 7 and 9) and after treating with aniline reagent (tracks 3, 5, 8 and 10). In both the modified-cleaved and the modified but uncleaved rRNAs, there is a major termination site corresponding to G_{2661} in the

Figure 42. Sequencing gel showing the primer extension products of PAP/RTA N-glycosidase activity on α-sarcin/ricin domain present in different substrates.
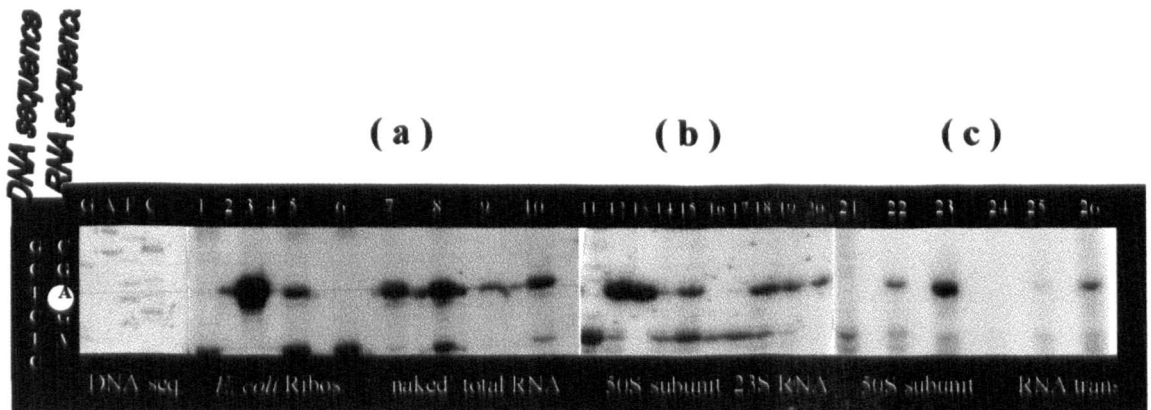
α-Sarcin/ricin domain contained on different substrates was incubated with and without PAP/RTA, with and without aniline reagent (where indicated).

Total rRNA was extracted after incubation, and 3μg were used as a template for primer extension as detailed in section 2.14.1.2. The products of primer extension were fractionated on a 6% (w/v) polyacrylamide gel and made visible by autoradiography (section 2.13.2.).

     1) *E. coli* ribosomes
     2) *E. coli* ribosomes + PAP (1:1 m.r.)
     3) *E. coli* ribosomes + PAP + aniline (1:1 m.r.)
     4) *E. coli* ribosomes + RTA (1:10 m.r.)
     5) *E. coli* ribosomes + RTA + aniline (1:10 m.r.)
     6) 'naked' total rRNA
     7) 'naked' total rRNA + PAP (1:1 m.r.)
     8) 'naked' total rRNA + PAP + aniline (1:1 m.r.)
     9) 'naked' total rRNA + RTA (1:10 m.r.)
     10) 'naked' total rRNA + RTA + aniline (1:10 m.r.)
     11) 50S subunit
     12) 50S subunit + PAP (1:1 m.r.)
     13) 50S subunit + PAP + aniline (1:1 m.r.)
     14) 50S subunit + RTA (1:10 m.r.)
     15) 50S subunit + RTA + aniline (1:10 m.r.)
     16) 23S RNA
     17) 23S rRNA + PAP (1:1 m.r.)
     18) 23S rRNA + PAP + aniline (1:1 m.r.)
     19) 23S rRNA + RTA (1:10 m.r.)
     20) 23S rRNA + RTA + aniline (1:10 m.r.)
     21) 50S subunit
     22) 50S subunit + PAP (1:1 m.r.)
     23) 50S subunit + PAP + aniline (1:1 m.r.)
     24) RNA_T
     25) RNA_T + PAP (1:10 m.r.)
     26) RNA_T + PAP + aniline (1:10 m.r.)

23S rRNA sequence, which is not present in the unmodified rRNA sample. Thus, the site of depurination can be inferred from this as one base to the 5' of the termination site at A_{2660}.

2. **Figure 42(b)** shows the products of primer extension derived from 50S subunit (tracks 11-15) and from 23S rRNA (tracks 16-20), after RIPs N-glycosidase activity (tracks 12, 14, 17 and 19) and with added aniline reagent (tracks 13, 15, 18 and 20). In both, the modified/cleaved and the modified/uncleaved 23S rRNAs extension, there is a major termination site characteristic of depurination at A_{2660}.

3. Finally, **Figure 42(c)** shows the products of primer extension derived from 50S subunit (tracks 21-23) and from RNA_T (tracks 24-26), after PAP's N-glycosidase activity only (tracks 22 and 25) and after treating with aniline reagent (tracks 23 and 26). Once more, in both the modified/cleaved and the modified/uncleaved 23S rRNAs extension, there is a major termination site characteristic of depurination at A_{2660}.

Thus, there was a major termination site characteristic of the depurination A_{2660} because of the PAP's N-glycosidase activity through the substrates assayed, proving that the α-sarcin/ ricin domain is present in the conformational structure sensitive to PAP although there is lack of activity of RTA on RNA_T.

7.7. Interaction of the TP50 Ribosomal Proteins with Domain VI

The r-proteins are presently viewed as fulfilling a subsidiary role in translation, such as protecting rRNA from degradation, stabilising rRNA conformations and facilitating conformational changes in the ribosomal RNA. (Douthwaite *et al.*, 1995).

The proteins bound to domain VI from 23S rRNA of *E. coli* ribosomes have been tentatively identified as L3 which binds strongly within subdomain VIA and L6 which binds weakly to the same subdomain (Leffers *et al.*, 1988). Furthermore, Uchiumi *et al.* (1999) found a cooperative interaction between both proteins. Their results showed that the binding of L6 and L3 together protected additional bases A_{2657}, A_{2662}, C_{2666} and C_{2667} in the α-sarcin/ricin loop, in addition to A_{2740}, A_{2741}, A_{2753}, A_{2764}, A_{2765} and A_{2766} in another stem loop (domain IV has 5 stem-loop structures) within domain VI

(helix 92, Raue *et al.*, 1988). Hence, the works mentioned suggested the protection of rRNA sequences and the conformational modulation of the highly conserved α-sarcin/ ricin domain depends on the protein binding.

Gel retardation electrophoresis is a method that allows protein-RNA complexes to be detected and which depends on the physical separation of complexes from free rRNA and protein. The complexed and the uncomplexed RNAs are separated by differences in electrophoretic mobility. It is based on the fact that generally, the larger size and reduced negative charge of the RNA: protein complex slows migration in a standard polyacrylamide gel (Draper, 1994). Gel retardation electrophoresis has been used by several authors in order to elucidate the interaction and the specificity of the interaction of ribosomal proteins or other ribosomal components with the rRNA (e.g. Bartel and Szostak, 1994; Karn *et al.*, 1994; Batey and Williamson, 1996; Serganov *et al.*, 1996, Uchiumi *et al.*, 1999).

In the present study, interactions of r-proteins (TP50) with RNA transcripts (Domain VI from 23S rRNA) were investigated. The domain VI RNA transcript (RNA_T) used contains the α-sarcin/ricin loop. Leffers *et al.* (1988) reported that the L3 binding site was at residue 2629, a nucleotide away from the 5'end of the domain VI RNA transcript used. Also Uchiumi *et al.* (1997) reported that the presence of L3 in that domain indicated also the presence of L6 with a low affinity, and both would affect the conformation of the a-sarcin/ricin loop in a cooperative way. It is unclear therefore whether L6 binding can take place independently of L3. The interaction of radiolabelled domain VI – transcript (^{32}P-RNA_T) and TP50 r-proteins was monitored using a native gel mobility shift assay based on works carried out by Batey and Williamson (1996) and by Serganov *et al.*, (1996). The proportion of TP50 to be added to domain VI-RNA_T was based on the stoichiometry studies by Nierhaus (1990) for 50S reconstitution from 23S rRNA and TP50. Because non-physiological RNA-RNA interaction can be problematic, the first experiment involved an investigation of whether prior heating and snap cooling of the ^{32}P-RNA_T affected its interaction with r-proteins. The results of titration are shown in **Figure 43**.

Figure 43. Effect of prior heating and snap-cooling treatment of ^{32}P-RNA$_T$ on its subsequent association with r-proteins, as monitored by mobility shift assays.
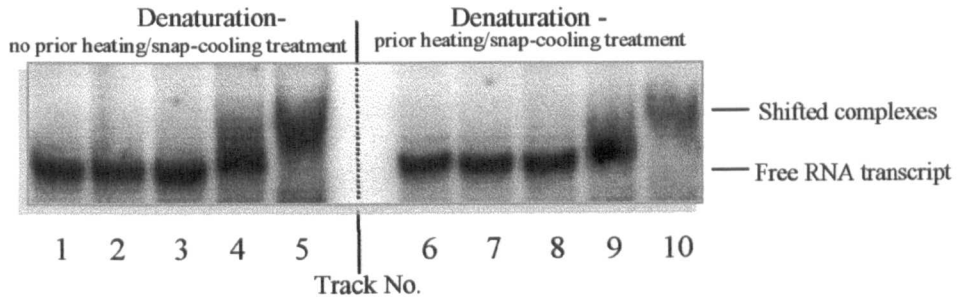
12% Non-denaturing gel electrophoresis. Samples electrophoresed during 1 h and 45 min.

(I) ^{32}P-RNA$_T$ denaturation – no prior heating and snap-cooling treatment.
     1) ^{32}P-RNA$_T$
     2) ^{32}P-RNA$_T$ + L3 (1:0.2 ratio)
     3) ^{32}P-RNA$_T$ + L3 (1:0.4 ratio)
     4) ^{32}P-RNA$_T$ + TP50 (1:2 ratio)
     5) ^{32}P-RNA$_T$ + TP50 (1:4 ratio)
(II) ^{32}P-RNA$_T$ denaturation - prior heating and snap-cooling treatment.
     1) ^{32}P-RNA$_T$
     2) ^{32}P-RNA$_T$ + L3 (1:0.2 ratio)
     3) ^{32}P-RNA$_T$ + L3 (1:0.4 ratio)
     4) ^{32}P-RNA$_T$ + TP50 (1:2 ratio)
     5) ^{32}P-RNA$_T$ + TP50 (1:4 ratio)

Re-folding step: 1min at 90°C followed by two minutes incubation on ice (heating and snap cooling treatment). Mobility shift buffer (MBS) composition consistes of: 10mM K-Hepes pH 7.5, 50mM potassium acetate, 0.1mM EDTA, 0.1mg/ml tRNA, 5µg/ml heparin, and 0.01% Nonidet P40 (Batey and Williamson, 1996). Each reaction contained 0.2pmol RNA$_T$. TP50 ratios based on section 2.16.2.

^{32}P-labelling for ^{32}P-RNA$_T$ was obtained following the procedure described at section 2.14.3.

The Max Planck Institut fuer Molekulare Genetik provide samples of several r-proteins pooled individually as well as a sample of TP50 containig L3 and L6 among them. **Figure 43** shows titration experiment with ^{32}P-RNA$_T$ and either L3 or TP50 (sections 2.16.1 and 2.16.2) to give a 1:0.2, 1:0.4, 1:2 and 1:4 ratio (^{32}P-RNA$_T$: TP50), where indicated. ^{32}P-RNA$_T$ was obtained as described at sections 2.14.3. and 2.14.5. The titration experiments were carried out as described in section 2.18.2. Final buffer composition of the sample prior to being loaded is shown at **Appendix 2**. The conditions chosen are based on the reasoning discussed by Batey and Williamson (1996). All of their reactions include a high concentration of tRNA to prevent non-specific interactions.

Figure 43 (I) (tracks 1 to 5) show the titration experiment of ^{32}P-RNA$_T$ without heating and snap-cooling treatment (re-folding step). **Figure 43(II)** (tracks 6 to 10) show the titration experiment of ^{32}P-RNA$_T$ subjected to a prior re-folding step; 1min at 90°C followed by two minutes incubation on ice (heating and snap-cooling treatment) (Batey and Williamson, 1996). According to Batey and Williamson (1996) the process of heating and snap-cooling RNA is a functionally adequate preparation of an RNA transcript for monitoring the association with r-proteins in an *in vitro* situation. (This procedure is not the same as a renaturation as understood in an *in vivo* situation). Since this study is an *in vitro* study the decision was taken to follow Batey and Williamson's (1996) method.

The behaviour of the two RNA$_T$ samples in titration with r-proteins is similar. Tracks 4, 5, 9, and 10 show also similar retarded mobility shift electrophoretic profiles. This suggests that the heating and snap cooling (re-folding) step of the RNA$_T$ is not significantly, affecting its quantitative behaviour in binding r-proteins. No L3 binding was obtained. However some binding was obtained when TP50 titration was assessed, and this can be postulated as being L6 binding (through low affinity binding proposed by Uchiumi *et al.*, 1997; 1999), but further investigation would be needed to prove this **(Figure 43)**.

In a second approach, the effect of TP50 titration was assessed **(Figure 44)**. To 6pmol ^{32}P-RNA$_T$ different quantities of TP50 were added to give a final ratio of 1:0.3, 1:0.5, 1:1, 1:2, 1:3, and 1:4 (where indicated, **Figure 44**). Electrophoresis was carried out for 105 min.

Figure 44, tracks 1 and 2 refer to controls of RNA transcripts in mobility shift buffer, without the reconstitution two step incubation (120min at 25°C instead of 60min at 25°C, 60min at 4°C) (track 1) and carrying out this procedure (track 2) (60min at 25°C, 60min at 4°C). Tracks

Figure 44. Interaction between ^{32}P-RNA$_T$ and TP50.
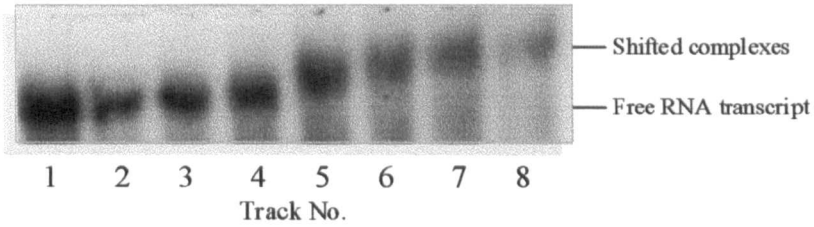
12% Non-denaturing gel electrophoresis. Samples electrophoresed during 105 min.

^{32}P-RNA$_T$ not subjected to heating and snap-cooling treatment prior to titration experiment. Ratios according to Nierhaus (1990) as described at section 2.16.2. For additional conditions see text.

    1) ^{32}P-RNA$_T$ (control 1)
    2) ^{32}P-RNA$_T$ (control 2)
    3) ^{32}P-RNA$_T$ + TP50   (1:0.3 ratio)
    4) ^{32}P-RNA$_T$ + TP50   (1:0.5 ratio)
    5) ^{32}P-RNA$_T$ + TP50   (1:1 ratio)
    6) ^{32}P-RNA$_T$ + TP50   (1:2 ratio)
    7) ^{32}P-RNA$_T$ + TP50   (1:3 ratio)
    8) ^{32}P-RNA$_T$ + TP50   (1:4 ratio)

^{32}P-labelling for ^{32}P-RNA$_T$ was obtained following the procedure described at section 2.14.3.

5 to 8 show that ^{32}P-RNA$_T$: TP50 complexes slow migration through the non-denaturing gel. Thus, ^{32}P-RNA$_T$ displays a reduction of mobility in a native-PAGE on binding to TP50. Titration curve should be extended to obtain the point of saturation binding.

In order to obtain more ^{32}P-labelling efficiently, ^{32}P-RNA$_T$ was obtained following the procedure described at section 2.14.4., which consists on obtaining the ^{32}P-labelling since the synthesis of the transcript trough SP6 transcription. Further experiments were carried out using a ^{32}P-RNA$_T$, which had not been subjected to a heating and snap-cooling (re-folding) step. The final buffer composition of the samples to be loaded is shown at **Appendix 2**.

Using tRNA as unrelated RNA further checked the specificity of binding. tRNA did not show competition for TP50 on a final amount of 4pmol, equivalent to 13.3x ^{32}P-RNA$_T$ quantity (Data not shown).

Figure 45 describes the specificity of binding, through the competition-binding experiments but now using related RNAs. Unlabelled RNA$_T$ and 23S rRNA were used to define the TP50 affinity for ^{32}P-RNA$_T$ as follows:

a) Tracks 1-3 (I and II) refer to the ^{32}P-RNA$_T$ in mobility shift buffer (MSB) (section 2.18.2), with and without the two steps incubation as controls (60min at 25°C, 60min at 4°C, or 120min at 25°C).

b) Tracks 4-9 (I) show the TP50 titration experiment at ratios of 1:1, 1:3, 1:6. 1:9, 1:12 and 1:15 ^{32}P-RNA$_T$: TP50 respectively.

c) Tracks 10-12 (I) and 13-14 (II) show the competition binding effect of unlabelled RNA$_T$ at different ratios (as indicated in the **Figure 45**), using a constant 1:15 ratio of ^{32}P-RNA$_T$:TP50. Track 14(II) refers to a second control without TP50 in order to elucidate any possible effect of ^{32}P-RNA$_T$: unlabelled-RNA$_T$ in terms of gel retardation.

d) Tracks 15 to 19 (II) show the competition-binding effect of 23S rRNA at different rations (as indicated in the **Figure 45**) using a constant 1:15 ratio of ^{32}P-RNA$_T$:TP50 complex as a starting complex. Track 19(II) refers to a third control without TP50 in order to elucidate any possible effect of 23S rRNA in terms of gel retardation.

Figure 45 shows that in the absence of a competitor, ^{32}P-RNA$_T$ formed a maximally retarded complex with TP50 in a 1:12. Howeverver, as expected, binding to ^{32}P-RNA$_T$ is reduced in the presence of unlabelled RNA$_T$.

Figure 45. Gel mobility shift assays for TP50 competition binding experiments.
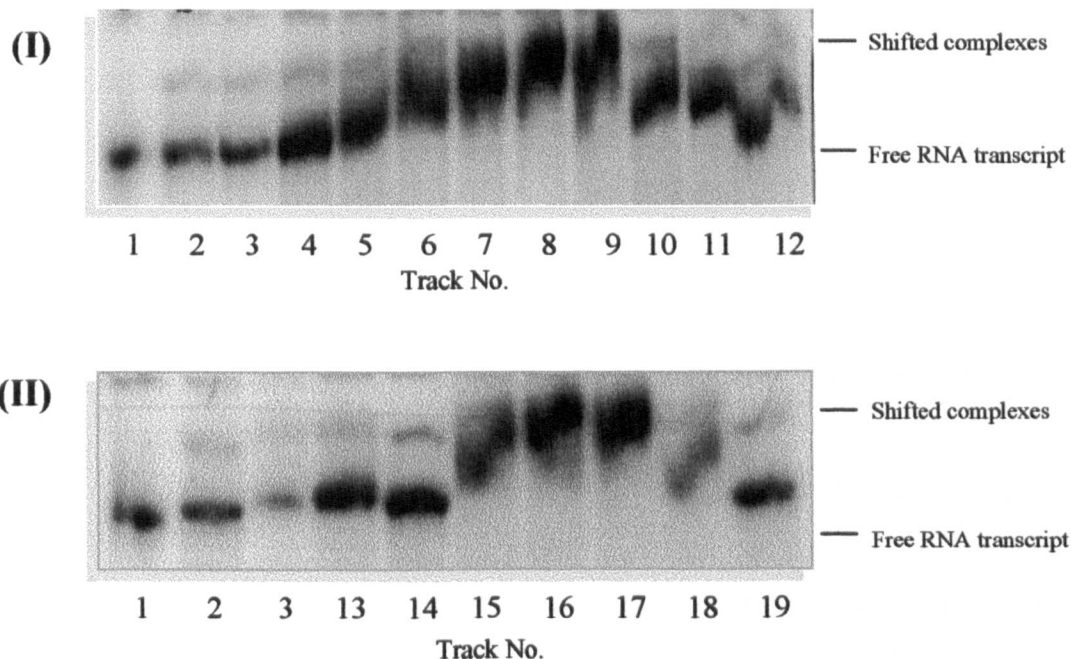
12% Non-denaturing gel electrophoresis. Samples electrophoresed during 3 h.

^{32}P-RNA$_T$ non-temperature treated prior titration experiment. Ratios according to Nierhaus (1990) as described at section 2.16.2.

(I) Titration and RNA-RNA binding-competition experiments

     1) 0.3pmol ^{32}P-RNA$_T$ + MSB

     2) 0.3pmol ^{32}P-RNA$_T$ + MSB

     3) 0.3pmol ^{32}P-RNA$_T$ + MSB (after two hours incubation)

     4) 0.3pmol ^{32}P-RNA$_T$ + 0.015e.u. TP50   (1:1 ratio)

     5) 0.3pmol ^{32}P-RNA$_T$ + 0.03e.u. TP50   (1:3 ratio)

     6) 0.3pmol ^{32}P-RNA$_T$ + 0.06e.u. TP50   (1:6 ratio)

     7) 0.3pmol ^{32}P-RNA$_T$ + 0.09e.u. TP50   (1:9 ratio)

     8) 0.3pmol ^{32}P-RNA$_T$ + 0.12e.u. TP50   (1:12 ratio)

     9) 0.3pmol ^{32}P-RNA$_T$ + 0.15e.u. TP50   (1:15 ratio)

     10) 0.3pmol ^{32}P-RNA$_T$ + 0.15e.u. TP50 + 1pmol RNA$_T$ (1:15:3.3 ratio)

     11) 0.3pmol ^{32}P-RNA$_T$ + 0.15e.u. TP50 + 2pmol RNA$_T$ (1:15:6.7 ratio)

     12) 0.3pmol ^{32}P-RNA$_T$ + 0.15e.u. TP50 + 3pmol RNA$_T$ (1:15:10 ratio)

(II) RNA-RNA and RNA-23S rRNA binding competition experiments

     1) 0.3pmol ^{32}P-RNA$_T$ + MSB

     2) 0.3pmol ^{32}P-RNA$_T$ + MSB

     3) 0.3pmol ^{32}P-RNA$_T$ + MSB (after two hours incubation)

     13) 0.3pmol ^{32}P-RNA$_T$ + 0.15e.u. TP50 + 4pmol RNA$_T$ (1:15:13.3 ratio)

     14) 0.3pmol ^{32}P-RNA$_T$ + 4pmol RNA$_T$ (1:0:3.3 ratio)

     15) 0.3pmol ^{32}P-RNA$_T$ + 0.15e.u. TP50 + 1pmol 23S RNA   (1:15:3.3 ratio)

     16) 0.3pmol ^{32}P-RNA$_T$ + 0.15e.u. TP50 + 2pmol 23S RNA   (1:15:6.7 ratio)

     17) 0.3pmol ^{32}P-RNA$_T$ + 0.15e.u. TP50 + 3pmol 23S RNA   (1:15:10 ratio)

     18) 0.3pmol ^{32}P-RNA$_T$ + 0.15e.u. TP50 + 4pmol 23S RNA   (1:15:13.3 ratio)

     19) 0.3pmol ^{32}P-RNA$_T$ + 4pmol 23S RNA   (1:0:3.3 ratio)

Finally, 23S rRNA was shown to be a less efficient competitor for TP50 than unlabelled transcripts with a $D_{1/2}$ of approx. 4 pmol (equivalent to 13.3x ^{32}P-RNA$_T$ quantity) ($D_{1/2}$ refers to the amount of competitor required to reduce binding by 50% according to Karn *et al.* (1994)). This could be explained because of the complexity of 23S rRNA/r-protein reconstitution. Batey and Williamson (1996) observed a similar effect with 16S rRNA competition for the binding S15 to a transcript of 16S rRNA. They suggested that the slow rate of association, compared to more efficient competitors was likely because, in spite of the requirement for a RNA: protein collision at the correct site for specific binding, not all the collisions would be productive. However, because TP50 bound to ^{32}P-RNA$_T$ and a condition of an excess of tRNA, it was demonstrated that the elements of the specific TP50-23S rRNA interaction were preserved in domain VI transcripts.

Figure 46(I) shows the stability of the complex, which was analysed using the experiments described at sections 2.18.2. and 2.18.3. The rational for the experiments is the following: An incubation is performed in which the ^{32}P-RNA$_T$/TP50 interaction obtains equilibrium. At this point, an excess of unlabelled RNA$_T$ is added and incubation continued. Samples are removed after various time of incubation and applied immediately to the non-denaturing gel. If the complex between the ^{32}P-RNA$_T$ and TP50 is relatively stable, then the amount of retarded labelled complex should not be influenced by the unlabelled competitor RNA. If on the other hand, the complex between ^{32}P-RNA$_T$ and TP50 is unstable, protein which dissociate from it would rebind to the excess unlabelled RNAT, resulting in a loss of the retarded, labelled complex with time.

The experiments were based on Batey and Williamson's (1996) work, but with the modifications described in the sections quoted. However, association and dissociation experiments were conducted at 25°C (instead of the two step procedure used in **Figures 43, 44** and **45**) in a dry block, by adding 0.3pmol ^{32}P-RNA$_T$ and 0.15 e.u. of TP50 (1:15 ratio, transcript: TP50). In dissociation experiments (**Figure 46(II)**), 2pmol of RNA transcript competitor were subsequently added to each reaction to give a final ratio

Figure 46. The ^{32}P-RNA$_T$:TP50 complex association and dissociation experiments
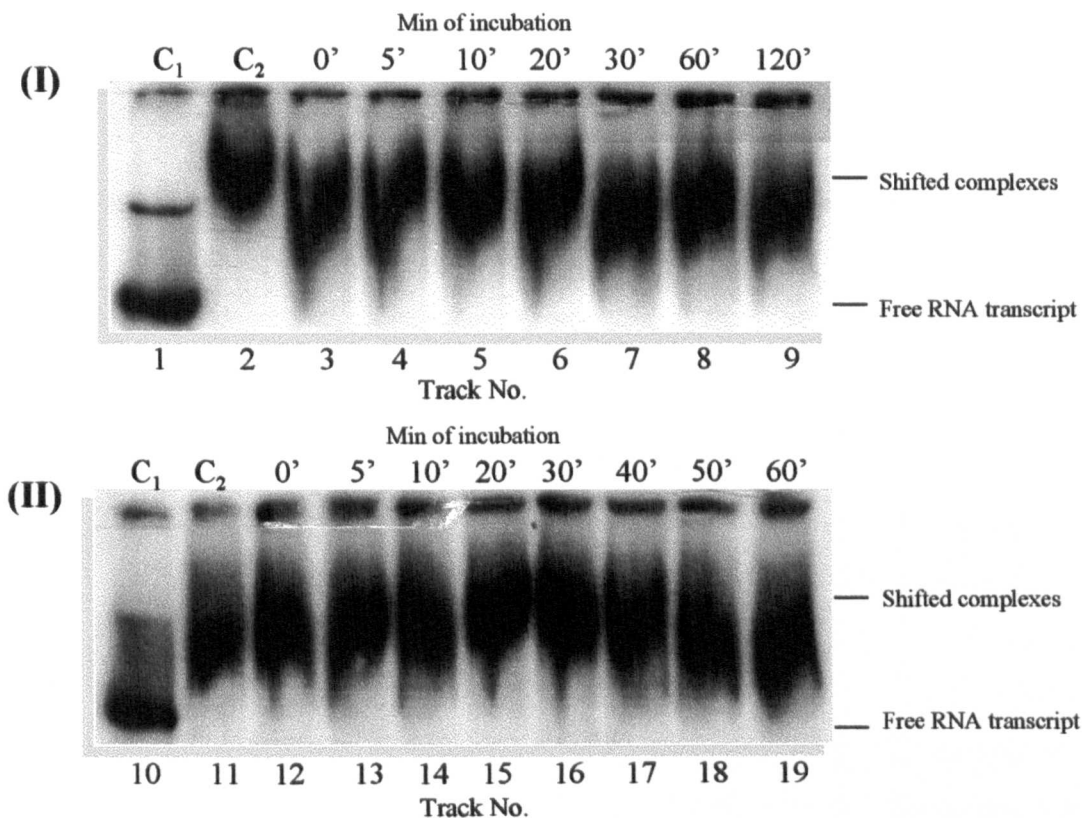
(I) Association experiments in a 1:15 ^{32}P-RNA$_T$:TP50 ratio, at 0 to 120 min of complex incubation, in MSB at 25°C. 12% acrylamide non-denaturing gel electrophoresed during 4 h at 20mA.

    1) 0.3pmol ^{32}P-RNA$_T$ + MSB (Control 1)
    2) 0.3pmol ^{32}P-RNA$_T$ + 0.15e.u. TP50 (1:15 ratio) (Control 2)
    3) 0.3pmol ^{32}P-RNA$_T$ + 0.15e.u. TP50 (1:15 ratio) after 0 min
    4) 0.3pmol ^{32}P-RNA$_T$ + 0.15e.u. TP50 (1:15 ratio) after 5 min
    5) 0.3pmol ^{32}P-RNA$_T$ + 0.15e.u. TP50 (1:15 ratio) after 10 min
    6) 0.3pmol ^{32}P-RNA$_T$ + 0.15e.u. TP50 (1:15 ratio) after 20 min
    7) 0.3pmol ^{32}P-RNA$_T$ + 0.15e.u. TP50 (1:15 ratio) after 30 min
    8) 0.3pmol ^{32}P-RNA$_T$ + 0.15e.u. TP50 (1:15 ratio) after 60 min
    9) 0.3pmol ^{32}P-RNA$_T$ + 0.15e.u. TP50 (1:15 ratio) after 120 min

(II) Dissociation experiments in a 1:15:6.7 ^{32}P-RNA$_T$: TP50: RNA$_T$ competitor ratio (complex with ^{32}P-RNA$_T$ was formed before the addition of the competitor RNA$_T$), at 0 to 60 min of mixture incubation, in MSB at 25°C. 12% acrylamide non-denaturing gel electrophoresed during 3 h at 20mA

    10) 0.3pmol ^{32}P-RNA$_T$ + MSB (Control 1)
    11) 0.3pmol ^{32}P-RNA$_T$ + 0.15e.u. TP50 (1:15 ratio) (Control 2)
    12) 0.3pmol ^{32}P-RNA$_T$ + 0.15e.u. TP50 + 2pmol RNA$_T$ (1:15:6.7 ratio) 0 min competition
    13) 0.3pmol ^{32}P-RNA$_T$ + 0.15e.u. TP50 + 2pmol RNA$_T$ (1:15:6.7 ratio) 5 min competition
    14) 0.3pmol ^{32}P-RNA$_T$ + 0.15e.u. TP50 + 2pmol RNA$_T$ (1:15:6.7 ratio) 10 min competition
    15) 0.3pmol ^{32}P-RNA$_T$ + 0.15e.u. TP50 + 2pmol RNA$_T$ (1:15:6.7 ratio) 20 min competition
    16) 0.3pmol ^{32}P-RNA$_T$ + 0.15e.u. TP50 + 2pmol RNA$_T$ (1:15:6.7 ratio) 30 min competition
    17) 0.3pmol ^{32}P-RNA$_T$ + 0.15e.u. TP50 + 2pmol RNA$_T$ (1:15:6.7 ratio) 40 min competition
    18) 0.3pmol ^{32}P-RNA$_T$ + 0.15e.u. TP50 + 2pmol RNA$_T$ (1:15:6.7 ratio) 50 min competition
    19) 0.3pmol ^{32}P-RNA$_T$ + 0.15e.u. TP50 + 2pmol RNA$_T$ (1:15:6.7 ratio) 60 min competition

of 1:15:6.7. The experiment was performed under these conditions because it had been shown in the competition experiments shown in **Figure 45** that they had resulted in a substantial reduction in the formation of the ^{32}P RNA$_T$: TP50 complex.

Thus, **Figure 46** shows the following reactions:

a) Tracks 1-2 (I) and 10-11 (II) show the ^{32}P-RNA$_T$ and ^{32}P-RNA$_T$:TP50 complex (after 2h incubation) as control.

b) Tracks 3 to 9 (I) show the profile of ^{32}P-RNA$_T$:TP50 complex after the indicated incubation times.

c) Tracks 12 to 19 (II) show the profile of ^{32}P-RNA$_T$:TP50: RNA$_T$ competitor, after the indicated incubation times.

Figure 46(I), track 3 (time 0) shows that the formation of a complex occurs rapidly. **Figure 46(II)** shows that RNA$_T$ competitor reduced binding but that is only apparent at incubation time of > 30min incubation. It is concluded that the ^{32}P-RNA$_T$: TP50 complex is relatively stable.

The stability of the complex between ^{32}P-RNA$_T$: TP50 (1:15 ratio) was also analysed in buffer 6 (20mM Tris/Cl pH7.4, 20mM Mg acetate, 400mM NH$_4$Cl, 1mM EDTA, 5mM 2-mercaptoethanol) and TKCa buffer in order to provide the conditions for the assay of substrate sensitivity for RIPs N-glycosidase activity. The substrates refer to ^{32}P-RNA$_T$ and ^{32}P-RNA$_T$:TP50 complex as a reconstituted domain VI.

Based in the assembly mapping protocol for the 50S published by Nierhaus (1990) as described in section 2.18.6., this alternative method was carried out. ^{32}P-RNA$_T$: TP50, was reconstituted in buffer 6 (**Figure 47**) then the sample was applied to a 10-30% sucrose gradient made up with the same reconstitution buffer. A sample of the same amount of ^{32}P-RNA$_T$ was similarly applied to a sucrose gradient . After centrifugation, the sucrose gradients were fractionated. The fractions were collected and the cpm was measured using a scintillation counter in order to obtain a sedimentation profile. The cpm/μl was plotted against the fraction number.

Figure 47. Sedimentation profile of ^{32}P-RNA$_T$ and ^{32}P-RNA$_T$:TP50 complex reconstituted in buffer 6 (20mM Tris/Cl pH7.4; 20mM Mg acetate, 400mM NH$_4$Cl, 1mM EDTA, 5mM 2-mercaptoethanol).
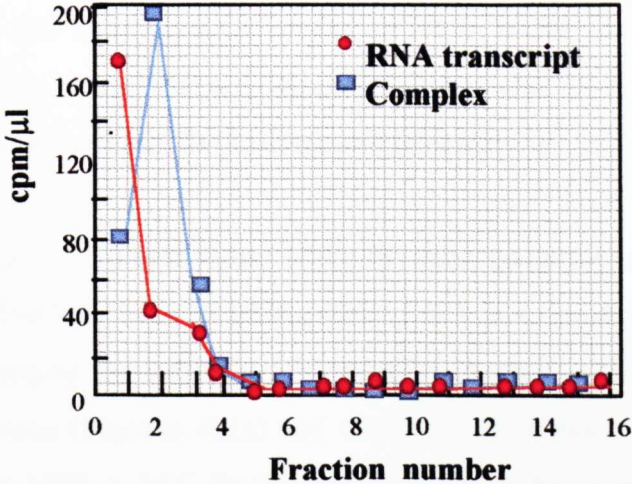
The direction of sedimentation is from left to right.

Figure 47 shows the sedimentation profiles of both ^{32}P-RNA$_T$ and ^{32}P-RNA$_T$:TP50 complex substrates. **Figure 48** shows the sedimentation profile of a similar experiment to that shown in **Figure 47** but this time the complex was formed in MSB and then equilibrated with TKCa buffer by Biogel P6 chromatographic column (section 2.18.5.) and applied to a sucrose gradient containing TKCa buffer. **Figure 47** and **Figure 48**, both show a clear and well-defined change in sedimentation profile from the free RNA$_T$ to the RNA$_T$: TP50 complex in the two buffers tested. These confirmed the complex formation during the centrifugation, under different buffer conditions. Thus, the following step was to assay PAP activity on ^{32}P-RNA$_T$ and ^{32}P-RNA$_T$:TP50 complex under the TKCa buffer selected for this research (Chapter V).

Gel retardation assays were carried out under the same non-denaturing conditions, but this time using ^{32}P-RNA$_T$ and ^{32}P-RNA$_T$:TP50 (1:15 m.r.) complex reconstituted in MSB and then changing the buffer for TKCa buffer (section 2.18.5.). The experiment was carried out twice (**Figures 49(a)** and **49(b)**). In both cases, the reconstitutions were carried out in MSB at 25°C for 30 min. Then, the buffer was changed for TKCa buffer (where indicated), followed by incubation under those conditions used for testing RIP sensitivity (30 min at 37°C). Results were compared to those incubated for a further 30-min at 25°C. The control experiments were carried out but using MSB under the two conditions described. The samples were electrophoresed for 105 min (**Figure 49(a)**), and for 50min (**Figure 49(b)**). The experiments were performed in both **Figures 49a/b**, as follows:

a) Tracks 1 and 2 show the profile of the two substrates reconstituted in MSB, and then incubated for 30 min at 37°C.

b) Tracks 3 and 4 show the profile of the two substrates reconstituted in MSB, and then incubated for 30 min at 25°C.

c) Tracks 5 to 6 show the profile of both substrates reconstituted in MSB; MSB was changed for TKCa buffer and then incubated for 30 min at 25°C.

d) Tracks 7 and 8 show the profile of both substrates reconstituted in MSB; MSB was changed for TKCa buffer and then incubated for 30 min at 37°C.

Figure 48. Sedimentation profile of ^{32}P-RNA$_T$ and ^{32}P-RNA$_T$:TP50 complex equilibrated in TKCa buffer (25mM Tris/HCl pH 7.6, 25mM KCl and 5mM CaCl$_2$).
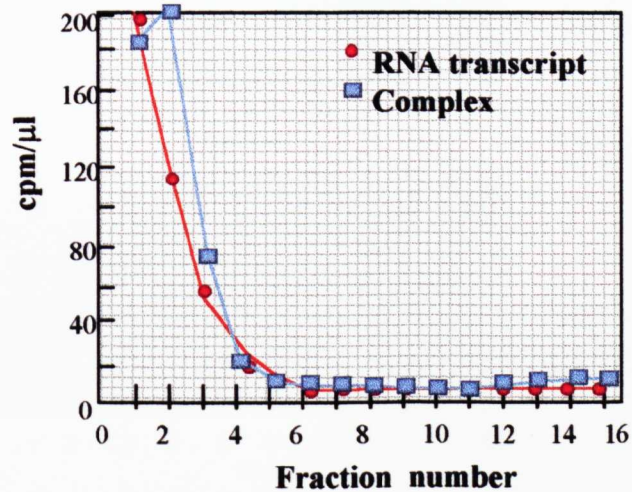
The direction of sedimentation is from left to right.

Figure 49. Non-denaturing gel retardation profile of ^{32}P-RNA$_T$ and ^{32}P-RNA$_T$: TP50 complex reconstituted in MSB at 25°C, then equilibrated in TKCa buffer and incubated at 25°C or 37°C.
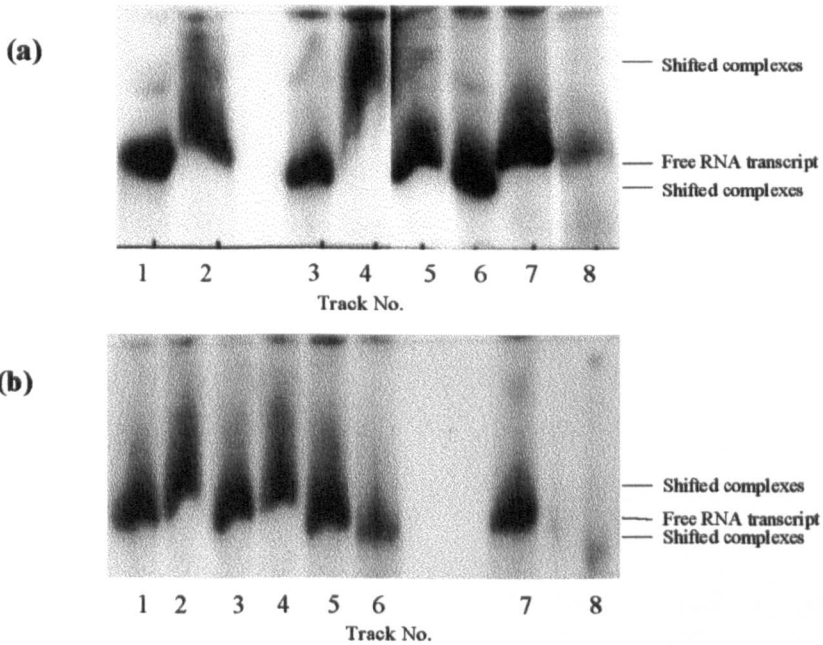
Samples reconstituted in MSB 30 min at 25°C, changing MSB for TKCa buffer (where indicated) and then incubated at 25°C or 37°C. 12% Non-denaturing gel electrophoresis.

(a) Samples electrophoresed for 1h and 45 min.
      1) ^{32}P-RNA$_T$ in MSB incubated at 37°C
      2) ^{32}P-RNA$_T$: TP50 reconstituted and then incubated at 37°C
      3) ^{32}P-RNA$_T$ in MSB, maintained at 25°C
      4) ^{32}P-RNA$_T$: TP50 reconstituted and maintained at 25°C.
      5) ^{32}P-RNA$_T$ equilibrated in TKCa and then incubated at 25°C.
      6) ^{32}P-RNA$_T$: TP50 equilibrated in TKCa and incubated at 25°C.
      7) ^{32}P-RNA$_T$ equilibrated in TKCa and then incubated at 37°C.
      8) ^{32}P-RNA$_T$: TP50 equilibrated in TKCa and incubated at 37°C.

(b) Samples electrophoresed for 50 min.
      1) ^{32}P-RNA$_T$ in MSB incubated at 37°C
      2) ^{32}P-RNA$_T$: TP50 reconstituted and then incubated at 37°C
      3) ^{32}P-RNA$_T$ in MSB, maintained at 25°C
      4) ^{32}P-RNA$_T$: TP50 reconstituted and maintained at 25°C.
      5) ^{32}P-RNA$_T$ equilibrated in TKCa and then incubated at 25°C.
      6) ^{32}P-RNA$_T$: TP50 equilibrated in TKCa and incubated at 25°C.
      7) ^{32}P-RNA$_T$ equilibrated in TKCa and then incubated at 37°C.
      8) ^{32}P-RNA$_T$: TP50 equilibrated in TKCa and incubated at 37°C.

Samples in tracks 2 and 8 (**a** and **b**), which refer to the ^{32}P-RNA$_T$:TP50 complex reconstituted and then incubated at 37°C, show less retardation than those performed at a constant 25°C, showing that the former are less stable (Tracks 4 and 6, **a** and **b**).

The complexes for which the buffer was changed to TKCa buffer and then incubated at 25°C (tracks 5 and 6, **a** and **b**) and at 37°C (tracks 7 and 8, **a** and **b**) differ from those shown above. In these cases the shifted complexes have a higher mobility than free RNA$_T$. However, under both buffer conditions the magnitude of the mobility shift is lower at 37°C than at 25°C, suggesting that the complex is less stable at the higher temperature. TKCa buffer caused the RNP to fold into a more compact structure (Bartel and Szostak, 1994; Serganov et al., 1996). This might be because of the cooperative influence of the Ca^{2+} and of the r-proteins.

Parallel experiments were carried out in order to assay the reconstituted ^{32}P-RNA$_T$: TP50 complex sensitivity to PAP and RTA N-glycosidase activity. Standardisation of conditions and electrophoretic profiles of E. coli ribosomes and its derivatives after RIP's activity were attempted.

Figure 50 shows the comparative results between the activity of PAP on E. coli ribosomes, 50S and 30S subunits (**Figure 50(I)**) and PAP activity on their respective 'naked' rRNAs (**Figure 50(II)**) in MSB buffer (EDTA containing). PAP was added to the mixtures to give a 1:10, 1:1 and 1:0.1 (where indicated) substrate: PAP molar ratio, with added aniline reagent (where indicated). Tracks 3-5, 8-10, 11-13 (I) and 16-18, 20-23, 26 (II) show non-specific activity of PAP with a smear like pattern. but when the depurination is superimposed on this smear like pattern, as shown in tracks 10 (I) and 18, 22 (II) the aniline fragment corresponding to A$_{2660}$ can be distinguished. These tracks represent a dilution of 1:0.1 m.r., 1:0.1 m.r. and 1:1 m.r. respectively. Although it may be assumed that the aniline fragment corresponding to A2660 is present in the tracks representing higher concentrations (tracks 9, 17 and 21), further analysis is required to prove its presence.

An analysis by non-denaturing PAGE using a different buffer was carried out in order to assay the reconstituted ^{32}P-RNA$_T$: TP50 complex sensitivity to PAP and RTA N-glycosidase activity and the results are suported on pages 213-217.

Figure 50. Comparative results between the activity of PAP on *E. coli* ribosomes, 50S, 30S subunits (I) and on their respective 'naked' RNAs (II) in MSB reaction buffer.
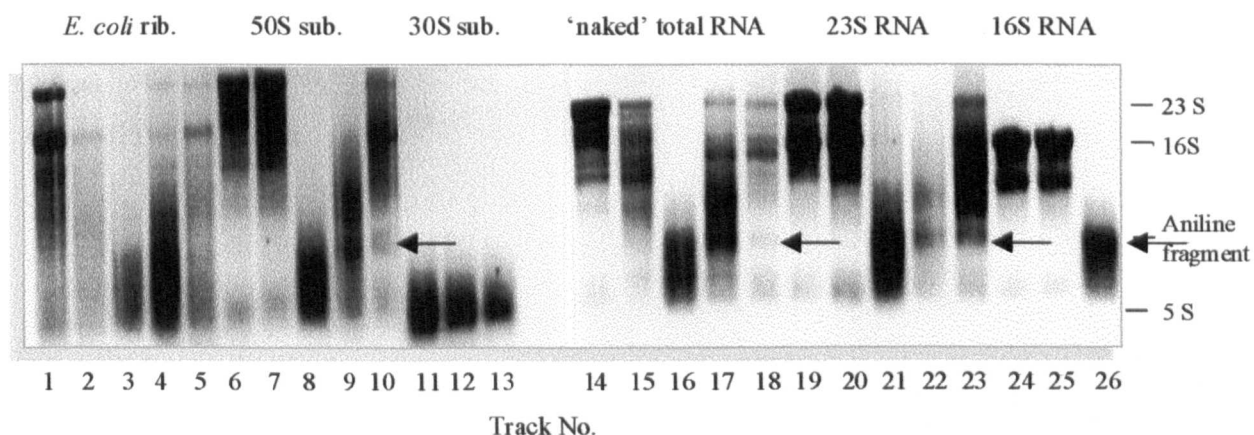
Electrophoretic profile of extracted RNA after incubation. 3μg were loaded onto a 1.2% agarose: formamide gel. MSB Reaction Buffer (Appendix 2) instead of TKCa buffer.

[I]PAP activity on *E. coli* ribos. (tracks 1-5), 50S subunits (tracks 6-10) and 30S subunits (tracks 11-13):

    1. *E. coli* ribosomes
    2. *E. coli* ribosomes + PAP   (1:10 m.r.)
    3. *E. coli* ribosomes + PAP + aniline   (1:10 m.r.)
    4. *E. coli* ribosomes + PAP + aniline   (1:1 m.r.)
    5. *E. coli* ribosomes + PAP + aniline   (1:0.1 m.r.)
    6. 50S subunit
    7. 50S + PAP   (1:10 m.r.)
    8. 50S + PAP + aniline   (1:10 m.r.)
    9. 50S + PAP + aniline   (1:1 m.r.)
    10. 50S + PAP + aniline   (1:0.1 m.r.)
    11. 30S subunit
    12. 30S + PAP   (1:10 m.r.)
    13. 30S + PAP + aniline   (1:10 m.r.)

[II]PAP activity on 'naked' total RNA (tracks 14-18), 23S RNA (tracks 19-23) and 16S RNA (tracks 24-26):

    14. 'naked' total rRNA
    15. 'naked' rRNA + PAP (1:10 m.r.)
    16. 'naked' rRNA + PAP + aniline (1:10 m.r.)
    17. 'naked' rRNA + PAP + aniline (1:1 m.r.)
    18. 'naked' rRNA + PAP + aniline (1:0.1 m.r.)
    19. 23S rRNA
    20. 23S rRNA + PAP   (1:10 m.r.)
    21. 23S rRNA + PAP + aniline   (1:10 m.r.)
    22. 23S rRNA + PAP + aniline   (1:1 m.r.)
    23. 23S rRNA + PAP + aniline   (1:0.1 m.r.)
    24. 16S rRNA
    25. 16S rRNA + PAP   (1:10 m.r.)
    26. 16S rRNA + PAP + aniline   (1:10m.r.)

'smear' of rRNA cleavage products, resulting from non-specific depurination. Similar results have been observed previously as shown in Chapter V. The pattern seems to be a reaction to the influence of chelating agents on the N-glycosidase activity.

So far, the ^{32}P-RNA$_T$:TP50 complex in MSB does not allow the analysis of A$_{2660}$ specific PAP activity on different substrates. Thus, a second and a third approach were attempted in order to elucidate the reconstituted substrate's sensitivity to PAP. The samples were analysed by non-denaturing gel electrophoresis as control (**Figure 51(I)**).

Figure 51 shows the comparative results between the activity of PAP on ^{32}P-RNA$_T$ and ^{32}P-RNA$_T$:TP50 complex in reaction buffers, TKCa and MSB. In all MSB cases, after the reconstitution incubation, PAP was added to give a 1:10, 1:1 and 1:0.1 m.r. (Substrate: PAP). The PAP activity was carried out in all cases for 30 min at 25°C followed by the rRNA extraction.

Figure 51 (I) shows the ^{32}P-RNA$_T$ and ^{32}P-RNA$_T$ after PAP's N-glycosidase activity with an added aniline reagent (tracks 1 and 2 respectively), both in TKCa buffer and as a control. **Figure 51 (II)** shows two experimental series of ^{32}P-RNA$_T$ (tracks 1-5) and ^{32}P-RNA$_T$: TP50 (tracks 6-10) both in MSB. The reactions were performed as follows:

a) Tracks 1(I), 1(II) and 6(II) show the electrophoretic pattern of reaction mixture containing ^{32}P-RNA$_T$ and ^{32}P-RNA$_T$: TP50 complex as the control reactions in which either PAP or aniline treatment has been omitted.

b) Tracks 2 and 7 (II) show the profile form the reaction mixtures with their respective substrate with added PAP to give a 1:10 substrate: PAP m.r. as controls and without aniline treatment.

c) Tracks 2(I), 3-5 (II) and 8-10 (II) show rRNA from reaction mixtures in their respective reaction buffers with PAP to give a 1:10, 1:1 and 1:0.1 m.r. (Substrate: PAP) with added aniline treatment.

Figure 51. Comparative results between the activity of PAP on ^{32}P-RNA$_T$ and ^{32}P-RNA$_T$: TP50 complex in both reaction buffers (TKCa and MSB), analysed by non-denaturing PAGE.
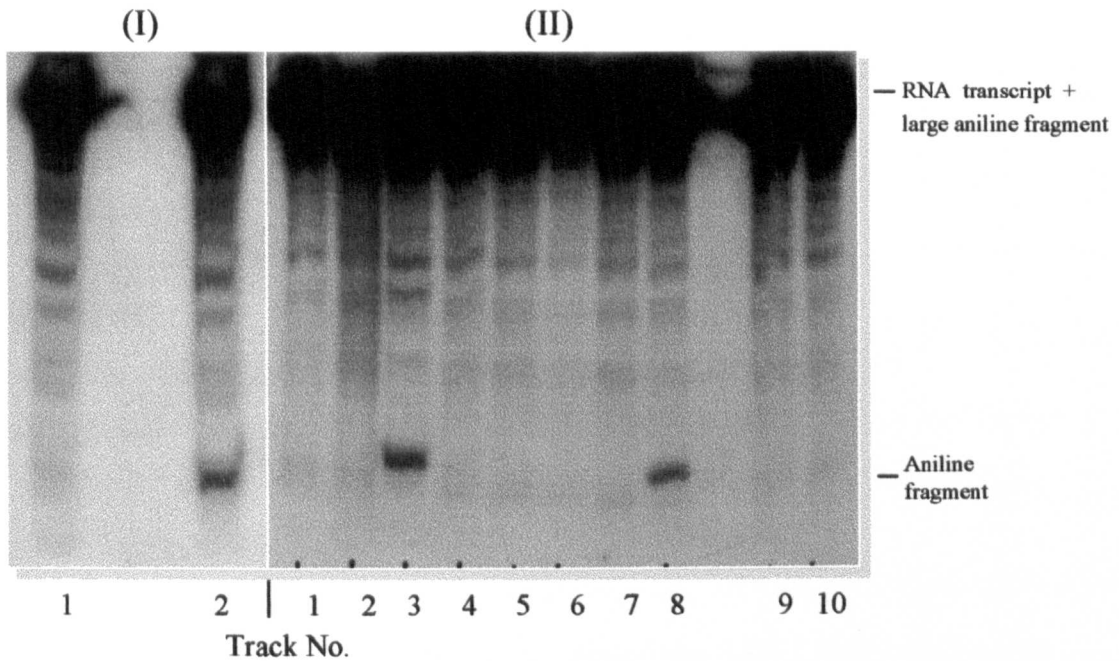
Samples were electrophoresed 50 minutes. 12% acrylamide non-denaturing gel.

(I) PAP activity on ^{32}P-RNA$_T$ in TKCa buffer.

     1) ^{32}P-RNA$_T$

     2) ^{32}P-RTA$_T$ + PAP + aniline (1:10 m.r.)

(II) PAP activity on ^{32}P-RNA$_T$ (tracks 1-5) and ^{32}P-RNA$_T$: TP50 complex (tracks 6-10), in MSB buffer.

     1. ^{32}P-RNA$_T$

     2. ^{32}P-RNA$_T$ + PAP   (1:10 m.r.)

     3. ^{32}P-RNA$_T$ + PAP + aniline   (1:10 m.r.)

     4. ^{32}P-RNA$_T$ + PAP + aniline   (1:1 m.r.)

     5. ^{32}P-RNA$_T$ + PAP + aniline   (1:0.1 m.r.)

     6. ^{32}P-RNA$_T$:TP50 (1:15 m.r.)

     7. ^{32}P-RNA$_T$:TP50 + PAP (1: 15: 10 m.r.)

     8. ^{32}P-RNA$_T$:TP50 + PAP + aniline (1: 15: 10 m.r.)

     9. ^{32}P-RNA$_T$:TP50 + PAP + aniline (1: 15: 1 m.r.)

     10. ^{32}P-RNA$_T$:TP50 + PAP + aniline   (1: 15: 0.1 m.r.)

Tracks 2(I), 3 (II) and 8 (II) show the small aniline fragment, presumably represent the 42nt fragment (accoring to the information presented in **Figure 33**) from the cleavage of RNA_T depurination at A_{2660}. The large aniline fragment and uncleaved RNA_T are not clearly resolved.

A comparison between this result, and those of previous experiments (**Figure 39**) suggest that under these conditions ^{32}P-RNA_T in TKCa buffer, and ^{32}P-RNA_T in MSB, have a similar sensitivity to PAP's N-glycosidase activity. ^{32}P-RNA_T and ^{32}P-RNA_T: TP50 complex in MSB also show the same sensitivity to PAP.

Although it has been demonstrated (**Figures 48** and **49**) that the ^{32}P-RNA_T:TP50 complex is relatively stable, it differs in its gel retardation profile, from complexes maintained in MSB, and thus, presumably, differs in its conformation. Nevertheless, the complexes formed in both buffers are equally sensitive to PAP depurination. Additionally, these results could provide evidence for the role of the divalent cation and for the role of r-proteins, in constraining or maintaining the rRNA structure where the α-sarcin/ricin loop still appeared to be exposed for RIPs depurination.

Lu and Draper (1994), showed that the 5'end of 23S rRNA appeared to show Mg^{2+} dependent stabilisation of the tertiary structures, supporting the idea of both the Mg^{2+} and the r-proteins together, or one of them (divalent cation or r-proteins) participate in the folding of the rRNA.

Figure 52 shows the comparative results between the activity of RTA on ^{32}P-RNA_T and ^{32}P-RNA_T:TP50 complex in MSB using PAP activity on ^{32}P-RNA_T as control.

Tracks 1-3 and 4-6 show the pattern of RNA from reaction mixture containing ^{32}P-RNA_T and RIPs (1-3 containing PAP, and 4-6 containing RTA), to give a 1:10 and 1:1 m.r. (substrate: RIP) (where indicated). Tracks 8-9 show aniline treated samples.

Figure 52. Comparative results between the activity of RTA on ^{32}P-RNA$_T$ and ^{32}P-RNA$_T$: TP50 complex in MSB, analysed through a non-denaturing PAGE and using PAP activity on ^{32}P-RNA$_T$ as control.
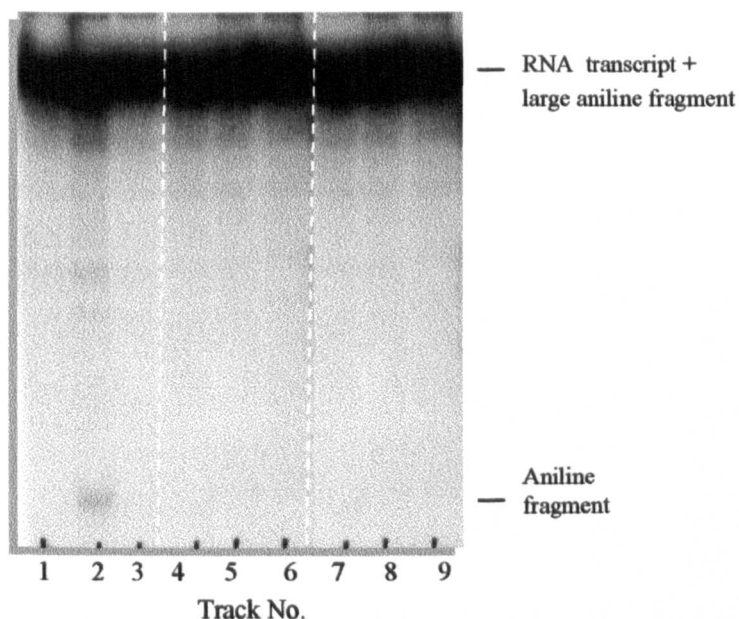
Samples were electrophoresed 50 minutes. 12% acrylamide non-denaturing gel.

(I) PAP activity on ^{32}P-RNA$_T$ in MSB buffer as control.
    1) ^{32}P-RNA$_T$
    2) ^{32}P-RTA$_T$ + PAP + aniline (1:10 m.r.)
    3) ^{32}P-RTA$_T$ + PAP + aniline (1:1 m.r.)

(II) RTA activity on ^{32}P-RNA$_T$ (tracks 1-5) and ^{32}P-RNA$_T$: TP50 complex (tracks 6-10), in MSB buffer.
    4. ^{32}P-RNA$_T$ + RTA   (1:10 m.r.)
    5. ^{32}P-RNA$_T$ + RTA + aniline   (1:10 m.r.)
    6. ^{32}P-RNA$_T$ + RTA + aniline   (1:1 m.r.)
    7. ^{32}P-RNA$_T$: TP50 + RTA   (1: 15: 10 m.r.)
    8. ^{32}P-RNA$_T$: TP50 + RTA + aniline   (1: 15: 10 m.r.)
    9. ^{32}P-RNA$_T$: TP50 + RTA + aniline   (1: 15: 1 m.r.)

The generation of the aniline fragment following the incubation of ^{32}P-RNA$_T$ with PAP (track 2) serves as a positive control. The lack of activity by RTA confirms previous results in this Chapter where RNA$_T$ was not sensitive to RTA activity in a 1:10 m.r. (Substrate: RTA) and analysed by 2% agarose: formamide gels and by primer extension (**Figures 39** and **40,** respectively). Furthermore, the ^{32}P-RNA$_T$ reconstituted with TP50 was also insensitive to RTA's N-glycosidase activity, under both MSB and TKCa reaction buffer conditions (**Figure 52**).

Finally in order to elucidate whether or not there is a RIP association and subsequent N-glycosidase activity, a comparative gel retardation electrophoresis was carried out. Gel retardation assay were used to investigate the possibility that the RIP: RNA$_T$ and for RIP: RNA$_T$: TP50 complex causes a sufficient mobility shift to be detected by this technique. The results of such an experiment are shown in **Figure 53**. ^{32}P-RNA$_T$ (tracks 1-3) and ^{32}P-RNA$_T$:TP50 complex (tracks 4-6), were incubated with PAP and RTA in MSB, and analyzed by non-denaturing PAGE, together with control samples incubated without the RIPs. for 30 min at 25°C prior to loading the samples onto a 12% acrylamide non-denaturing gel.

The results show that PAP does not cause retardation of either ^{32}P-RNA$_T$ or ^{32}P-RNA$_T$:TP50 complex (compare lanes 1 and 2, 4 and 5). In contrast RTA causes retardation of both ^{32}P-RNA$_T$ and ^{32}P-RNA$_T$:TP50 complex (compare lanes 1 and 3, 4 and 6).

Summing up:

1) PAP was active on both domain VI transcript and reconstituted RNA transcript: TP50 complex, at a ten-fold higher concentration than that of the substrate.

2) The activity of PAP on MSB in the presence of aniline reagent when agarose gel electrophoresis is used, occurred at multiple sites in the rRNA of ribosomes, subunits and 'naked' rRNAs, termed non-specific activity (as shown by agarose:formamide gels). A similar non-specific activity had been previously demonstrated in other EDTA-containing buffers (Chapter V). Nevertheless, **Figure 51** clearly shows PAP' specific cleavage of the RNA$_T$ in this buffer.

3) The rRNA N-glycosidase activity of PAP was similar on domain VI transcripts and such transcripts reconstituted with TP50. However, both were relatively poor

Figure 53. Comparative gel retardation assays after PAP or RTA were added to ^{32}P-RNA$_T$ and ^{32}P-RNA$_T$: TP50 complex in MSB.

RNA complex

Free RNA transcript

1   2   3   4   5   6

Track No.
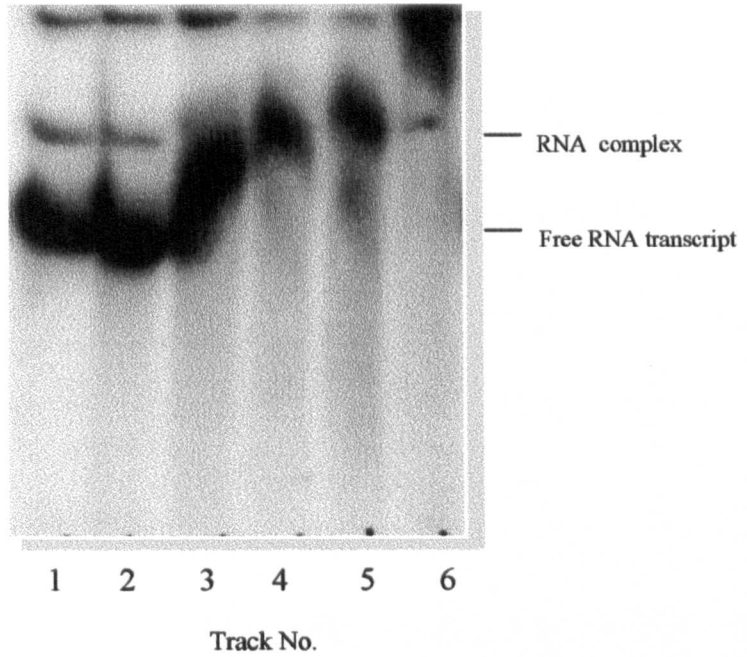
Samples were electrophoresed 2h 45min. 12% Acrylamide non-denaturing gel. Reactions in MSB buffer.
1) ^{32}P-RNA$_T$
2) ^{32}P-RTA$_T$ + PAP (1:10 m.r.)
3) ^{32}P-RTA$_T$ + RTA (1:10 m.r.)
4) ^{32}P-RNA$_T$:TP50 (1:15 m.r.)
5) ^{32}P-RNA$_T$:TP50 + PAP (1: 15: 10 m.r.)
6) ^{32}P-RNA$_T$:TP50 + RTA (1: 15: 10 m.r.)

substrates for PAP action. This suggests that the structure of the α-sarcin/ricin loop in the native ribosome and in intact 23S rRNA may differ from that on the domain VI transcript.

4) RTA was not active on both domain VI transcripts and such transcripts reconstituted with TP50 in TKCa and MSB buffers. Thus, *E. coli* native ribosomes and domain VI-RNA transcripts are the only α-sarcin/ricin loop containing substrates, insensitive to RTA activity. The former case could be due to the fact that the depurination site is protected. The latter could again be explained by the possibility that an optimal structure for RTA activity requires the involvement of long range tertiary interactions of the type described by Brimacombe (1995).

5) Unexpectedly, it was found that RTA appeared to form a complex with both RNA transcript and RNA transcript: TP50 complex in MSB as shown by the non-denaturing gel electrophoresis. This is the more surprising because in spite of the binding to the complex, there is no N-glycosidase activity on the substrates.

7.8. Conclusions

In order to gain a greater insight into the r-protein influence on RIPs' activity, the individual domain VI of 23S rRNA from *E. coli* ribosomes was transcribed and reconstituted with the TP50 so that RIP's activity on these reconstituted substrates could be tested.

In this chapter the step by step construction of a pGEM-4Z, carrying the cloned domain VI obtained by PCR methodology, from the 3' end of *E. coli* 23S *rrn*B operon (Brosius *et al.*, 1981a/b) is shown. *E. coli* DH5α cells were transformed and screened through colour selection protocols. Further purification of recombinant pGEM-4Z was carried. The plasmid was *Bam*HI restricted to linearize the DNA and to obtain the RNA transcript after SP6 RNA polymerase enzyme and rNTPs were added. RNA transcript sensitivity to PAP and to RTA was assayed, and primer extension was done in order to elucidate that the depurination has occurred at the highly conserved α-sarcin/ricin $GA_{2660}GA$ sequence. Primer extension also was done for the *E. coli* ribosome and its derivatives, all of them showing the same DNA electrophoretic pattern with its characteristic stop at the $GA_{2660}GA$.

The reconstitution of the domain VI RNA transcript was attempted, by adding TP50 since it is well recognised that domain VI binds strongly to L3 r-protein (Leffers *et al.*, 1988). L6 only binds weakly and furthermore, that there is a cooperative interaction between both proteins through an apparent conformational modulation of the highly conserved α-sarcin/ricin loop (Leffers *et al.*, 1988; Uchiumi *et al.*, 1997; 1999).

RNA transcript reconstitution was carried out and the complex was analysed by gel retardation electrophoresis, where it was expected that the migration of the complex would be slower than the transcript because the complex has an increased mass and reduced negative charge due to the basicity of r-proteins. The results of the titration, reconstitution stability and competition described in the methods showed the rapid formation of a stable complex, whose assembly was not affected by the presence of unrelated RNA (tRNA). In contrast, the formation of the complex was reduced in the presence of unlabelled domain VI transcripts and 23S rRNA. This suggests that the complex formation shows RNA sequence specificity.

Using the standard agarose: formamide gel system, it was not possible to observe the two fragments of aniline cleavage (resulting from depurination at A_{2660} in the ^{32}P-RNA_T) because the small fragment might be lost. However, the small aniline fragment of 42nt was clearly resolved in PAGE on the 12% acrylamide non-denaturing gel system used to analysed protein/RNA complexes, and this was used as an assay system for depurination of ^{32}P-RNA_T and RNA_T: TP50 reconstituted complex. Using this assay, it was shown that free domain VI transcript and that complexed with TP50 showed similar sensitivity to PAP in both MSB and TKCa buffer.

8. CHAPTER VIII:

GENERAL DISCUSSION AND FUTURE WORK

8.1. General Discussion

The selective activity of RIPs on different substrates is still only partially understood. It has been reported that all RIPs possess a similar active site structure to depurinate all ribosomes, but they differ in their activity one with another. It is also well known that RIPs' N-glycosidase activity takes place in a highly conserved rRNA sequence at the 23S-like ribosomal RNA site. It might be considered the possibility that ribosome preparations, are not homogeneous with respect to their susceptibility to RIPs. The above consideration might include that they are not homogeneous because different conformations, some associated with elogation factors, and these factors might differ between prokaryotic and eukaryotic species. Furthermore, it has been suggested that the presence or absence of certain ribosomal proteins and their ability to interact with RIPs, can affect the substrate's sensitivity to the RIPs.

It is well known that the majority of RIPs are active on 'naked' substrates (either 23S-like RNA or synthetic oligoribonucleotides that mimics the α-sarcin/ricin loop) and the specificity of depurination at a single site is retained. However, the catalytic constant (K_{cat}) is approx. 10^5-fold lower on these RNA substrates than rat liver ribosomes, implying that r-proteins play a very important role in RIP catalysis. The general characteristics of PAP and RTA activity on both native *E. coli* ribosomes and deproteinised (naked) total rRNA were established as a model for research. Before this, it is known that PAP modifies 23S rRNA in native *E. coli* ribosomes (Hartley *et al.*, 1991) in contrast to the toxic A-chains of the type 2 RIPs abrin and ricin, which are inactive against *E. coli* ribosomes. Nevertheless, PAP and RTA catalyse depurination of the rRNA in the 'naked' state. Thus, it was assumed that from the structure of diverse RIPs and above all the conservation of the active site, they would recognise the same identity elements in RNA. Marchant and Hartley (1995) showed that PAP has less stringent identity element requirements than RTA. Hence, in order to study the influence of r-proteins on the susceptibility of the RIP target site to depurination by PAP and RTA, it was necessary to first establish the characteristics of action of those RIPs on *E. coli* ribosomes and 'naked' rRNA

The results of the N-glycosidase assays showed that the activity of PAP decreased on 'naked' rRNA by a factor of approx. 10 compared to that on the native substrate, confirming the influence of r-proteins in increasing the efficiency of depurination, possibly because r-proteins support a conformation which is optimal for PAP. In the case of RTA, no activity could be demonstrated on any substrate tested at a 1:1 m.r.

(Substrate: RTA) in TKMg reaction buffer. It was found that the use of divalent cation: chelating agent effectively increased the RIPs' activity on the substrates and even in some cases, allowed RIPs N-glycosidase activity at depurination sites other than A_{2660} in 23S rRNA. Results showed that under several conditions, the r-proteins in the substrates affected their sensitivity to RIP's activity. PAP showed high activity on the native *E. coli* ribosomes in all cases compared to the deproteinised rRNA substrates. Furthermore, there was a marked difference in the activity of PAP on the dissociated subunits, where with 50S there was approx. 100x more activity than with coupled 70S ribosomes. However, the protection is not absolute since dissociated 50S subunits did serve as substrate for RTA's activity, albeit a poor substrate. A similar observation has been made for the activity of RTA on yeast ribosomes. It was shown RTA expressed from an inducible promoter preferentially modified the rRNA in free 60S subunits (Gould *et al.*, 1991).

There is evidence that most activities of ribosomes are rRNA mediated, and that peptide bond formation is catalysed in a compartment that was shown to be predominantly composed of rRNA (Steiner *et al.*, 1988) and turned out to be resistant to partial ribosomal protein extraction procedures but sensitive to RNase or EDTA treatment (Noller *et al*, 1992). Polacek and Barta (1998) have also reported, for all RNA-catalysed reactions known to date that there is interaction with other parts of the ribosome. They have emphasised the influence of divalent metal ions, where it has been assumed that structurally and functionally important metal ions are coordinated to highly ordered rRNA structures. Their experiments were done in order to show the site-specific cleavage of RNAs due of the exposure of the ribosomes to divalent metal ions such as Pb^{2+}, Mg^{2+}, Mn^{2+} and Ca^{2+}. The basis of their research is that the ribosomes have to deal specifically with the problem of packing rRNA secondary structure elements into highly ordered complexes capable of deciphering the genetic code. Thus, positively charged ions, including polyamines, monovalent ions, and divalent ions are required for counterbalancing the electrostatic repulsion of the polyanionic rRNA and for the promotion of rRNA structures. Pan *et al.* (1993) showed that metal ions are known to promote nucleic acid folding and can even participate directly in RNA catalysis. RNA catalysed reactions, either require or are

catalysed reactions, either require or are greatly stimulated by, divalent ions, which can play structural roles or participate directly in RNA catalysis (Pan *et al.*, 1993).

When Mg^{2+} was substituted by Ca^{2+} by using the TKCa buffer instead of the TKMg buffer, there was enhanced RIP activity and the effect of the r-proteins in influencing the sensitivity of the substrates to RIPs became clear. Thus, the TKCa buffer was chosen for the further experiments. Our results might suggest a protective effect of Mg^{2+} at A_{2660} for RIPs N-glycosidase activity, but when EDTA was present or when Ca^{2+} was substituted for Mg^{2+}, this well conserved sequence containing the site of depurination by RIPs, became more accessible in the *E. coli* ribosomes and their derivatives. However, RTA showed a non-specific depurination activity on *E. coli* ribosomes in the presence of EDTA. These results suggest that the activity of RTA with rRNA in an EDTA medium is influenced by the presence of r-proteins, being higher when r-proteins are present. During the development of this work, it has been hypothesised that another possible reason for this enhancement of RIPs activity on the substrates, might be because the depletion of Mg^{2+} either by the presence of chelating agents, or by the substitution with another divalent cation. It is well known that the depletion of Mg^{2+} influence the coupled ribosome conformation dissociating it into ribosomal subunits and so making the structures more sensitive to both RIPs (as it was shown for RTA activity on ribosomal subunits -Chapter VI-). Furthermore, on the 30S subunit and the 16S rRNA depurination, the presence of Ca^{2+} instead of Mg^{2+}, could explain the possibility that RTA acted on A_{1269} where previously this was reported to be an insensitive structure.

The influence of r-proteins on the substrates sensitivity to RIPs was assessed using the partial and total dissociation of rRNA/r-proteins as reported by Nierhaus (1990). r-Proteins were split off from the ribosome with salt solutions in such a way that the higher the ionic strength, the more the proteins were split off. Using this technique certain ribosomes and subunits were assayed for PAP and RTA activity. *E. coli* ribosomes, 50S and 30S subunits, P37 and 3.5c subparticles and 23S rRNA (all containing the highly conserved α-sarcin/ricin domain) obtained from 50S subunits. Finally, possible additional depurination sites on 30S subunit and 16S rRNA were sought. The experiments were monitored by analytical agarose: formamide gel electrophoresis, and the reaction buffer chosen was the TKCa buffer because of its ability to give a consistent and clear differentiation pattern of the RIPs N-glycosidase activity with the substrates. The length of the main fragment produced by the cleavage with the aniline reagent after the N-glycosidase activity of RIPs was characteristic of the previously reported depurination at $GA_{2660}GA$ from 23S rRNA in the highly and universally conserved

α-sarcin/ricin loop. However, two depurination sites were found in 16S rRNA; $GA_{1014}GA$ (already established) and putatively at 16S rRNA $GA_{1269}GA$, a new site appeared as a result of the RIP's activity under some of the different reaction buffer conditions.

RTA was active on both native 50S and 30S subunits, as well as on 23S and 16S rRNA. The activity on these substrates was similar and the specificity on the 23S rRNA was identical to that on 'naked' rRNA.

RTA showed no activity in a 1:10 m.r. (Substrate: RTA) for *E. coli* ribosomes but when dissociated into 50S and 30S subunits, this RIP concentration was enough to obtain well characterised RTA N-glycosidase activity. Even with the partial and total deproteinisation of the subunits, there was still depurination activity, suggesting that only the native *E. coli* ribosomes were insensitive to RTA, and that dissociation into subunits changed the rRNA conformation and exposed the depurination sites. Considering Polacek and Barta's (1998) results, where they have shown that most of the observed metal ion induced cleavages in the 3' minor domain on naked 16S rRNA were not detected in 70S ribosomes, it is possible that the ribosomal proteins or structural rearrangements of the rRNA in the RNP particle play a protective role.

The individual domain VI of 23S rRNA from *E. coli* ribosomes was transcribed and reconstituted with the TP50 for testing RIPs' activity on these reconstituted substrates. A pGEM-4Z plasmid was constructed carrying the cloned domain VI obtained by PCR methodology, from the 3' end of *E. coli* 23S in pKK3535 (derived from the *rrn*B operon; Brosius *et al.*, (1981a/b)). RNA transcript sensitivity to PAP and to RTA was assayed, and primer extension was done in order to make sure that the depurination had occurred at the highly conserved α-sarcin/ricin $GA_{2660}GA$ sequence. Primer extension was also done for the *E. coli* ribosome and its derivatives, all of them showing the same DNA electrophoretic pattern with its characteristic stop at the $GA_{2660}GA$.

The gel retardation (for measuring the transcript reconstitution) which had been hypothesised for the binding domain at L3 was not obtained. The explanation for this was provided when Uchiumi published his results in 1999. On the other hand, when TP50 was added to the transcript of domain VI the hypothesised retardation was obtained. Had Uchiumi's information been available in 1997 a longer transcript would have been chosen for this research which would have included the binding site for L3.. Nevertheless, it is well recognised that there is a cooperative interaction between both L3 and L6 proteins through an apparent conformational modulation of the highly conserved α-sarcin/ricin loop (Leffers *et al.*, 1988; Uchiumi *et al.*, 1997; 1999). The results showed an immediate formation of a stable complex, which did not show any affinity to unrelated RNA (tRNA). This allowed binding-competition with related RNA for r-proteins, suggesting that the RNA transcript and its complex contained the characteristics of the domain VI present on 23S rRNA, and that this RNA competed with unlabelled RNA transcript to bind with the r-proteins. In further assay there was also competition between the complex and the 23S rRNA to bind with the r-proteins. The resuspension of domain VI into TKCa buffer however was not enough to obtain a consistent gel retardation profile because of the addition of TP50 to the domain VI - RNA transcript as was the case when MSB was used. Using non-denaturing PAGE for analysing the RNA transcript and the reconstituted RNA transcript sensitivity to both PAP and RTA, it was possible to obtain a profile of the sensitivity of the substrates to RIP activity. The results suggest that under the described conditions, there was no difference between the sensitivity of both substrates (transcript and reconstituted transcript). Furthermore, there was no difference in sensitivity, using either TKCa or MSB as reaction buffer. This suggests that the presence or absence of Ca^{2+} or other divalent cations does not alter the reconstituted conformation of the transcript because even in the presence of EDTA, the activity of neither RIPs was changed. This might suggest also that EDTA buffer acts on the conformation of RNA and not on the RIPs, as suggested from the similar profile presented by the action of RIPs on RNA transcript resuspended in TKCa or in MSB. Although there was no N-glycosidase activity of RTA on either the RNA transcript or the reconstituted transcript, a complex was observed between RTA and the substrate under MSB and non-denaturing electrophoresis conditions.

In keeping with earlier reports (reviewed by Hartley and Lord, 1993) native *E. coli* 70S ribosomes were not susceptible to RTA. Surprisingly purified 50S and 30S subunits prepared from ribosomes dissociated by lowering Mg^{2+} were both sensitive to

RTA. From this, it is concluded that alterations in ribosome structure can significantly affect RTA sensitivity. The accessibility of the sarcin/ricin loop, and the stem loop containing A_{1014} in 16S rRNA could influenced by subunit association/dissociation, or sensitivity could be influenced by the conformational 'switches' in rRNA which have been proposed to occur during subunit dissociation (reviewed by Zimmerman, 1996). A similar increase in the sensitivity of naturally derived 60S subunits in yeast to RTA action was reported by Gould *et al.*, (1991). However, in the case of *E. coli* it can be assumed that *in vivo*, free ribosomal subunits are not substrates for RTA activity because biologically active rRTA can be expressed at very high levels (approx. 10% of total protein) without affecting growth (O'Hare. 1987).

The role of Mg^{2+} in the α-sarcin/ricin loop.

Macbeth and Wool (1999) have shown that the flexible region of the α-sarcin/ricin stem loop structure, comprising a non canonical A-A pair and unpaired C, C and U, C residues, and located below the bulged G, is an important determinant for both ricin and α-sarcin action. In particular, the deletion of the A-A pair leads to loss of RTA action. The authors propose that this flexible region may permit reversible conformational changes in the α-sarcin/ricin stem loop that allow the alternate binding of EF-Tu (EF-1) and EF-G (EF-2) to the ribosome. It is interesting to note that this flexible region has been proposed to form a binding pocket for 3 divalent metal ions. It is conceivable that the replacement of Mg^{2+} by Ca^{2+} alters the stability of the loop structure, and hence its susceptibility to RTA and PAP.

8.2. Future Work

The influence of r-proteins on the sensitivity of RIPs to substrates, which is the objective of this research project, has been only partially resolved. The results obtained give rise to new issues that require further investigation. Among the most important of these are: The need to establish the effect of r-proteins on the 23S rRNA transcript conformation, which would resolve further investigation of RIP's activity on the substrate. We reasoned that the different functional effects of the two RIPs probably have a basis in their physical interaction with 23S rRNA, most likely within

the protein-RNA complex, the structure of which may be influenced by divalent cations. To test the idea, it would be necessary to employ a range of chemical reagents and ribonucleases to probe the domain VI-RNA transcript structure before and after the reconstitution compared to the protection at the 23S rRNA structure, before and after the reconstitution and to assay the sensitivity to RIPs.

The influence of Mg^{2+} and Ca^{2+} on the structure of the rRNA. Recognising that L6 binding depends on L3 binding to the domain VI (Leffers *et al.*, 1988; Uchiumi *et al.*, 1997; Uchiumi *et al.*, 1999), this research project suggested that the presence of the divalent cations Ca^{2+} and Mg^{2+} can obtain a different rRNA conformation. An examination of how this occurs requires foot printing experiments using different chemical, enzymatic and RIPs probes.

Further investigation of the influence of r-proteins on the activity of RIPs in the EDTA containing buffer is necessary in attempt to explain the marked difference in activity of the non-specific depurination which is observed both in the presence/absence of the r-proteins on *E. coli* ribosome and its derivatives.

9. CHAPTER IX:

REFERENCES

Aagaard, C., Rosendahl, G., Dam, M., Powers, T. and Douthwaite, S. (1991). Specific structural probing of plasmid-coded ribosomal RNA from *Escherichia coli*. Biochimie **73**(12): 1439-1444.

Anderson, C., Stratus, J.W. and Dudock, B.S. (1983). Preparation of a cell-free protein-synthesising systems from wheat germ. Chapter 41. Methods Enzymol. **101:** 635-644.

Arnstein, H.R.V., Cox, R.A. (1992). Protein biosynthesis. Rickwood, D. (Ed.). IRL Press, Oxford University Press. New York.

Asano, K., Svensson, B. and Poulsen, F.M. (1984). Isolation and characterisation of inhibitors in cell-free protein synthesis from barley seeds. Carlsberg Res. comm. **49**: 619-626.

Barbieri, L., Battelli, M.G., and Stirpe, F. (1982). Reduction of ricin and other plant toxins by thiol: protein disulphide oxidoreductase. Arch. Biochem. Biophys. **216**(1): 380-383.

Barbieri, L., Battelli, M.G. and Stirpe, F. (1993). Ribosome-inactivating proteins from plants. Biochimica et Biophysica Acta. **1154**(3-4): 237-282.

Barbieri, L., Stoppa, C. and Bolognesi, A. (1987). Large scale chromatographic purification of ribosome-inactivating proteins. J. Chromatography **408**: 235-243.

Barbieri, L., Valbonesi, P., Bonora, E., Gorini, P., Bolognesi, A., Stirpe, F. (1997). Polynucleotide: adenosine glycosidase activity of ribosome-inactivating proteins: effect on DNA, RNA and poly(A). Nucleic Acids Res. **25**: 518-522.

Bartel, D. P. and Szostak, J.W. (1994). Study of RNA-protein recognition by *in vitro* selection. Chapter 11. In 'RNA-protein interactions'. Nagai, K. and Mattaj, I.W. (Eds.). Frontiers in Molecular Biology. Oxford University Press. Reprinted 1996. pp. 248-268.

Batey, R.T. and Williamson, J.R. (1996). Interaction of the *Bacillus stearothermophilus* Ribosomal Protein S15 with 16S rRNA: I. Defining the Minimal RNA Site. J. Mol. Biol. **261**(4): 536-549.

Batielli, M.G., Enzo, L., Stirpe, F., Cella, R. and Parisi, B. (1984). Differential effect of ribosome inactivating proteins on plant ribosome activity and plant cell growth. J. Exp. Bot. **35**(155): 882-889.

Bolegnesi, A., Barbieri, L., Abbondanza, A., Falasca, A.I., Carnicelli, D., Batelli, M.G. and Stirpe, F. (1990). Purification and properties of new ribosome-inactivating proteins with RNA N-glycosidase activity. Biochim. Biophys. Acta. **1087**(3): 293-302.

Boness, M.S., Ready, M.P., Irvin, J.D., and Mabry, T.J. (1994). Pokeweed antiviral protein inactives pokeweed ribosomes, implications for the antiviral mechanism. Plant J. **5**(2): 173-183.

Brimacombe, R. (1995). The structure of ribosomal RNA. A 3-Dimensional jigsaw puzzle. Eur. J. Biochem. **230**(2): 365-383.

Brimacombe, R., Greuer, B., Mitchell, P., Osswald, M., Rinkel-Appel, J., Schuler, D., and Stade, K. (1990). Three dimensional structure and function of *Escherichia coli* 16S and 23S rRNA as studied by cross-linking techniques. In 'Structure, function, and evolution of ribosomes'. Hill, W., Dahlberg, A., Garrett, P.B., Moore, D., Schlessinger, and Warner, J. (Eds.). American Society for Microbiology, Washington, D.C. pp 93-106.

Brimacombe, R., Stiege, W., Kyriatsoulis, A., and Maly, P. (1988). Methods Enzymol. **164**, Noller, H.F. and Moldave, K. (Eds.). p.287. Academic Press Inc. San Diego.

Brosius, J., Dull, T.J., Sleeter, D.D., Noller, H.F. (1981). Gene organisation and primary structure of a ribosomal RNA operon from *Escherichia coli*. J. Mol. Biol. **148**(2): 107-127.

Brosius, J., Ullrich, A., Raker, M.A., Gray, A., Dull, T.J., Gutell, R.B., Noller, H.F. (1981). Construction and fine mapping of recombinant plasmids containing the *rrn*B ribosomal RLNA operon *E. coli*. Plasmid **6**(1): 112-118.

Carnicelli, D., Brigotti, M., Montanaro, L. and Sperti, S. (1992). Differential requirement of ATP and extra-ribosomal proteins for ribosome inactivation by eight RNA N-glycosidases. Biochem. Biophys. Research Comm. **182**(2): 579-582.

Cawley, D.B., Hedblom, M.L., Hoffman, E.J., and Houston, L.L. (1977). Differential Ricin Sensitivity of Rat Liver and Wheat Germ Ribosomes in Polyuridylic Acid Translation. Arch. Biochem. Biophys. **182**: 690-695.

Cawley, D.B., Hedblom, M.L. and Houston, L.L. (1979). Protection and Rescue of Ribosomes from the Action of Ricin A chain. Biochemistry 18(12): 2648-2654.

Cech, T.R. (1987). The chemistry of self splicing RNA and RNA enzymes. Science 236(4808): 1532-1535.

Chaddock, J.A., Roberts, L.M., Jungnickel, B. and Lord, M. (1995). A hydrophobic region of ricin A chain which may have a role in membrane translocation can function as an efficient non-cleaved signal peptide. Biochem. Biophys. Research Comm. 217(1): 68-73.

Chaddock, J.A., Monzingo, A.F., Robertus, J.D., Lord, M., and Roberts, L.M. (1996). Major structural differences between pokeweed antiviral protein and ricin A-chain do not account for their differing ribosome specificity. Eur. J. Biochem. 235(1-2): 159-166.

Chen, Z.C., White, R.F., Antoniw, J.F. and Lin, Q. (1991). Effect of pokeweed antiviral protein (PAP) on the infection of plant viruses. Plant Pathology 40(4): 612-620.

Chen, X.-Y., Link, T.M., and Schramm, V.L. (1998). Ricin A-chain: Kinetics, mechanisms, and RNA stem-loop inhibitors. Biochemistry 37(33): 11605-11613.

Chien, A.S., Edgard, B. and Trela, J.M. (1976). DNA polymerase from the extreme thermophile *Thermus aquaticus*. J. Bacteriology 127(3): 1550-1557.

Coleman, W.H. and Roberts, W.K. (1981). Factor requirement for the tritin inactivation of animal cell ribosomes. Biochem. Biophys. Acta 654(1): 57-66.

Dahlberg, A.E. (1989). The functional role of ribosomal RNA in protein synthesis. Cell 57(4): 525-529.

Dahlberg, A. E. and Zimmermann, R.A. (1992). Ribosomes. In 'Encyclopedia of Microbiology'. Lederberg, J. (Ed.). p 573-583. Academic Press Ltd, London.

D'Alessio, J.M. (1982) In 'Gel electrophoresis of Nucleic Acids'. Rickwood, D. and Hames, B.D. (Eds.). IRL Press, Oxford, pp. 173-179.

Datta, D., Changchien, L.-M. and Craven, G. (1986). Studies on the kinetic sequence on *in vitro* assembly using cibacron F3GA as a general assembly inhibitor. Nucleic Acids Res. 14(10): 4095-4111.

Dijk, J. and Littlechild, J. (1979) Purification of Ribosomal Proteins from *Escherichia coli* under Nondenaturing Conditions. Chapter 40. Methods Enzymol. **59**: 481.

Dore, J.M., Gras, E., Depierre, F. and Wijdenes, J. (1993). Mutations dissociating the inhibitory activity of the pokeweed antiviral protein on eukaryotic translation and *Escherichia coli* growth. Nucleic Acids Res. **21**(18): 4200-4205.

Dosio, F., Brusa, P., Delprino, L., Ceruti, M., Gerosa, G., Cattel, L., Bolognesi, A. and Barbieri, L. (1993). A new solid-phase procedure to synthesize immunotoxins (antibody-ribosome inactivating protein conjugates). Farmaco **48**(1):105-115.

Douthwaite, S., Voldborg, B., Hansen, L.H., Rosendahl, G. and Vester, B. (1995). Recognition determinants for proteins and antibiotics within 23S rRNA. Biochem. Cell Biol.-Biochim. Biol. Cell. **73**(11-12): 1179-1185.

Draper, D.E. (1994). RNA-protein interactions in ribosomes. Chapter IV. In "RNA-Protein Interactions". Nagai, K., and Mattaj, L.W. (Eds.). Frontiers in Molecular Biology. IRL Press. Oxford University Press, Inc., New York.

Egebjerg, J., Douthwaite, S. and Garrett, R. (1989). Antibiotic interactions at the GTPase-associated centre within *Escherichia coli* 23S rRNA. EMBO J. **8**(2): 607-611.

Endo, Y., Gluck, A., Chan, Y., Tsurugi, R. and Wool, I.G. (1990). RNA-Protein Interaction: An analysis with RNA oligonucleotides of the recognition by α-sarcin of a ribosomal domain critical for function. J. Biol. Chem. **265**(4): 2216-2222.

Endo, Y., Gluck, A. and Wool, I.G. (1991). Ribosomal RNA identity elements for ricin A-chain recognition and catalysis. J. Mol. Biol. **221**(1): 193-207.

Endo, Y., Mitsui, K., Motizuki, M., and Tsurugi, K. (1987). The Mechanism of Action of Ricin and Related Toxic Lectins on Eukaryotic Ribosomes. J. Biol. Chem. **262**(12): 5908-5912.

Endo, Y. and Tsurugi, K. (1987). RNA N-glycosidase of ricin A chain: Mechanism of action of the toxic lectin ricin on eukaryotic ribosomes. J. Biol. Chem. **262**(17): 8128-8130.

Endo, Y. and Tsurugi, K. (1988). The RNA N-glycosidase activity of ricin A-chain. J. Biol. Chem. **263**(18): 8735-8739.

Endo, Y., Tsurugi, K. and Ebert, R.F. (1988). The mechanism of action of barley toxin: a type 1 ribosome-inactivating protein with RNA N-glycosidase activity. Biochem. Biophys. Acta **954**(2): 224-226.

Endo, Y., Tsurugi, K., and Lambert J.M. (1988). The site of action of six different ribosome-inactivating proteins from plants on eukaryotic ribosomes: The RNA N-glycosidase activity of the proteins. Biochem. Biophys. Res. Comm. **150**(3): 1032-1036.

Ferreras, J.M., Barbieri, L., Girbés, T., Battelli, M.G., Rojo, M.A., Arias, F.J., Rocher, M.A., Soriano, F., Mendéz, E. and Stirpe, F. (1993). Distribution and properties of major ribosome-inactivating proteins (28S rRNA glycosidase) of the plant *Saponaria officinalis* L. (Caryophyllaceae). Biochem. Biophys. Acta **1216**(1): 31-42.

Fourmy, D., Recht, M.I., Blanchart, S.C., Puglisi, J.D. (1996). Structure of the A Site of *Escherichia coli* 16S Ribosomal RNA Complexed with an Aminoglycoside Antibiotic. Science **274**(5291): 1367-1371.

Franceschi, F.I. and Nierhaus, K.H. (1990). Ribosomal protein-L15 and protein-L16 are mere late assembly proteins of the large ribosomal-subunit. Analysis of an *Escherichia coli* mutant lacking L15. J. Biol. Chem. **265**(27): 16676-16682.

Franceschi, F., Weinstein, S., Avila, H., Sagi, I., Levin, I., Paulke, C., Srinivas, R., Morlang, S., and Yonath, A. (1997). Proteins and rRNA-proteins complexes as tools for derivatization in ribosome crystallography. In 'Structural Aspects of Protein Synthesis' Abstracts., Tallberg, Sweden. September 17-20, 1997.

Frankel, A., Welsh, P., Richardson, J. and Robertus, J.D. (1990). The role of arginine 180 and glutamic acid 177 of ricin toxic A chain in the enzymatic inactivation of ribosomes. Mol. Cellular Biol. **10**(12): 6257-6263.

Gesteland, R.F. (1966). Unfolding of *Escherichia coli* ribosomes by removal of magnesium. J. Mol. Biol. **18**: 356-371.

Geyl, D., Bock, A., and Isono, K. (1981). An improved method for two-dimensional gel electrophoresis analysis of mutationally altered ribosomal-proteins of *Escherichia coli*. Mol. Gen. Genet. **181**(3): 309-311.

Girbés, T., Citores, L., Iglesias, R., Ferreras, J.M., Muñoz, R., Rojo, M.A., Arias, F.I., García, J.R., Méndez, E., and Calonge, M. (1993a). Ebulin I, a nontoxic novel

type 2 ribosomes-inactivating protein form *Sambucus ebulus* L. leaves. J. Biol. Chem. **268**(24): 18195-18199.

Girbés, T., Citores, L., Ferreras, J.M., Rojo, M.A., Iglesias, I., Muñoz, R., Arias, F.J., Calonge, M., García, J.R. and Méndez, E. (1993b). Isolation and partial characterisation of nigrin b, a non-toxic novel type 2 ribosome-inactivating protein from the bark of *Sambrus nigra* L. Plant Mol. Biol. **22**(6): 1181-1186.

Girbés, T., Ferreras, J.M., Iglesias, R., Citores, L., DeTorre, C., Carbajales, M.L., Jiménez, P., DeBenito, F.M., Muñoz, R. (1996). Recent advances in the uses and applications of ribosome-inactivating proteins from plants. Cell. Mol. Biol. **42**(4): 461-471.

Gluck, A., and Wool, I.G. (1996). Dependence of depurination of oligoribonucleotides by ricin A-chain on divalent cations and chelating agents. Biochem. Mol. Biol. International **39**(2): 285-291.

Gluck, A., Endo, Y. and Wool, I.G. (1992). Ribosomal RNA identity elements for ricin A-chain recognition and catalysis. Analysis with tetraloop mutants. J. Mol. Biol. **226**(2): 411-424.

Gluck, A., Endo, Y., and Wool I.G. (1994). The ribosomal RNA identity elements for ricin and for α-sarcin: mutations in the putative CG pair that closes a GAGA tetraloop. Nucleic Acids Res. **22**(3): 321-324.

Green, R. and Noller, H.F. (1996). *In vitro* complementation analysis localizes 23S rRNA posttranscriptional modifications that are required for *Escherichia coli* 50S ribosomal subunit assembly and function. RNA **2**: 1011-1021.

Gould, J.H., Hartley, M.R., Welsh, P.C., Hoshizaki, D.K., Frankel, A., Roberts, L.M. and Lord, J.M. (1991). Alteration of an amino acid residue outside the active site of the ricin A chain reduces its toxicity towards yeast ribosomes. Mol. Gen. Genet. **230**: 81-90.

Habuka, N., Kataoka, J., Miyano, M., Tsuge, H., Ago, H. and Noma, M. (1993). Nucleotide sequence of a genomic gene encoding tritin, a ribosome-inactivating protein from *Triticum aestivum*. Plant Mol. Biol. **22**(1): 171-176.

Habuka, N., Murakami, Y., Noma, M., Kudo, T. and Horikoshi, K. (1989). Amino acid sequence of *Mirabilis* antiviral protein, total synthesis of its gene and expression in *E. coli*. J. Biol. Chem. **264**(12): 6629-6637.

Hackl, W. and Stoffler-Meilicke (1988). Immunoelectron miscroscopic localisation of ribosomal proteins from *Bacillus stearothermophilus* that are homologous to *Escherichia coli* L1, L6, L23 and L29. Eur. J. Biochem. **174**(2): 431-435.

Hagenbuchle, O., Santer, M., Steitz, J.A. and Mans, R.J. (1978). Conservation of the primary structure at the 3' end of 18S ribosomal ribonucleic acid from eukaryotic cells. Cell **13**: 551-563.

Hames, B.D. (1990). Gel electrophoresis of proteins. 2nd. Edition. Hames and Rickwood (Ed.). IRL Press.

Hanahan, D. (1983). Studies on transformation of *Escherichia coli* with plasmids. J. Mol. Biol. **166**(4): 557-580.

Hanahan, D. (1985). Techniques for transformation of *E. coli*. DNA cloning volume I. A practical approach. Glover, D.M. (Ed.). IRL Press Oxford.

Harley, S.H., and Beevers, H. (1982). Ricin inhibition of *in vitro* protein synthesis by plant ribosomes. Proc. Natl. Acad. Sci. USA. **79**(19): 5935-5938.

Harlow, E. and Lane, D. (1988). Antibodies. A Laboratory Manual. Harlow, E. and Lane, D. (Eds.). Cold Spring Harbor Laboratory, USA.

Harris, E.L.V. (1989). Concentration of the extract. In 'Protein purification methods: A practical approach'. Harris, E.L.V. and Angal, S. (Eds.). IRL Press, Oxford, pp.125-161.

Hartley, M.R. and Lord, J.M. (1993). Structure, function and applications of ricin and related cytotoxic proteins. Ch. 6. In "Biosynthesis and Manipulation of Plant Products"., Don Grierson (Ed.). Blackie Academic & Professional, University Press, Cambridge. UK. pp. 210-239.

Hartley, M.R., Chaddock, J.A. and Bonness, M.S. (1996). The structure and function of ribosome-inactivating proteins. Review. TIPS **1**(8): 254-260.

Hartley, M.R., Legname, G., Osborn, R., Chen, Z. and Lord, J.M.(1991). Single-chain ribosome inactivating proteins from plants depurinate *Escherichia coli* 23S ribosomal RNA. FEBS Lett. **290**(1,2): 65-68.

Hedblom, M.L. Cawley, D.B. and Houston, L.L. (1976). The specific binding of ricin and its polypeptide chains to rat liver ribosomes and ribosomal subunits. Arch. Biochem. Biophys. **177**: 46-55.

Hosur, M.V., Nair, B., Satyamurthy, P., Misquith, S., Surolia, A., Kannan, K.K. (1995). X-ray structure of Gelonin at 1.8 angstrom resolution. J. Mol. Biol. **250**(3): 368-380.

Hui, I. and Dennis, P.P. (1985). Characterisation of the ribosomal RNA gene clusters in *Halobacterium cutirubrum*. J. Biol. Chem. **260**(2): 899-906.

Iglesias, R., Arias, F.J., Rojo, M.A., Escarmis, C., Ferreras, J.M., Girbes, T. (1993). Molecular action of the type-1 ribosome-inactivating protein from saporin-5 on *Vicia sativa* ribosomes. FEBS Lett. **325**(3): 291-294.

Iglesias, R., Escarmis, C., Alegre, C., Ferreras, J.M., Girbes, T. (1993). Fusidic acid-dependent ribosomal complexes protect *Escherichia coli* ribosomes from the action of the type-1 ribosome-inactivating protein crotin-2. FEBS Lett. **318**(2): 189-192.

Ippoliti, R., Lendaro, E., Bellelli, A. and Brunori, M. (1992). A ribosomal protein is specifically recognised by saporin, a plant toxin which inhibits protein synthesis. FEBS Lett. **298**(2,3): 145-148.

Irvin, J.D. (1975). Purification and partial characterisation of a protein from *Phytolacca amaricana* which inhibits eukaryotic protein synthesis. Arch. Biochem. Biophys. **169**: 522-528.

Irvin, J.D., Kelly, T. and Robertus, J.D. (1980). Purification and properties of a second antiviral protein from *Phytolacca americana* which inactivates eukaryotic ribosomes. Arch. Biochem. Biophys. **200**: 418-425.

Jackson, A.D. and Larkins, B.A. (1976). Influence of ionic strength, pH and chelation of divalent metals on isolation of polyribosomes from tobacco leaves. Plant Physiology **57**: 5-10.

Jiménez, A. and Vázquez, D. (1985). Plant and fungal protein and glycoprotein toxins inhibiting eukaryotic protein synthesis. Ann. Rev. Microbiol. **39**: 649-672.

Kaledin, A.S., Slyusarenko, A.G. and Gorodetski, J.I. (1980). Isolation and properties of DNA polymerase from extremely thermophilic bacterium aquaticus. Biokhimiya **45**(4): 651-664.

Karn, J., Gait, M.J., Churcher, M.J., Mann, D.A., Mikaélian, I. and Pitchard, C. (1994). Control of human immunodeficiency virus gene expression by the RNA-binding proteins tat and rev. Chapter 9. In 'RNA-protein interactions'.

Nagai, K. and Mattaj, W. (Eds.). Frontiers in Molecular Biology. Oxford University Press Inc., New York. Reprinted 1996. pp. 192-220.

Katzin, B.J., Collins, E.J. and Robertus, J.D. (1991). Structure of ricin A-chain at 2.5Å. Proteins-Struc. Fuc. Genet. **10**(3): 251-259.

Kiss, A., Sain, B. and Venetianer, P. (1977). The number of rRNA genes in *Escherichia coli*. FEBS Lett. **79**: 77-79.

Kolb, V.A., Kommer, A., Makayer, E., Spirin, A. (1997). Intraribosomal tunnel for nascent peptide: does it exist? In 'Structural Aspects of Protein Synthesis' Abstracts., Tallberg, Sweden. September 17-20, 1997.

Kubo, S., Ikeda, T., Imaizumi, S., Takanami, Y. and Mikami, Y. (1990). A potent plant virus inhibitor found in *Mirabilis jalapa* L. Ann. Phytopath. Soc. Japan **56**: 481-487.

Kumon, K., Sasaki, J., Sejima, M., Takeuchi, Y. and Hayashi, Y. (1990). Interaction between tobacco mosaic virus, pokeweed antiviral proteins and tobacco cell wall. Phytopathology **80**(7): 636-641.

Kurland, C.G. (1971). Purification of Ribosomes from *Escherichia coli*. Chapter 39. Methods Enzymol. **20**: 379-381.

Laemmli, UK. (1970). Cleavage of structural proteins during the assembly of the head of bacteriophage T4. Nature **227**: 680-685.

Lee-Huang, S., Kung, H.F., Huang, P.L., Bourinbaiar, A.S., Morell, J.L., Brown, J.H., Huang, P.L., Tsai, W-P., Chen, A.Y., Huang, H.I., Chen, H.C. (1994). Human immunodeficiency virus type 1 (HIV-1) inhibition, DNA-binding, RNA-binding, and ribosome inactivation activities in the N-terminal segments of the plant anti-HIV protein GAP31. Proc. Natl. Acad. Sci. USA **91**(25):12208-12212.

Leffers, H., Egebjerg, A., Andersen, A., Christensen, T., and Garret, R.A. (1988). Domain VI of *Escherichia coli* 23S ribosomal RNA; structure, assembly and function. J. Mol. Biol. **204**(3): 507-522.

Legault, P. and Pardi, A. (1997). Unusual dynamics and pK$_a$ shift at the active site of a lead-dependent ribozyme. J. Am. Chem. Soc. **119**(28): 6621-6628.

Logemann, J., Jack, G., Tommerup, H., Mundy, J., Schell, J. (1992). Expression of a barley-inactivating protein leads increased fungal protection in transgenic tobacco plants. Bio-Tech. **10**(3): 305-308.

Lord, J.M., Hartley, M. and Roberts, L.M. (1991). Ribosome inactivating proteins of plants. Cell Biol. **2**: 15-22.

Lu, M. and Draper, D.E. (1994). Bases defining an ammonium and magnesium ion-dependent tertiary structure within the large subunit ribosomal RNA. J. Mol. Biol. **244**(5): 572-585.

Lundquist, S. and Nygard, O. (1997). Secondary structure of eukaryote specific expansion sequence II in 28S ribosomal RNA. Structural Aspects of Protein Synthesis Abstracts., Tallberg, Sweden. September 17-20, 1997. pp.18.

Macbeth, M.R. and Wool, I.G. (1999). Characterisation of *in vitro* and *in vivo* mutations in non-conserved nucleotides in the ribosomal RNA recognition domain for the ribotoxins ricin and sarcin and the translation elongation factors. J. Mol. Biol. **285**(2): 567-580.

MacGrath, M.s., Huang, K.M., Caldwell, S.E., Gaston, I., Luk, K.-G., Wu, P., Ng, V.L., Crowe, S., Daniels, J., Marsh, J., Deinhart, T., Lekas, P.V., Vennari, J.C., Yeung, H.-W. and Lifson, J.D. (1989). GLQ223: An inhibitor of human immunodeficiency virus replication in acutely and chronically infected cells of lymphocyte and mononuclear phagocyte lineage. Proc. Natl. Acad. Sci. USA **86**(8): 2844 -2848.

Marchant, A. and Hartley, M. (1994). Mutational studies on the α-sarcin loop of *Escherichia coli* 23S ribosomal RNA. Eur. J. Biochem. **226**(1): 141-147.

Marchant, A. and Hartley, M. (1995). The action of pokeweed Antiviral Protein and ricin A-chain on mutants in the α-sarcin loop of *Escherichia coli* 23S Ribosomal RNA. J. Mol. Biol. **254**(5): 848-855.

Maruta, H., Tsuchiya, T. and Mizuno, D. (1971). *In vitro* reassembly of functionally active 50S ribosomal particles from ribosomal proteins and RNAs of *E. coli*. J. Mol. Biol. **61**: 123-134.

Massiah, A.J. (1994). Studies on wheat ribosome-inactivating proteins. A thesis submitted for the degree of Doctor of Philosophy at the University of Warwick, United Kingdom.

Massiah, A.J. and Hartley, M. (1995). Wheat ribosome-inactivating proteins: Seed and leaf forms with different specificities and cofactor requirements. Planta **197**(4): 633-640.

Matheson, A.T., Davies, J., Dennis, P.P., Hill, W.E. (1995). Frontiers in translation. Biochem. Cell Biol. **73**: 739-1227.

Meyer, H-A., Triana-Alonso, F., Spahn, C.M.T., Twardowski, T., Sobkiewicz, A. and Nierhaus, K.H. (1996). Effects of antisense DNA against the α-sarcin stem loop structure of the ribosomal 23S rRNA. Nucleic Acids Res. **24**(20): 3996-4002.

Miyano, M., Appelt, K., Arita, M., Habuka, N., Kataoka, J., Ago, H., Tsuge, H., Noma, M., Ashford, V. and Xuong, N.H. (1992). Crystallization and preliminary X-ray crystallographic analysis of Mirabilis antiviral protein J. Mol. Biol. **226**(1): 281-283.

Moazed, D., and Noller, H.F. (1989). Interaction of transfer RNA with 23S rRNA in the ribosomal A-sites, P-sites and E-sites. Cell **57**(4): 585-597.

Moazed, D., Robertson, J.M. and Noller, H.F. (1988). Interaction of elongation factors EF-G and EF-Tu with a conserved loop in 23S RNA. Nature **334**(28): 362-364.

Moazed, D., Stern, S. and Noller, H.F. (1986). Rapid chemical probing of conformation in 16S ribosomal RNA and 30S ribosomal subunits using primer extension. J. Mol. Biol. **187**(3): 399-416.

Moazed, D., Van Stolk, B.J., Douthwaite, S. and Noller, H.F. (1986). Interconversion of active and inactive 30S Ribosomal Subunits is accompanied by a conformational change in the Decoding Region of 16S rRNA. J. Mol. Biol. **191**(3): 483-493.

Montford, W., Villafranca, J.E., Monzingo, A.F., Ernst, S.R., Katzin, B., Rutenber, E., Xuong, N.H., Hamlin, R. and Robertus, J.D. (1987). The three dimensional structure of ricin at 2.8Å. J. Biol. Chem. **262**(12): 5398-5403.

Moore, P.B. (1988). The ribosome returns. Nature **331**(6153): 223-227.

Moore, P.B. (1997a). Ribosomes: Protein synthesis in slow motion. Current Biology **7**(3): R179-R181.

Moore, P.B. (1997b). The conformation of ribosomes and rRNA. Curr. Op. Str. Biol. 7: 343-347.

Moya, M., Dantry-Varsat, A., Goud, B., Louvard, D. and Boquet, P. (1985). Inhibition of coated pit formation in Hep2 cells blocks the cytotoxicity of diphtheria toxin but not that of ricin. J. Cell Biol. 101: 548-559.

Monzingo, A.F. and Robertus, J.D. (1992). X-ray analysis of substrate analogs in the ricin A-chain active site. J. Mol. Biol. 227(4): 1136-1145.

Monzingo, A.F., Collins, E.J., Ernst, S.R., Irvin, J.D. and Robertus, J.D. (1993). The 2.5 Å structure of pokeweed antiviral protein. J. Mol. Biol. 233(4): 705-715.

Munishkin, A. and Wool, I.G. (1995). Systematic deletion analysis of Ricin A-chain function. Single amino acid deletions. J. Biol. Chem. 270(51): 30581-30587.

Munishkin, A. and Wool, I.G. (1995). The ribosome-in-pieces: Binding of elongation factor EF-G to oligoribonucleotides that mimic the sarcin/ricin and thiostrepton domains of 23S ribosomal RNA. Proc. Natl. Acad. Sci. USA 94: 12280-12284.

Munishkin, A. and Wool, I.G. (1997). Binding of EF-G to sarcin/ricin domain oligoribonucleotides. In '.Structural Aspects of Protein Synthesis' Tallberg, Sweden. September 17-21. 1997.

Nierhaus, K.H. (1990). Reconstitution of ribosomes. Chapter 8. In 'Protein Synthesis. A practical approach'. p 161-189. Spedding, G. (Ed.). Oxford University Press. NY USA

Nierhaus, K.H. and Dohme, F. (1974). Total reconstitution of functionally active 50S ribosomal subunits from E. coli. Proc. Natl. Acad. Sci. USA. 71: 4713-4717.

Nierhaus, K.H., Schilling-Barteztko, S., and Twardowski, T. (1992). The two main states of the elongating ribosome and the role of the α-sarcin stem-loop structure of 23S rRNA. Biochimie. 74: 403-410.

Nitta, I., Nambu, H., Okado, T., Yoshinari, S., Ueda, T., Endo, Y., Nierhaus, K.H., and Watanabe, K. (1998). A novel cell-free system for peptide synthesis driven by pyridine. Biol. Chem. 379: 819-829.

Nitta, I., Ueda, T., Watanabe, K. (1998). Possible involvement of Escherichia coli 23S ribosomal RNA in peptide bond formation. RNA-A Publication of the RNA Society 4(3): 257-267.

Noller, H.F. (1980). Structure and topography of ribosomal RNA. In 'Ribosomes: Structure, Funct. and Genetics'. Chambliss, G., Craven, G.R., Davis, J., Davis, K., Kahna, L. and Nomura, M. (Eds.). pp 3-22. University Park Press Baltimore.

Noller, H.F. (1984). Structure of ribosomal RNA. Ann. Rev. Biochem. **53**: 119-162.

Noller, H.F. (1991). Ribosomes: Drugs and the RNA world. Nature **353**(6342): 302-303.

Noller, H.F. (1991). Ribosomal RNA and translation. Ann. Rev. Biochem. **60**: 191-227.

Noller, H.F. and Nomura, M. (1987). Ribosomes. Chapter 10. In ''*Escherichia coli* and *Salmonella typhimurium*. Cellular and Molecular Biology'' (Neidhardt, F.C., Ingraham, J.L., Magasanik, B., Low, K.B., and Schaechter, M., Editors). Am. Soc. Microbiol. Washington, D.C. pp.167-180.

Noller, H.F., Hoffarth, V., Zimniak, L. (1992). Unusual resistance of peptidyl transferase to protein extraction procedures. Science **256**(5062): 1416-1419.

Noller, H.F., Green, R., Heilek, G., Hoffarth, V., Huttenhofer, A., Joseph, S., Lee, I., Lieberman, K., Mankin, A., Merryman, C., Powers, T., Viani-Puglisi, E., Samaha, R.R. and Weiser, B. (1995). Structure and function of ribosomal RNA. Biochem. Cell Biol. **73**: 997-1009.

Nomura, M. (1990). History of ribosome research: A personal account. Chapter 1. In 'The Ribosome: Structure, function & evolution'. Hill, W.E., Dahlberg, A., Garret, R.A., Moore, P.B., Schelessinger, D., Warner, J.R. (Eds.). Am. Soc. Microbiol., Washington, D.C.

Nowotny, V. and Nierhaus, K.H. (1982). Initiator proteins for the assembly of the 50S subunit from *Escherichia coli* ribosomes. Proc. Natl. Acad. Sci. USA. **79**(23): 7238-7242.

Oakes, M.I., Scheinman, A., Atha, T., Shankweiler, G. and Lake, J.A. (1990). Ribosome structure: Three-dimensional locations of rRNA and proteins. In 'The Ribosome. Structure, function and evolution'. Hill, W.E., Moore, P.B., Dahlberg, A., Schlessinger, D., Garrett, R.A. and Warner, J.R. (Eds.). Am. Soc. Microbiol. Washington, D.C. pp 150-193.

O'Hare, M., Roberts, L.M., Thorpe, P.E., Watson, G.J., Prior, B. and Lord, J.M. (1987). Expression of ricin A chain in *Escherichia coli*. FEBS Lett. **216**(1): 73-78.

Olsnes, S. and Pihl, A. (1973). Isolation and properties of abrin: a toxic protein inhibiting protein synthesis. Evidence for different biological functions of its two constituent peptide chains. Eur. J. Biochem. **35**: 179-185.

Olsnes, S. and Pihl, A. (1982). Toxin lectins and related proteins. In 'Molecular Action of Toxins and Viruses'. Cohen, P. and vanHeyringen, J. (Eds.). Elsevier, Amsterdam, pp. 51-105.

Orita, M., Nishikawa, F., Kohno, T., Senda, T., Mitsui, Y., Endo, Y., Taira, K. and Nishikawa, S. (1996). High-resolution NMR study of a GdAGA tetranucleotide loop that is an improved substrate for ricin, a cytotoxic plant protein. Nucleic Acids Res. **24**(4): 611-618.

Osborn, R.W. (1990). The action of ricin A chain on eukaryotic ribosomes. PhD thesis, University of Warwick, UK

Osborn, R.W. and Hartley, M.R. (1990). Dual effects of the ricin A chain on protein synthesis in rabbit reticulocyte lysate. Inhibition of initiation and translocation. Eur. J. Biochem. **193**(2): 401-407.

Ostergaard, P., Phan, H., Johansen, L.B., Egebjerg, J., Ostergaard, L., Porse, B.T. and Garret, R.A. (1998). Assembly of proteins and 5S RNA to transcripts of the major structural domains of 23S rRNA. J. Mol. Biol. **284**(2): 227-240.

Pan, T., Long, D.M. and Unlenbeck, O.C. (1993). Divalent metal ions in RNA folding and catalysis. In 'The RNA world' Gesteland, R.F. and Atkins, J.F. (Eds.). Cold Spring Harbor, New York. Cold Spring Harbor Laboratory Press. pp 271-302.

Peattie, D.A. (1979). Direct chemical method for sequencing RNA. Proc. Natl. Acad. Sci. USA **76**: 1760-1764.

Piatak, M., Lane, J.A., Laird, W., Bjorn, M.J., Wang, A. and Williams, M. (1988). Expression of fully functional ricin A-chain in *Escherichia coli* is temperature-sensitive. J. Biol. Chem. **263**(10): 4837-4843.

Pleij, C.W.A. (1990). Pseudoknots: A new motif in the RNA game. Trends Biochem. Sci. **15**(4): 143-147.

Polacek, N. and Barta, A. (1998) Metal ion probing of rRNAs: Evidence for evolutionarily conserved divalent cation binding pockets. RNA-A Publication of the RNA Society 4(10): 1282-1294.

Powers, T. and Noller, H.F. (1993). Evidence for functional interaction between elongation factor Tu and 16S ribosomal RNA. Proc. Natl. Acad. Sci. USA. **90**(4): 1364-1368.

Powers, T., Daubress, G., and Noller, H.F. (1993). Dynamics of in vitro assembly of 16S RNA into 30S ribosomal subunits. J. Mol. Biol. **232**(2): 362-374.

Prestle, J., Hornung, E., Schonfelder, M., Mundry, K.W. (1992). Mechanism and site of action of a ribosome-inactivating protein type-1 from *Dianthus barbatus* which inactivates *Escherichia coli* ribosomes. FEBS Lett. **297**(3): 250-252.

Prince, J.B., Gutell, R.R., and Garrett, R.A. (1983). A consensus model of the *E. coli* ribosome. Trends Biochem. Sci. **8**(10): 359-363.

Purohit, P. and Stern, S. (1994). Interactions of a small RNA with antibiotic and RNA ligands of the 30S subunit. Nature **377**(6491): 659-662.

Ramakrishnan, V., Capel, M., Kjeldgaard, M., Engelman, D.M. and Moore, P.B. (1984). Positions of proteins S14, S18 and S20 in the 30S ribosomal subunit of *Escherichia coli*. J. Mol. Biol. **174**(2): 265-284.

Raué, H.A., Klootwijk, J. and Musters, W. (1988). Evolutionary conservation of structure and function in high molecular weight ribosomal RNA. Prog. Biophys. Mol. Biol. **51**(2): 77-129.

Ready, M.P., Kim, Y. and Robertus, J.D. (1991). Site directed mutagenesis of ricin A chain and implications for the mechanism of action. Proteins **10**(3): 270-278.

Ready, M.P., Brown, D.T., and Robertus, J.D. (1986). Extracellular localisation of pokeweed antiviral protein. Proc. Natl. Acad. Sci. USA. **83**(14): 5053-5056.

Shih, N.J.R., McDonald, K.A., Girbes, T., Iglesias, R., Kohlhoff, A.J. and Jackman, A.P. (1998). Ribosome-inactivating proteins (RIPs) of wild Oregon cucumber (*Marah oreganus*). Biol. Chem. **379**(6): 721-725.

Rice, R.H. and Means, G.E. (1971). Radioactive labelling of proteins in Vitro. J. Biol. Chem. **246**(3): 831-832.

Richardson, P.T., Westby, M., Roberts, L.M. Gould, J.H., Coleman, A. and Lord, J.M. (1989). Recombinant proricin binds galactose but does not depurinate 28S ribosomal RNA. FEBS Lett. **255**(1): 15-20.

Roberts, H.K. and Stewart, T.S. (1979). Purification and properties of a translation inhibitor from wheat germ. Biochemistry **18**(12): 2615-2621.

Röhl, R. and Nierhaus, K.H. (1982). Assembly map of the large subunit (50S) of *Escherichia coli* ribosomes. Proc. Natl. Acad. Sci. USA. **79**(3): 729-733.

Romero, D.P., Arredondo, J.A. and Traut, R.R. (1990). Identification of a region of *Escherichia coli* ribosomal protein L2 required for assembly of L6 into the 50S subunit. J. Biol. Chem. **265**(30): 18185-18191.

Romero-Zepeda, H. and Hartley, M.R. (1997). Interaction of Ribosomes-Inactivating Proteins and Ribosomes. Structural Aspects of Protein Synthesis Abstracts., Tallberg, Sweden. September 17-20, 1997. pp.17.

Rutenber, E. and Robertus, J.D. (1991). Structure of ricin b-chain at 2.5Å resolution. Proteins. Struct. Funct. Genet. **10**(3): 260-269.

Saiki, R.K., Gelfand, D.H., Stoffel, S., Scharf, S.J., Higushi, R., Horn, R., Mullis, K.B. and Erlich, H.A. (1988). Primed-directed enzymatic amplification of DNA with a thermostable DNA polymerase. Science **239**(4839): 487-491.

Sambrook, J., Fritsch, E.F. and Maniatis, T. (1991). Molecular cloning. A laboratory manual. 2nd. Edition, Cold Spring Harbor Laboratory Press, New York.

Sanger, F., Nicklen, S. and Coulsen, A.R. (1977). Proc. Nat. Acad. Sci. USA USA **74**: 5463-5467. In 'Moazed *et al.*, (1986)', J. Mol. Biol. **187**: 399-416.

Schlossman, D., Withers, D., Welsh, P., Alexander, A., Robertus, J.D. and Frankel, A. (1989). Role of Glu177 of the ricin toxin. A chain in enzymatic inactivation of ribosomes. Mol. Cell Biol. **9**(11): 5012-5021.

Seggerson, K. and Moore, P.B. (1998). Structure and stability of variants of the sarcin-ricin loop (SRL) of 28S rRNA: NMR studies of the prokaryotic SRL and a functional mutant. RNA-A Publication of the RNA Society **4**(10): 1203-1215.

Serganov, A.A., Masquida, B., Westhof, E., Cachia, C., Portier, C., Garber, M., Ehresmann, B. and Ehresmann, C. (1996). The 16S rRNA binding site of *Thermus thermophilus* ribosomal protein S15: Comparison with *Escherichia*

coli S15, minimum site and structure. RNA- A publication of the RNA Society **2**(11): 1124-1138.

Sigmund, C.D., Ettayebi, M., Borden, A. and Morgan, E.A. (1988). Antibiotic resistance mutations in ribosomal RNA genes of *Escherichia coli*. Methods Enzymol. **164**: 673-690.

Spirin, A.S. (1986). Ribosome structure and protein biosynthesis. The Benjamin/ Cummings Publishing Company, Inc. California.

Spirin, A.S. (1990). Ribosome preparation and cell-free protein synthesis. Chapter 2. In 'The Ribosome: Structure, function & evolution'. Hill, W.E., Dahlberg, A., Garret, R.A., Moore, P.B., Schelessinger, D., Warner, J.R. (Eds.). Am. Soc. Microbiol. Washington, D.C.

Stark, H., Rodnina, M., Rinke-Appel, J., Brimacombe, R., Wintermeyer, W., van Heel, M. (1997). Three dimensional cryomicroscopy of the translating *E. coli* ribosomes. Structural Aspects of Protein Synthesis. Abstracts. Tallberg, Sweden. September 17-20, 1997. pp 2.

Steiner, G., Kuechler, E., Barta, A. (1988). Photo-affinity labelling at the peptidyl transferase centre reveals two different positions for the A- and P- sites in domain V of 23S rRNA. EMBO J. **7**(12): 3949-3955.

Stern, S., Moazed, D. and Noller, H.F. (1988). Structural analysis of RNA using chemical and enzymatic probing monitored by primer extension. Chapter 33. Methods Enzymol. **164**:.481.

Stern, S., Powers, T., Changchien, L.-M., Noller, H.F. (1989). RNA-Protein Interactions in 30S Ribosomal Subunits: Folding and function of 16S rRNA. Science **244**(4906): 783-790.

Stirpe, F. and Barbieri, L. (1986). Ribosome inactivating proteins up to date. FEBS Lett. **195**(1-2): 1-8.

Stirpe, F., Bailey, S., Miller, S.P. and Bodley, J.W. (1988). Modification of ribosomal RNA by ribosomes inactivating proteins from plants. Nucleic Acids Res. **16**(16): 1349-1357.

Stirpe, F., Gasperi-Campani, A., Barbieri, L., Falasca, A., Abbondanza, A. and Stevens, W.A. (1983). Ribosome-inactivating proteins from the seeds of *Saponaria offinalis* L. (soapwort), of *Agrostemma officinalis* L. (corncockle)

and of *Asparagus officinalis* L. (asparagus), and form the latex of *Hura crepitans* L. (sandbox tree). Biochem. J. **216**(3): 617-625.

Stirpe, F., Olsnes, S. and Pihl, A. (1980). Gelonin, a new inhibitor of protein synthesis non-toxic to intact cells. Isolation, characterisation and preparation of cytotoxic conjugates with concanavalin A. J. Biol. Chem. **255**: 6947-6955.

Stirpe, F., Williams, D.G., Onyon, L.J. and Legg, R.F. (1981). Dianthins, ribosome-damaging proteins with anti-viral properties form *Dianthus caryophyllus* L. (carnation). Biochem. J. **195**(2): 399-405.

Szewczak, A.A., Chan, Y-L., Moore, P.B. and Wool, I.G. (1991). On the conformation of the alpha-sarcin stem-loop of 28S rRNA. Biochimie **73**(7-8): 871-877.

Szewczak, A.A. and Moore, P.B. (1995). The sarcin/ricin loop, a modular RNA. J. Mol. Biol. **247**(1): 81-98.

Szewczak, A.A., Moore, P.B., Chan, Y.-L. and Wool, I.G. (1993). The conformation of the sarcin/ricin loop from 28S ribosomal RNA. Proc. Natl. Acad. Sci. USA **90**(20): 9581-9585.

Tapprich, W.E. and Dahlberg, A.E. (1990). A single base mutation at position 2661 in *E. coli* 23S ribosomal RNA affects the binding of ternary complex to the ribosome. EMBO J. **9**(8): 2649-2655.

Taylor, G.R. (1991). Polymerase chain reaction: basic principles and automation. In 'PCR. A practical approach' Vol. 1. McPherson, M.J., Quirke, P. and Taylor, G.R (Eds.). Oxford University Press. Reprint 1994.

Taylor, S., Massiah, A., Lomonossoff, G., Roberts, L.M., Lord, J.M. and Hartley, M.R. (1994). Correlation between the activities of five Ribosome-Inactivating Proteins in depurination of Tobacco Mosaic Virus Infection. Plant J. **5**(6): 827-835.

Terao, K., Uchiumi, T., Endo, Y. and Ogata, K. (1988). Ricin and α-sarcin alter the conformation of 60S ribosomal subunits at neighbouring but different sites. Eur. J. Biochem. **174**(3): 459-463.

Thrush, G.R., Lark, L.R., Clinchy, B.C. and Vitetta, E.S. (1996). Immunotoxins: An update. Ann. Rev. Immunol. **14**: 49-71.

Traub, P., Mizushiman, S., Lowry, V. and Nomura, M. (1971). Reconstitution of ribosomes from subribosomal components. Chapter 41. Methods. Enzymol. **20**: 391-407.

Uchiumi, T., Sato, N., Wada, A., Kominami, R., Hachimori, A. (1997). Interaction of the alpha-sarcin domain of 23S ribosomal RNA with proteins L3 and L6. Structural Aspects of Protein Synthesis Abstracts. Tallberg, Sweden. September 17-20, 1997. pp.15.

Uchiumi, T., Sato, N., Wada., Hachimori, A. (1999). Interaction of the sarcin/ricin domain of 23S ribosomal RNA with proteins L3 and L6. J. Biol. Chem. **274**(2): 681-686.

Unlenbeck, O.C. (1987). A small catalytic oligoribonucleotide. Nature **328**(6131): 596-600.

Uhlenbeck, O.C. (1995). Keeping RNA happy. RNA -A Publication of the RNA Society **1**(1): 4-6.

Van de Peer, Y., Caers, A., De Rijk, P. and De Wachter, R. (1998). Database on the structure of small ribosomal subunit RNA. Nucleic Acids Res. **26**(1): 179-182.

vanDeurs, B., Pederson, O.W., Sundan, A., Olness, S. and Sandvig, K. (1985). Receptor-mediated endocytosis of a ricin-colloidal gold conjugate in Vero cells. Intracellular routing to vacuolar and tubulo-vesicular portions of the endosomal system. Exper. Cell Res. **159**: 287-304.

Varani, G. and Pardi, A. (1994). Structure of RNA. Chapter I. In ''RNA-Protein Interactions''. Nagai, K., and Mattaj, L.W. (Eds.). Frontiers in Molecular Biology. IRL Press. Oxford University Press, Inc., New York.

Vater, C.A., Bartle, L.M., Leszyk, J.D., Lambert, J.M. and Goldmacher, V.S. (1995). Ricin A chain can be chemically cross-linked to the mammalian ribosomal proteins L9 and L10. J. Biol. Chem. **270**(21): 12933-12940.

Verschoor, A., Srivastava, S., Grassucci, R. and Frank, J. (1996). Native 3D structure of Eukaryotic 80S ribosome: Morphological homology with the *E. coli* 70S ribosome. J. Cell Biol. **133**(3): 495-505.

Wachinger, M., Samtleben, R., Gerhauser, C., Wagner, H., Erfle, V. (1993). Byodin, a single-chain ribosome-inactivating protein, selectively inhibits the growth of

HIV-1-infected cells and reduces HIV-1 production. Res. Exp. Med. **193**(1): 1-12. ABS

Weitzmann, C.J., Cunningham, P.R. and Ofengand, J. (1990). Cloning, *in vitro* transcription, and biological activity of *Escherichia coli* 23S ribosomal RNA. Nucleic Acids Res. **18**(12): 3515-3520.

Weston, S.A., Tucker, A.D., Thatcher, D.R., Derbyshire, D.J. and Pauptit, R.A. (1994). X-ray structure of recombinant ricin A-chain at 1.8Å resolution. J. Mol. Biol. **244**(4): 410-422.

Westhof, E. and Michel, F. (1994). Prediction and experimental investigation of RNA secondary and tertiary foldings. Chapter 2. In 'RNA-proteins interactions'. Nagai, K. and Mattaj, I.W. (Eds.). Oxford University Press. Reprinted 1996. pp. 25-51.

Wilson, K.S. and Noller, H.F. (1998). Mapping the position of translational elongation factor EF-G in the ribosome by directed hydroxyl radical probing. Cell. **92**(1): 131-139.

Wool, I.G. (1979). The structure and function of eukaryotic ribosomes. Ann. Rev. Biochem. **48**: 719-754.

Wool, I.G., Endo, Y., Chan, Y.-L. and Gluck, A. (1990). Structure, function and evolution of mammalian ribosomes. In 'The Ribosome: Structure, Function and Evolution'. Hill, W.E. (Ed.). American Society for Microbiology, Washington, D.C. pp. 203-217.

Wool, I.G., Gluck, A. and Endo, Y. (1992). Ribotoxin recognition of ribosomal RNA and a proposal for the mechanism of translocation. TIBS **17**(7): 266-269.

Wool, I.G., Chan, Y-L. and Gluck, A. (1995). Structure and evolution of mammalian ribosomal proteins. Biochem. Cell Biol. **73**(11-12): 933-947.

Yoshinari, S., Yokota, S., Sawamoto, H., Koresawa, S., Tamura, M. and Endo, Y. (1996). Purification, characterisation and subcellular localisation of a type-1 ribosome-inactivating protein from the sarcocarp of *Cucurbita pepo*. Eur. J. Biochem. **242**(3): 585-591.

Yoshinari, S., Koresawa, S., Yukota, S., Sawamoto, H., Tamura, M., Endo, Y. (1997). Gypsophila, a new type1 ribosome-inactivating protein from

Gypsophila elegans: Purification, enzymatic characterisation and subcellular localisation. Biosci. Biotech. and Biochem **61**(2): 324-331.

Youvan, D.C. and Hearst, J.E. (1979). Reverse transcriptase pauses at N^2-methylguanine during *in vitro* transcription of *E. coli* 16S rRNA. Proc. Natl. Acad. Sci. USA. **76**:3571-3574.

Zehner, Z.E., Shepherd, R.K., Gabryszuk, J., Fu, T-F., Al-Ali, M. and Holmes, W.M. (1997). RNA-protein interactions within the 3' untranslated region of vimentin mRNA. Nucleic Acids Res. **25**(16): 3362-3370.

Zhong, P., Shortridge, V.D., Edalji, R.P., Walter, K.A., Cao, Z., Holzman, T.F. and Katz, L. (1997). Molecular cloning of ErmAM RNA methyltransferase and the effect of magnesium on the substrate foldings. Structural Aspects of Protein Synthesis Abstracts. Tallberg, Sweden. September 17-20, 1997.p. 19.

10. CHAPTER X:
APPENDIX

Appendix 1. The strategy for the cloning of the domain VI - DNA encoding fragment.
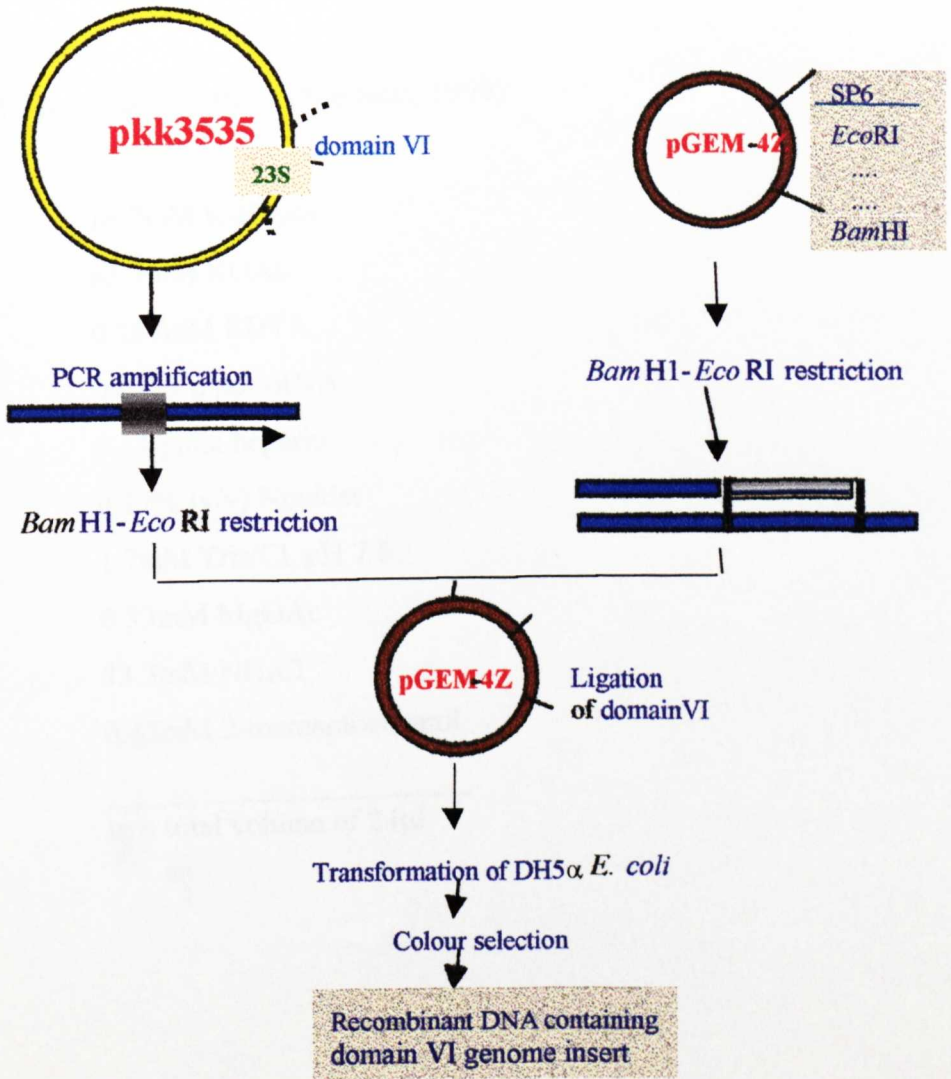
Appendix 2. Final buffer composition on RNA$_T$-Protein complex.

Final buffer composition on RNA$_T$-Protein complex in MSB (based on Batey's and Williamson's (1996) work):

- 20µl MSB (Batey and Williamson, 1996)
- + 2µl RNA$_T$,
- + 2µl r-proteins in buffer 4 (Nierhaus, 1990):

16.7mM K-Hepes

83.3mM KOAc

0.187mM EDTA

0.0129 pmol tRNA

0.11 pmol heparin

0.17% (v/v) Nonidet

1.7mM Tris/Cl, pH 7.6

0.33mM MgOAc

33.3mM NH$_4$Cl

0.42mM 2-mercaptoethanol

In a total volume of 24µl